APPLICATION OF FABRICATED GRAPHENE BASED MATERIALS CONCURRENT WITH OTHER TREATMENT METHODS TO ELIMINATE ORGANIC POLLUTANTS FROM AQUEOUS PHASE

Thesis submitted for the Award of the Degree of

DOCTOR OF PHILOSOPHY

(SCIENCE)

by

ANTARA GANGULI

Registration Index No.: **36/15/LifeSc./23**

Under the Supervision of

PROF PAPITA DAS

PROF SIDDHARTHA DATTA

JADAVPUR UNIVERSITY

KOLKATA - 700032

INDIA

2022

CERTIFICATE FROM THE SUPERVISOR(S)

This is to certify that the thesis entitled "**APPLICATION OF FABRICATED GRAPHENE BASED MATERIALS CONCURRENT WITH OTHER TREATMENT METHODS TO ELIMINATE ORGANIC POLLUTANTS FROM AQUEOUS PHASE**" Submitted by Smt. **ANTARA GANGULI** who got her name registered on 23.04.2015 for the award of Ph. D. (Science) degree of Jadavpur University, is absolutely based upon her own work under the supervision of Prof Papita Das and Prof Siddhartha Datta, Professor, Department of Chemical Engineering, Jadavpur University and that neither this thesis nor any part of it has been submitted for either any degree / diploma or any other academic award anywhere before.

29/6/22

(Signature of the Supervisor date with official seal)

Dr. Papita Das
Professor
Dept. of Chemical Engineering
Jadavpur University, Kolkata

29/6/2022

(Signature of the Supervisor date with official seal)

Ex-Professor (Retd.)
CHEMICAL ENGINEERING DEPARTME
JADAVPUR UNIVERSIT
Kolkata-700 032

Title : APPLICATION OF FABRICATED GRAPHENE BASED MATERIALS CONCURRENT WITH OTHER TREATMENT METHODS TO ELIMINATE ORGANIC POLLUTANTS FROM AQUEOUS PHASE

INDEX No. : 36/15/LifeSc./23

Abstract : The present work and its findings aim to fabricate graphene oxide and reduced graphene oxide analogous materials and its utilization to treat organic pollutants present in the aqueous matrix. Organic pollutants possess serious threat to aquatic organisms as well as it affects health conditions of humans. Generally, the organic pollutants are considered to have teratogenic, mutagenic and carcinogenic properties thereby treatment of organic pollutant contaminated water is of utmost important research niche. The laboratory fabricated nanomaterials were utilized for treatment of model organic pollutant compounds solely as well as they were also used in combination with other treatment methods to improve the efficiency of the remediation methods. The nanomaterial was used in concurrent with gamma radiation to treat model organic pollutant from aqueous matrix. Biodegradation still remains the preferred choice for treatment of hazardous pollutants for its cost effectiveness, easiness as well as wide applicability. The fabricated materials were also used in concurrent to microorganisms to remove PAH compounds and phenol (organic contaminants) from its aqueous solutions. The laboratory fabricated nanomaterial occurred to be biocompatible with microorganism as it showed little to no antibacterial effects against gram-positive and gram-negative microorganisms and thus obligated a synergistic effect in removal of aromatic pollutants. Adsorption treatment method is widely accepted for its simplicity but has a major drawback in terms of waste generation. Combination of sorption – biodegradation thus solves the problem of pollutant laden waste generated by the adsorption process. Residual toxicity of the treated synthetic wastewater was estimated by germination and root length analysis of plant model *Cicer arietinum* (Chickpea).

Thus, fabrication of graphene family nano materials and its utilization in various treatment processes were investigated in synthesized wastewater along with the detoxification efficiency was elucidated via chickpea plant model. Real time petrochemical effluent treatment was also done for upscaling the bench top scale experiment and to further investigate real time utilization of the fabricated materials.

Keywords : Graphene oxide and reduced graphene oxide analogous material, Fabrication, Gram-positive and Gram-negative bacteria, Positive synergism, Organic aqueous pollutants

Antara Ganguli
29/06/2022

Dr. Papita Das
Professor
Dept. of Chemical Engineering
Jadavpur University, Kolkata

29/6/22

29/6/2022
Ex-Professor (Retd.)
CHEMICAL ENGINEERING DEPARTMENT
JADAVPUR UNIVERSITY
Kolkata-700 032

Dedication

This Thesis is dedicated to my father Mr. **Anup Kumar Ganguli**, my mother Mrs. **Alpana Ganguli** for believing and supporting me.

Special thanks to my husband Mr. **Saumabha Bhattacharya** for his constant love, support, motivation, and constructive criticism which kept me going.

I am grateful to my in laws Mr. **Prodip Kumar Bhattacharya** and Mrs. **Bulbul Bhattacharya** for their support during the period.

A big thanks to my brother Mr. **Arnab Ganguli** and sister-in-law Mrs. **Moumita Ganguli** for their affection and positivity.

Special mention to my uncle Prof **Ganapati Mukherjee** for the constant motivation.

Acknowledgement

My doctoral trajectory would not have been possible without the constant support, motivation and care of many individuals at Jadavpur University, Kolkata, India. Firstly, I would like to express my gratitude and indebtedness to my mentor **Prof Papita Das** for her patience, guidance and motivation which led to the completion of this journey. I am grateful to her for the mental support she provided during the whole period.

I am also sincerely thankful to my guide **Prof Siddhartha Datta** as it was a memorable experience to work under his guidance and to learn to find the researcher side of myself in this journey.

I am grateful to the **Head of the Department of Chemical Engineering** for allowing me to work in the department and for the help received through usage of central laboratories and instrumental facilities to carry out many experimental activities of the doctoral learning.

Special mention to **Dr Abhijit Saha**, Centre – Director, UGC-DAE Consortium for Scientific Research, Kolkata Centre for giving me permission to carry out a portion of my thesis work in the gamma radiation facility center of UGC - DAE.

I am thankful to all the **Professors of the Department of Chemical Engineering** for their support and scholastic guidance whenever required.

I am much obliged to the **Department of Life Science and Biotechnology** for accepting my registration for PhD and to the Head of the Department and the Professors of the Department for their support.

Special mention to the Head of the Department and Professors of the **Department of Environmental Sciences, University of Calcutta** for their guidance whenever my steps faltered and also to my seniors, batchmates and juniors of the department for being a part in this journey.

As the doctoral journey involves teamwork so I am thankful to all my lab mates and co - researchers from other labs, my lab seniors, my lab juniors and everyone who joined me in my journey of doctoral learning. Special mention to **Ms Priya Banerjee** and **Mr. Sudipta Goswami** for their support during the initial phase of my doctoral journey. My heartfelt thanks to all the co-authors who have contributed to the research work associated with the thesis.

Distinct mention to few people who remained constant through thick and thin during the tough times due to unprecedented COVID and also being great buddies. Thankful to **Mr. Niladri Shikhar Saha, Mr. Sandipan Bhattacharya, Ms Arundhati Sarkar** for their immense help during my doctoral journey and gifting me beautiful memories to cherish lifelong.

During my doctoral endeavor I was assigned for assisting several **B.Tech** and **M.Tech** candidates for fulfillment of their project work and I am thankful to each of them for enriching my knowledge as learning is a dynamic process and information can flow both ways.

I would like to extend my gratitude to all the **technical staffs** of Department of Chemical Engineering and central departmental facility of Jadavpur University, Gamma Radiation Facility of UGC-DAE Consortium for Scientific Research, CRNN (Centre for Research in Nanoscience and Nanotechnology) University of

Calcutta for their positive cooperation to carry out my research work. Thankful to all the technical personnel for providing me assistance during my PhD journey and making the experience a lot easier.

Met lots of people in this long journey of doctoral research and I am thankful to each one of them for providing all sorts of experiences which led to me being more evolved. All the experiences helped to shape my life and build up my ability to cope with any circumstances. The journey of PhD is thus aptly named as the journey of life and is not just merely an academic transition phase.

I want to acknowledge **UGC** (University Grants Commission) for providing me UGC – NET JRF fellowship and contingency grants during the tenure to carry out my research work with ease.

Furthermore, my biggest gratitude is for my family and my extended family members, friends, well - wishers for their constant motivation, positive criticism and instilling confidence in me which fueled me to complete this journey of infinite possibilities. A special mention to my grandmother **Late Nanibala Mukherjee** and my uncle(s) **Late Ajit Ganguly** and **Late Mihir Chatterjee** who always blessed me in every sphere of life.

Lastly, my pet indie dog (**Kaalu Bhattacharya**) is worth mentioning as he acted as my greatest stressbuster through the tough times and helped me overcome major writer blocks.

The journey of PhD is indeed a path full of enthusiasm and adventure of exploring infinite possibilities and uncertainties and thus it requires constant motivation for hard work without any expectation, so I dedicate my work to **Myself**. Started the journey from the prefix Miss to Mrs. and now awaiting Dr. it has been a blessed journey of fulfillment with both highs and lows, but the greatest lesson comes from the fiascos as it is aptly said failure is the greatest teacher.

Above all I am highly grateful to the **Almighty** and the Supreme powers above for the countless blessings showered upon me.

Thanking you,

ANTARA GANGULI

"Research is creating new knowledge."

- ***Neil Armstrong***

LIST OF PUBLICATIONS :

- Lopamudra Das, Niladri Saha, **Antara Ganguli**, Papita Das, Avijit Bhowal, and Chiranjib Bhattacharjee. "Calcium alginate bentonite/activated biochar composite beads for removal of dye and Biodegradation of dye-loaded composite after use: Synthesis, removal, mathematical modeling and biodegradation kinetics. Environmental Technology & Innovation (2021): 101955. http://dx.doi.org/10.1016/j.eti.2021.101955

- **Antara Ganguli**, Preetha Ganguly, Papita Das, and Abhijit Saha. Integral approach for the treatment of phenolic wastewater using gamma irradiation and graphene oxide. Groundwater for Sustainable Development 10, (2020): 100355. https://doi.org/10.1016/j.gsd.2020.100355

- Preeti Das, Shouvik Mahanty, **Antara Ganguli**, Papita Das and Punarbasu Chaudhuri. Role of Manglicolous fungi isolated from Indian Sunderban mangrove forest for the treatment of metal containing solution: Batch and optimization using response surface methodology. Environmental Technology & Innovation 13 166–178 (2019). https://doi.org/10.1016/j.eti.2018.11.006

- Swapnila Roy, Suvendu Manna, Shubhalakhsmi Sengupta, **Antara Ganguli**, Sudipta Goswami, Papita Das. Comparative assessment on Defluoridation of waste water using chemical and bio-reduced graphene oxide: Batch, Thermodynamic, Kinetics and Optimization using Response Surface Methodology and Artificial Neural Network. Process Safety and Environmental Protection, 111, 221–231, (2017). ISSN: 0957-5820 https://doi.org/10.1016/j.psep.2017.07.010

LIST OF PATENTS : Nil

LIST OF NATONAL / INTERNATIONAL WORKSHOP / SEMINAR / CONFERENCE

- Selected for Oral presentation at ICSWRM-2020 (International Conference on Sustainable Water Resources Management under Changed Climate) held at Jadavpur University entitled "Abatement of Phenol from aqueous solution by Gram Positive and Gram-Negative bacteria – Its Degradation Kinetics and Biochemical Characterization.
  PAPER CODE : **216/SWRMCC/2020**

- Selected for Oral presentation at ATIPC-2018 (International Conference on Advanced Technologies for Industrial Pollution Control) held at Indian Institute of Engineering Science and Technology, Shibpur entitled "Removal of Phenol from Its Aqueous Solution by Bacteria Immobilized Graphene Oxide Nanocomposite.
  PAPER CODE : **108**

- Selected for Oral presentation at CHEMCON-2017 (70th annual session of Indian Institute of Chemical Engineers) held at Haldia Institute of Technology entitled "Modelling and optimization of removal of phenol by nanomaterial. PAPER CODE : **NT00481**

TABLE OF CONTENTS

PREFACE

The present work and its findings aim to fabricate graphene oxide analogous materials and its utilization to treat organic pollutants present in the aqueous matrix. Organic pollutants possess serious threat to aquatic organisms as well as it affects health conditions of humans. Generally, the organic pollutants are considered to have teratogenic, mutagenic and carcinogenic properties thereby treatment of organic pollutant contaminated water is of utmost important research niche. The laboratory fabricated nanomaterials were utilized for treatment of model organic pollutant compounds solely as well as they were also used in combination with other treatment methods to improve the efficiency of the remediation methods. The nanomaterial was used in concurrent with gamma radiation to treat phenol from aqueous matrix. Biodegradation still remains the preferred choice for treatment of hazardous pollutants for its cost effectiveness, easiness as well as wide applicability. The fabricated materials were also used in concurrent to microorganisms to remove PAH compounds and phenol (organic contaminants) from its aqueous solutions. The laboratory fabricated nanomaterial occurred to be biocompatible with microorganism as it showed little to no antibacterial effects against gram-positive and gram-negative microorganisms and thus obligated a synergistic effect in removal of aromatic pollutants. Adsorption treatment method is widely accepted for its simplicity but has a major drawback in terms of waste generation. Combination of sorption – biodegradation thus solves the problem of pollutant laden waste generated by the adsorption process. Residual toxicity of the treated synthetic wastewater was estimated by germination and root length analysis of plant model *Cicer arietinum* (Chickpea).

In the first part of the research study fabrication of graphene-based nanomaterials – named as GOaN (Graphene oxide analogous nanomaterial) and rGOaN (reduced Graphene oxide analogous nanomaterial) were done by modifying Hummer's method. The aim was to judiciously use lesser chemical products to fabricate Graphene oxide and reduced Graphene oxide from Graphite powder purchased commercially. The prepared materials were tested by various characterization methods and it was seen that in most of the cases it was similar to commercially available Graphene Oxide and Graphene powder. Thus, the term "analogous" was included while naming our materials. The cost efficiency of the process is calculated for judicious reasoning for usage of adsorbent in further steps.

In the second part of the research study the prepared nanomaterial (GOaN) was utilized to assess the removal efficacy of aromatic compounds specifically Poly aromatic hydrocarbons (LMW – Naphthalene ;

HMW – Pyrene) and Phenol from its aqueous phase. The adsorption kinetics, thermodynamics and reaction order were analyzed by batch scale study using OFAT (One factor at a time) approach. Optimizations of the process parameters of the iterative experimentations were also done by RSM (Response Surface Methodology) of Design – Expert Software program for statistically significant approach and also to elucidate intra parameter factors interaction. The batch processes showed Langmuir isotherm model was best fitted in major cases with low linear error (χ^2) and the rate kinetics experiment followed pseudo second order model with high regression coefficient (R^2) value. Thermodynamic study concludes that the reaction is spontaneously endothermic with high randomness. RSM study correlates the experimental data with statically significant modelling data.

In the third part of the research work the prepared nanomaterial (GOaN) was utilized in combination with an avant – garde mode of treatment of organic pollutants by using ionizing radiation. In this case gamma radiation treatment was opted as a choice of removal technique of aromatic pollutant and the effect of gamma radiation on fabricated nanomaterial was elucidated. It was observed that there was no effect on the prepared nanomaterial adsorbents at the chosen dosage of radiation. The removal efficiency is increased when fabricated GOaN (Graphene oxide analogous nanomaterial) is used along with gamma radiation for removal of phenol from synthesized wastewater. RSM modelling helped to investigate the intra parameter interactions occurring during the experimental study.

In the fourth part the Poly aromatic compounds [LMW – Naphthalene (Np); HMW – Pyrene (Pr)] and Phenol (Ph) were degraded by utilizing MTCC (Microbial Type Cell Culture) – purchased microorganism and also by an isolated microorganism from marine water. As biodegradation is the ultimate solution for complete degradation of pollutants thus the research study was executed to find suitable microorganism for degradation. Effect of fabricated nanomaterial on the chosen microorganisms were also studied and biocompatibility of the fabricated nanomaterial was established.

In the fifth part the comparison study between only microorganism and microorganism – fabricated GO nanocomposite was observed for pollutant removal where the combination effect turned out to be more efficient in removing organic pollutants in a shorter span of time. Adsorption process renders huge quantity of toxic laden adsorbent sludge which must be mitigated before disposal into the environment. Biodegradation process helps to solve the drawback of adsorption sludge formation and also combination of sorption – biodegradation has its own benefits. Nanomaterials acts as scaffolds for bacterial attachment and proliferation thereby increasing the efficiency of the process.

In the last part the prepared nanomaterial (GOaN) in single and in combination with microorganism was utilized for real time effluent treatment to study the future prospect of upscaling the bench – top experimental methods. In real world problem, the fabricated nanocomposite (GOaN +P) performs better thereby ascertaining the fact that complex pollutant needs combination / hybrid solutions. The treated water was tested for residual toxicity by germination and root length study of Chickpea (*Cicer arietinum*) plant model. Detoxification efficiency of gram negative – graphene oxide analogous material was observed to be the highest among all the combinations.

Thus, fabrication of graphene family nano materials and its utilization in combination with other treatment processes were investigated in synthesized wastewater. Interaction of the material with microorganism was also elucidated and composite formation between the bacteria – GOaN was observed. Real time effluent treatment was done with the formed bio nanocomposite for upscaling the bench top scale experiments and to further investigate real time utilization of the fabricated materials. The detoxification efficiency was elucidated via chickpea (*Cicer arietinum*) plant model to estimate the residual toxicity and whether the treated solutions are rendered fit for discharge into the environment or reutilized in secondary activities to promote reduce, reuse and recycle.

LIST OF TABLES

LIST OF FIGURES

GLOSSARY – SYMBOLS AND ABBREVIATIONS

® : Registered Marked
°C : Degree Celsius
µ : Specific Growth Rate (cells /hr)
Θ : Angle of Diffraction
Λmax : Lambda max
R2 : Correlation Coefficient
ANOVA : Analysis of Variance
AO : Acridine Orange
BLAST : Basic Local Alignment Search Tool
BOD : Biological Oxygen Demand
CCD : Central Composite Design
cm : Centimeter
COD : Chemical Oxygen Demand
CPCB : Central Pollution Control Board
DA : Dalton
dl : Decilitre
DNA : Deoxyribonucleic Acid
DOE : Design of Experiments
ECD : Electron Capture Detector
EDAX : Energy Dispersive X-Ray Spectroscopy
EPA : Environmental Protection Agency
EtBr : Ethidium Bromide
FID : Flame Ionization Detector
FS : Fluorescence Spectroscopy
FT-IR Spectroscopy : Fourier Transform Infrared Spectroscopy
G : Graphene (pristine)
GLC : Gas Liquid Chromatography
GO : Graphene Oxide
GOaN : Graphene Oxide analogous Nanomaterial
GOaN + B : Graphene Oxide analogous Nanomaterial + *Bacillus sp*
GOaN + P : Graphene Oxide analogous Nanomaterial + *Pseudomonas sp*
Gr : Graphite
HMW PAH : High Molecular Weight Poly aromatic Hydrocarbons
HPLC : High Performance Liquid Chromatography
IMViC : Indole, Methyl Red, Voges – Proskauer and Citrate
Kow : Octanol / Water Partition Coefficient
LB Media : Luria Broth Media
LLE : Liquid – Liquid Extraction

LMW PAH : Low Molecular Weight Poly Aromatic Hydrocarbons
mins : Minutes
ml : Milliliter
MLG : Multi Layered Graphene
MS : Mass Spectroscopy
MSM : Minimal Salts Media
MTCC : Microbial Type Culture Collection
NB Media : Nutrient Broth Media
Np : Naphthalene
OFAT : One - Factor -at- a - Time
PAH(s) : Poly Aromatic Hydrocarbons
PDI : Poly Dispersity Index
Phe : Phenol
ppb : Parts per Billion
ppm : Parts per Million
Pr : Pyrene
PSUF : Polymer supported Ultra Filtration
pXRD : Powder X-Ray Diffraction
rGO : Reduced Graphene Oxide
RGOaN : Reduced Graphene Oxide analogous Nanomaterial
RSM : Response Surface Methodology
SDG(s) : Sustainable Development Goals
SEM : Scanning Electron Microscope
SPCBs : State Pollution Control Board
SPE : Solid Phase Extraction
TGA : Thermo Gravimetric Analysis
™ : Trade Marked
UF : Ultra Filtration
UN : United Nations
USEPA : United States Environmental Protection Agency
UV – ViS Spectro : Ultra Violet – Visible Spectroscopy
WHO : World Health Organization
ZP : Zeta potential

CHAPTER 1

1. INTRODUCTION AND LITERATURE REVIEW

1.1 CONTEXTUAL INFORMATION

The technological progression in addition to scientific advancements has always been a central driving force leading to an exponential growth of human civilization. The 21st (twenty -first) century is the era of digitalization and globalization which acts as a fillip for the exponential rise of industrialization. With the introduction of novel scientific technologies and global increase in population there is a rapidly escalating trend for the upsurge of industrialization to meet the current demand. This majorly impacts all the spheres of the planet explicitly the atmosphere, biosphere, hydrosphere, lithosphere, geosphere and even cryosphere. The Sustainable Development Goals (SDGs) were set up by United Nations (UN) for realizing a better sustainable future for the progenies to come. The focal point of these goals was to use Earth's finite resources more judiciously and preserve the Earth's bounty for the forthcoming generations to survive on. As water remains an indispensable part of life, the increase in global anthropogenic population along with advancement of industrialization leads to unsurmountable amount of waste generated and disposed into the water bodies (Ganguli et al., 2020; Hashemi et al., 2022). Thus, this scenario poses threat of contaminating the ever-dwindling sources of freshwater supply. According to a report by World Health Organization (WHO) polluted water still remains the major cause of infanticide and global deaths all across the world particularly in developing countries like India (Salvia & Schneider, 2019). By 2025, it is predicted that majority of the population will thrive under scarcity or severe shortage of fresh water (Zhao et al., 2019). Treatment and management of waste entering into the aquatic ecosystem along with reclamation of water thus remains priority for scientists across the globe (Hashemi et al., 2022; Schwarzenbach et al., 2010).

A wide array of carbon-based and other non-carbon compounds predominates the composition of wastewater released from the industries. As increase in anthropogenic activities occur, huge number of pollutants is released due to leakage from industrial effluent or sewage effluent into our ecosystem cycles on a daily basis. Sometimes, spillage or improper handling of petroleum products also disposes large amounts of organic pollutants into the aquatic or terrestrial biomes. Among them the organic compounds

specifically the aromatics requires a special mention. The organic compounds mostly Polyaromatic Hydrocarbons (PAHs) and Phenolic compounds are categorized as carcinogen, mutagen and as chemicals possessing ability for teratogenic occurrences (Qiao et al., 2020). As they are listed as priority pollutants, their concentrations in the environment should be regularly checked and kept well under the maximum tolerance limits defined by the authoritative regulations provided by environmental protection bodies like Environmental Protection Agency (EPA) of United States and Central Pollution Control Board (CPCB) of India (Mojiri et al., 2019). Adsorption still remains the preferred choice for removal of pollutants from industrial wastewater (Basheer, 2018). With the increase in the complexity of pollutants emitted into the ecosystem, novel materials should be utilized as themselves or as well as in combination with other treatment methods for better waste management. The booming trend of utilization of nanomaterials in various environmental applications particularly pollutant removal and remediation has caught the attention of researchers all across the globe (X. Li et al., 2016). As nanotechnology is regarded as platform technology, nanomaterials bring new perspective to the already existing conventional methods (Campbell et al., 2019; Obayomi et al., 2022). Nanomaterials possess unique physical-chemical and optical properties as well as it is easily tunable which makes it more adaptable to be utilized in combination with already prevailing procedures. Reduced mass transfer complication and larger specific surface area with increased reactivity are key advantages of nano dimensioned materials. The reuse of treated wastewater for non-potable purposes such as watering lawns, golf courses and parks, flushing toilets and industrial cooling is a common way of reducing demand for fresh water. Reuse of water may also reduce costs and energy usage. Thus, reclamation of water means that a large portion of the wastewater is returned to the environment in a form that can be reused in secondary activities e.g., for agriculture or other industrial purposes. Three major reasons about the apprehension against reusage of wastewater in most Indian cities and towns are due to: 1) Lack of awareness 2) Cost of treatment and distribution of reused water 3) Lack of infrastructure

This doctoral research study includes laboratory fabrication of graphene family nanomaterials and its utilization as adsorbent as themselves as well as in addition with other treatment methods of organic pollutants like Low Molecular Weight (LMW) polyaromatic compound, High Molecular Weight (HMW) polyaromatic compound and Phenol. Interaction of the prepared nanomaterial with microorganisms is elucidated. The prepared nanocomposite material is finally applied for treatment of a real time petrochemical effluent and the efficiency is confirmed by the study of residual toxicity analysis by phytotoxic effects on Chickpea (*Cicer arietinum*) plant model.

1.2 WATER POLLUTANT - PAH(s) AND PHENOL

The National Water Quality Monitoring Program, initiated by the Central Pollution Control Board (CPCB) in association with Pollution Control Committee of State Pollution Control Board (SPCBs) specifies organic pollution to be one of the major causes of water pollution in India. Water quality of rivers and wetlands are constantly monitored via the Pollution Control Boards of various states and union territories, through a network of monitoring tools and stations. Small and medium scale industries pollute the environment just as much as the larger industrial unit does. In India, the number of small scale and medium scale industries sum up to approximately 3 million units. Most of these units lack adequate infrastructure for safe and monitored waste disposal systems. Moreover, they cannot afford it, yet they continue to practice highly polluting manufacturing technologies. As a commodity precursor substance Poly aromatic hydrocarbons (PAHs) and phenolic compounds are utilized with immense potential applications in almost all major industrial sections like petrochemical industries, pharmaceutical industries, plastic manufacturing units, paints, dyes, disinfectant and other allied substances producing industries (Mojiri et al., 2019; Patel et al., 2020; Sonwani et al., 2019). Thereby it can be assumed that these compounds are ubiquitously found in the environment as they are also obtained from natural sources too. Natural sources accounts for a minimum share in the pollution and may include catastrophic events like volcanic eruption or forest fires to release pollutants into the environment. But the main alarming source of these pollutants happens to be manmade synthetic origin as it increases with the infinite rise in the demand of synthetic commodity produce. PAH and phenol coexist predominantly in a large quantity in wastewater obtained from refinery and coking operations. Burning fossil fuels, agricultural wastes and biofuels as well as rapid deforestation and increase in industrialization are major contributors to the global rise in PAH pollution (Wilcke et al., 2014). Vehicular emissions too add up the pollution level. Recently various wildfires are contributing to the already raised levels of pollution. All these compounds produce alarming risk to the human health as well as affects other faunal world due to their toxic carcinogenic and mutagenic properties (Chu et al., 2016). Damage to central nervous system along with liver, kidney and other major organs are inevitable as human bodies are susceptible to high concentrations of aromatic pollutants. According to European Commission and USEPA (United States Environmental Protection Agency) such compounds are integrated within the list of primary pollutants as majority of them has been identified as carcinogenic chemicals having mutagenic properties (Balati et al., 2015; J. Shen et al., 2017). Aromatic compounds have tremendous persistence character due to the highly stable C – C bonds and less bioavailable portion. Two or several fused benzene rings in various structural (linear, stacked or angular) patterns gives rise to polycyclic aromatic hydrocarbons (Mahgoub, 2019). PAHs are generally hydrophobic

by nature has high octanol/water partition coefficient (Kow) and also requires large amount of energy to disrupt i.e. high desorption energy is needed for breaking the bonds (Johnsen & Karlson, 2005; Lamichhane et al., 2016a; Shin et al., 2006). PAHs can be classified into low molecular weight (LMW having 2-3 membered ring structure compounds) and high molecular weight (HMW having more than 4 membered ring structure compounds) based on the molecular structure. Solubility in water linearly decreases with the increase of molecular complexity and mass of the compound. Thus, the characteristic feature of PAHs includes low hydrophilicity, high boiling and melting points, etc. It also possess characteristic UV absorbance spectra thereby making UV – Vis spectrophotometer a common tool for identification of PAHs (Abdel-Shafy & Mansour, 2016). Naphthalene is a ringed aromatic compound produced as an essential by-product in the chemical industry and is extensively used in various consumer products. Naphthalene is also present in crude oil and thus is acutely lethal and has carcinogenic effect on humans. Its toxicity is also proven in organisms present in aqueous sphere. Naphthalene is a type of homocyclic aromatic compound as it contains only carbon atoms in its structure and are not substituted by any other atoms in its ring structure. It is the simplest of poly aromatic compounds consisting of two fused benzene rings and thus it is classified as LMW PAH (low molecular weight polyaromatic hydrocarbon compound). Naphthalene is characteristically a discreetly volatile compound with a boiling point of 218 °C and low hydrophilicity (aqueous solubility) of 31.7 mg/L (20 °C). Its log value of octanol/water (Kow) partition coefficient is 3.29, which implies its affinity for lipid tissues and thus is a potent applicant for bioaccumulation. Pyrene on the other hand is classified as HMW PAH (high molecular weight polyaromatic hydrocarbon compound) and it is also found ubiquitously in petrogenic and pyrogenic materials.

Phenol is a type of heterocyclic aromatic compound as it has -OH group substitution in its ring which is a non-carbon compound. It is the simplest of the phenolic compounds and serves as the parent compound for other phenolics. Phenol and its byproducts are found in a wide variety of industrial wastewater including wastewater from coal and coke plants, petrochemical refineries, pulp and paper mills, etc. (Sun et al., 2015). The phenolic compounds are also capable of mutagenic and carcinogenic activities when long term exposure to the pollutant occurs (Barik et al., 2021).The chemical structure of phenol is C_6H_5OH which depicts the OH bond attachment with the aromatic fragment. All the carbon atoms in aromatic structures are sp2 hybridized. The following table represents the physico-chemical properties of the above-mentioned toxicants.

Table 1.1 : Common properties of the pollutants analyzed in this research study

POLLUTANT	FORMULA	STRUCTURE	MOLECULAR WEIGHT (g/mol)	MELTING POINT (°C)	BOILING POINT (°C)
NAPHTHALENE	C10H8	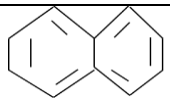	128.17	80.26	218
PYRENE	C16H10	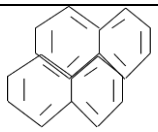	202.26	156	393
PHENOL	C6H6O	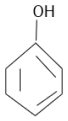	94.11	40.5	181.7

1.3 ROUTE OF EXPOSURE – PAH(s) AND PHENOL

PAHs generally tends to be lipophilic due to their easy solubility in organic solvents. Due to high affinity for organic matter, PAHs (with lesser fused benzene rings) breaks down due to volatilization, dissolution and degradation and becomes more toxic to the aquatic life present in the environmental matrix. PAHs with more fused benzene rings can remain in the sediments for years. The route of exposure of PAH to humans widely varies from inhalation of contaminated air from vehicular exhausts, smoking and cooking gases to ingestion of food containing PAHs (Abdel-Shafy & Mansour, 2016). Recently, massive wildfires and bushfires are contributing to the global pollution of earth with aromatic pollutants (P. Gong & Wang, 2021; Wentworth et al., 2018). Agricultural biomass also contains PAHs and thus dietary intake maybe another source of exposure along with burning of crops and other agricultural by-products (Gadi et al., 2012; Samburova et al., 2016; Zhang et al., 2022). Thus, entry via food chain also plays a role in human exposure to PAHs. Exposure to PAHs also occurs from occupational sites like factories, refineries, mining and metal related industries. Recently e - waste processing sites are also one of the sources of PAH contamination particularly atmospheric PAH. Factory personnel inhaling or having contact with the toxic fumes are more susceptible to higher levels of PAH exposure.(H. Chen et al., 2019; Luo et al., 2015) Urban landfill sites and municipal dumping areas also contribute to PAH contamination by transported air,

surface soil leaching and runoffs.(Melnyk et al., 2015) Smokers also contribute to PAH exposure to themselves. Domestic cooking methods may also be a source of PAH exposure as well as indoor paints or ambient air. Thus, exposure to PAH may occur from a variety of sources and thus dietary intake, inhalation or occupational hazards may contribute to the same. Regulation of PAH levels is thus mandatory for various food and other indoor and outdoor sites. Deposition of aerosols or runoffs from land or water or soil leachates are main routes for entry in to the food chains.(Gupte et al., 2016)

The major source of phenol discharged into the aqueous environment is done by the sectors of coal processing and coking operations (Saputera et al., 2021). Together they account for nearly 75% of total phenol released in the wastewater along with other major industrial operations (Raza et al., 2019). Other industrial sources include Textile, Leather, Rubber, Paper pulp processing industries, Wood and Resin units, Paint manufacturers, Iron and Petroleum refineries, pharmaceutical manufacturing units, etc. (Barik et al., 2021; Sun et al., 2015). Though a few types of phenolic compounds occurs naturally but the risks are caused by industrial, agricultural and anthropogenic byproducts being dumped into the environment non – judiciously. Inhalation and ingestion by oral route are also sometimes source of toxic phenol exposure.

1.4 TOXIC EFFECTS DUE TO EXPOSURE – PAH(s) AND PHENOL

Acute PAH exposure leads to various symptoms like eye irritability, nauseous feeling and diarrheal state. Chronic exposure may lead to cytotoxic and genotoxic effects where DNA (Deoxyribonucleic acid) damage may occur which ultimately paves the way for cancer of various organs (Andersen et al., 2018; Bai et al., 2017). Cardiopulmonary systems are also affected due to long term exposure to PAH (Holme et al., 2019). Biomarkers are thus chosen to keep track of the PAH levels ranging from urine to check human exposure to molluscs for the aquatic matrices(J. Gong et al., 2015; Lacroix et al., 2015; Z. Yang et al., 2021). Naphthalene causes serious allergic response in animals and humans, thereby it is known to be a direct skin irritant. Repeated exposure leads to skin redness and inflammation. Hemolytic effects can be observed if chronic exposure to a large amount of Naphthalene is done (Diggs et al., 2011). Diminished immune response is another symptom of chronic PAH exposure along with other long term serious health complications. Genetic mutations via base pair substitutions, addition or deletion of base pairs, strand breakage, chromosomal alterations are reported in various laboratory studies (Abdel-Shafy & Mansour, 2016; Jung et al., 2013). Reproductive system is also affected due to long exposure and thus teratogenic

abnormalities are reported as chronic effects of these PAHs compounds (Adeniji et al., 2018; Bolden et al., 2017).

Phenol on the other hand is toxic even at low concentrations and thus it is difficult to biodegrade phenol at higher concentrations. It imparts mutagenic, teratogenic, carcinogenic toxic effects on chronic exposure at high concentration (Leong et al., 2011). In high concentration , phenol may bioaccumulate in fishes which in turn ends up being staple diet of many people thereby having a chance of biomagnification through trophic levels (Liang et al., 2015). Acute exposure of phenol beyond 50 mg/L may lead to immediate effects as blisters on skin, burning sensation in the exterior skin and internally in the eyes, severe muscle feebleness, uneven breathing patterns, tremors, coma and may also lead to cessation of life in humans (Villegas et al., 2016). It also affects the central nervous system, vascular system, kidneys, biliary ducts of liver in humans and abnormal fetal development in animals due to prolonged exposure (Sun et al., 2015). Endocrine disorders are also one of the symptoms due to chronic exposure to high levels of phenol (Villegas et al., 2016).

1.5 TREATMENT TECHNOLOGIES FOR ABATEMENT - PAH AND PHENOL

For PAH samples pre-treatment is a prerequisite and it consists of several crucial steps. These steps are important as they help in reducing cost, time and sample volume to work with (Manousi & Zachariadis, 2020). The steps are as follows:

a) Extraction – Proper extraction of the samples is required for accuracy of the result as trace quantity is available in aqueous medium owing to low hydrophilicity of PAH(s). The extraction techniques can be divided into various types depending on the extraction method such as – Solid Phase Extractive method (SPE), Liquid – Liquid Extractive method (LLE) and other microextraction techniques. Ultrasonicators , Soxhlet extractors and Mechanical Stirrers may also be utilized for extraction and concentration of PAH from diluted samples (Erawaty Silalahi et al., 2021).

b) Concentration of the extract – Concentration of the extracted samples is done to increase the value of PAH (s) to a detectable amount being analyzed by the instruments. Thus, validation of method for extraction and concentration of organic samples, specifically PAH samples is necessary.

c) Cleaning up of the concentrate – In order to analyze the extracted samples by the scrutinizing equipment, cleaning up of the extracted phase is necessary. To verify the purity of the concentrated samples, cleaning up of the concentrate is required.

d) Eluent concentration – As cleaning up is done, the eluent obtained is further concentrated and purified for analysis. Utmost care is taken to remove the aqueous phase to undiluted pure sample for analytical purposes

e) Analysis – Chromatographic techniques are beyond a doubt the widely used techniques for PAH estimation along with UV spectral analysis. Analysis by HPLC (High Performance Liquid Chromatography) and GLC (Gas – Liquid Chromatography) methods are by far the most common methods. UV (Ultra – Violet) and FS (Fluorescence spectroscopy) are the most common detectors used in the HPLC system. FID (Flame ionization detector), ECD (Electron capture detector), or MS (Mass Spectrometry) are coupled with GLC systems for analysis. Both qualitative and quantitative measurements are done with these sophisticated analytical instruments. The sensitivity of the instruments is adequate to trace parts per billion (ppb) or parts per million (ppm) levels of PAH (s) in the sample (Adeniji et al., 2018).

Several technologies are implied for abatement of the PAH and phenol pollutants including various physical and chemical processes (Alkhuraiji et al., 2017). In situ remediation of hydrocarbons has been successfully accomplished with different approaches, including chemical and biological methods. In the natural environment PAH undergoes various physical and chemical processes like adsorption, volatilization, chemical degradation and photocatalytic degradation. Biological degradation or biodegradation also forms a major part in the abatement of aromatic pollutants like PAH and phenol. Biological remediation specifically microbial degradation remains the major removal pathway of these persistent compounds It involves either bio stimulation or bioaugmentation of the microorganism and can be of different type depending on the type of biological species utilized. Biodegradation can either be InSite or ExSite depending on the site of degradation with In Situ techniques gaining more preference over Ex Situ ones (Shah, 2014). In the current scenario management of waste is of utmost importance for the healthy functioning of the society and its living beings. With the advent of more persistent chemicals due to anthropogenic activities newer and more innovative technologies are being utilized for treatment of pollutants.

Various conventional methods of treatment of organic contaminants are listed below:

1.5.1 COAGULANTS OR FLOCCULANTS

The coagulation-flocculation mechanism is based on the pivotal principles to define the electrostatic interface between pollutants and coagulator - flocculant agents. Coagulation process reduces the net external surface charge of the colloidal elements to stabilize by overpowering electrostatic revulsion forces. Flocculation process continually increases the particle size to form discrete particles through additional collision forces and interaction with inorganic polymers or by the organic polymers added. Once discrete particles are flocculated into larger particles, the sludge generated can be removed or separated by filtration, straining or floatation (Shabeer et al., 2014). Different electrolytes like magnesium chloride, ferric chloride, sulphates of magnesium or aluminum are utilized for this simple process. Production of huge quantity of sludge, application of chemicals and allocation of toxic compounds into solid phase are core drawbacks of this process (Balati et al., 2015). Separation of the constituents pose hindrance to the smooth operational parameters of the process.

1.5.2 FILTRATION MEMBRANE

Filtration of pollutants by membrane separation has gathered considerable attention for the treatment of various contaminants. (Z. Yang et al., 2020) This energy intensive process requires precise pressure, temperature and other working conditions to operate at full capacity. The process is noisy as it requires vacuum pump for its operational activity. The membranes are subjected to harsh conditions which might lower the longevity of the membranes. This technique has been further subdivided into various forms of ultrafiltration, osmosis and reverse osmosis processes.

- **Ultrafiltration** (UF) utilizes permeable membrane to separate heavy metals, macromolecules and suspended solids from inorganic solution on the basis of the pore size (5–20 nm) and molecular weight of the separating compounds (1000 – 100,000 Da). Polymer-supported ultrafiltration (PSUF) technique adds water soluble polymeric ligands to bind metal ions and form macromolecular complexes by producing a free targeted metal ions effluent (Sun et al., 2015). Recently nano dimensional materials are being utilized as nanofiltration units for achieving better efficiency (Jin et al., 2013) .

- **Reverse osmosis** utilizes the principle of osmotic differences but in an opposite manner. As it is reverse in nature so pressure is required for the process to occur. As osmosis requires semi permeable membrane same is the requirement criteria for reverse osmosis. Thus, the process turns out be costly although recently researchers are opting for low-cost materials to act as the membrane filter. Membrane pore bottleneck is one of the key drawbacks of this method along with precision in conditions which makes the process difficult to comprehend (Jin et al., 2013; Liu et al., 2013). A major roadblock for reverse osmosis process is the generation of brine so sea side location is a criteria for reverse osmosis facility setup (Gholami et al., 2006).

1.5.3 OXIDATION

Various oxidation processes have been widely studied for removal of organic pollutants. Oxidation processes can be subdivided into groups according to the type of oxidation namely –

- **Chemical oxidation** – Destructive oxidation by using common chemicals like chlorine, ferrate, permanganate have been extensively studied .But the major drawback of these chemicals are they operate at narrow range of conditions and are sometimes exothermic in nature so there is potential risk in handling the chemicals (Yates et al., 2014).

- **Electrochemical oxidation** – This process eliminates the handling of potential hazardous chemicals but it requires installation of equipment and energy consumption thereby making the process costly. Here the pollutants are adsorbed at the anodic surface and the material of the anode is further investigated using various raw material (Martínez-Huitle & Ferro, 2006).

- **Catalytic Air oxidation** - this process requires high temperature, high pressure and in presence of catalyst can eliminate organic pollutants which are recalcitrant in nature (Izquierdo-Colorado et al., 2019). It is an energy intensive and a temperature dependent process which makes it less economical.

- **Advanced oxidation processes** – This process utilizes array of methods which can form OH (hydroxyl) radical (Suzuki et al., 2015). The OH radical is capable of mineralizing organic pollutants are widely researched now a days. Advanced oxidation process is used in combination to various other forms of treatment to increase the efficacy of removal of noxious organic pollutants. The most widely used Fenton's reagent and ozonation are part of advanced oxidation processes. More detailed information about advanced oxidation process is included in Chapter 5 of this doctoral thesis.

1.5.4 ADSORPTION

The most widely accepted and used technique for removal of various sorts of pollutants. The field of adsorption is ever exploratory due to its uncomplicatedness, cost effectiveness and ease of usage. The difference between adsorption and absorption is that the former involves only surface interfacial reactions whereas the latter one involves the whole material. Basic principle lies in the mass transfer process where an amount of solute is transfer from the fluid phase to the surface of solid adsorbent and bound by the physical or chemical or both forces together on the nature of bonding interactions adsorption can be reversible physical process or irreversible chemical process. Physical interaction involves weaker forces like Van der Waals, Electrostatic interactions, Hydrogen bonding whereas chemical bond formation occurs in case of chemical interaction (Zhao et al., 2019). Thus, based on physical or chemical forces acting on the process it is named as physisorption and chemisorption respectively. An endless voluminous literature is available for low-cost adsorbents which are already studied and creation of novel materials are generating endless prospect to develop the newer and novel adsorbents which poses high efficiency while keeping the thought of cost effectiveness in mind.

1.5.5 BIOLOGICAL DEGRADATION

Biological treatment methods are attractive because they are easier, energy efficient, ecofriendly, viable, safer than chemical approaches. To achieve sustainable development goals along with economically viable options, bioremediation still remains the preferred choice (Imam et al., 2021). Biotechnology or biological technologies can be used as efficient and low-cost technology in comparison to other physical or chemical

methods. Bioremediation is the green approach to mitigate waste products and other hazardous materials as they have no deteriorating effect on the environment and ecosystem (Villegas et al., 2016). It is the "Ecofriendly option" which is chosen by many researchers for treatment of hazardous pollutants even in extreme conditions. It uses the principle of treating waste products using biotic forms mainly microorganisms although phytoremediation and fungal remediation are of equivalent importance too. Biological treatment methods of aromatic hydrocarbons include

- Bioremediation using bacteria
- Fungal remediation
- Phytoremediation.

Wide variety of enzymes may also be utilized for treatment of organic contaminants thus gaining potential as biodegradation. Enzymes like laccases, peroxidases, etc. are extensively used for catalytic removal of pollutants (Kurnik et al., 2015). The major difference between bioremediation and enzymatic catalytic process lies in the fact that the latter one polymerizes and precipitate the pollutant and not metabolize it (Ba et al., 2013).

The section on Biodegradation is discussed in details in chapter 6 of this doctoral thesis with special reference to bacterial degradation.

Below is the tabulated form on the various research study conducted across globe for removal of PAHs (Np, Pr) and Ph using different methods: (NR = Not reported)

Table 1.2 : **Various forms of treatment of organic contaminants and their efficiency in terms of PAHs (LMW PAH - NP; HMW PAH – PR) – a global scenario**

POLLUTANT	MATERIAL (S)	TREATMENT METHOD	REMOVAL EFFICIENCY	COUNTRY	REFERENCE (DOI INCLUDED)
Naphthalene	*Eichhornia crassipes*	Bioaccumulation (Phytoremediation)	>75%	Israel	(Nesterenko-Malkovskaya et al., 2012)

	(water hyacinth)				https://doi.org/10.1016/j.chemosphere.2012.01.060
Naphthalene Pyrene	Porous carbon (Petroleum coke derived)	Adsorption	>80% >75%	China	(Yuan et al., 2010) https://doi.org/10.1016/j.jhazmat.2010.05.130
Naphthalene	C60 Fullerene	Adsorption	>55%	USA	(X. Cheng et al., 2004) https://doi.org/10.1021/je030247m
Naphthalene Pyrene	Aspen wood fibres	Adsorption	>90%	USA	(Boving & Zhang, 2004) https://doi.org/10.1016/j.chemosphere.2003.07.007
Naphthalene	Graphene/Graphene oxide nanosheet from rice straw	Adsorption	>60%	India	(Das et al., 2016) https://doi.org/10.15761/fnn.1000107
Naphthalene	Chemically activated biochar	Adsorption	>80%	China	(Qu et al., 2021)

					https://doi.org/10.1016/j.jhazmat.2020.123292
Naphthalene	Activated Carbon from Coal	Adsorption	NR	Spain	(Cabal et al., 2009) https://doi.org/10.1016/j.chemosphere.2009.04.002
Naphthalene	Modified Zeolites	Adsorption	NR	China	(N. Li et al., 2017) https://doi.org/10.4236/jep.2017.84030
Naphthalene Pyrene	Ripe orange peels	Adsorption	NR	Nigeria	(Owabor & Audu, 2010) https://doi.org/10.4314/gjpas.v16i1.62822
Naphthalene	Nano chitosan / sodium alginate composite	Adsorption	NR	India	(Sathish et al., 2021) https://doi.org/10.1007/s00289-021-03926-0
Naphthalene	Rice Husk activated carbon RHAC	Adsorption	NR	Egypt	(Yakout et al., 2013) https://doi.org/10.1260/0263-6174.31.4.293

Naphthalene	Borassus flabellifer (Asian Palm Kernel Shell) Charcoal	Adsorption	NR	India	(J. et al., 2016) https://doi.org/10.5897/AJB2016.15650
Naphthalene	Oleic acid modified palm shell activated carbon	Adsorption	>65%	India	(J. A. Kumar et al., 2018) https://doi.org/10.5004/dwt.2018.22066
Naphthalene	Fatty acid modified walnut shells	Adsorption	NR	China	(M. Zhu et al., 2016) https://doi.org/10.1016/j.chemosphere.2015.10.050
Pyrene	Bacterial – fungal consortium consisting of *Serratia marcescens* L-11, *Streptomyces rochei* PAH-13 and *Phanerochaete chrysosporium* VV-18	Hybrid technique (Biological – Biological)	>60%	India	(A. Sharma et al., 2016) https://doi.org/10.1016/j.jenvman.2016.08.024

Naphthalene	Ni-doped titanium nanocomposite	Hybrid adsorption /photocatalytic degradation	NR	Korea	(A. Sharma & Lee, 2015) https://doi.org/10.1016/j.jenvman.2015.03.008
Pyrene	*Pseudomonas taiwanensis* PYR1 and *Acinetobacter baumannii* INP1 immobilised on cinder beads	Bacterial consortium Immobilization	<75%	China	(R. Huang et al., 2016) https://doi.org/10.1016/j.marpolbul.2015.11.044
Naphthalene Pyrene	Enzyme (Laccase) immobilised electrospun fibres	Enzyme mediated electrospinning process	>65% >60%	China	(Niu et al., 2013) https://doi.org/10.1016/j.jhazmat.2013.01.017
Pyrene Naphthalene	Mixed bacterial cultures DAK11	Mixed consortium Bioremediation	70 -75%	India	(Patel et al., 2018) https://doi.org/10.1016/j.biortech.2018.01.049

Table 1.3 : **Various forms of treatment of organic contaminants and their efficiency in terms of Phenol – a global scenario**

POLLUTANT	MATERIAL (S)	TREATMENT METHOD	REMOVAL EFFICIENCY	COUNTRY	REFERENCE (DOI INCLUDED)
Phenol	Titanium oxide (TiO2)	Adsorption	NR	Algeria	(Bekkouche et al., 2004) http://dx.doi.org/10.1016/j.desal.2004.06.090
Phenol	Activated Carbon from rubber seed coat	Adsorption	>90%	South Korea	(Rengaraj, 2002) https://doi.org/10.1016/S0304-3894(01)00308-9
Phenol	Activated sewage sludge	Adsorption	NR	Spain	(Otero et al., 2003) https://doi.org/10.1016/S0143-7208(03)00005-6
Phenol	Chemical treated bentonite	Adsorption	NR	Jordan	(Al-Asheh et al., 2003)

					https://doi.org/10.1016/S1383-5866(02)00180-6
Phenol	Carbon-encapsulated iron nanoparticles, carbon nanotubes and activated carbon	Adsorption	>75%	Poland	(Strachowski & Bystrzejewski, 2015) http://dx.doi.org/10.1016/j.colsurfa.2014.11.044
Phenol	Coal, residual coal and chemically treated coal	Adsorption	NR	India	(Ahmaruzzaman & Sharma, 2005) https://doi.org/10.1016/j.jcis.2005.01.075
Phenol	Activated charcoal – chitosan mixture (1:1)	Adsorption	>90%	China	(R. Huang et al., 2014) https://doi.org/10.1002/ep.11844
Phenol	Ultrathin MgO coated Ag/TiO2 nanocomposite	Photocatalytic degradation	NR	USA	(Scott et al., 2019) https://doi.org/10.1016/j.chemosphere.2018.10.083

Phenol	Montmorillonite, activated carbon and cement based composite geomaterials	Static sorption	80%	France	(Houari et al., 2014) https://doi.org/10.1016/j.cej.2014.06.065

1.6 GRAPHENE FAMILY NANOMATERIAL AS AN INNOVATIVE ADSORBENT FOR ABATEMENT OF ORGANIC POLLUTANTS

Nanomaterials being the basis of nanotechnological advancements occurring in the twenty first century. New treatment technologies involving nanomaterials is turning out to be panacea for water pollutants (Alvarez et al., 2018). Carbon based nanomaterials are widely explored as adsorbents due to their excellent properties (Sarma et al., 2019). Graphene family nanomaterial encompasses a wide range of materials showing different surface properties and characteristic edgy features (Volkov et al., 2017). Structurally graphene appears to be like a honeycomb lattice as it is consists of tightly packed monolayer of carbon atoms in hexagonal array (X. Li et al., 2009). It is obtained through the process of exfoliation of graphite and has many fascinating structural and optical properties (Geim & Novoselov, 2007; Y. Huang et al., 2011) It is primarily the building block of all allotropes of carbon which are sp-2 hybridized mainly (Jia et al., 2011). The other members of the graphene family are derivatives of graphite by oxidation and reduction of the oxidized form namely oxidized graphene/graphite and reduced graphene/graphite. The term graphene / graphite is sometimes used interchangeably although there may exist difference in the properties. The sp2 bonding is disrupted while using strong oxidizing agents for the oxidation of graphite powder to form graphene oxide. Formation of sp3 bonds in case of oxidized graphene and removal of sp2 bonds when the oxidized form is reduced for achieving tunable properties hypothesizes bond disruption. The advantage of graphene oxide over pristine graphene or graphite is in its hydrophilic nature. Thus, due to chemical oxidation of graphite, graphene oxide consists of surface functional groups which enables dispersion in aqueous matrix along with heterogeneity which increases activity range of the material. Graphene oxide is aptly termed as a wonder material due to its applicability in every field of biological,

medical, energy, optical, electronic and environmental aspects (Balati et al., 2015; Hernández et al., 2014; Ranjan et al., 2018).

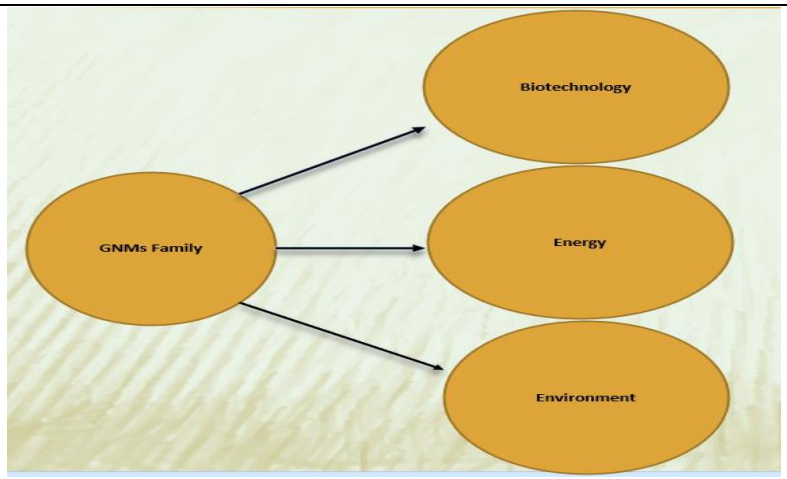

Fig 1.1 : Application of Graphene family nanomaterials in various sectors

Last few decades exploitation of the astounding property of Graphene oxide is utilized in pollutant degradation specifically for recalcitrant pollutants as their removal is not easily achieved. Similarly, Graphene oxide has been widely used for aromatic pollutant degradation with remarkable results. But as mentioned earlier novel materials are being synthesized on a daily basis. Such novel materials require more better and efficient treatment processes which would yield results faster and effectively. Thus, graphene oxide in combination of other treatment methods have been currently a hot spot for all the researchers globally. Below the increasing research pattern could be seen about exploiting the synergistic effect between graphene oxide and bacteria for organic pollutant removal. The trendline data was collected as a part of literature survey within the timeframe 2015 – 2021. The string words used were “GRAPHENE” “GRAPHENE OXIDE” “SYNERGISTIC EFFECT” “BACTERIA” “ORGANIC POLLUTANT” etc. Much of the literature survey consisted of grey papers (which are not useful) and thus were omitted from the search history using exclusion of keywords which were not needed. There was opulence of papers relating to the antibacterial effect but very few studies were present about synergistic effect of nanomaterial and bacteria for treatment of aromatic pollutants. Similarly, research studies on organic pollutant treatment by combination effect of Gamma radiation and Graphene oxide from synthesized aromatic solutions were

also in dearth. Thus, these extensive literature survey helps to shape the research motives of the present doctoral study which is discussed in details in the next chapter.

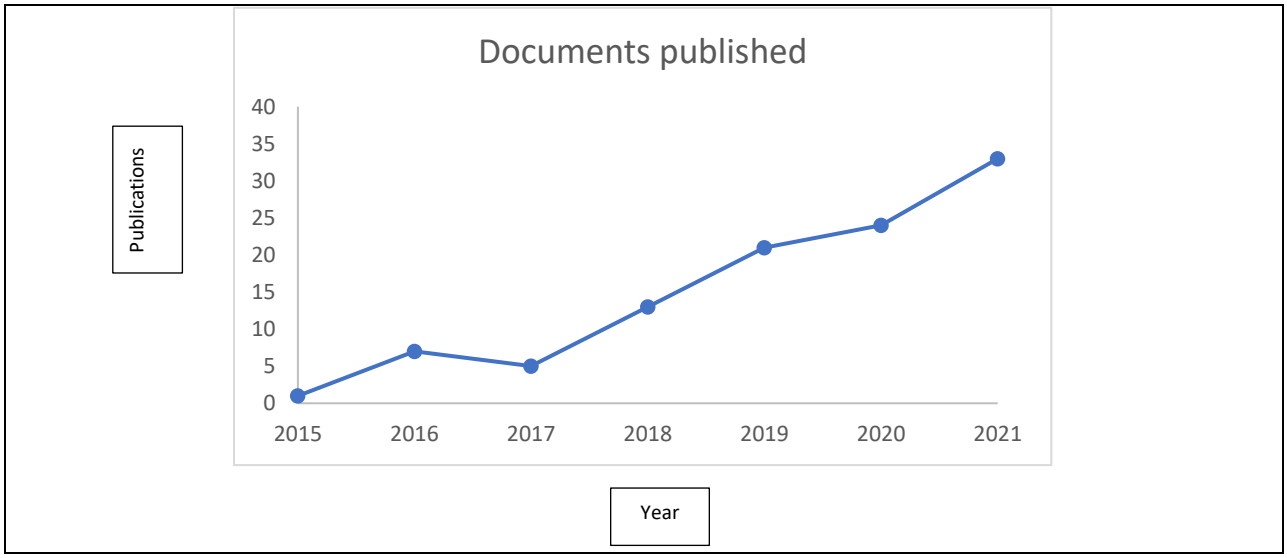

Reference : Scopus (updated on December 31st, 2021)

Fig 1.2 : Documents published under the string words "Graphene oxide" "Microorganism" "Synergistic organic pollutant removal"

CHAPTER 2

2. OBJECTIVE OF THE PRESENT STUDY

2.1 CONTEXTUAL IMPETUS

The literature review in the previous chapter (Chapter 1) has shown the huge potential of using nanomaterials in various environmental applications. Carbon based nanomaterials specifically Graphene family nanomaterials have been used in extensive range of applications in the arena of biomedical sciences, pollutant remediation, electronics, material sciences etc. But in all the research papers it was seen that the fabrication process of graphene family nanomaterials impacted the physical – chemical properties of the synthesized material. Ionization radiation is an avant – garde method of treatment of recalcitrant pollutants as it treats pollutant without formation of sludge. Thus, the effect of ionizing radiation on pollutant removal is an interesting area for research recently. But the major constraint lies in the availability of gamma radiation facility and cost of the procedure. The major drawback of adsorption process also depends on the generation of pollutant laden waste which can be mitigated in presence of biological microorganism. But the interface of material science and biotechnology is research in progress. Thus, the standardized methods of preparation of Graphene family materials must be tweaked to prepare biocompatible material which can be utilized in concurrent with other treatment methods. The biocompatibility helps in stabilizing microbial population for better removal of pollutants from the aqueous medium and can be applied in solving real world problems.

2.2 OBJECTIVES OF THE STUDY

- Fabrication and characterization of Graphene based nanomaterials
- Application of prepared nanomaterials to remove model organic pollutants (LMW PAH, HMW PAH, Phenol) in shake flask studies with Equilibrium, Kinetics, Thermodynamics study of the adsorption process
- Simulation of the removal process parameters and understanding inter – parameter interactions by Response Surface Methodology (RSM) of Design – Expert software

- Application of prepared nanomaterial concurrent with ionizing radiation treatment by gamma radiation to remove model organic pollutant
- Effect of interaction between process parameters elucidation by RSM optimization and validation.
- Modelling of the experimental data by Artificial Neural Network (ANN)
- Selection of prototypical Gram-positive bacteria and Gram-negative bacteria for removal of PAHs and Phenol from synthesized solutions
- Interaction of Gram positive and Gram-negative bacteria prototypes with fabricated nanomaterial
- Viability study of bacteria after composite formation to prove biocompatibility and synergistic interaction between microorganism and nanomaterial.
- Utilization of sorption – biodegradation effect of the bio nanocomposite for removal of model organic pollutant from synthesized solution
- Application of the prepared nanocomposite material in real effluent treatment process
- Toxicological analysis of the treated synthetic wastewater by Germination and Root length study of *Cicer arietinum* (Chick pea plant)

2.3 RESEARCH FOCUS

As it is observed from literature review that graphene-based materials are widely used as adsorbent for removal of extensive variety of pollutants it is thus an important research area to explore further possibilities. Graphene-based nanomaterials can also be used in concurrent to other existing treatment methods for better efficiency and thus nanomaterials act as platform on which the efficiency of other treatment technologies can be improved. The primary focus of this experimental study remained in the fabrication of biocompatible graphene-based material with simple facile techniques. Exploitation of the prepared nanocomposites to remove aromatic compounds from aqueous phase was the prima facie research focus. Utilization of the prepared material along with new treatment techniques to improve the removal efficiency of pollutants were further studied during the experiments planned and conducted. The prepared nano adsorbent was utilized in conjunction with ionizing radiation of gamma rays for treatment of model organic pollutant from its aqueous phase. But as with adsorption process the major concern is the formation of pollutant laden adsorbent and its proper disposal. Biodegradation is the preferred choice

for mitigation of toxic waste into metabolites thereby decreasing the chances of contamination in the environmental aspect. The interaction of microorganism and fabricated graphene-based nanomaterial is an evolving research field. Interaction of biological organisms on the nanomaterial surface depends on many controlling factors and may yield antibacterial or biocompatible effects. The biocompatibility of the prepared material with gram positive and gram-negative microorganism was further investigated by growth of microorganisms in presence of graphene family nanomaterials. Finally, utilization of the adsorbent material in combination with biodegradation method for improving removal of the aromatic pollutant in aqueous phase and in real time effluent was explored. In Situ cosorption – biodegradation of aromatic compound is thus one of the research motives behind the experiments conducted. To lower the effect of toxicity of aromatic compounds in aqueous phase, to increase the efficiency of the fabricated nanomaterial and to turn the water suitable for discharge into the environment or utilized in secondary practices like agriculture or washing purposes has been the driving forces behind the experimental study plan and conducted during the course of the doctoral study.

CHAPTER 3

3 FABRICATION AND CHARACTERIZATION OF BENCH SCALE SYNTHESIZED GRAPHENE-BASED MATERIALS

3.1 CONTEXTUAL INFORMATION

As previously discussed in Chapter 1, Graphene family nanomaterials have caught the attention of the researchers due to its wonderful physical topography and chemical properties and easy tunability and applicability in many areas. Graphene oxide is a widely sought-after material and it is aptly termed as the wonder material for its utilization in many niche areas ranging from electronics, energy, environment to biomedical areas (Priyadarsini et al., 2018). The unique physical and chemical properties along with high flexibility with stiffness and high compatibility due to its exceptional surface functionality makes it a special material. Graphene oxide acts as the parent material to the other materials available of the graphene family. Synthesis of Graphene oxide (GO) has primary involved chemical reactions of oxidation and exfoliation of graphite by strong oxidizing agents. Graphene oxide (GO) serves as a precursor substrate to form its reduced morphs like reduced Graphene oxide (rGO), multi layered Graphene (MLG) and pristine Graphene (G)(Priyadarsini et al., 2018). Thus, production of Graphene oxide is of utmost importance to explore the fascinating properties of Graphene family nanomaterials. Synthesis of Graphene involves mechanical exfoliation, chemical vapor deposition, thermal reduction or chemical reduction or exfoliation (S. Kumar & Parekh, 2020). Historically the fabrication of Graphene oxide (GO) was credited to Brodie in 1859 when the material was not known as Graphene oxide (GO). Brodie created “oxide de graphite” by treating graphite mixture with a strong oxidizing mixture consisting of Potassium chlorate ($KClO_3$) and Nitric acid (HNO_3) in a concentrated form (Brodie Benjamin Collins, 1859). Several other researchers followed the preparation pathway mechanism of Graphite oxide and corroborated the findings of Brodie. The researchers over the years started making modifications to produce better yield of the substance. Staudenmaier modified the process by incorporating Sulphuric acid (H_2SO_4) with fuming Nitric acid (HNO_3) to yield better oxidation results. The modern method of preparation of Graphene oxide was proposed by Hummers and Offeman which changed the primary reactant products to graphite and Sodium nitrate ($NaNO_3$) suspension in Sulphuric acid removing $KClO_3$ (Potassium chlorate) and gradual addition of Potassium permanganate ($KMnO_4$). The most recent and successful adaptation of modified

Hummer's method was put forward by Marcano which has reduced the emission of toxic gases (NO_x) and eliminated interferences by impurities through exhaustive washing procedure. The evolution of the process of preparation of graphene oxide is depicted in the figure below.

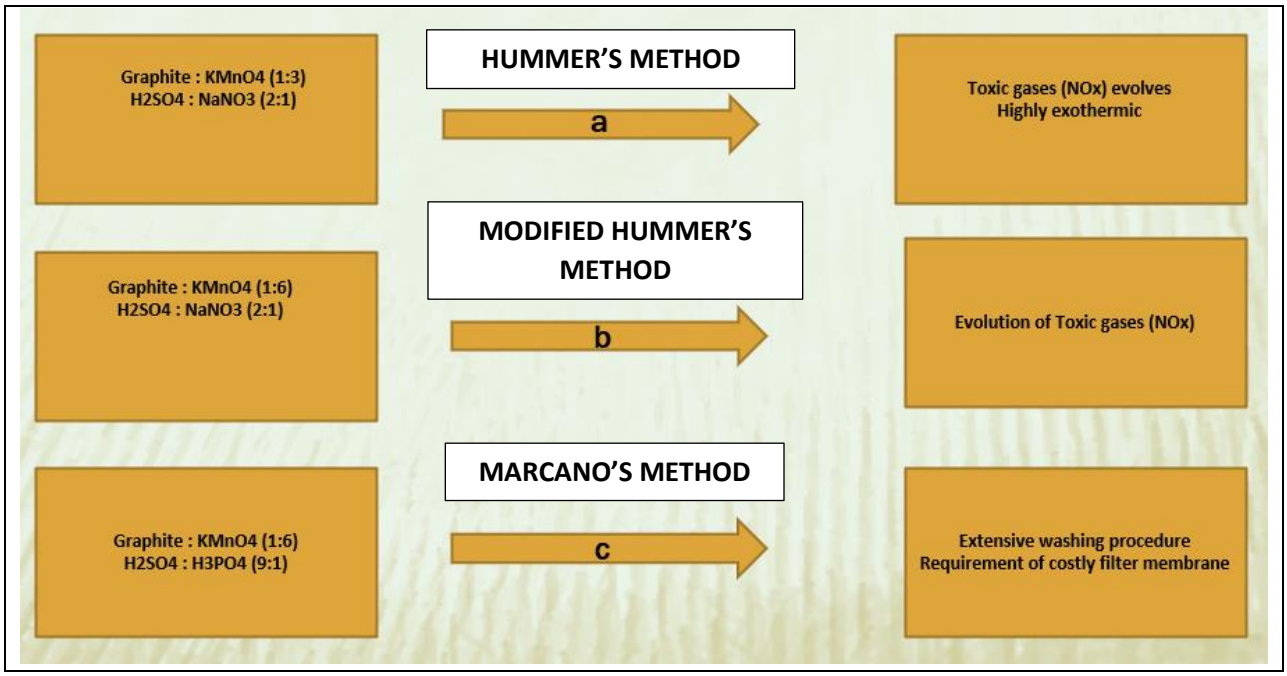

Fig 3.1 : Evolution of Graphene oxide preparation method with starting reactants , conditions and drawbacks of the processes.

3.2 STRUCTURAL ASPECT OF GRAPHENE OXIDE – AN INSIGHT

Structurally, graphene oxide, the oxidized form of graphite and the precursor of all graphene family nanomaterial is a 2 -D planar carbon structure with oxygen rich O2 functional groups attached to it. The O2 rich functional moieties include carboxyl, carbonyl, hydroxyl and epoxy groups attached to its outer edges as well as intra-atomic spaces. The oxygenated functional groups are dispersed along the edges as well as in interstitial spaces of the carbon framework. The oxygenated functional groups render the material to be hydrophilic and thus forming stable aqueous suspensions. Thus easy dispersibility in hygroscopic solutions is an added virtue of graphene oxide unlike its reduced forms which are generally hydrophobic and forms a distinct layer in aqueous solutions (Alam et al., 2017).

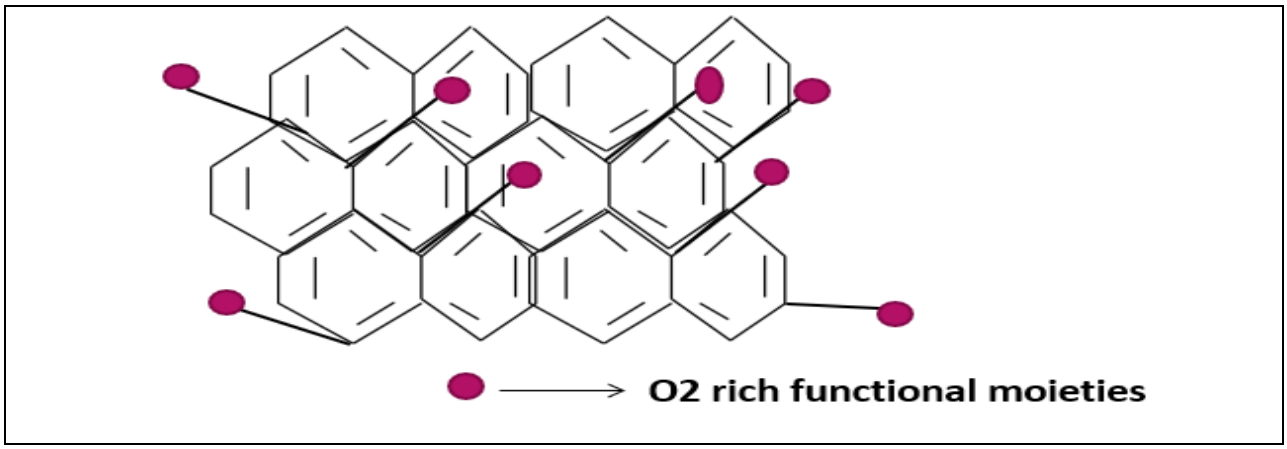

Fig 3.2 : Schematic structure of Graphene oxide as reported in literature

3.3 METHODOLOGY OF PREPARATION OF GOaN and rGOaN NANOMATERIALS

3.3.1 CHEMICALS REQUIRED FOR PREPARATION – All chemicals used are of analytical grade and used without further purifying the chemicals. The glassware used were from Borosil® and were thoroughly washed to remove any unwanted interferences. All the solutions were prepared in double distilled water to not alter the chemical constituents of the prepared solutions. The chemicals required for this section of experimental study have been tabulated as below :

Table 3.1 : Chemicals used for fabrication of graphene based nanomaterials

CHEMICAL NAME (CHEMICAL FORMULA; PURITY; CHEMICAL COMPANY NAME)
Graphite powder (Gr; Purity 99%; Loba Chemicals)
Potassium permanganate (KMnO4; Purity 98%; Merck)
Sulfuric acid (H2SO4; Purity 98%; Merck)
Hydrogen peroxide (H2O2; Purity 30%; Merck)
Hydrazine hydrate (N2H4; Purity 99%; Merck)
Double distilled water (H2O; Purity 99%; Milli Q - Millipore)

3.3.2 PREPARATION OF GRAPHENE OXIDE ANALOGOUS NANOADSORBENT (GOaN)

The experimental study was designed based on modified Hummer's method but with introductions of several modifications. The first modification is to avoid the usage of NaNO3 as oxidizing agent. The major

drawback in Hummer's method is the evolution of toxic NOx gases which is a byproduct of the reaction due to the presence of $NaNO_3$ as precursor reactant. So, to avoid emission of toxic fumes and making it more environmentally adaptable we bypassed the usage of $NaNO_3$. Next modification was done regarding the ratio of Graphite:$KMnO_4$ (Potassium permanganate) as in our study the ratio between the two was selected to be 1:4 whereas in conventional Hummer's method the ratio was 1:3. Another modification was introduced regarding the condition in which the first phase of reaction occurs. Addition of $KMnO_4$ to the suspension of graphite powder and concentrated H_2SO_4 (Sulphuric acid) occurs in chiller ice box which does not allow the temperature to go beyond 10°C. Another point to be mentioned is the precooling of graphite powder before the initiation of the reaction and 99% pure graphite powder of 60 mesh is taken as precursor reactant. The detailed steps for preparation of GOaN nanomaterial –

- First phase – Graphite powder was weighed carefully by weighing balance (Sartorius) and kept in a cool area. The preweighted amount (5gm) of pre cooled graphite powder is taken in an Erlenmeyer flask to which concentrated H_2SO_4 (100ml) is added slowly while continuously stirring. The whole setup is kept in a chiller ice box to retain the temperature with 10°C.
- The slurry was then stirred for 1hr under chilled conditions before addition of $KMnO_4$ (20gm) which is done with extreme care as it is highly exothermic reaction.
- After addition of $KMnO_4$ under ice – cold conditions the mixture is again kept for shaking for 2hrs. this allows the reaction to take place slowly and gradually preventing any unwanted mishaps. The mixture turns dark green in appearance as mentioned by other researchers (Vinodhkumar et al., 2018)
- After the stipulated time of (varied from 0 -120 mins) , double distilled water (150ml) was added and stirred for 30mins at 30°C. The mixture now tuned to dark brown in color as suggested in this step by other researchers (Vinodhkumar et al., 2018)
- Finally, 350ml of water is added at room temperature and 50ml of Hydrogen peroxide was added and left overnight.
- The slurry obtained is washed till pH is neutralized and the obtained powder is air dried and stored in a cool dry dark place.

The obtained final products are then characterized by various analytical procedures and compared to the literature present for preparation of graphene oxide nanomaterial.

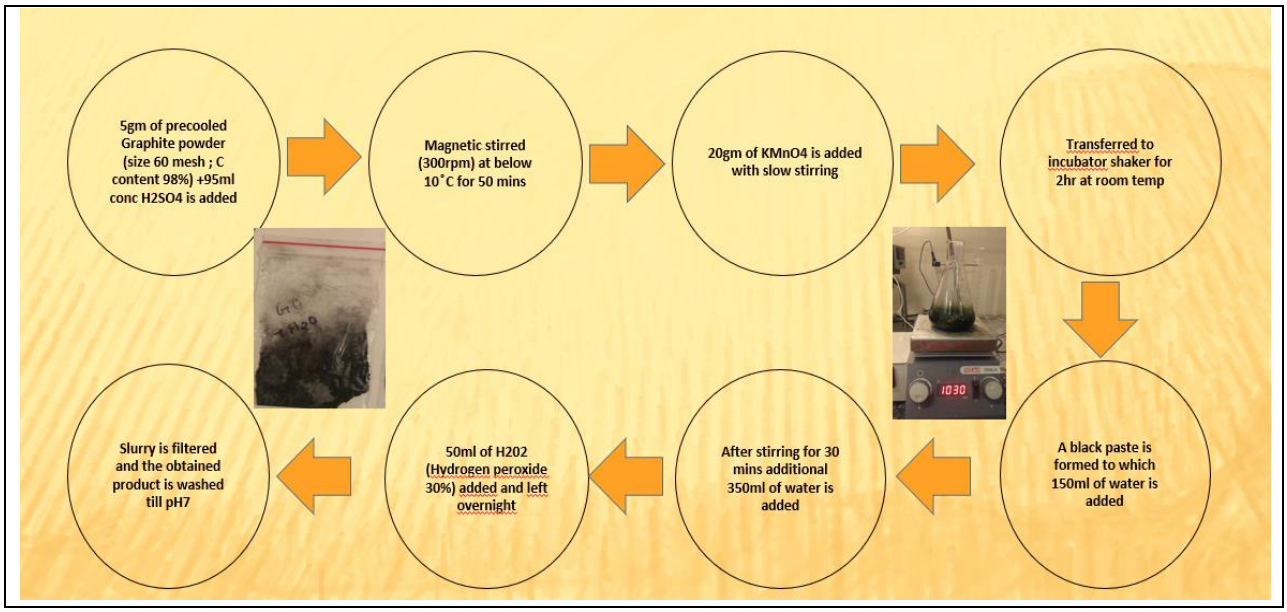

Fig 3.3 : Flow chart showing fabrication steps of GOaN nanomaterial (with pictorial inset)

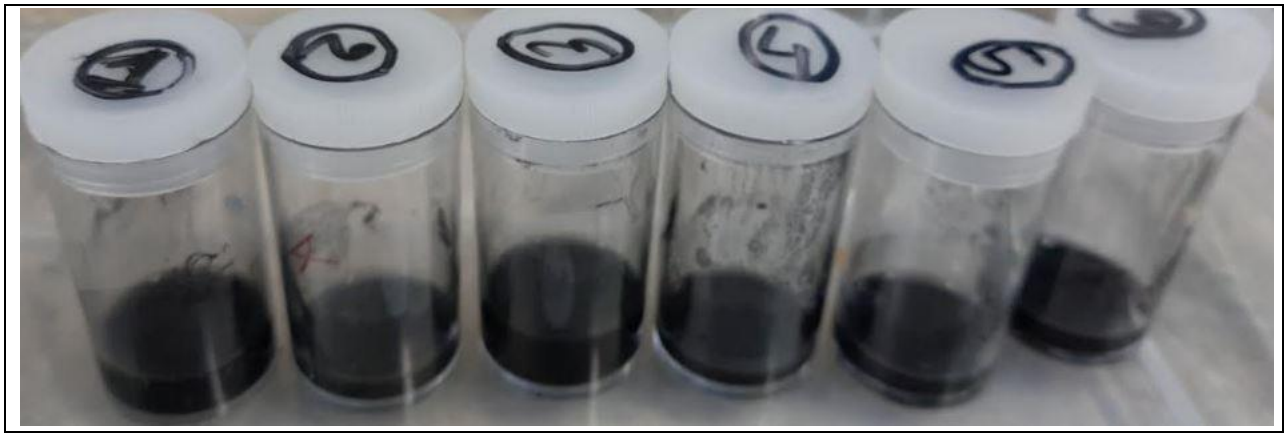

Fig 3.4 : Photographic representation of various GOaN formed by varying retention times

3.3.3 PREPARATION OF REDUCED GRAPHENE OXIDE ANALOGOUS (rGOaN) NANOADSORBENT

Graphene oxide acts as the parent compound from which reduced forms of graphene family nanomaterials namely Reduced GO (RGO) to pristine graphene may be formed. Graphene differs in properties from its precursor graphene oxide in terms of dispersibility in aqueous media. Chemical reduction along with thermal or ultrasonication exfoliation treatment helps in preparation of reduced

forms with increased conductivity. (Deemer et al., 2017). The properties differ in case of reduced form of graphene oxide from the precursor material. As the oxygen rich functional groups were reduced by the chemical reductive processes the hydrophilicity of the material also gets diminished and thus reduced GOaN forms a layer on top of the aqueous layer. The stages for formation of reduced form of the precursor material formed in the earlier step is depicted below in the chart form.

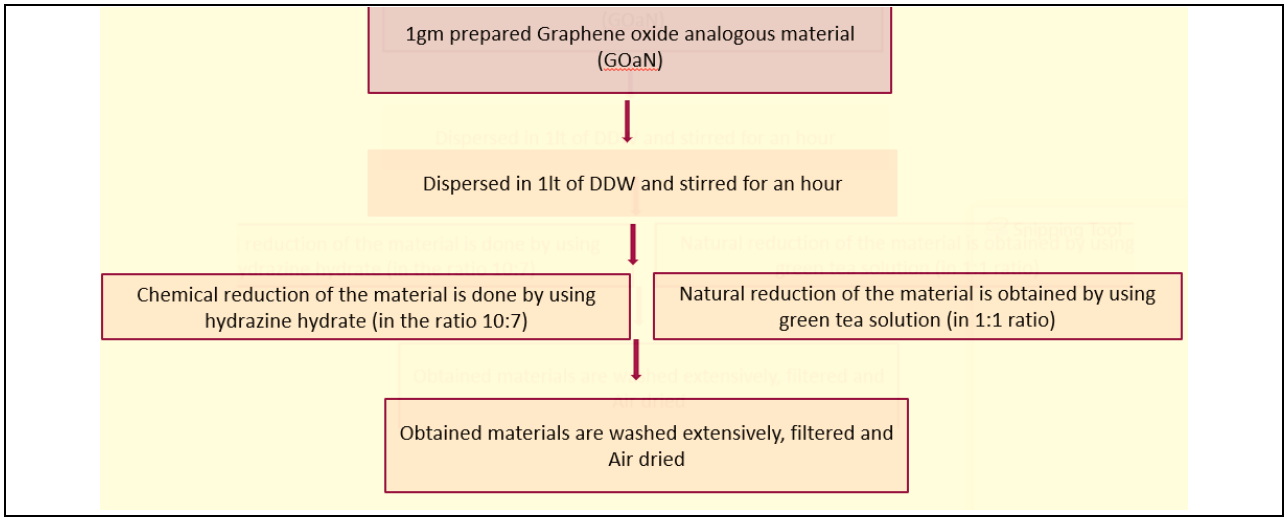

Fig 3.5 : Flow chart showing fabrication steps of rGOaN (reduced GOaN) nanomaterial

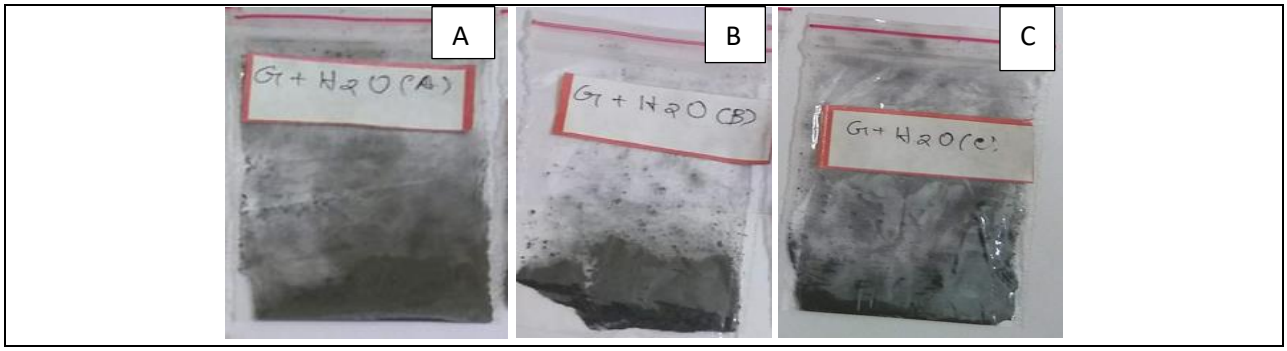

Fig 3.6 : Photographic representation of rGOaN prepared (From L-R - (A) Autoclave reduced GOaN (B) Hydrazine hydrate reduced GOaN (C) Green tea solution reduced GOaN. The maximum yield % was obtained in case of (B) and thus it was further characterized and analyzed.

3.4 CHARACTERIZATION STUDY OF THE PREPARED NANOMATERIAL

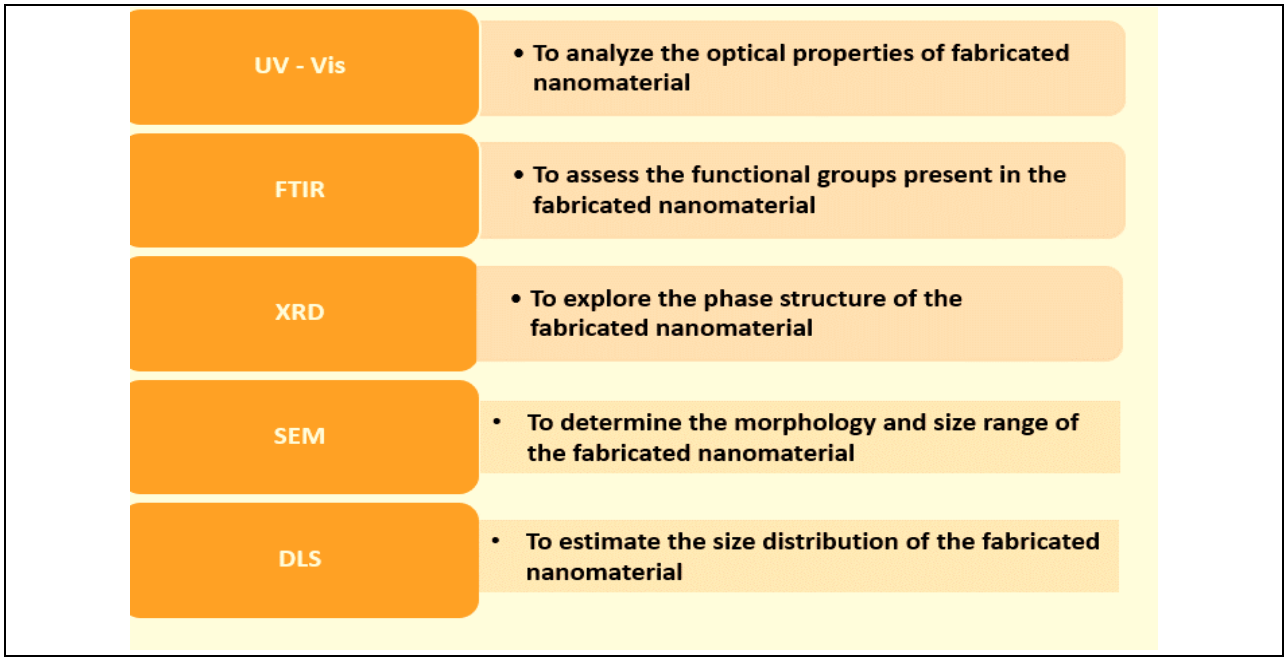

Fig 3.7 : List of various physicochemical techniques for characterization of fabricated nanomaterial

3.4.1 FOURIER TRANSFORM INFRARED SPECTROSCOPIC TECHNIQUE

Fourier Transform – IR spectroscopy is a popular tool for easier, faster, cost effective and reliable analysis of the samples (Chirman & Pleshko, 2021). The sample analysis was done and the spectra was obtained by FTIR spectrophotometer [Perkin Elmer]. FTIR spectra provides a structural fingerprint of the material although the main drawback lies in the fact that the chemicals analyzed into broader classification. Potassium bromide KBr is used as mulling agent in the ratio 1:10. For analysis of structural pattern as well as functional groups intercalation, FTIR proves to be a facile mode of analysis. Samples were cast into pellets with potassium bromide (KBr; FTIR analytical grade; Merck) and scanned in the range of 500–4000cm−1 with a resolution of 4cm–1. The ATR (Attenuated Total Reflectance) mode doesn't require sample preparation and can be utilized directly.

3.4.2 UV – ViS (UV – Visible) SPECTROSCOPIC TECHNIQUE

In case of UV – Visible spectroscopy it's a fast, facile mode of characterizing a prepared material due to its easiness and wide availability. The theory uses Beer – Lambert's law which correlates absorbance with

mass concentration in well dispersed suspension. The spectroscopic analyses were performed using the Perkin Elmer spectrophotometer. All the analyses were carried out in 1ml quartz cuvette. Small amount of sample diluted in double distilled water were used for the analysis. Baseline was measured every time and it was subtracted to obtain the result. The acquired spectra are in the range of 200 – 700nm, with resolution of 1nm, scanning speed of 10nm/sec and optical path length of 1cm. 200 – 500nm is considered to be the UV range and beyond that the visible range starts with automatic change of lamp at 585nm.

3.4.3 RAMAN SPECTROSCOPIC TECHNIQUE

Raman spectroscopy is an efficient, rapid and non-destructive type of characterization method. This spectroscopic technique is used to determine the molecular vibrational mode. The characteristic feature of Raman spectra of Graphene based materials include D band, G band and 2D or G' band. The integrated intensity ratio between D band and G band (ID/IG), the G band's position, and its corresponding full width at half maximum (FWHM) are all recognized as indicators for the structural disorder of carbon materials (Llosa Tanco & Pacheco Tanaka, 2016). The fabricated sample was analyzed in the range of 500 – 4000 cm -1. The Raman analyses utilized the following parameters: Raman spectroscope (Horiba) sample analysis method = mapping review, z = −500, excitation wavelength (nm) = 532 nm, power % = 10%, time (s) = 1 s, scanning wavelength (nm) = 500–4000 nm.

3.4.4 FLUORESCENCE SPECTROSCOPIC TECHNIQUE

In the fluorescence spectrophotometer (the excitation wavelength could be varied from 200-700 nm by using a 450 W xenon lamp with an excitation monochromator and emission could be collected from 300-800 nm by an emission monochromator. The fluorescence spectrophotometer (Agilent) was utilized to compare the fabricated GOaN nanomaterial with commercially available and purchased GO nanomaterial powder.

3.4.5 SCANNING ELECTRON MICROSCOPIC TECHNIQUE

Scanning electron microscope (Zeiss) as the name suggests scans the surface of the materials and gives us the information about the topographical analysis of the material. Focused beams of electrons are used as

source of illumination to produce signals which are then processed to form the images. ImageJ software helps in processing the SEM images to give us lateral dimensions and size of the graphene oxide flakes. For Sem analysis the diluted samples are drop casted on to glass slides and air dried. Then the samples were coated by gold coater (Quorum, 150 R ES) to make them conducive for the analysis. Under high vacuum the electrons are emitted in narrow beams having larger depth of field which leads to more detailed three-dimensional micrograph of the samples. The sensitivity of FESEM (Field Emission Scanning Electron Microscope) is much higher than normal SEM and thus the samples can be magnified 100 times more than it could be in normal SEM. The samples are destroyed and no micrographs are obtained if the laser is too close to the sample in normal SEM. The samples are coated with conducting elements to create a homogenous surface for image analyzing.

3.4.6 EDAX (ENERGY DISPERSIVE X-RAY)TECHNIQUE

The analysis was carried out EDAX spectroscopy (Bruker) which is generally attached with SEM analysis. EDAX is requisite to get an idea about the chemical configuration of the substance and quantify the elements present in the material.

3.4.7 POWDER X-RAY DIFFRACTION (pXRD) TECHNIQUE

To analyze the structural integrity, phase formation and to check the crystalline or amorphous state of the substance pXRD provides an indispensable tool. The interaction between X-ray and the sample is recorded and thus pXRD proves to be nondestructive technique for fast identification of sample. The X Ray Diffractogram (pXRD) data obtained by diffractometer (Shimadzu) having monochromatic Cu Kα, radiation (λ=1.5409 A°). Data were collected from 10° to 80° at a scan rate of 0.05° per 10.26 seconds.

3.4.8 THERMOGRAVIMETRIC TECHNIQUE

To understand the change of a sample mass according to the temperature, thermogravimetric analysis is done. Thus, to determine the percentage of oxygen containing functional group the method of TGA is applied. In TGA analysis the sample is heated in a sequence of steps over a period of time to give

corroborating data on the change in the mass of the sample. The thermogram was recorded and analysis was done by using Perkin Elmer TGA under nitrogen flow conditions.

3.4.9 ZETA SIZER AND ZETA POTENTIAL TECHNIQUE

To ascertain the size of the particles fabricated and to get information about the homogeneity in formation of the material molded and the overall composition is homogenous or not, Zetasizer is an efficient tool. it uses the principle of Dynamic light scattering implying Brownian motion code to get the estimate about the dimensions of the materials fabricated along with the homogeneity or heterogeneity is calculated by PDI (Poly Dispersity Index). The instrument used is Zetasizer (Malvern)

Zeta potential gives an assumption of the surface charge of a particle. it is an important parameter to understand the stability of the particles to form colloidal dispersive media. This charge is developed at the interfacial layer between the surface of a solid adsorbent and the aqueous surface of the adsorbate solution.

3.5 DATA FINDINGS AND DISCUSSIONS

3.5.1 FTIR SPECTRAL ANALYSIS

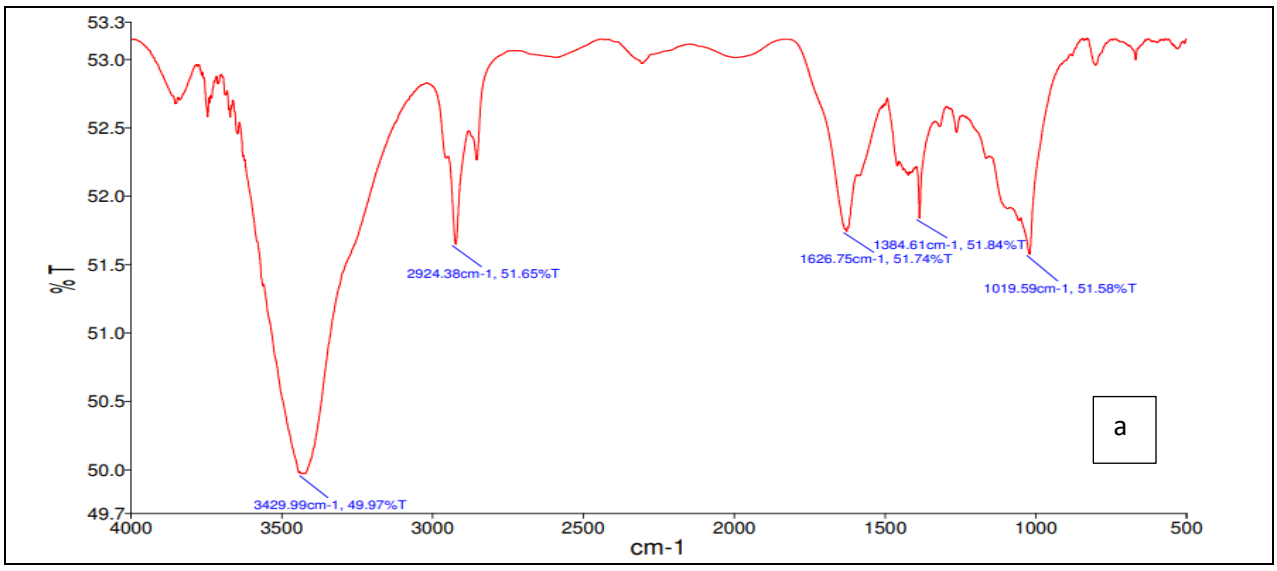

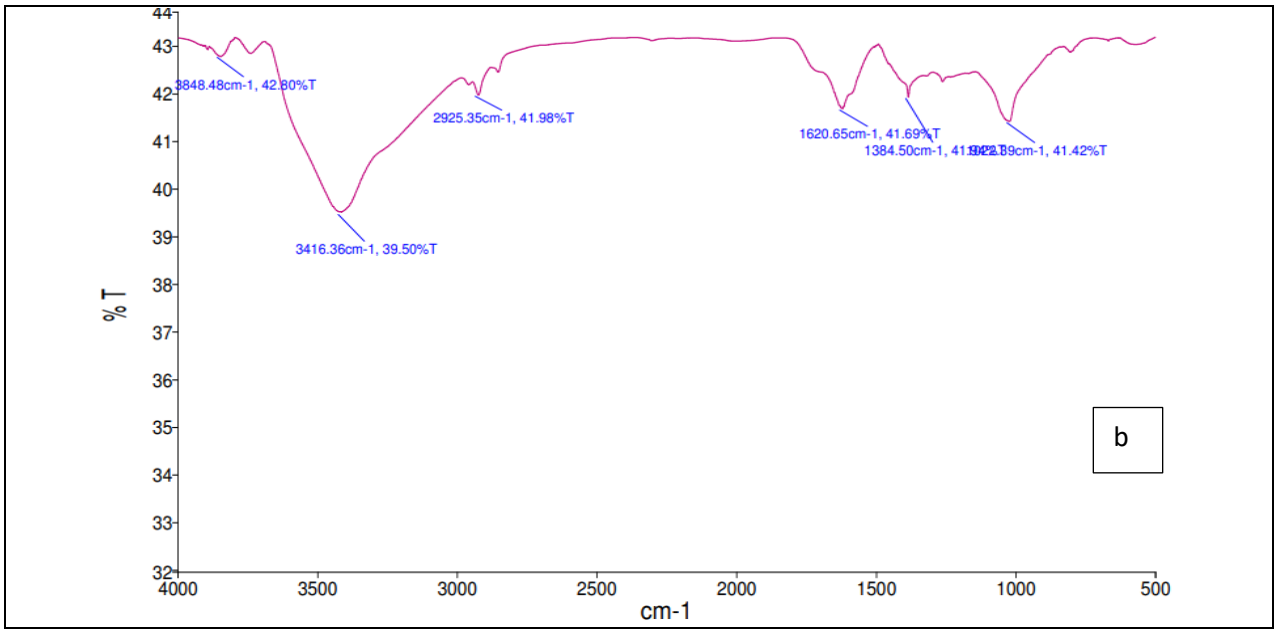

Fig 3.8 : FTIR spectra of prepared nanomaterial a) rGOaN reduced Graphene oxide analogous nanomaterial

b) GOaN Graphene oxide analogous nanomaterial

%T = Transmittance percentage

cm-1 = Wavelength unit

The broad peak observed in the wavenumber range of 2800–3550cm−1 can be accredited to the stretching mode of the O-H groups as compared to the narrow and sharp peak of reduced graphene oxide. The O-H groups in GOaN are attached to the parent carbon web at various sites (may range from the center of the carbon skeleton of the sheet to its borders). The corresponding shifts in the frequency of vibration of the O-H bonds lead to a resultant expansion and shortening of the band. Presence of residual water molecules intercalated between the GO sheets also contributes to the broadening of the O-H band.(Ranjan et al., 2018).1635cm−1 can be ascribed to the stretching vibration of C=O bonds in carboxyl/carbonyl groups. The band at 1626 cm−1 can be attributed to the vibration of O-H groups in water molecules adsorbed on GO sheets. Similarly, the bands at 1324 cm−1 and 1015 cm−1 can be attributed to the stretching vibrations of the C–OH group and the C–O (epoxy) group respectively. No

substantial peak at ≈1570 cm−1 (corresponding to the stretching vibrations within graphitic domains) directs to a high-quality synthesized GO sample with less impurities.

3.5.2 UV – ViS SPECTRAL ANALYSIS

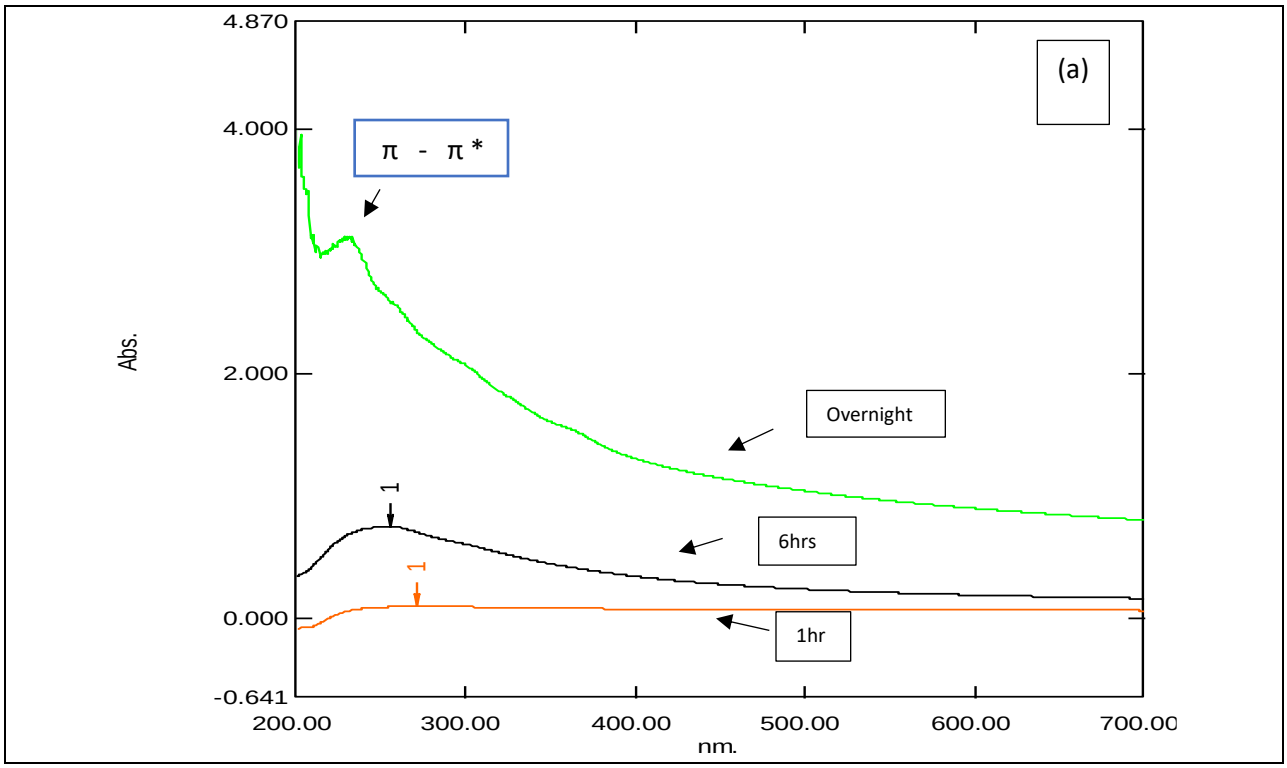

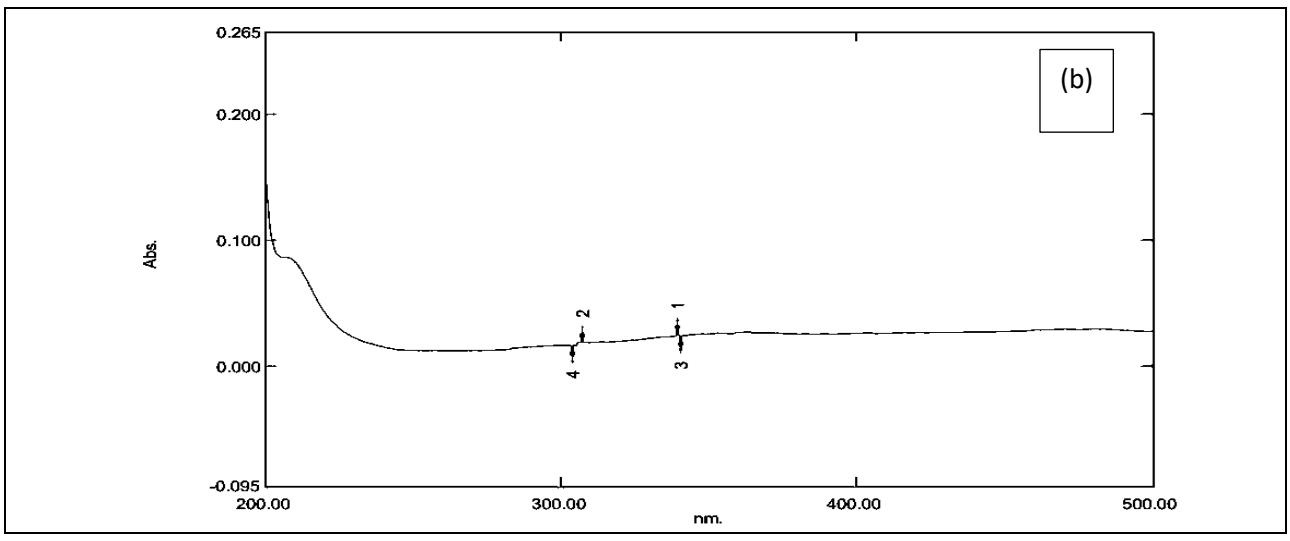

Fig 3.9 : UV spectral analysis of (a) fabricated GOaN of various saturation time and (b) fabricated rGOaN (chemical reduction by N2H4)

Peak shift is noticed from 260nm to 235nm with increase in reaction time

Abs = Absorbance

nm = wavelength (λ) unit

A prominent peak at 231 -233 nm comes from the pi-pi* (π-π*) transition of C-C and C=C bonds in sp2 hybrid regions and a subordinate shoulder broad peak at 285 - 303 nm is due to pi-pi* (π-π*) transition of the C=O bond in sp3 hybrid regions (Ranjan et al., 2018). In the above spectra peak is observed near 233nm but diffused peaks are noticed due to variation in oxidation degree. The peak is prominent with higher intensity after overnight retention time. It was observed in many papers that GO shows absorption at shorter wavelength of 230nm due to change in π–π* transitions of aromatic C–C bonds due to oxidation whereas graphitic structure gives peak at 265nm. There is no peak at 265nm which concludes that oxidation has occurred and GOaN has been produced. In case of reduced form of Graphene oxide analogous nanomaterial intensity of the peaks are lowered and smaller peaks around 290nm – 330nm is detected by the UV probe software. The less intense peaks may be attributed to removal of oxygen – containing functional groups by hydrazine hydrate reducing agent. The spectrum obtained for reduced form is coherent with other reported literature (Emiru & Ayele, 2017). For spectral analysis it is noted that the sample concentration should be less than 0.5 mg/ml otherwise interferences may occur(Hu et al., 2017). The sample dilution also should not be less than 0.005mg/ml as resultant absorbance will be too small for detection and false data may be produced.

3.5.3 RAMAN SPECTRAL ANALYSIS

In the spectra we could observe prominent and sharp peaks at D, 2D and G region for the reduced form of GOaN fabricated nanomaterial. Disorderness or defects within the graphite layers are marked by D peak (1320 – 1350 cm -1) whereas the G peak (1580 – 1605 cm -1) or G’ peak (2640 – 2680 cm -1) denotes hexagonal lattice structure and stretching or modifications in sp2 hybridized C=C bonds. Sometimes another short peak may be observed around (1625 cm -1) which is denoted by D’ band and is caused by structural defects or double resonance, but it was not observed in this case. (Hu et al., 2017). The

structural defect modifications due to intercalation of oxygen rich functional groups is thus denoted by D bands (Ranjan et al., 2018).In reduced form sharp peaks of D and G bands is seen whereas in oxidized form shorter and broader peaks were observed with background noise due to fluorescence. The peaks in the oxidized forms gets diffused and thus shorter broader peaks were observed in GOaN nanomaterial. It is seen in literature that oxygen rich sites create defects in the graphitic structure which is directly proportional to the fluorescence. Thus sharp peaks could be observed in reduced form of GO as it is void of many oxygen rich sites. (Shang et al., 2012). Broadening of the D band in GOaN is thus attributed to oxygenation of rGOaN and reduction of sp^2 domains due to creation of defects, vacancies, and distortions during oxidation. The I_D/I_G ratio was found to increase after oxygenation to 1.35 from 1.12. This confirms that oxygen containing functional groups were fixed to the graphitic planes.

The ratio of the relative intensities of both D and G bands corresponds to the degree of disorder in the microstructures of oxidized or reduced graphene oxide samples. Higher ID/IG ratios indicate that more sp3 hybridized carbon domains are present i.e., higher defects are formed in microstructurally while lower ratios indicate structure dominated by sp2 hybridized carbon. ID/IG ratio also increases when reduction takes place thereby producing improved signal to noise ratio.(S. Yang et al., 2020).

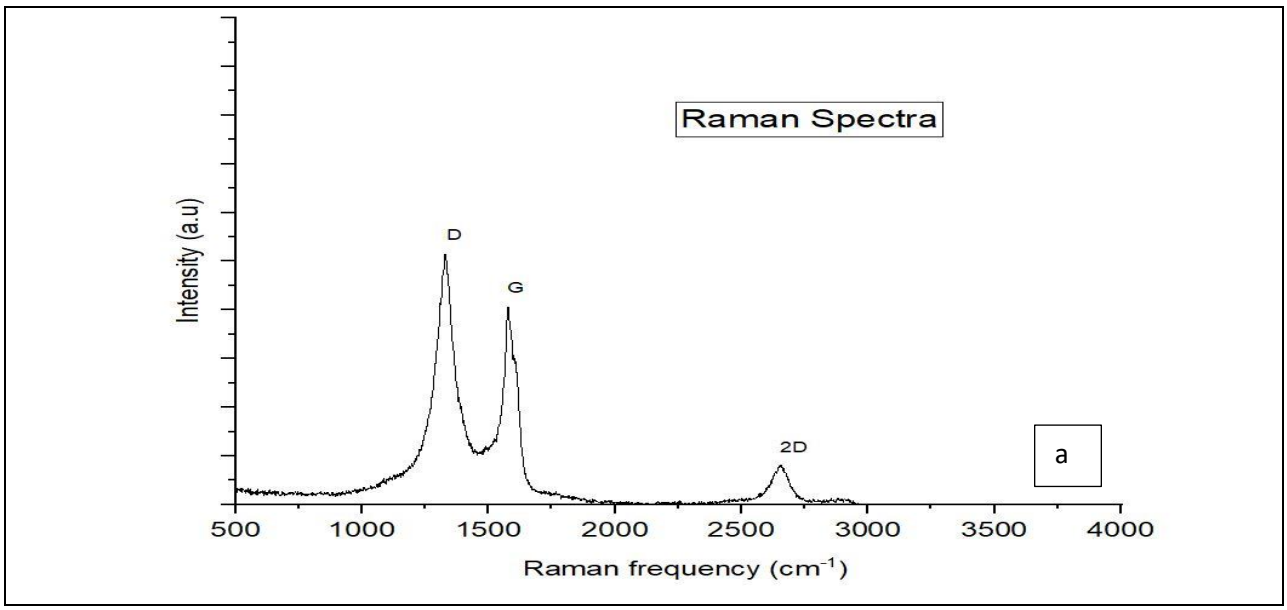

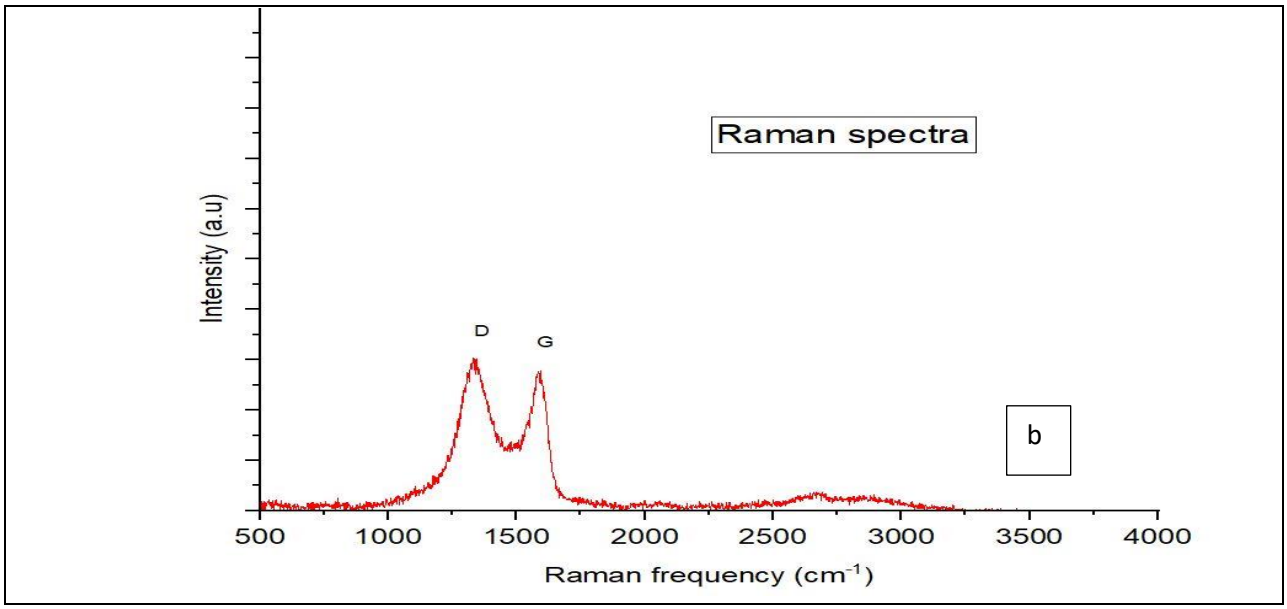

Fig 3.10 : Raman spectral analysis of prepared nanomaterial a) Raman spectra of rGOaN with prominent 2D peak b) Raman spectra of GOaN devoid of 2D peak

3.5.4 FLUORESCENCE SPECTRAL ANALYSIS

GO fluorescence is due to electron-hole recombination from conduction band (CB) bottom and nearby localized electronic states to wide-range valance band (VB). In view of atomic structure, the GO emission is predominantly from the electron transitions among/between the non-oxidized carbon region (-C = C-) and the boundary of oxidized carbon atom region (C-O, C = O and O = C-OH).(Shang et al., 2012) All three kinds of functionalized groups C-O, C=O and O= C-OH are involved in the fluorescence of GO.(Marcano et al., 2010). The laboratory fabricated GOaN was compared with respect to commercially purchased GO nano powder and it was observed that the fluorescence intensity was lesser but the spectra was similar to the commercially purchased GO powder. The measured fluorescence intensity indirectly occurs due to contributions from COOH and C- OH groups indicating presence of oxygen – rich functional groups in the material. Hence confirming the laboratory fabricated GOaN nano material was analogous to commercially purchased GO.

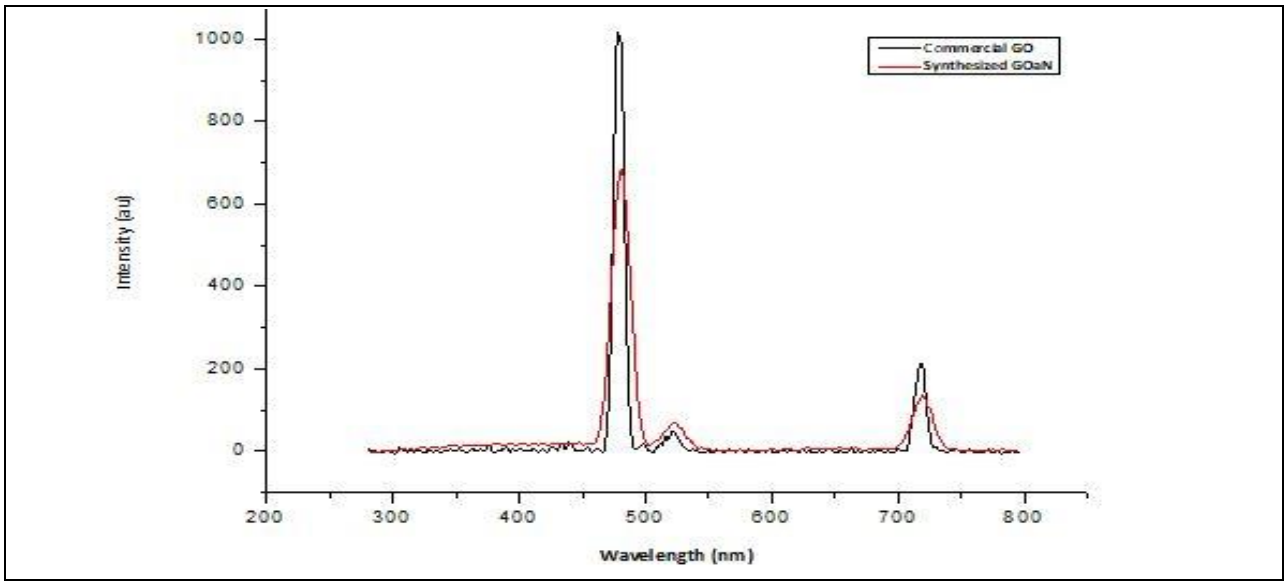

Fig 3.11 : Fluorescence spectra of fabricated GOaN (1mg/dl) and commercially purchased GO nanopowder (1mg/dl) [excitation wavelength 495nm]

3.5.5 SEM IMAGING ANALYSIS

In the images available we can observe oxidation of graphite powder has created layers in the otherwise solid structure of graphite. This exfoliated nature confirms oxidation has taken place and graphene oxide (GOaN) has been formed. The lamellae which are formed are not sharp knifed like structure but various canals and lacunae have developed which increases the surface area and adsorption sites for pollutants. The interconnected layers could be noticed from the SEM images which gives rise to three-dimensional network, thereby acting as a better adsorbent at the nanoscale level. At the preliminary investigation by SEM micrographs, it can be concluded that the nanomaterial may be conducive to bacterial attachment and proliferation. The “pillars” and “caves” that are formed are ideal places for bacterial attachment although smooth surfaces may cause a hindrance for attachment as reported in many literature (Y. Cheng et al., 2019; Zheng et al., 2021). In case of reduced form of graphene oxide analogous nanomaterial, the edges are observed to be sharper and more pronounced wrinkle effect is seen (Nguyen et al., 2019).

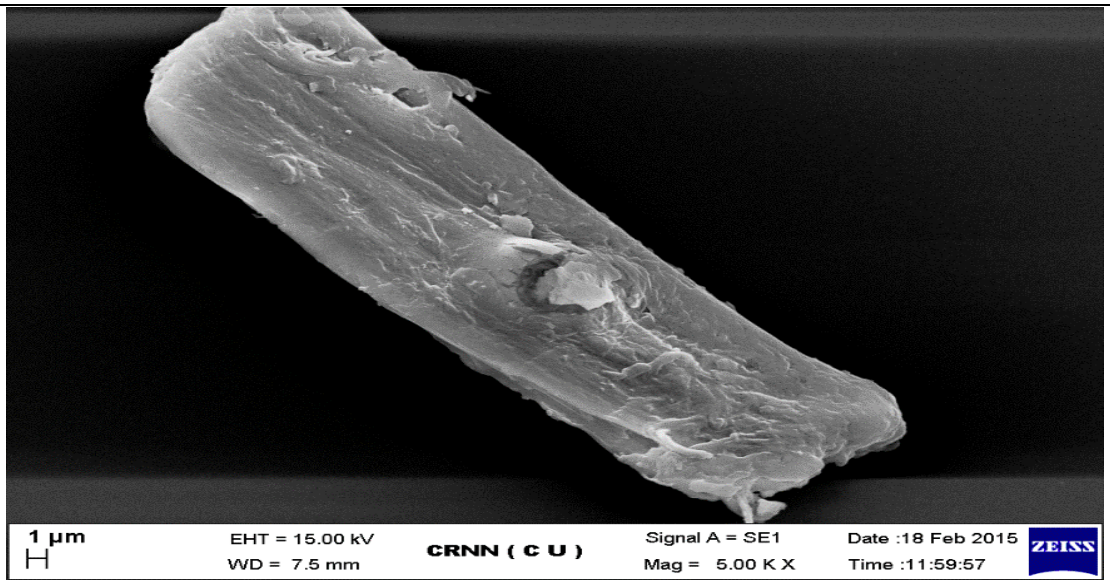

Fig 3.12 : SEM Microimage of graphite flake (in powder form)

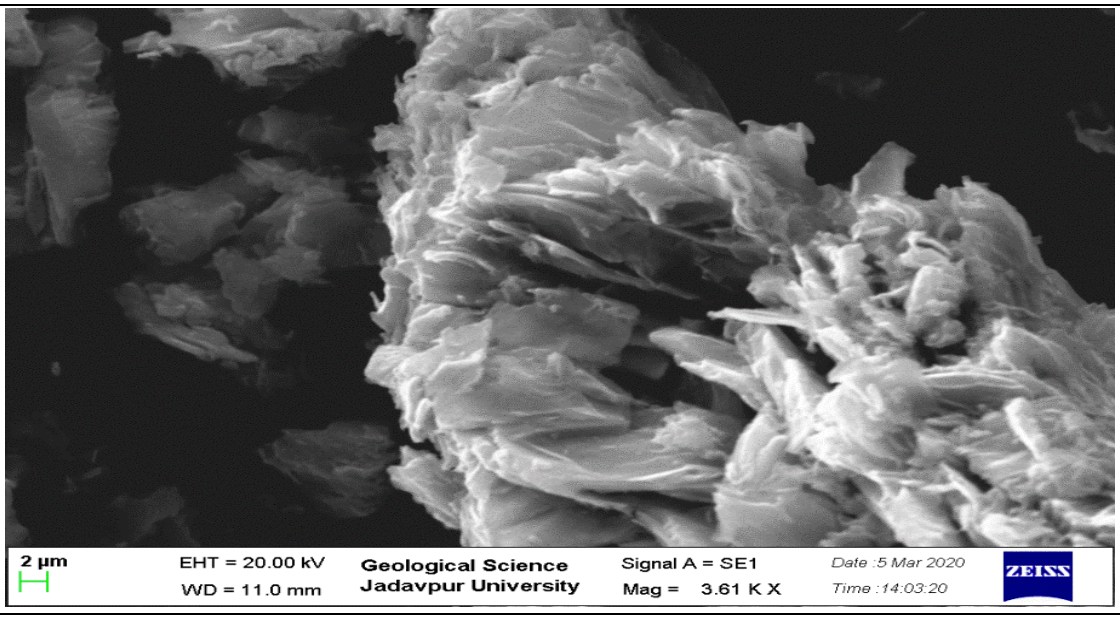

Fig 3.13 : SEM Microimage of fabricated GOaN nanomaterial

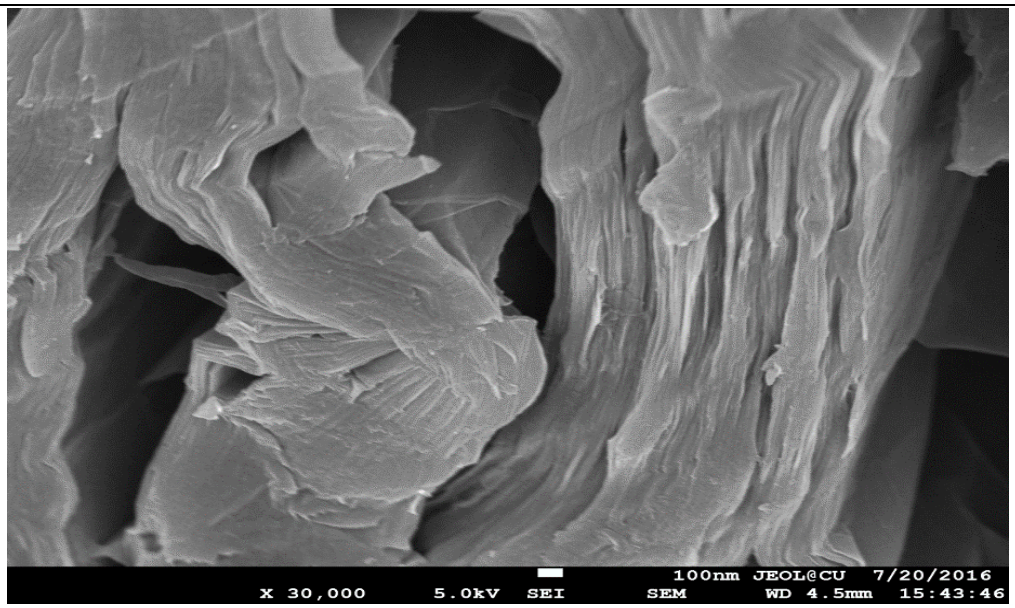

Fig 3.14 : FESEM Microimage of fabricated GOaN nanomaterial

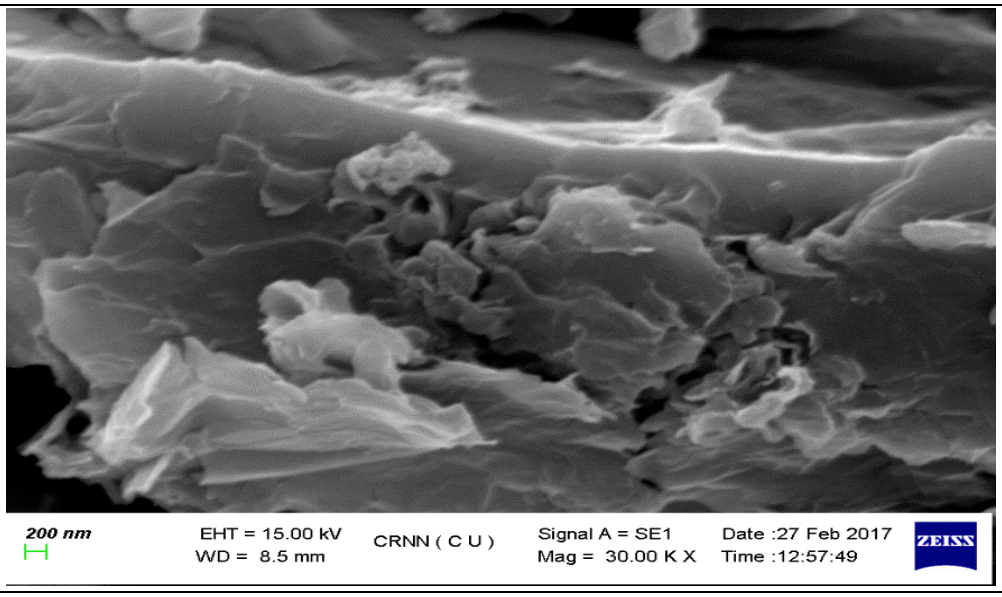

Fig 3.15 : SEM Microimage of fabricated rGOaN nanomaterial

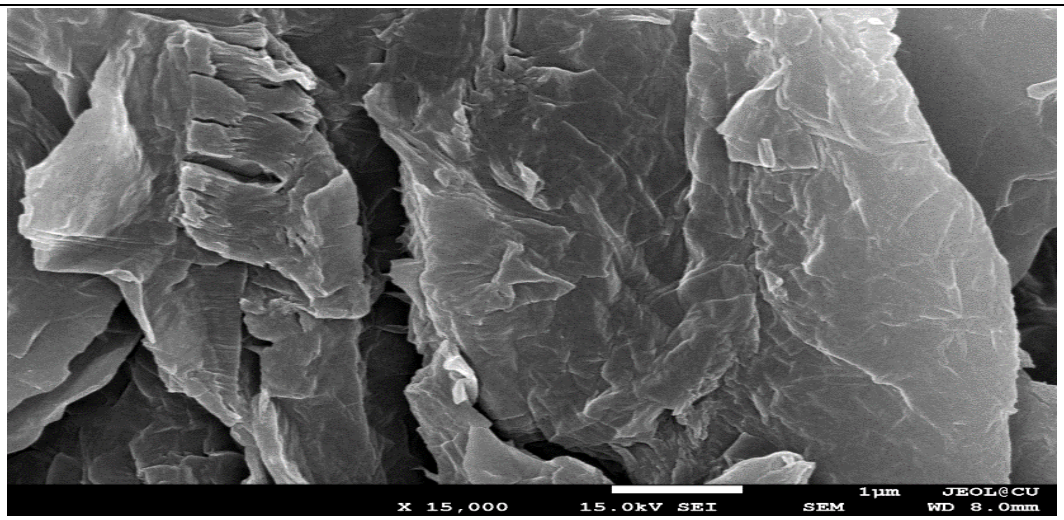

Fig 3.16 : FESEM Microimage of fabricated rGOaN nanomaterial

3.5.6 EDAX ELEMENTAL ANALYSIS

The elemental composition shows the presence of Oxygen in GOaN nanomaterial concluding oxidation of the substance has occurred. A negligible amount of presence of Sulphur may be due to the concentrated acid used and remained even after extensive water wash. But as it in nullable amount so it does not affect the bulk properties of fabricated GOaN nanomaterial. Presence of sulphur in the Edx analysis of graphene oxide have been reported by other researchers also (Narayan et al., 2018). In the other image it can be seen that the oxygen level is significantly diminished proving that reduction of GOaN has occurred and its reduced form rGOaN is formed. The percentage of carbon is higher in both the cases whereas trace amount of nitrogen has been detected by the analytical instrument.

Table 3.2 : EDX report of GOaN nanomaterial

Element	Weight %	Atomic %
Carbon (C)	69.38	75.37
Oxygen (O)	30.62	24.63
Total	100.00	100.00

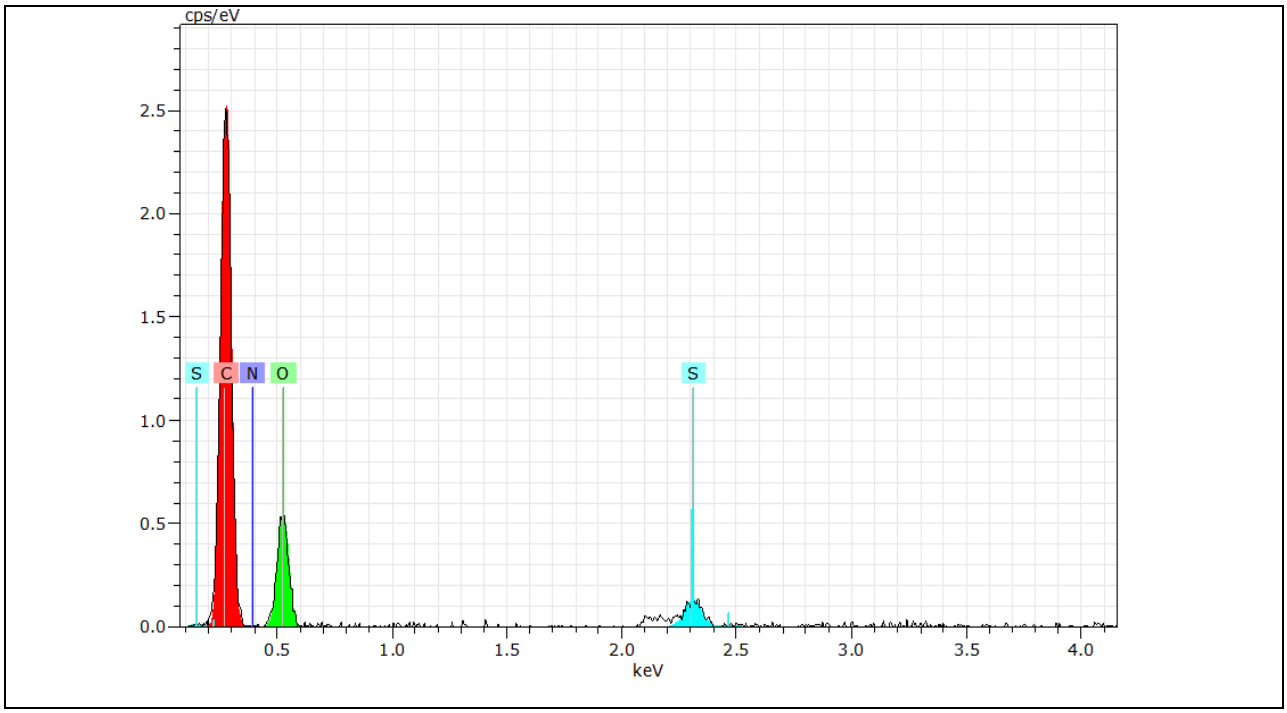

Fig 3.17 : EDX analysis of fabricated GOaN nanomaterial

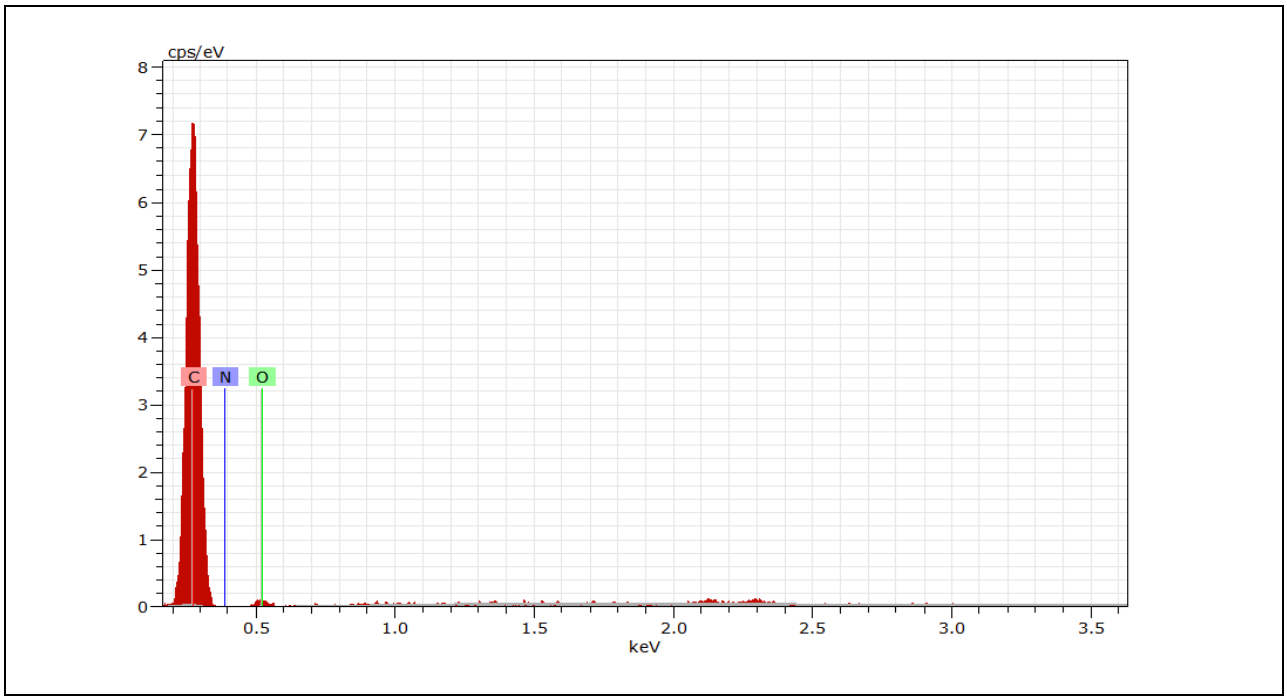

Fig 3.18 : EDX analysis of fabricated rGOaN nanomaterial

Table 3.3 : EDX report of rGOaN nanomaterial

Element	Weight %	Atomic %
Carbon (C)	89.18	75
Oxygen (O)	10.82	25
Total	100.00	100.00

3.5.7 X -RAY DIFFRACTION ANALYSIS

Broader peaks are observed in the diffractogram which indicates less of regular pattern structure with the peak formed at around 2θ = 12.5° which is observed by other researchers as well. (Ranjan et al., 2018). Due to interlayer spacing occurring by the incorporation of oxygen rich functional groups like hydroxyl, epoxy, carbonyl on carbon skeleton along with intercalation of water molecules during oxidation many diffuse peaks are observed. In case of graphite a sharp peak at 2θ = 24° indicates regular patterned carbon structure.

No peaks corresponding to Mn were observed indicating no leftover residue of Mn is present in the sample corresponding to good quality sample produced.

Interlayer spacing gives estimation about the intercalation of oxygen rich moieties (Ranjan et al., 2018)

The characteristic of GO XRD spectra is in the fact that peak corresponding to 26.5° is diminished proving formation of oxidized form of graphene.

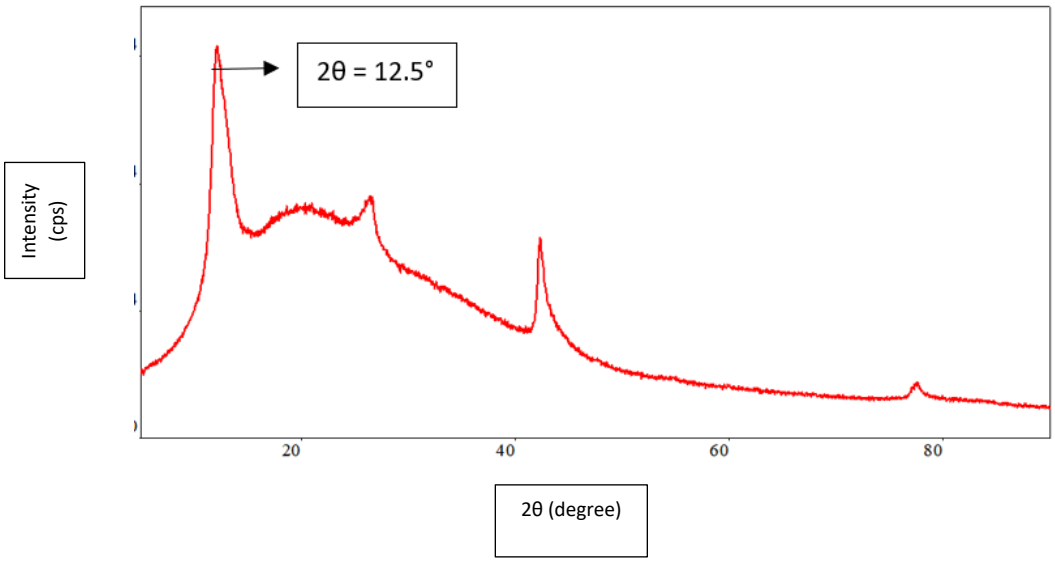

Fig 3.19 : XRD diffractogram analysis of fabricated GOaN nanomaterial

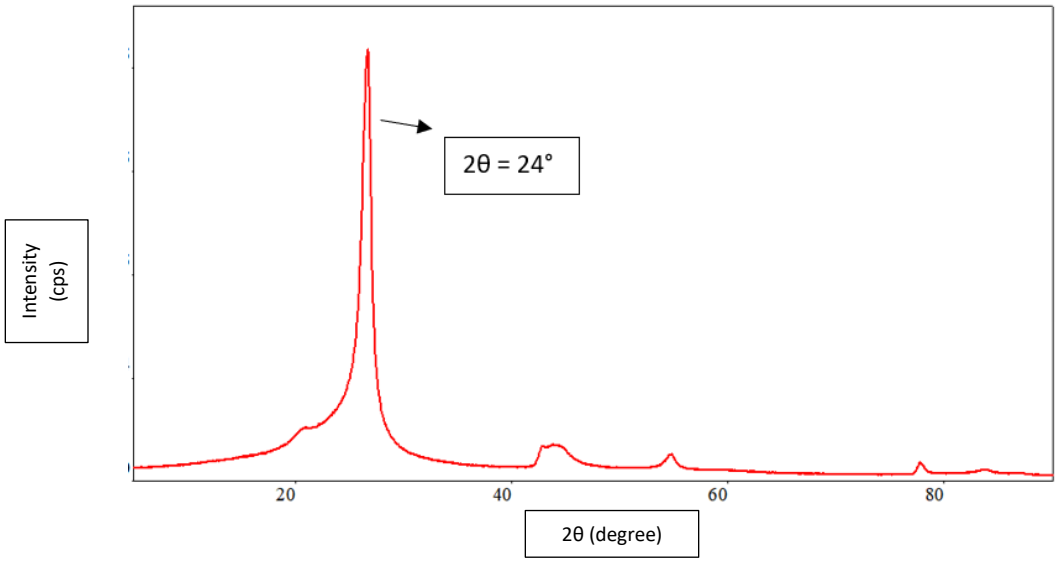

Fig 3.20 : XRD diffractogram analysis of fabricated rGOaN nanomaterial

3.5.8 TGA ANALYSIS

As carbon structure is resistant to heat changes so the graph of graphite (Gr) or rGOaN (reduced graphene oxide) doesn't show much change in the mass till 500 °C (Not shown here). But as Graphene oxide (GOaN) primarily consists of oxygenated functional moieties, they are degraded at an early stage. About 15% mass loss occurred at the temperature of less than 100˚C primarily due to the loss of H2O (water) molecules in GOaN. In the second stage, roughly 45% mass loss takes place occurring at a temperature of ~200˚C due to the thermal decomposition of unstable oxygen-containing functional groups. This is due to the pyrolysis of oxygen-containing functional groups such as hydroxyl, carbonyl and carboxylic acid to yield CO, CO2, and H2O. Therefore, thermolabile GO is expected to be effectively reduced into highly-conductive reduced GO (rGO) at around this temperature. Finally, a mass loss of about 40% occurred at 620˚C mainly due to the combustion of the carbon skeleton. Generally, it is estimated that at around 500˚C the combustion of GO is considered to be completed (Narayan et al., 2018).

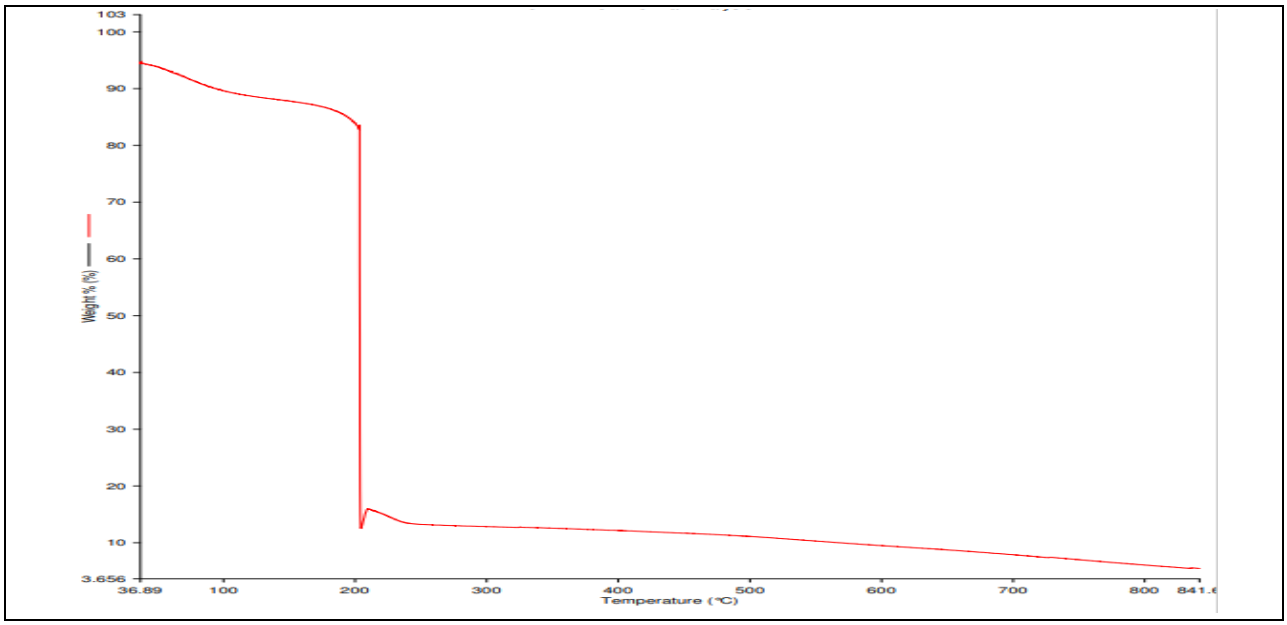

Fig 3.21 : TGA analysis of fabricated GOaN nanomaterial

X axis = Temperature (°C)

Y axis = Weight (%)

3.5.9 ZETASIZER AND ZETA POTENTIAL ANALYSIS

Zeta potential of GO is measured on the overall net charge on its surface at the neutral range. GO is an 2D amphiphilic material which consists of negatively charged hydrophobic graphite containing core and hydrophilic oxygen containing functional groups (Wang et al., 2016). It is known that GO dispersions are charged negatively in aqueous solution as because the flanking edge of the GO sheets consists of carboxylic groups predominantly ($-COO^-$). The electrostatic repulsive forces act greater than Van der Waals and thus it forms stable suspension with agglomerating, coagulating or flocculating. According to ASTM standard, zeta potential <30 mV (maybe + or -)shows high stability due to electrostatic repulsion and 30 – 40 mV has moderate stabilization (Krishnamoorthy et al., 2013)

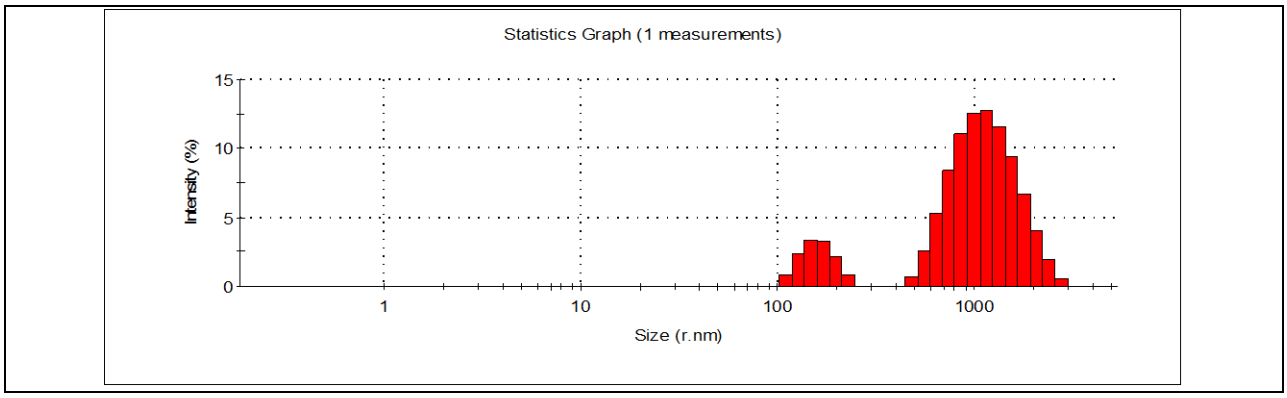

Fig 3.22 : Zetasizer analysis of fabricated GOaN nanomaterial

Table 3.4 : PDI Index calculation by Zetasizer of GOaN nanomaterial at 25°C

Temp (°C)	Z -Avg (r.mn)	Scattering angle°	PDI
25	584.4	90	0.383

Generally, samples having index partaking PDI < 0.1 monodisperse, 0.1 < PDI < 0.2 narrow particle size distribution, 0.2 < PDI < 0.5 wide particle size distribution (Lohrke et al., 2008). The nano sample fabricated in the laboratory shows PDI at 0.4 which establishes the wider particle size distribution.

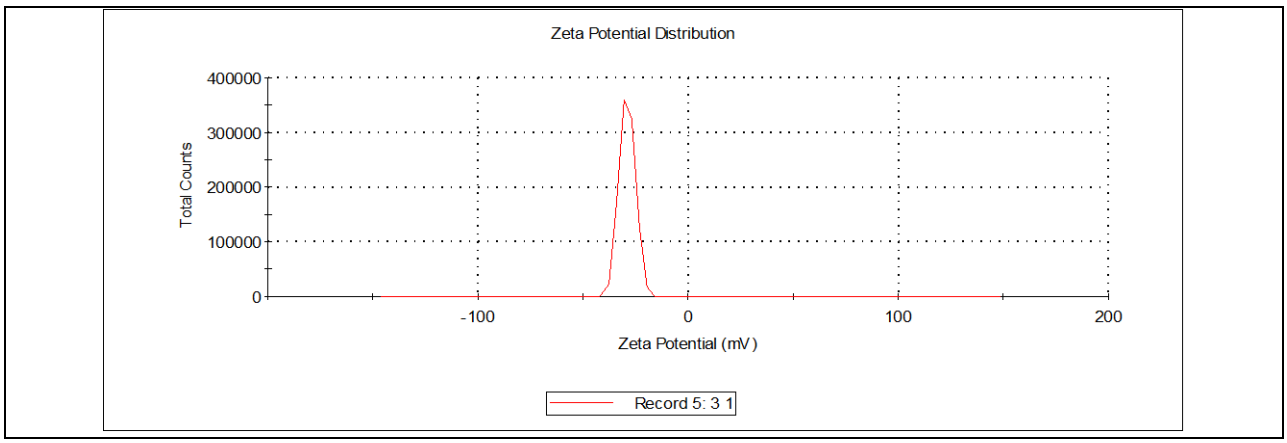

Fig 3.23 : Zetapotential analysis of fabricated GOaN nanomaterial at neutral pH

Table 3.5 : Zetapotential value and conductivity at 25°C of fabricated GOaN nanomaterial at neutral pH

Temp (°C)	ZP (mV)	Conductivity mS/cm
25	584.4	90

3.6 COST CALCULATION OF PREPARED GOaN NANOMATERIAL

Cost calculation of any prepared adsorbent involves the calculation of unit price of chemicals required and equipment used during the fabrication phase. In this chapter the nano adsorbents fabricated in the bench top method and its cost analysis is done in comparison to outsourced prepared Graphene Oxide nano powder and Reduced Graphene Oxide nano powder. The cost of the laboratory fabricated nanomaterial is mentioned in the following table :

Table 3.6 : Cost calculation of the primary chemicals required during fabrication process of GOaN

CHEMICALS UTILIZED FOR FABRICATION	TOTAL AMOUNT	UNIT COST (RS)	TOTAL COST (RS)
Graphite powder	5gm	0.6	3
Potassium permanganate	20gm	0.4	8
Sulphuric acid	100ml	0.5	50
Hydrogen peroxide	50ml	0.55	27.5
Double distill water	500ml	0.006	3
			Total = 91.5

In this experiment the instrumental cost is lowered by utilizing the process of air drying instead of using hot air oven which requires energy. The only instrument used is the magnetic stirrer for approximately 2hours. The wattage of magnetic stirrer (Remi) is about 50 watts which culminates to 0.15 kWh (kilowatt – hours). The electricity bill (CESC bill) in the local area provides us for the unit price for 1kWh as Rs 4.69. Thus, the total cost for unit gram of laboratory fabricated graphene oxide material is Rs 92.9 or 1.19 USD. Total cost of a substance includes equipment usage cost incurred during the fabrication period and cost of chemicals required for the process of fabrication. 100gms of commercially purchased graphene oxide nano powder costs Rs 9995.00 (inclusive of taxes) or 127.79 USD or approximately the cost is 1.28 USD per gram of graphene oxide nanomaterial. But in case of preparation of reduced form of graphene oxide the cost is escalated in our case as more chemicals are added and instrument usage also adds up to the cost.

Thereby it can be concluded that the fabrication process is cost effective in case of GOaN nanomaterial than the purchased nano powder yielding similar characteristic features of the material. Thus, the laboratory fabricated material is termed as Graphene oxide analogous nanomaterial and is the base material for all the experiments henceforth.

3.7 CONCLUDING REMARKS

Laboratory fabrication of graphene family nanomaterial has been investigated by tweaking the Hummer's protocol for synthesis of graphitic oxides. The characterization data was obtained and in various cases were corroborated with commercially purchased graphene powder (Platonik). The data shows that the laboratory fabricated nanomaterial was at par with the market available expensive graphene oxide in terms of characterization analysis. Cost calculation for an adsorbent preparation is important as feasibility and sustainability of the process depends on cost effectiveness and easiness of the fabrication method. In this chapter the fabrication process was simplified using lesser amount of chemicals and utilizing normal air-drying process for drying of the adsorbents.

CHAPTER 4

4. UTILIZATION OF FABRICATED GRAPHENE – BASED NANOADSORBENT MATERIAL TO ELIMINATE PAH(s) AND PHENOL IN SYNTHESIZED AQUEOUS MATRIX.

4.1 CONTEXTUAL INFORMATION

To redress the problem of any persistent pollutants, adsorption is one of the popular preferred choices among others due to its simplicity, feasibility, ecofriendly promising measures. Adsorption, absorption and ionic bonds are inclusive of the process of sorption (Lamichhane et al., 2016b). In adsorption the mass transfer process occurs at interfacial areas only. If the interaction process is guided by physical reversible bonding it is named as physisorption and chemisorption as the name suggests involves chemical bonding between the adsorbent and the adsorbate at the molecular level. But in many cases, it is noticed that both physisorption and chemisorption occurs simultaneously. As adsorption is advantageous in terms of simplicity, ease of usage, low capital investment, thus it is regarded as a promising tool for degradation of toxic pollutants (Alcántara et al., 2009).

GO (Graphene oxide) has been a promising contender in the field of adsorption and thus it is widely used for abatement of organic pollutants like dyes (Ramesha et al., 2011), phenolic compounds, PCBs (polychlorinated biphenyls), PAHs (polyaromatic hydrocarbons) and so on and so forth. Carbonaceous compounds are used extensively in the field of adsorption due to its easiness, low-cost solutions and wide variety of benefits. As mentioned in the previous chapter utilization of graphene-based materials have been the area of interest for many researchers due to easy tunability, unique properties at nanoscale levels, high surface area to volume ratio. Graphene structure mainly composed of sp2 hybridized planar - monolayer whereas the oxidized form graphene oxide consists of sp3 layered structure (Abu-Nada et al., 2021) . The oxygen containing moieties of graphene oxide when ionized in water offers positive (hydroxy and epoxy groups) and negative sites (carboxylic groups) for attachment of anions and cations respectively. Thus, a wide range of pollutant species can be adsorbed by graphene oxide nanomaterial. The surface edges consists mainly of carboxylic (-COOH) and hydroxylic (-C-OH) groups which forms chelation with other radical species through hydrogen bond (Abu-Nada et al., 2021).

4.2 EXPERIMENTAL SETUP

4.2.1 CHEMICALS REQUIRED

All chemicals used are of analytical grade and used without further purifying the chemicals. The list of chemicals for preparation of adsorbent is provided in the Table No. 3.1. The glassware used were from Borosil® and were thoroughly washed to remove any unwanted interferences. All the solutions were prepared in double distilled water to not alter the chemical constituents of the prepared solutions. Solution pH is maintained according to the requirement of the experimental need. In case of pH modification was needed (in case of pH experimental setup), it is done by using 0.1N HCl (LOBA chemie) or 0.1N NaOH (Merck) solutions. The solution pH was determined by a pH meter (Eutech Instruments). The other chemicals for preparation of adsorbate required are tabulated below :

Table 4.1 : Chemicals required for adsorbate preparation

Chemical	Formula	Purity	Make
Naphthalene	C10H8	98%	Sigma Aldrich
Pyrene	C16H10	98%	Sigma Aldrich
Phenol	C6H6O	98%	Merck
Acetone	C3H6O	98%	Merck
Hydrochloric acid	HCl	98%	Merck
Sodium hydroxide	NaOH	98%	Merck

4.2.2 PREPARATION OF GRAPHENE OXIDE ANALOGOUS NANOADSORBENT (GOaN)

Adsorbent preparation has been discoursed in details in the previous chapter (chapter 3) along with characterization of the prepared adsorbent according to standardized protocols. Briefly, Graphene oxide (GO), the precursor material of GFMs (graphene family-based materials) is prepared by modifying the

modified Hummer's method. The sample obtained is termed as GOaN and is utilized for other experiments planned and perceived henceforth for this doctoral study.

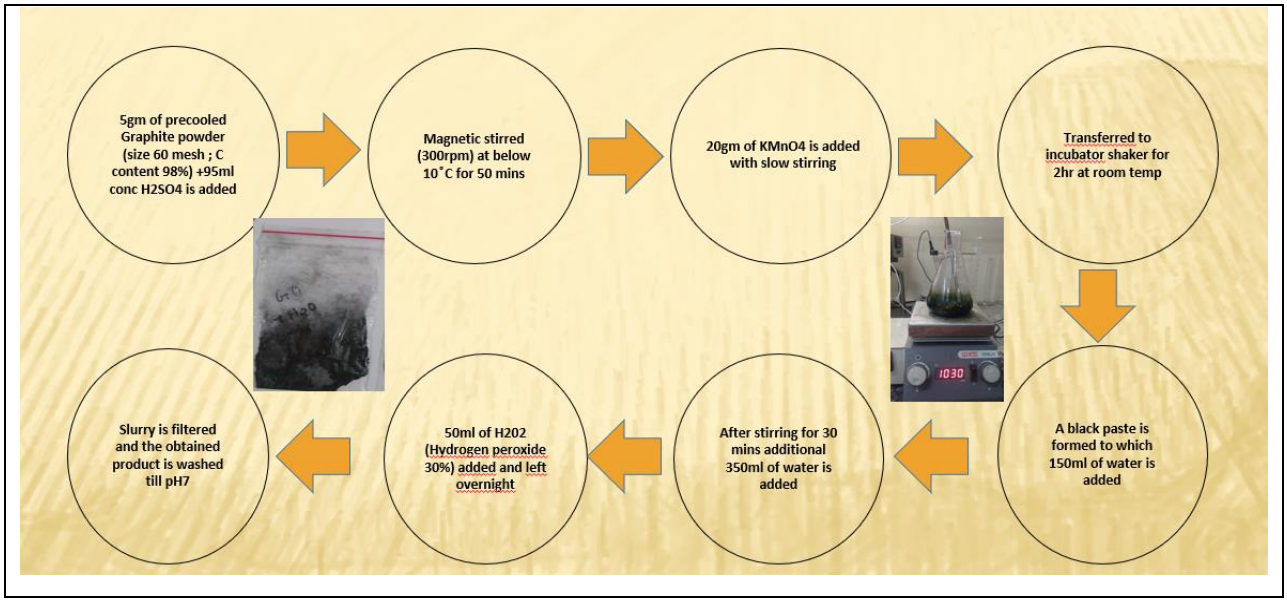

Fig 4.1 : Flow chart showing fabrication steps of GOaN nanomaterial with pictorial inset

4.2.3 PREPARATION OF ADSORBATE SOLUTIONS

4.2.3.1 PAH(s) SOLUTIONS - Synthetic waste water mirroring pollutant media were prepared in distilled water as the adsorbate solution. For PAH(s) compound the preparation of the stock aqueous media is a bit different as they are fairy insoluble in water. The dissolution of PAH compounds was obtained by dissolving the required amount of NP (Naphthalene) and Pr (Pyrene) in 5ml acetone and vortexing (REMI CM101 plus) it to form homogenous solution. The concentrated solution of PAH is then added to distill water to prepare volume up to 1000ml thereby obtaining 100mg/L concentration. The total volume of the liquid was then stirred at heated (<60°C) magnetic stirrer (REMI) to remove excess acetone. Required aliquots were homogeneously mixed with distilled water to obtain various concentrations of naphthalene, pyrene solution (s) for further experimental studies. Solution pH is maintained according to the requirement of the experimental need. In case of pH change was needed, it is done by using 0.1N HCl or 0.1N NaOH. The solution pH was determined by a pH meter (Eutech Instruments)

4.2.3.2 PHENOL SOLUTION - Synthetic waste water mirroring phenol media was prepared in distilled water directly as phenol is fairly soluble in water. 1000ml of 100mg/L concentration of phenol solution is prepared and mixed thoroughly by magnetic stirrer to prepare a homogenous solution. Various aliquots of predicted concentrations are prepared by diluting the stock solution with distilled water. Solution pH is maintained according to the requirement of the experimental need. In case of pH change was needed, it is done by using 0.1N HCl or 0.1N NaOH. The solution pH was determined by a pH meter (Eutech Instruments)

4.2.4 BATCH SCALE STUDY USING OFAT APPROACH

Comparative analysis of batch adsorption capacity to remove various pollutants such as PAH(s) [Naphthalene, Pyrene] and Phenol was performed by using laboratory fabricated GOaN. Experimental set up included the following steps-

In 100ml Erlenmeyer flasks 50ml sample volume is taken and preweighted adsorbent was added and the mixture was agitated in a rotary shaker incubator at 140rpm.The batch adsorption experiments were performed at multiple combinations of parameters including adsorbent dosage (g/L), initial pollutant concentration (mg/L), pH, shaking speed of the incubator (rpm) and ambient temperature (K) of the adsorption system with respect to time until it reached equilibrium. Residual concentration of the above-mentioned toxicants was analyzed by UV Spectrophotometer (Shimadzu) at respective wavelength (λmax) of each respectively (Naphthalene λmax 219nm; Pyrene λmax 293nm Phenol λmax 264nm). The λmax values were obtained by scanning the prepared adsorbate solutions within the wavelength range of 200 – 800 nm by the UV-Vis spectrophotometer. As the solutions are colorless the 200 – 500nm wavelenghth range can be useful for analysis as wavelength beyond 550nm is suitable for coloured solutions. Solution pH is maintained according to the requirement of the experimental need. In case of pH change was needed, it is done by using 0.1N HNO3 or 0.1N NaOH. The solution pH was determined by a pH meter (Eutech Instruments).

In this experiment one factor at a time (OFAT) method is followed to study the effect of variable factors of the experimental parameters on the removal efficiency of prepared nanomaterials (GOaN). To study the residual concentration of toxicant, the solution is sampled at a given time and assessed spectrophotometrically by UV -ViS Spectrophotometer. All experiments were repeated minimum thrice times to minimize the human experimental error. The average errors were all within range ± 5% of the

mean value. The values obtained were converted using EndMemo converter. The various experimental parameters considered for the batch scale studies is tabulated as below:

Table 4.2 : Defined and Variable parameters of the experimental set

EXPERIMENTAL SET	SET PARAMETERS	VARIABLE PARAMETER
1	Initial Pollutant Concentration (10mg/L) Solution pH 6.5 Temperature 30°C RPM 120	Dosage of adsorbent (0.05g/L, 0.075 g/L, 0.1g/L, 0.2g/L)
2	Adsorbent dose 0.1g/L Solution pH 6.5 Temperature 30°C RPM 120	Initial Pollutant Concentration (10mg/L, 20mg/L, 50mg/L, 100mg/L)
3	Initial Pollutant Concentration (10mg/L) Adsorbent dose 0.1g/L Temperature 30°C RPM 120	Solution pH 2, 4, 6, 8, 10
4	Initial Pollutant Concentration (10mg/L) Adsorbent dose 0.1g/L Solution pH 6.5 RPM 120	Temperature (25 °C, 30 °C, 35 °C, 40 °C)
5	Initial Pollutant Concentration (10mg/L) Adsorbent dose 0.1g/L Solution pH 6.5 Temperature 30°C	RPM (80, 100, 120)

4.2.5 RSM – OPTIMIZATION TOOL OF PROCESS PARAMETERS

Response Surface Methodology (RSM) is a prevailing technique for quantifying the impacts of each factor on one another and their interactions through effective process optimization (Rahman et al., 2022). Statistical designing of the experiments is essential and judiciously reasonable for evaluating important information with minimum number of experiments performed. Thus, these modelling techniques helps in reducing cost by saving time as well as material cost by performing lesser number of experiments to achieve the end goal. It is a tool which established the relation between mathematical and statistical model. RSM combines experimental strategies, mathematical methodologies, and statistical inferences to provide an efficient empirical investigation of the system of interest. This approach depicts the combined effect of all process parameter. In actuality, scaling up studies is time consuming and also necessitates huge number of experiments to confirm the optimum level and thus the net cost of the process and time required increases. These limitations can be eradicated by optimizing the process using statistical experimental design by Response Surface Methodology (RSM). The RSM's crucial advantage is that it drastically decreases the number of experiments needed for assessment, analysis, and optimization thereby making it is a faster and more cost-effective strategy for data congregation. Design expert 7.0 software (Stat – ease, USA) was applied to optimize the best combination of parameters to obtain maximum removal efficiency. The important variable parameters like pH of the solution, adsorbent dosage, initial pollutant concentration and time required to treat the pollutant are the independent test variable. RSM chart was prepared and batch experiments were performed according to the RSM chart. Hence, obtained responses i.e., removal percentage were feed to the software to provide an idea about the resemblance between predicted and actual removal efficiency. To find out combined effects of parameters on adsorption efficiency and optimum process conditions of the iterative experiments were evaluated by applying a factorial Central composite design (CCD) of Response Surface Methodology (RSM). The response model may be expressed as an empirical form-

$$Y = f(X1, X2, X3 \ldots\ldots Xn) \pm e$$

Where Y is the response, f is a response function and Xi is the process independent variables. Response function (f) was calculated by second-degree polynomial equation and evaluating the effect of independent process variable on response function. The linear form of quadratic polynomial equation as follows-

$$Y = \beta_0 + \sum_{i=1}^{n} \beta_i X_i + \sum_{i=1}^{n} \beta_{ii} X_i^2 + \sum_{i=1}^{n-1} \sum_{i=1}^{n} \beta_{ij} X_i X_j + e$$

where Y is the response, Xi and Xj are independent process variable, β0 is the constant coefficient, βi ith linear coefficient, βii is the quadratic coefficient, βij ijth interaction coefficient, n is the number of independent process variables. Thus, RSM is essential to get maximum information with minimum experimental runs due to parallel processing of factors in the experiments and also accounts for the interactive factors between the variables at the same time.

4.2.6 REUSABILITY STUDY OF THE ADSORBENTS

The adsorbent used in the above experimental set up was subjected to adsorption/desorption cycle to analyze the reusability potential of the adsorbent. The eluent emitted from the adsorbent is assessed spectrophotometrically at respective wavelength (Naphthalene λmax 219nm; Pyrene λmax 293nm Phenol λmax 264nm) to check the amount of toxicant released from the adsorbent with time or if subjected to extreme conditions of acidic/alkaline.

4.2.7 CALCULATIONS AND THEORETICAL CONSIDERATION

4.2.7.1 REMOVAL % OF POLLUTANTS

Equilibrium adsorption of the solute using laboratory fabricated GOaN nanomaterial was carried out in a set of 100mL Erlenmeyer flasks at agitation speed of 80 - 120rpm, at varying temperature ranges (20 to 40° C), adsorbent dosage (0.05 g/L to 0.2 g/L) on dry weight of adsorbent, initial pollutant concentrations of (5 to 50mg/l), and neutral pH (except pH variation study from pH 2 to pH 10). Samples were collected at 15mins intervals until equilibrium was established. Experimental samples are centrifuged to remove optical hindrance caused by adsorbent at 10000 rpm for 15mins. The collected supernatant is then analyzed by UV–Vis Spectrophotometer at respective lambda max values. Each experiment was conducted minimum thrice times and the results are expressed as the mean value of the obtained results. The removal percentage of adsorbate concentration were calculated by following equation:

$$\boldsymbol{Removal}\ \% = \frac{\boldsymbol{Ci - Cf}}{\boldsymbol{Ci}} * \mathbf{100} \quad (1)$$

Ci is the initial adsorbate concentration (mg/l),

Cf adsorbate concentration at any time interval (mg/l).

The regression coefficient (R2) value indicates the model stability. If R2 value of a model is near to one so this model was better representing the experimental data.

4.2.7.2 EFFICACY OF ADSORBENT

The adsorption behavior of the samples can be assessed properly by evaluating the adsorption capacity from the following relations

$$\boldsymbol{Qt} = \frac{(\boldsymbol{Ci} - \boldsymbol{Cf})\boldsymbol{v}}{\boldsymbol{w}} \quad (2)$$

$$\boldsymbol{Qe} = \frac{(\boldsymbol{Ci} - \boldsymbol{Ce})\boldsymbol{v}}{\boldsymbol{w}} \quad (3)$$

where q_t (mg g-1) and q_e (mg/g) were denoted as adsorption capacity at time(t) and at equilibrium conditions respectively, V (L) signifies the volume of the experimental solution and W (g) denotes the weight of the adsorbent utilized.

4.2.7.3 ADSORPTION ISOTHERM

An adsorption isotherm represents the equilibrium relationship between the adsorbate concentration in the liquid phase and that on the adsorbent surface at a solid phase at a given condition (Foo and Hameed, 2010). In equilibrium, a certain relationship prevails between solute concentration and adsorbate surface in solid phase. Typically, isotherms which constitute an important role towards the modeling analysis.

Data obtained experimentally were analyzed using Langmuir, Freundlich and Temkin models of adsorption isotherm.

4.2.7.3.1 LANGMUIR ADSORPTION ISOTHERM MODEL

The model is based on the assumption that the adsorption of adsorbate molecules occurs only at specific sites of a homogeneous adsorbent surface consist of fixed number of active sites present into the system and saturation of these active sites ends the adsorption process. The Langmuir model thus signifies the monolayer adsorption process.

The **Langmuir isotherm model** is expressed as linearized form

$$\frac{\boldsymbol{Ce}}{\boldsymbol{qe}} = \frac{\mathbf{1}}{\boldsymbol{KLQm}} + \frac{\boldsymbol{Ce}}{\boldsymbol{Qm}} \quad \textbf{(4)}$$

KL = Adsorption constant of Langmuir isotherm (L/mg)

Qm = Maximum adsorption capacity at theoretical value (mg/g)

Ce = Equilibrium adsorbate concentration (mg/L)

qe = Sorption capacity at equilibrium (mg/g)

4.2.7.3.2 FREUNDLICH ADSORPTION ISOTHERM MODEL

The model implies that, amount of solute adsorbed in the summation of adsorption on all the active sites present in the adsorbent and bounded by the bond energy. Where stronger binding sites occupied first until the process energy was exponentially decrease upon the completion of adsorption process. The model signifies the multilayer adsorption process.

The **Freundlich isotherm model** is best expressed as linearized form:

$$\boldsymbol{logqe} = \boldsymbol{logKf} + \frac{\mathbf{1}}{\boldsymbol{nlogCe}} \quad (5)$$

Kf= Adsorption constant of Freundlich isotherm (1/g)

1/n = Heterogeneity factor

qe denotes amount of adsorbate adsorbed at equilibrium (mg/l)

Ce denotes that adsorbate concentration at equilibrium (mg/l)

4.2.7.3.3 TEMKIN ADSORPTION ISOTHERM MODEL

The effect of indirect adsorbate / adsorbent interaction occurs at the adsorption isotherms. The isotherms model assumes that the heat of adsorption process decreases with the increase of coverage of the adsorbent used. The process is considered by uniform binding energy.

Temkin isotherm model can be best explained by the equation,

$$\boldsymbol{Qe = BtLnKt + BtLnCe} \quad (6)$$

Where Kt and Bt are Temkin constant

Qe denotes amount of pollutant adsorbed at equilibrium (mg/l),

Ce equilibrium concentration of adsorbate in aqueous phase (mg/l).

4.2.7.4 ADSORPTION KINETICS

To investigate the reaction mechanism and potential rate-controlling steps which include mass transfer and adsorption rate constant kinetics is always desirable. The pseudo 1st order and 2nd order kinetic models were fitted with the obtained adsorption data. The prediction of adsorption mechanism of the system is important and crucial for evaluating the affinity of adsorbent towards the adsorbate. This is also important to determine the efficacy of the process and simultaneously find out the adsorption capacity of the adsorbent. It is significant to determine how the reaction rates depends on the adsorbate concentration and therefore effecting the adsorption capacity of adsorbent. For this purpose, Pseudo first order, Pseudo second order and intra-particle diffusion models were analyzed. Following are the representation of both the kinetic model.

4.2.7.4.1 PSEUDO FIRST ORDER

Pseudo 1st order is expressed as

$$\boldsymbol{log\,(qe - qt) = logqe - k1t\ 2.303} \quad (7)$$

Where k1 is the 1st order rate constant.

qe and qt are amount of adsorbate adsorbed at equilibrium and at time t (mg/g)

4.2.7.4.2 PSEUDO SECOND ORDER

Pseudo 2nd order can be expressed in linear form

$$t\,qt = 1 / k2\,qe^{2} + t/qe \quad (8)$$

qe and qt are the amounts of adsorbate adsorbed (mg/g) at equilibrium and at time t (min-1).

And, k2 is the 2nd order rate constant with the unit g mg-1min-1.

4.2.7.5 THERMODYNAMICS

Temperature is the most significant and important parameters which govern the adsorption process by revise the adsorption capacity of the adsorbent for a specific adsorbate. The variation of adsorption efficiency with the variation of temperature was better expressed by the adsorption thermodynamics. Therefore, an estimation of thermodynamic parameters for adsorption process is extremely necessary to better understanding the effect of temperature on adsorption. During this study the activation parameters (activation energy, enthalpy and entropy) and thermodynamics variable parameters (Gibb's free energy, standard enthalpy and entropy) were calculated for the experimental data and analyzed their nature leads to the adsorption separation process**.**

Activation energy is needed to overcome the inter-molecular force of attraction by the adsorbate ions/molecules and get react or interact with the active functional groups presents in the adsorbent molecules. The value of activation energy may give an idea about the type of adsorption process. The adsorption mainly classified in two types Physisorption and Chemisorption. Physisorption is basically reversible in nature due to small amount of activation energy (< 40 kJ/mol) is required to start the reaction. Chemisorption is irreversible process, large amount of activation energy (> 40 kJ/mol) is required to start the reaction

Activation enthalpy, entropy and free energy

To get an insight of the adsorption process, the process activation enthalpy (ΔH0 , kJ/mol), activation entropy (ΔS0 , kJ/mol) and free energy of activation (ΔG0 , kJ/mol) were evaluated for the adsorption

process. In general, the negative value of ΔG0 indicates the feasibility and spontaneous nature of the process. A positive value of ΔH0 suggest that the process is endothermic in nature. The magnitude and sign of ΔS0 indicates the amount of randomness present between solid/liquid interface of the system

All the thermodynamic parameters and the characteristics of the adsorption system were derived by the following empirical formula

$$Kc = Ca / Ce \quad (9)$$

$$\Delta G = - RT \ln Kc \quad (10)$$

$$\ln Kc = - \Delta G / RT = - \Delta H / RT + \Delta S / R \quad (11)$$

Where Kc denotes the adsorption distribution coefficient, ΔG is the Gibbs free energy difference, and ΔS denotes entropy fluctuations. Similarly, Enthalpy difference, ideal gas constant, and absolute temperature are represented by ΔH, R, and T, respectively. The amount of dye adsorbed per unit mass of adsorbent is denoted by Ca.

4.2.7.6 MASS TRANSFER EXPERIMENT

Data from the batch study was fitted to the intraparticle diffusion model proposed by Webber and Morris. This model suggests that adsorption of any material varies proportionally with √t i.e., square root of time rather than with contact time t. The empirical formula used to obtain the model parameters is

$$qt = kam\sqrt{t} + Cam\ t \quad (12)$$

kam is the rate parameter and Cam is the constant defining boundary layer.

4.3 DATA FINDINGS AND DISCUSSIONS

To delineate the optimum conditions of the process single – factor experiments were performed with OFAT approach.

4.3.1 BATCH SCALE PROCESS PARAMETERS

4.3.1.1 INFLUENCE OF AMOUNT OF ADSORBENT (DOSAGE)

The efficiency of an adsorbent is estimated by its uptake capacity performance. Uptake capacity is analyzed by the dose analysis. Dose analysis is important from economical viewpoint as it estimates the minimum amount of adsorbent required to do the job efficiently and excellently. It was seen that an increasing trendline is observed till 0.1gm/L after which there is no significant change. The increase in the adsorbent dose leads to increase in active sites present on the adsorbent. At higher dosage the efficiency remains similar or in some cases may reduce which may be hypothesized by the fact that overcrowding of the adsorbent eventually leads to congregated adsorbents, clumping together and reducing the n umber of activity sites. Thus, the adsorbent dose was standardized to be 0.1g/L.

Efficiency of adsorbent depends on the availability of active sites on its surface area. 10 ppm PAH solutions (Naphthalene, Pyrene,) and Phenol solution was utilized as the fixed concentration of adsorbate to study the effect of varying adsorbent (GOaN material) dosage parameter on the adsorption process utilizing OFAT approach. It was observed and indicated in the graph that 0.1g/L showed the maximum removal after which there was no significant change in the removal percentage. Higher concentration of adsorbent in a fixed area may lead to aggregation and thereby reduces or equals the removal efficiency. Thereby 0.1g/L was chosen to be the adsorbent amount for further experiments to judiciously lessen the wastage of adsorbent.

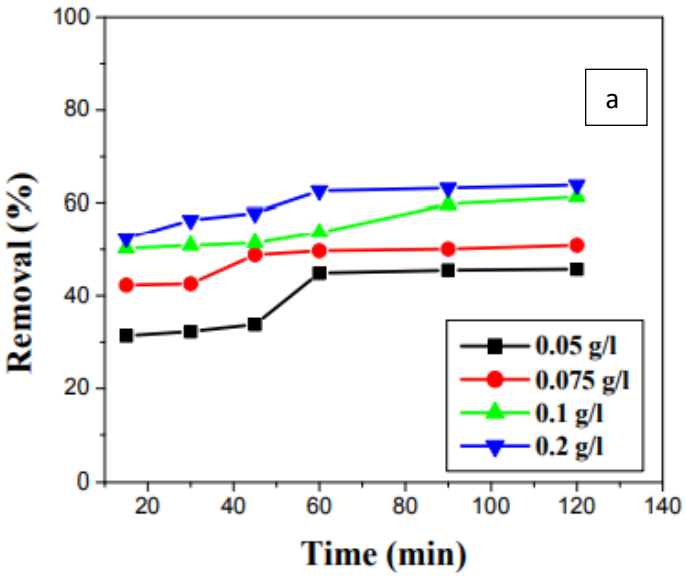

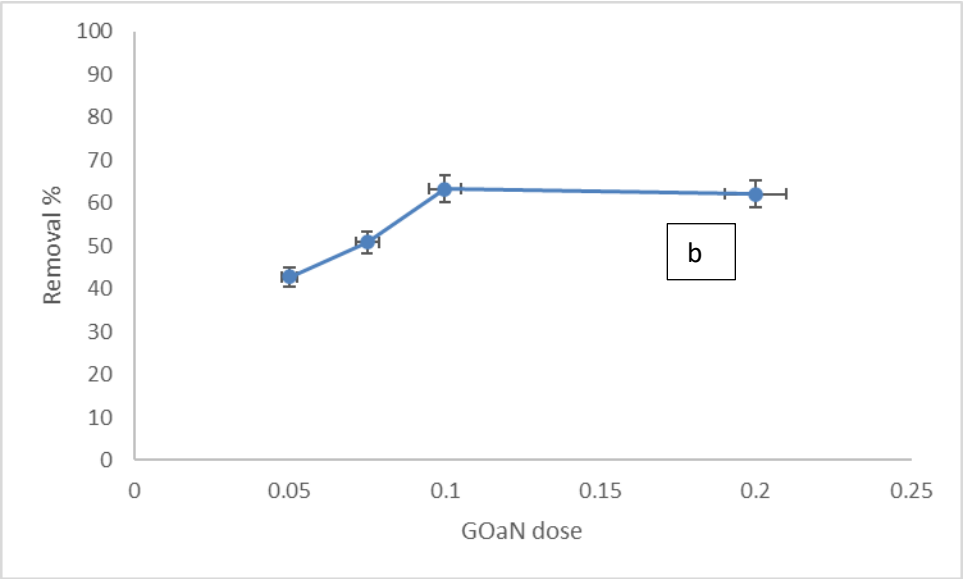

Fig 4.2 : (a) Naphthalene removal % with time by various GOaN dosage (g/L)

(b) Effect of GOaN dose (g/L) on removal % of naphthalene (10mg/L)

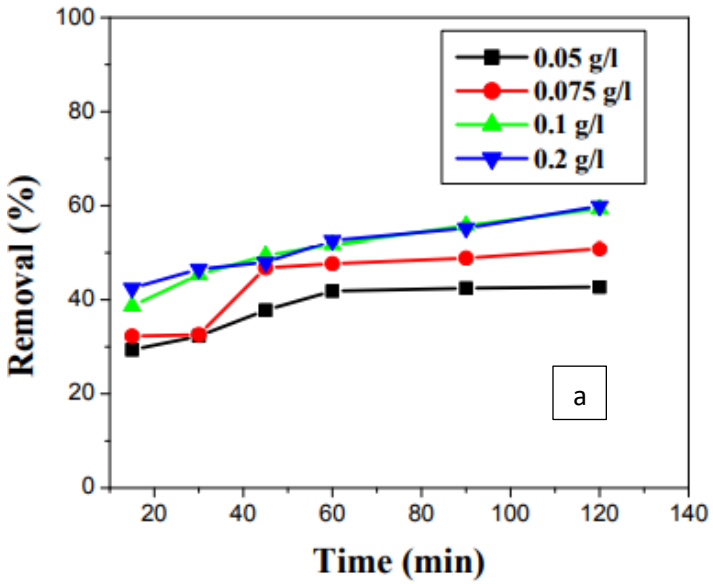

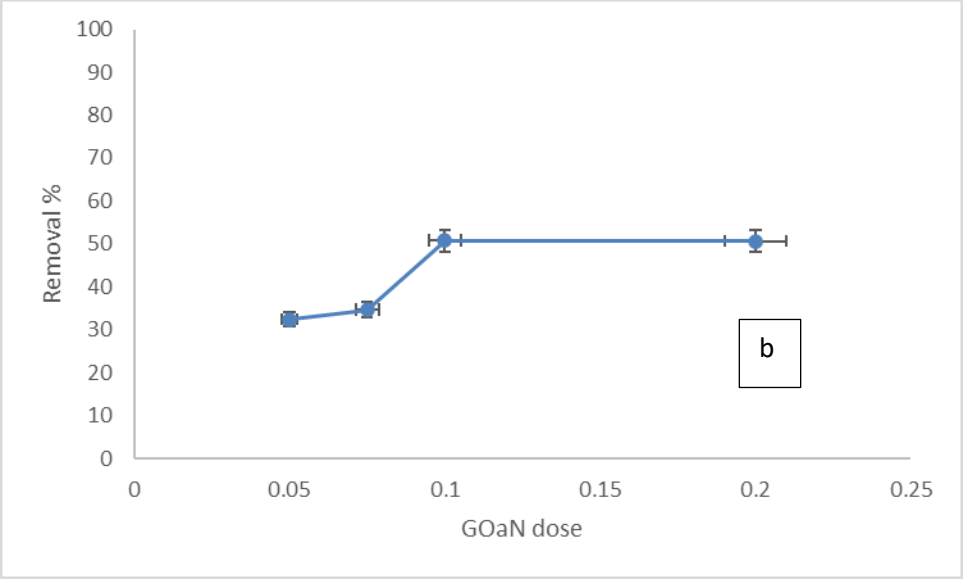

Fig 4.3 : (a) Pyrene removal % with time by various GOaN dosage (g/L)

(b) Effect of GOaN dose (g/L) on removal % of pyrene (10mg/L)

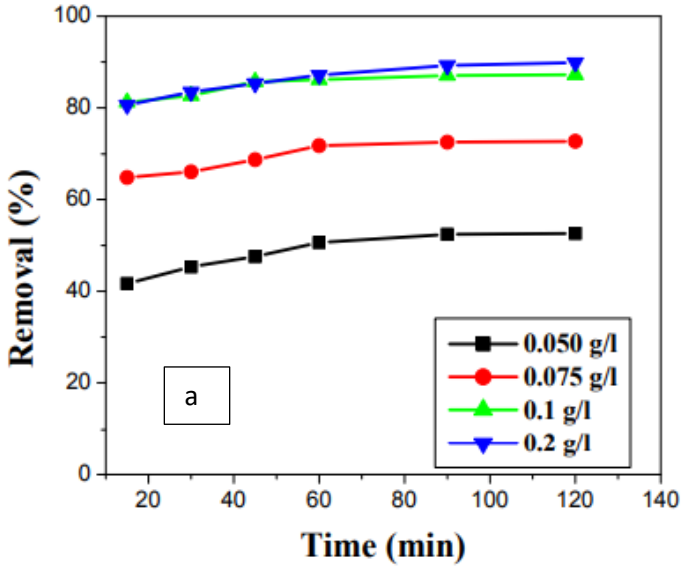

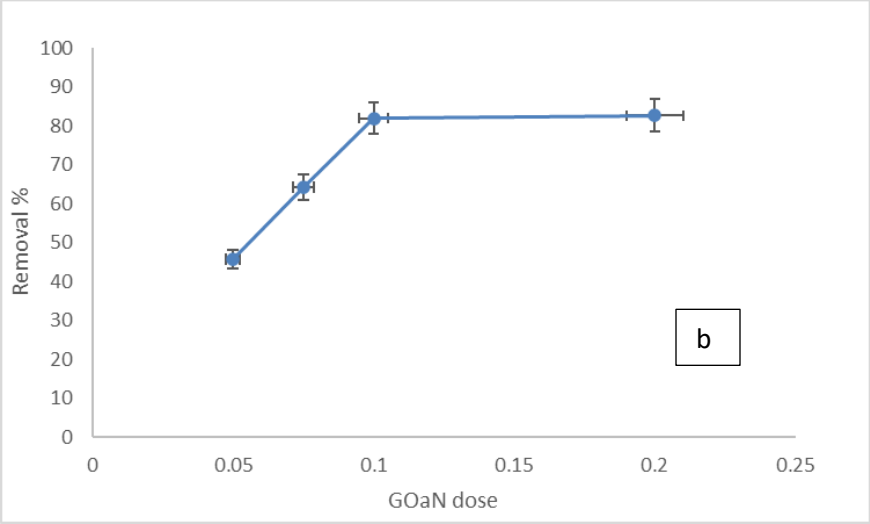

Fig 4.4 : (a) Phenol removal % with time by various GOaN dosage (g/L)

(b) Effect of GOaN dose (g/L) on removal % of phenol (20mg/L)

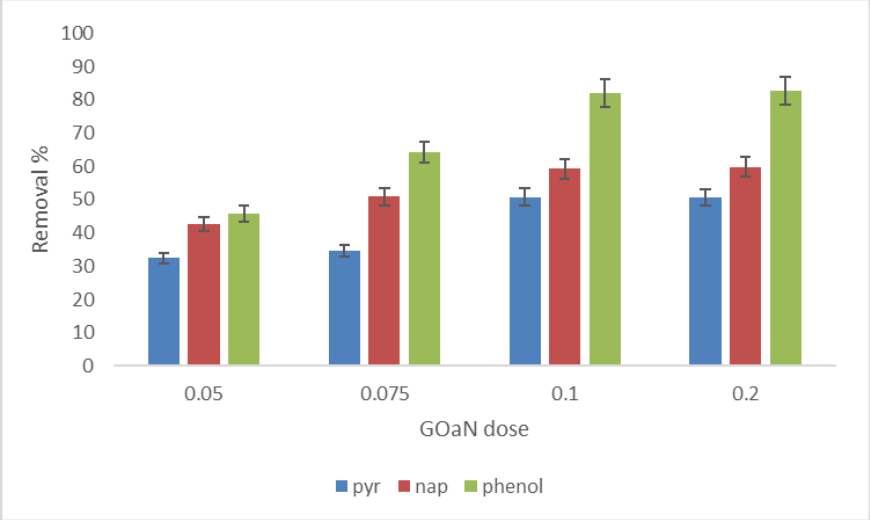

Fig 4.5 : Effect of dosage of GOaN on removal % of Pyrene, Naphthalene , Phenol

4.3.1.2 INFLUENCE OF INITIAL POLLUTANT CONCENTRATION

The primary pollutant concentration is varied from 10mg/L to 100mg/L for the experimental set up. Finite amount of adsorbent consists of definite number of active sites for adsorption. Higher concentration of

pollutants may decrease the efficiency of the adsorbents as the active sites gets filled up very quickly. Thus, adsorption capacity reduces with increase in the initial pollutant concentration. It was observed than beyond 25mg/L for PAH(s) compounds, the removal % is low. This might be due to large number of unsaturated molecules remaining in the solution and the constant competition arising between the already saturated molecules and the unsaturated ones. In case of phenol, it was seen till 20mg/L, the removal % was on the higher range after which there is a decrease in the removal percentage.

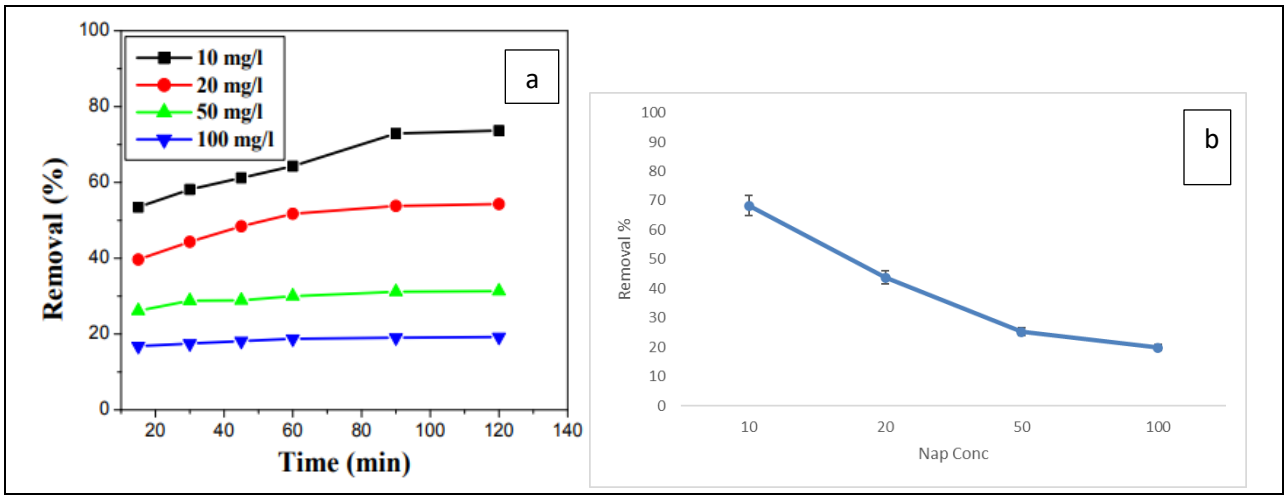

Fig 4.6 : Effect of initial naphthalene concentration on removal % by GOaN (a) with time (b) Removal % decrease with increase in Nap concentration (mg/L)

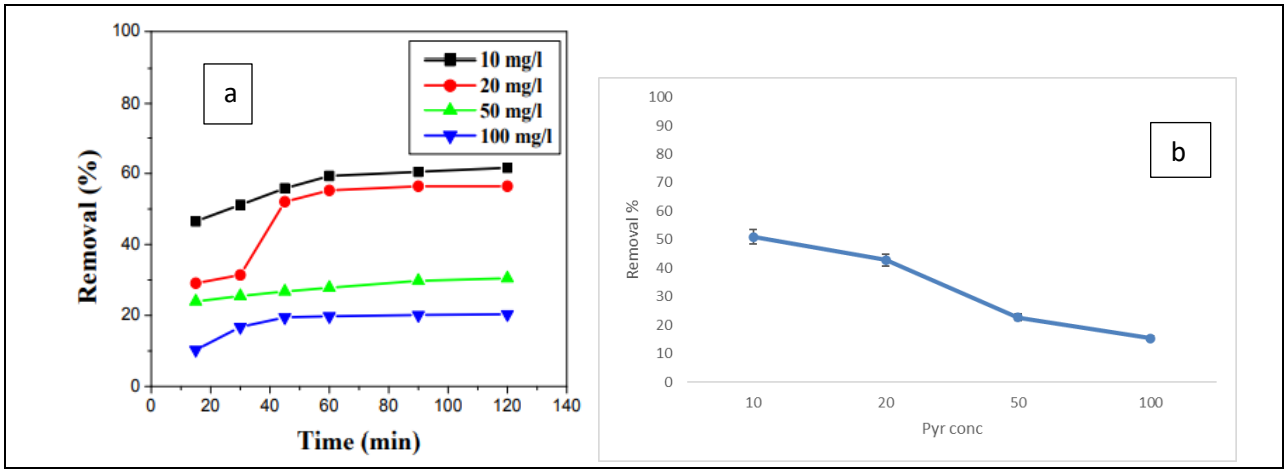

Fig 4.7 : Effect of initial pyrene concentration on removal % by GOaN (a) with time (b) Removal % decrease with increase in Pyr concentration (mg/L)

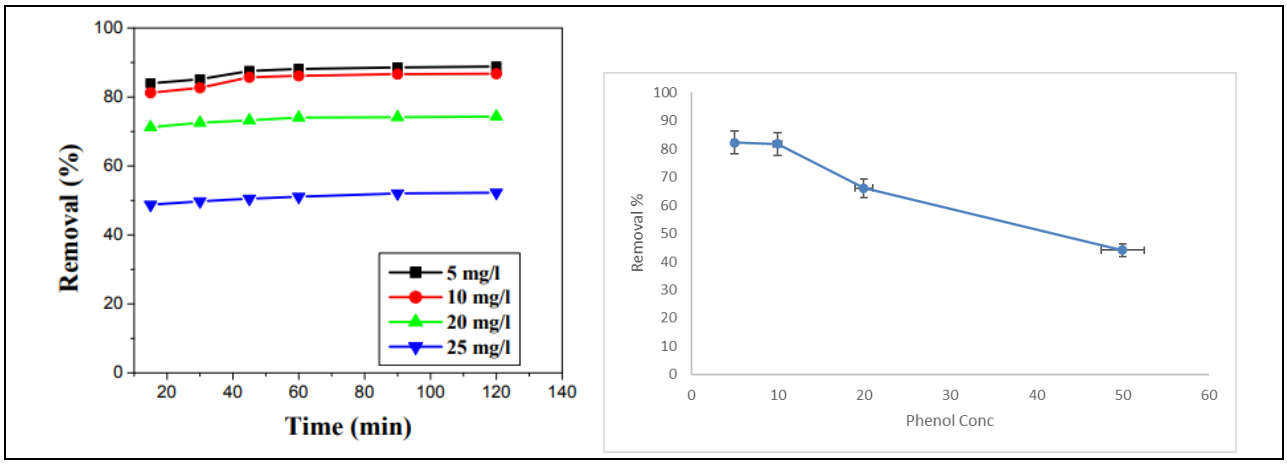

Fig 4.8 : Effect of initial phenol concentration on removal % by GOaN (a) with time (b) Removal % decrease with increase in Phenol concentration (mg/L)

4.3.1.3 INFLUENCE OF TEMPERATURE

It is a well-known fact that diffusion is an endothermic process. With increase in temperature the ions diffuse freely with less opposite retarding forces acting thereby increasing the sorption of ions on to the adsorbent surfaces. Adsorption process is influenced by many external parameters among which temperature plays a crucial role. It was observed that with increase in temperature, the vibration at molecular level increases which eventually increases the desorption rate of the contaminants. From the experimental results it was concluded that the maximum removal occurred at ambient temperature of 35 °C and thus the temperature parameter was set to be at 35°C. The experimental temperature range was set to be from 20°C to 40°C. It was observed that naphthalene and pyrene showed better removal % at higher temperature than phenol. This may be explained by the fact that better dissolution of these hydrophobic compounds occurs at higher temperature.

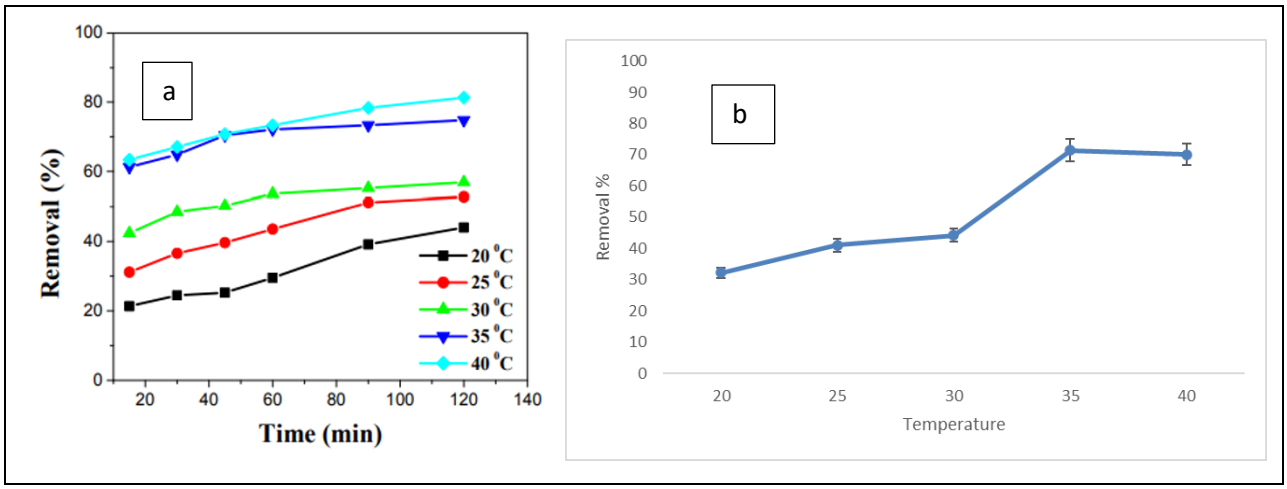

Fig 4.9 : Effect of Temperature on Naphthalene removal % (a) with time (b) Change in removal % with temperature (°C) change

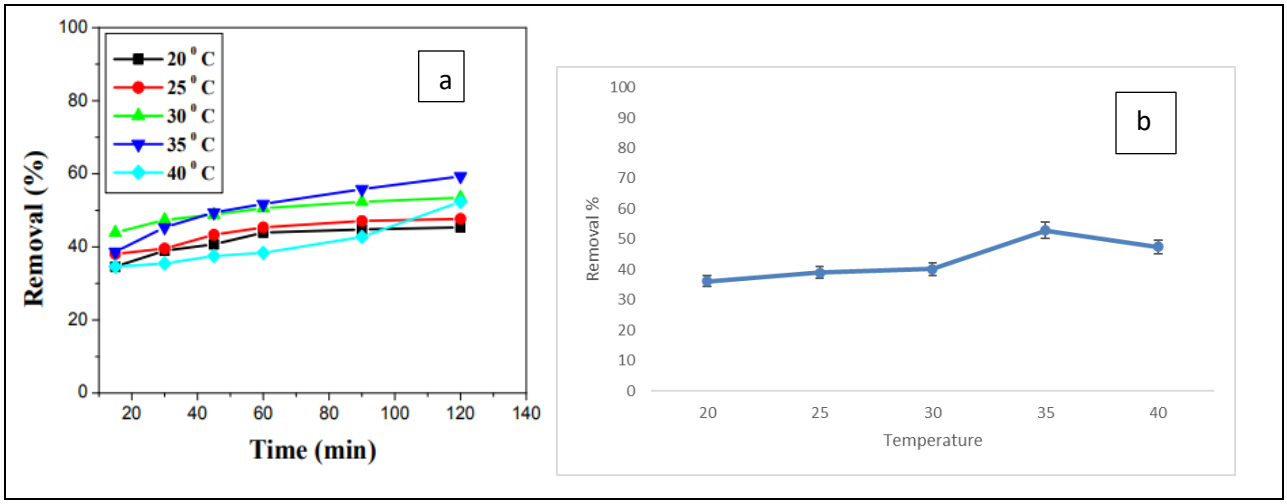

Fig 4.10 : Effect of Temperature on Pyrene removal % (a) with time (b) Change in removal % with temperature (°C) change

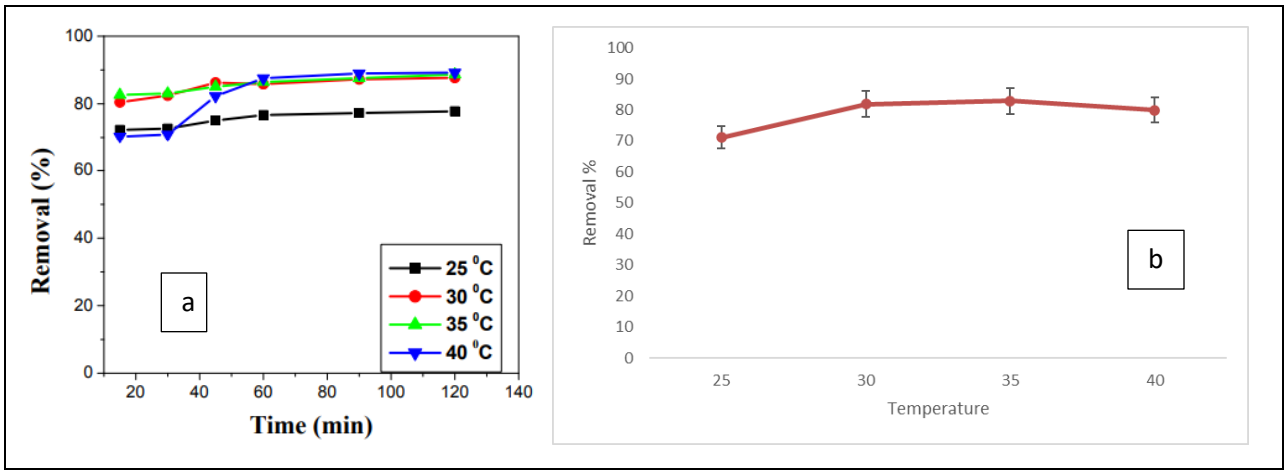

Fig 4.11 : Effect of Temperature on Phenol removal % (a) with time (b) Change in removal % with temperature (°C) change

4.3.1.4 INFLUENCE OF pH

pH factor is crucial for adsorption study as it can influence the electrostatic bonding between adsorbent molecules and retains its stability. The electrostatic interaction between oxygen rich moieties on GOaN and the cationic adsorbate is influenced by the pH of the adsorbate solution. At highly acidic and basic range the removal percentage is lower as the stability between the adsorbent and adsorbate is compromised. Maximum removal is observed at the optimal pH range between 5 – 7 and thus electrostatic interactions between the adsorbent and the adsorbate occurs. Repulsive forces due to pi – pi interactions between benzene rings of GOaN and organic pollutants is lessened in the optimal range thereby better uptake is observed.

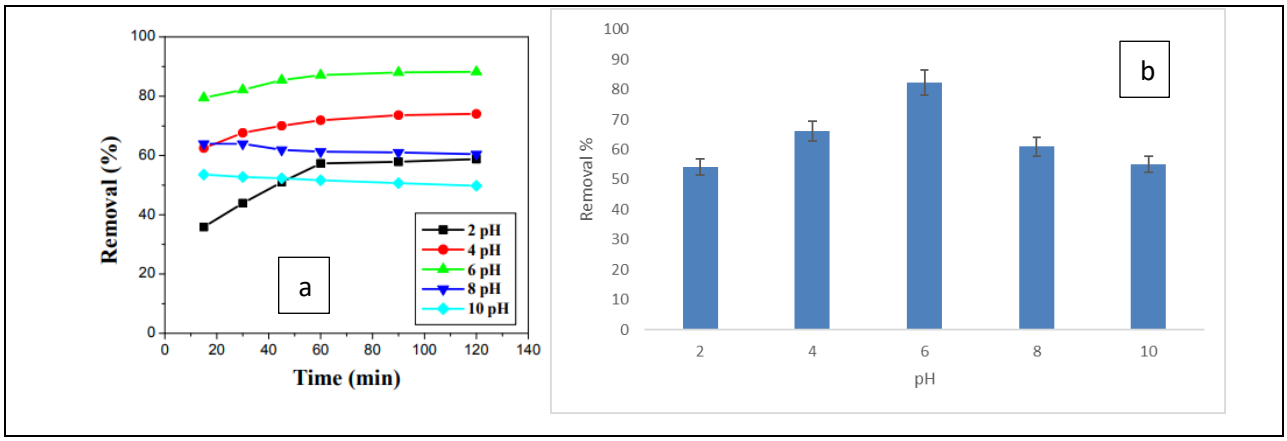

Fig 4.12 : Effect of pH on Naphthalene removal % (a) with time (b) Change in removal % with pH change

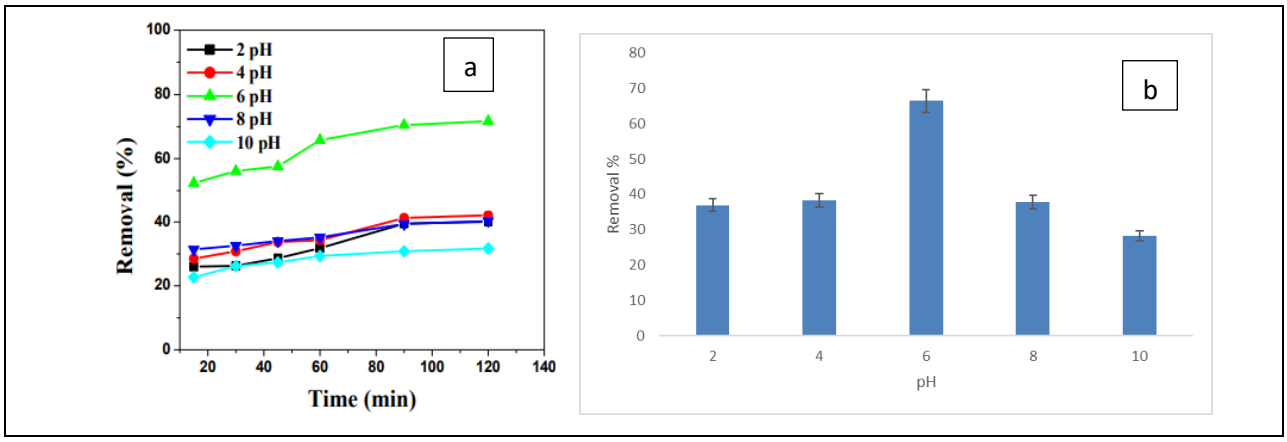

Fig 4.13 : Effect of pH on Pyrene removal % (a) with time (b) Change in removal % with pH change

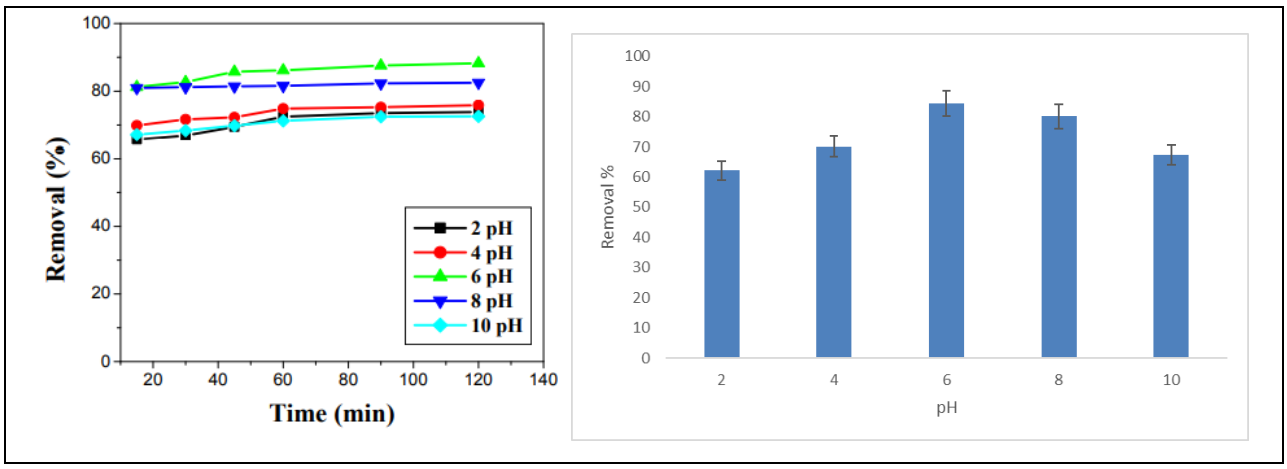

Fig 4.14 : Effect of pH on Phenol removal % (a) with time (b) Change in removal % with pH change

The batch scale parameters showed that GOaN was better suited for removal of Phenol amounting to > 85% , followed by Naphthalene > 60% but pyrene was removed at a very low value (< 50%) . This may be explained by the complex nature and recalcitrant property of high molecular weight PAH (s). As the size

of the HMW PAH molecules are greater than LMW PAH (Naphthalene) so less removal was observed by the fabricated GOaN nanomaterial.

4.3.2 ISOTHERM, THERMODYNAMICS AND KINETIC MODELLING

All the data of LMW PAH (Naphthalene) and Phenol (at temperature of 30 °C) are provided in a tabular format :

Table 4.3 : Adsorption isotherm values for LMW PAH (Naphthalene), HMW (Pyrene) and Phenol

POLLUTANT	ISOTHERM MODEL	PARAMETER	VALUE(S)	R2
Phenol	Langmuir	qo (mg/g)	5.2159	0.9763
		K (L/mg)	18.067	
	Freundlich	KF (L/mg)	20.584	0.9170
		n (g/L)	5.1170	
	Temkin	BT (J/mol)	1.6430	0.7422
		KT (L/mg)	1.0987	
Naphthalene	Langmuir	qo (mg/g)	2.0127	0.9402
		K (L/mg)	13.456	
	Freundlich	KF (L/mg)	10.050	0.8815
		n (g/L)	3.1730	
	Temkin	BT (J/mol)	1.5753	0.7079
		KT (L/mg)	1.5449	
Pyrene	Langmuir	qo (mg/g)	0.8320	0.9172
		K (L/mg)	1.0433	
	Freundlich	KF (L/mg)	2.7349	0.7943
		n (g/L)	0.0713	
	Temkin	BT (J/mol)	1.0155	0.5447
		KT (L/mg)	1.0094	

Among the three models Langmuir model was better represent of the experimental data with high regression coefficient and smallest error value for both the cases showing monolayer adsorption occurring.

Table 4.4 : Kinetic modelling values for LMW PAH (Naphthalene), HMW PAH (Pyrene) and Phenol

ADSORBATE TYPE	CONCENTRATION	$q_{e(exp)}$	PSEUDO 1ST ORDER			PSEUDO 2ND ORDER			INTRAPARTICLE DIFFUSION		
			K_1(1/min)	$q_{e1(cal)}$	R^2	K_2(1/min)	$q_{e2(cal)}$	R^2	K_{am}(mg/g√min)	C_am	R^2
Phenol	20 mg/L	20.77	0.11520	22.61	0.815	0.01014	26.14	0.988	0.9961	--	0.796
Naphthalene	20 mg/L	22.27	-0.06727	26.49	0.838	0.06811	27.46	0.975	0.3501	--	0.778
Pyrene	20mg/L	7.5	0.00115	8.36	0.742	0.0100	12.39	0.904	0.1837	-	0.695

The kinetics model viz., Pseudo-first-order, Pseudo-second-order and Inter particle diffusion model were consider to finding out the experimental adsorption rate constant. For the pseudo-first order linear plot of ln (qe-qt) vs t provides poor R2 value. Pseudo-second-order kinetics model is the most significant and acceptable kinetics model in adsorption process. The linear plot of t/qt vs t with greater R2 value was obtained for both the organic contaminants.

Table 4.5 : Thermodynamic values for LMW PAH (Naphthalene), HMW PAH (Pyrene) and Phenol

Temperature(K)	PHENOL			NAPHTHALENE			PYRENE		
	ΔG (J/mol)	ΔH (J/mol)	ΔS (J/mol K)	ΔG (J/mol)	ΔH (J/mol)	ΔS (J/mol K)	ΔG (J/mol)	ΔH (J/mol)	ΔS (J/mol K)
303	-5.66	89.14	3.59	-1.53	59.52	1.78	-1.77	22.43	8.74

308	-86.03			-1.91			-13.11		
313	-87.58			-30.34			-14.53		

Linear plot of lnK versus 1/T indicates that the adsorption process is physisorption in nature. The values of enthalpy (ΔH) and entropy (ΔS) were calculated from slope and intercept of the linear plot ln K versus 1/T. The positive value of ΔH indicates the process is endothermic in nature and positive value of ΔS indicated that the increased randomness between solid-solute interface is present. The value of Gibbs free energy (ΔG0) determines the nature of process whether it is physisorption or chemisorption in nature. The negative value of ΔG for various temperatures correspond to the spontaneous nature of adsorption. All the values are given in the table.

4.3.3 RSM OPTIMIZATION AND VALIDATION

The statistical model analysis generated by Design expert software (version 7.0) of the individual parameter (adsorbent dose, solution pH and reaction time) and their interactive effects of process variables on response (removal percentage) within the experimental range were obtained through three dimensional responses surface plots. ANOVA was used for the creation of mathematical relation functions between the variables to establish a link between them (Rahman et al., 2022). R^2 measures the dispersion of data points around a fitted line of regression. Higher R-squared values indicates that there are fewer disparities between the observed and estimated values of the experimental similar set of data. ANOVA estimates whether the process factors and their interactions with each other has an impact on the response of removal % and is statistically significant (probability < 0.05). High value of R2 (0.9162) and a realistic agreement of predicted R2 (0.8961) with adj. R2 value (0.8851) verified the capability of the fitted quadratic model for Naphthalene removal. High value of R2 (0.9562) and a realistic agreement of predicted R2 (0.8895) with adj. R2 value (0.9145) verified the capability of the fitted quadratic model for Phenol removal by adsorption.

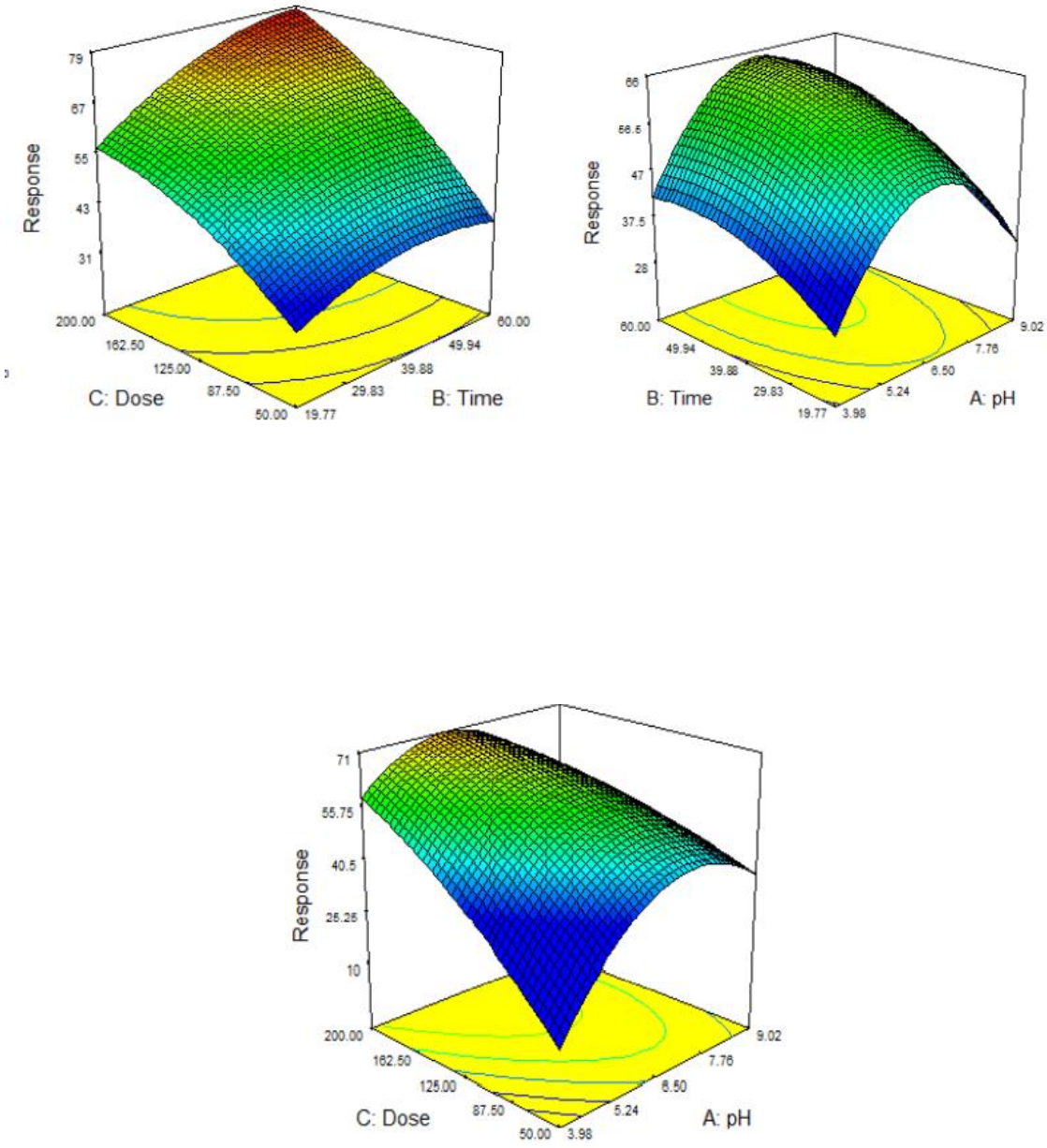

Fig 4.15 : RSM 3D plots for Naphthalene removal by GOaN

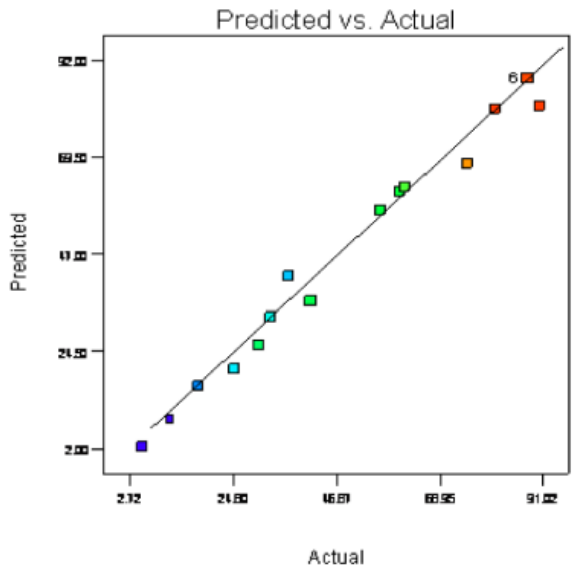

Fig 4.16 : Predicted and experimental values using Response surface methodology (Naphthalene)

Response (Removal Percentage) = -178.81705 + 46.91128 * pH + 0.82279* Time + 0.64815* Adsorbent dose + 0.018750* pH *Time - 0.055676* pH* Adsorbent dose - 0.26046* Time* Adsorbent dose - 3.55848* pH2 -0.011928 * Temperature2 – 0.84496*Adsorbent dose2

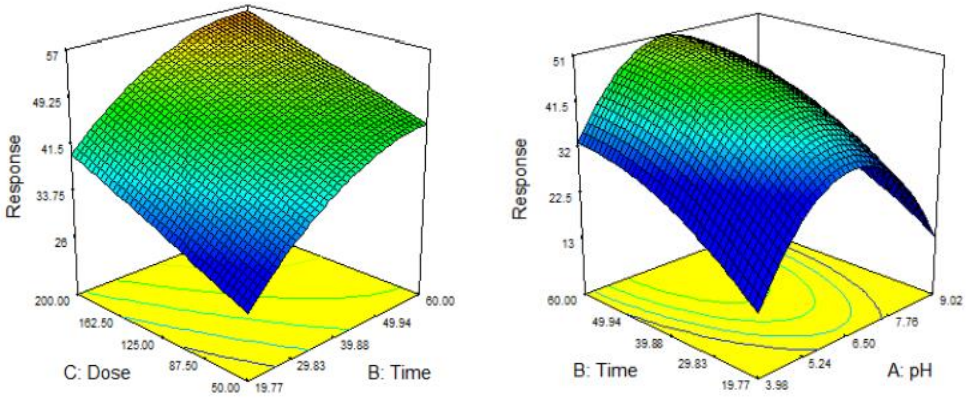

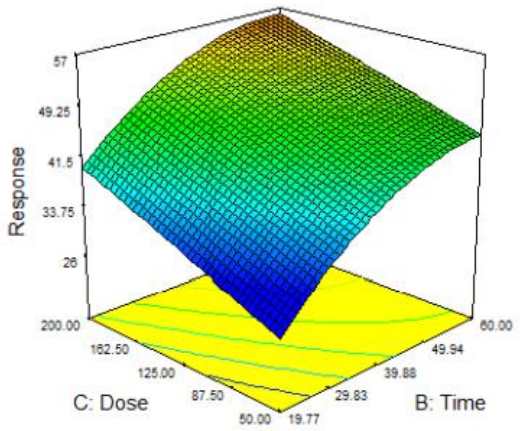

Fig 4.17 : RSM 3D plots for Phenol removal by GOaN

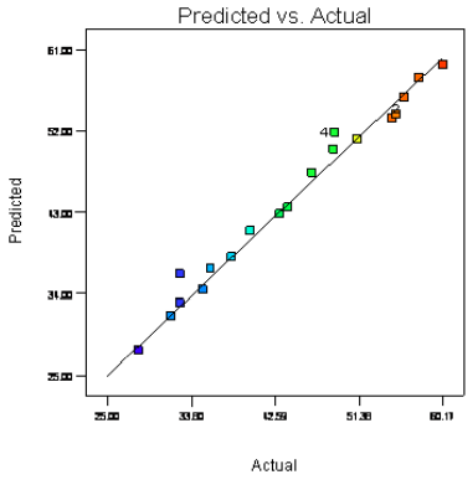

Fig 4.18 : Predicted and experimental values using Response surface methodology (Phenol)

Response (Removal Percentage) = -165.03700 + 48.18788 * pH + 1.52737* Time + 0.28302* Adsorbent dose - 0.032300* pH *Time - 0.029716* pH* Adsorbent dose -0.452187* Time* Adsorbent dose + 3.29658* pH2 - 0.010617 * Temperature2 – 1.84754*Adsorbent dose2

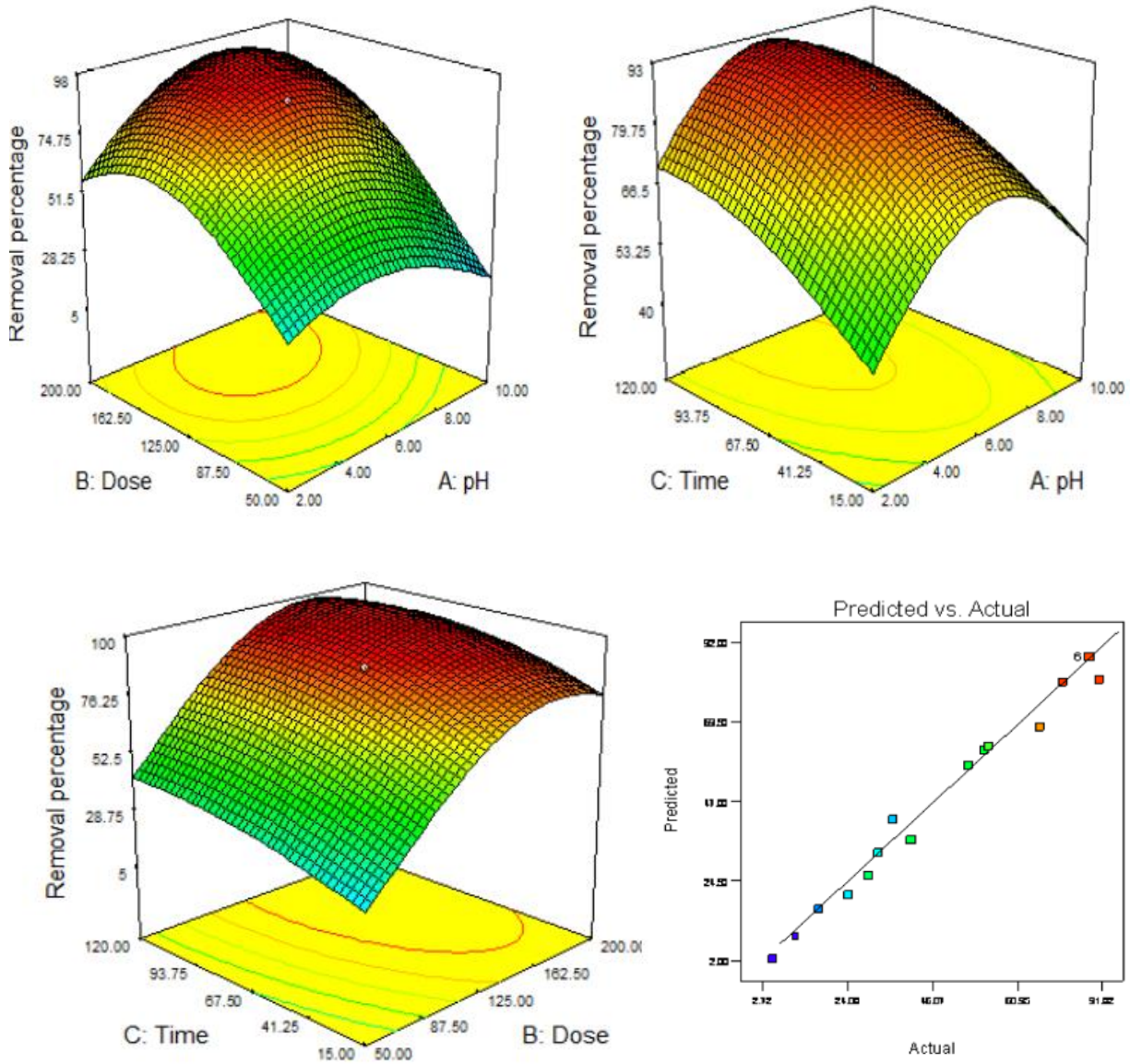

Fig 4.19 : RSM 3D plots for Pyrene removal by GOaN with predicted and experimental values

4.3.4 REUSABILITY STUDY OF GOaN

Regeneration study was conducted up to third adsorption–desorption cycle. It was done by 1 N HCl and or 1 N NaOH solution depends up on the treated adsorbate solution pH. After third cycle the efficiency reduced drastically.

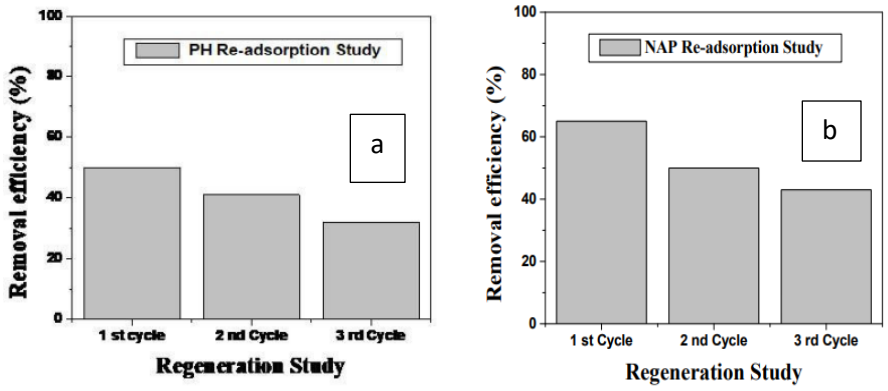

Fig 4.20 : Regeneration study of GOaN nanomaterial a) using Phenol as adsorbate b) using Naphthalene as adsorbate

4.4 CONCLUDING REMARKS

The Batch scale study shows that Phenol removal was higher by GOaN nanomaterial than the poly aromatic compounds (Naphthalene, Pyrene). But in the regeneration study the removal efficiency was lesser in case of phenol adsorbate. Thus, integral approaches involving other treatment types should be chosen for better removal of the organic contaminant. Data obtained from the adsorption studies at equilibrium condition were fitted to isotherm models Langmuir model. The adsorption kinetics for all three adsorbents were observed to fit the Pseudo second-order model better indicating that the overall rate of the adsorption process was controlled by both physisorption and chemisorption exchange between the adsorbent and adsorbate. The adsorption mechanism was mainly found to be surface diffusion along with intraparticle diffusion that was governed by external mass transfer. The predicted and experimental values were well fitted by the RSM method hence the model is validated.

CHAPTER 5

5. REMOVAL OF MODEL ORGANIC POLLUTANT BY INTEGRATED APPROACH OF SORPTION - GAMMA RADIATION

5.1 CONTEXTUAL INFORMATION

As discussed in the previous chapters that new materials are being constantly created on a daily basis with increasing complexity. Thus, complex and novel materials may turn out to new pollutant if their limits in the environmental sphere exceeds the standard level. Thus, newer technologies are being developed and exploited for removal of such pollutants. As mentioned earlier novel materials or recalcitrant products require newer technologies for more efficient removal. Ionizing radiation is one of a such Avant – Garde technique in scientific field. Degradation by ionizing radiation utilizes the power of splitting the water molecule to generate radicals in reactive state like hydrogen, hydroxyl, or electrons. These reactive species then helps in completely removing toxicants from the aqueous phase (Zhuan & Wang, 2019)

The field of combining two or more technologies for pollutant removal is a newly found research area and thus more and more insights are being gained each day. Graphene family nanomaterial specifically graphene oxide is regarded as platform for usage in various sectors. The idea of utilizing ionizing radiation of gamma and GO is an upcoming research hotspot as very few studies have been recorded about the synergistic effect of the two processes.

The objective of this present study was to investigate the catalytic degradation of Phenol (model organic pollutant chosen for the study) in aqueous solution using gamma-ray irradiation combined with laboratory fabricated GOaN nanoparticles. Since secondary materials of toxic nature is not produced by ionizing radiation, thus it is considered to be one of the promising methods of treatment of recalcitrant products (Chitose et al., 2003; Rubio-Clemente et al., 2014). IR has already been reported for treating many kinds of industrial waste water: textile industry, petroleum refining industry, coke making processes as well as municipal and sewage wastewater (Alkhuraiji et al., 2017). The formation of highly reactive radical species along with the reaction taking place at room temperature and without any production of harmful secondary products proves the advantages of the advanced oxidation process but the major drawback lies in its high cost (Chu et al., 2016; Martínez-Morlanes et al., 2011). Thus, high costs and low availability of Gamma radiation setup, may be involved in the less usage of the radiation source and shielding

scientific community from usage of gamma in explorative fields of research. Utilization of hybrid techniques are required to increase approachability of the technique and reduction of cost of the process (Kongmany et al., 2014).

Herein, simultaneous effect of graphene oxide on the degradation of phenol under the influence of gamma irradiation was studied. RSM (response surface methodology) was employed for optimization of the process parameters and to obtain the best condition for maximum degradation efficiency of the process. Additionally, an artificial neural network (ANN)-based model was developed to predict the relationship between the experimental variables and the degradation efficiency.

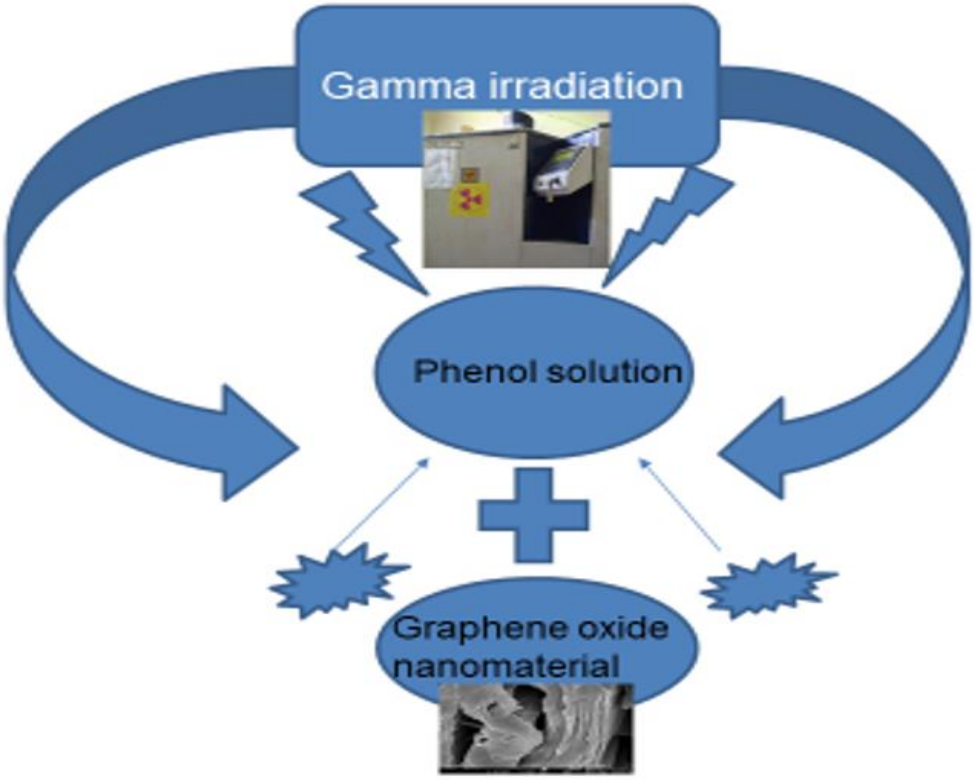

Fig 5.1 : Schematic representation with pictorial inset of the experimental set up

5.2 EXPERIMENTAL SETUP

5.2.1 PREPARATION OF ADSORBATE SOLUTION

As mentioned previously 100 mg/L stock solution of phenol (Merck 99% purity) is prepared by dissolving the pre weighed sample in double distilled water (Millipore). Then further aliquots of dilutions were done for the experimental set up. All the experiments were done under normal temperature and pressure conditions. All the chemicals used in the experiment are of analytical grade and used without further purification. Solution pH is maintained according to the requirement of the experimental need. In case of pH change was needed, it is done by using 0.1N HCl or 0.1N NaOH. The solution pH was determined by a pH meter (Eutech Instruments)

5.2.2 PREPARATION OF GOaN NANOADSORBENT

Adsorbent preparation has been discoursed in details in the previous chapter (chapter 3) along with characterization of the prepared adsorbent according to standardized protocols. Briefly, Graphene oxide (GO), the precursor material of GFMs (graphene family-based materials) is prepared by modifying the modified Hummer's method. The sample obtained is termed as GOaN and is utilized for other experiments planned. Below the flowchart of the preparation steps is mentioned.

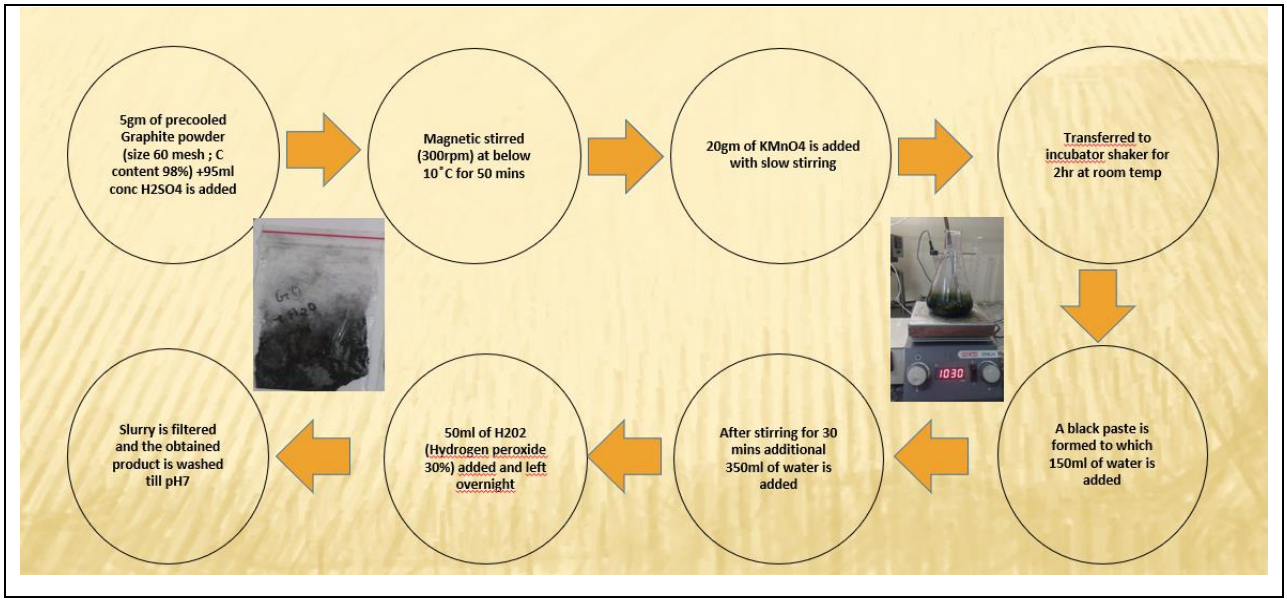

Fig 5.2 : Flowchart of preparation of GOaN nanoadsorbent

5.2.3 GAMMA IRRADIATION SETUP

All the experiments were performed in the UGC DAE gamma irradiation facility which has the following specifications – Irradiation Source Co-60, Strength 3.7kCi, cylindrical sample chamber with diameter of 10.6cm and height of 14.2cm. Dosimeters were provided to ensure the safety of the experimenters. Radiation dosage was measured in Gray (Gy) which denotes absorption of one joule of radiation energy per kilogram of matter. Radiation dose variation was performed at 1kGy, 2kGy, 4kGy, 6kGy and 8 kGy with 6kGy (Kilogray) being the choice of radiation dosage for RSM analysis study. Rate of dosage being at 1.8 kGy per hour. The phenol solutions were taken in special test tubes and the nanomaterial was added precisely just before the initialization of radiation experiments. After the required contact period is given, the test tubes were immediately removed from the gamma chamber with utmost care. Initial concentration of phenol solution was 20 mg/L. All the experiments were performed triplicate and average data was used. The amount of phenol removed from the aqueous solution is analyzed by the following equation:

$$Removal\ \% = \frac{Initial\ Concentration - Final\ Concentration}{Intial\ Concentration} * 100 \quad (1)$$

5.2.4 ANALYTICAL PROCEDURES

The experimental solutions after gamma irradiation were analyzed immediately by UV-Vis spectroscopic methods. Standard curve of the known concentration of phenol solution was prepared prior the experimental work. Lambda max was observed to be at 264.5 nm by scanning the phenol solution in the UV spectrum (Perkin Elmer, USA) range and the resultant solutions were also analyzed by HPLC using C18 general column (Waters) and GCMS analysis using TG-5MS column (ThermoScientific).

For HPLC 60:40 ratios were maintained for acetonitrile and water as the mobile phase, flow rate at 1.4ml/min and the detector were set at 254nm.

In case of GCMS the operating conditions are as follows –MS source temperature 225℃, MS acquisition mode 45-450 amu, Transfer line temperature 300℃, Column flow rate 1.5ml/min, Injector temperature 275℃, Injection type split less, Oven temperature program 60℃ for 5mins then 300℃ for 10mins at the rate of 8℃/min.

5.2.5 RSM OPTIMIZATION – TOOL FOR EXPERIMENTAL DESIGN AND PREDICTIVE MODELING

Response Surface Modeling (RSM) is a crucial tool to analyze and determine the optimum conditions between the interactive factors within the design space of the experimental study. It involves doing several experiments simultaneously using the results of first few single factor at a time experiments thereby it provides an insight into the steps to be planned for carrying out the experiment. Thus, RSM is a collection of both mathematical and statistical techniques to form the empirical model which will help in prediction of the design of experiments (Ba-Abbad et al., 2013). The major advantage of RSM over doing full scale experiments lies in the fact that it can reduce the experimental time and also limits the unnecessary use of chemicals for performing large scale batch operations. In this experimental study, Central Composite Design (CCD) and Box Behnken Design was adopted to study the integrated effects of process variable such as pH of the solution, contact period of adsorbate and adsorbent and dosage of the nano adsorbent.

The second order polynomial equation was used to relate the independent variables of the experiment and their responses:

$$Y = \beta_0 + \beta_1 A + \beta_2 B + \beta_3 C + \beta_{12} AB + \beta_{13} AC + \beta_{23} BC + \beta_{11} A^2 + \beta_{22} B^2 + \beta_{33} C^2 + e_i \quad (2)$$

where Y is the response; A, B, C are variables; β_0 is the model intercept coefficient; interaction coefficient of linear (β_1 β_2 β_3), quadratic (β_{11} β_{22} β_{33}) and the second order terms (β_{12} β_{13} β_{23}); e_i is the error term. To optimize the parameters for better removal of phenol, 3 parameters response surface methodology using Box Behnken design was chosen. pH (range 3-9), Dose (1 g/L – 2 g/L) and time (10-30 min) were chosen as independent variables and removal of phenol was chosen as response in this study. Total 17 experiments were performed according to the Design Expert software tools.

5.2.6 MODELING USING ARTIFICIAL NEURAL NETWORK

In this study, a three-layer feed forward backpropagation neural network with a linear transfer function was developed for modeling of phenol removal using combined effect of both gamma irradiation and adsorption by graphene oxide nano-materials.

MATLAB 7 was used in this study to develop the neural network model. In this study, ANN architectures were chosen as feed-forward networks which were trained by the input data using backpropagation algorithm (Saha, Srivastava, et al., 2013). Linear transfer function 'POSLIN' was chosen for the input to hidden layer mapping while a purely linear transfer function 'PURELIN' was chosen for the hidden layer to the output layer mapping. The values of correlation coefficient (R) were calculated among the best of 17 repeated run.

5.3 DATA FINDINGS AND DISCUSSIONS

5.3.1 EFFECT OF DIFFERENT EXPERIMENTAL PARAMETERS ON REMOVAL

It was observed that using solely gamma irradiation waves removal of phenol from aqueous solution was about 30.1%, but using both gamma irradiation and graphene oxide nanomaterial present in the synthetic solution simultaneously the removal resulted to be 81.4% after only about 30 minutes exposure under gamma radiation and dosage of 100 mg/dL of GO nanomaterial. The reason for the increase in the removal percentage may be due to combined or simultaneous approach effect of both gamma irradiation and graphene oxide nanomaterial (using 1 g/L of graphene oxide, 20 mg/L of phenol in solution at 6 kGy gamma radiation for 30 min). It was observed that as the irradiation dose of gamma radiation increased, removal was also increased. As the exposure dose increased, ionization of the phenol solution increased and as a result removal of phenol present in solution increased. It was also observed that as the dose of adsorbent increased, removal of phenol from the aqueous medium increased. But as the dose increased from 0.5 g/L, no further increase in removal was observed. The reason listed for this phenomenon may be that almost all the phenol present in solution can be adsorbed at 0.5 g/L dosage amount of adsorbent and thus further increase in adsorbent surface had no effect on the removal of phenol. It was observed that as the time of simultaneous exposure/adsorption increased, due to combined effect of ionization and adsorption, removal increased and almost 89.25% removal was observed at 60 min of combined effect of exposure and ionization.

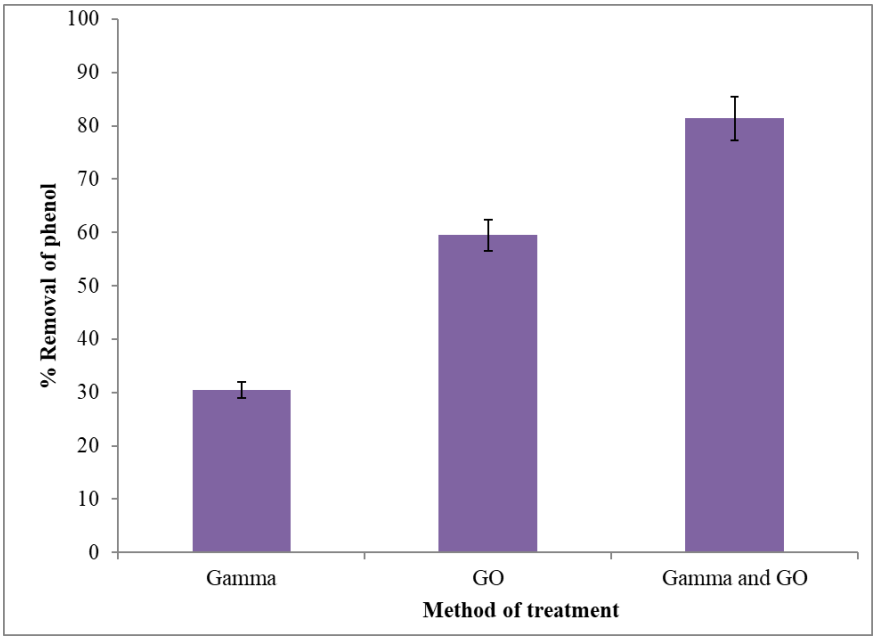

Fig 5.3 : Comparison between phenol removal % of the different modes of treatment

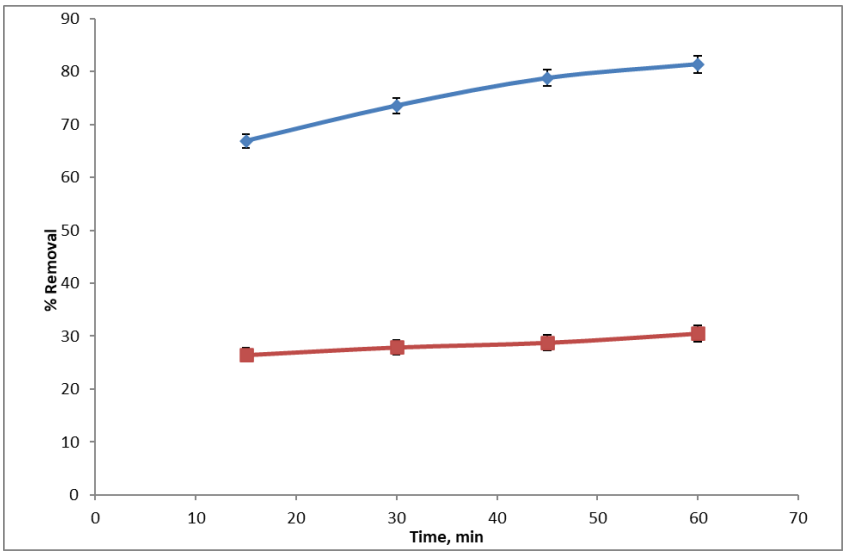

Fig 5.4 : Comparison between removal % of simulated phenol solution by GOaN (denoted by red line) and GOaN + Gamma radiation integral method (6kGy) (denoted by blue line) over time period.

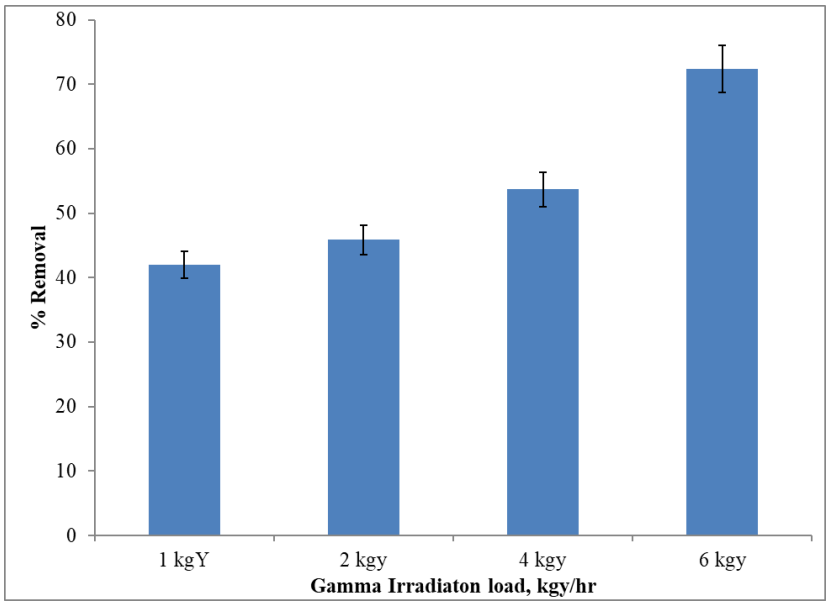

Fig 5.5 : Removal % of phenol from simulated solution by various gamma irradiation dose (GOaN dosage of 50mg/dl) in integral method

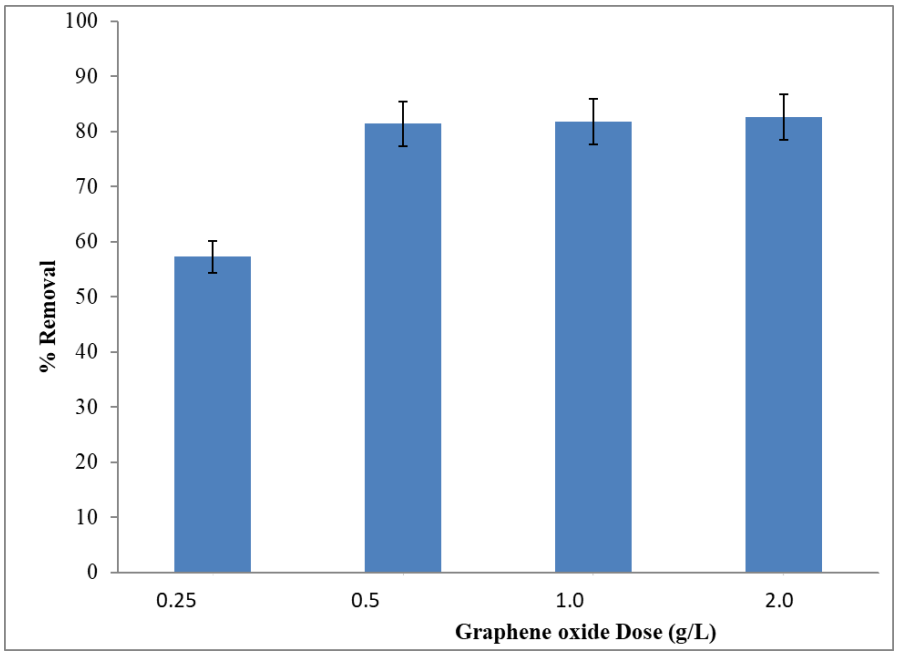

Fig 5.6 : Removal % of phenol from simulated solution by various GOaN dose (Gamma irradiation 6kGy) in integral method

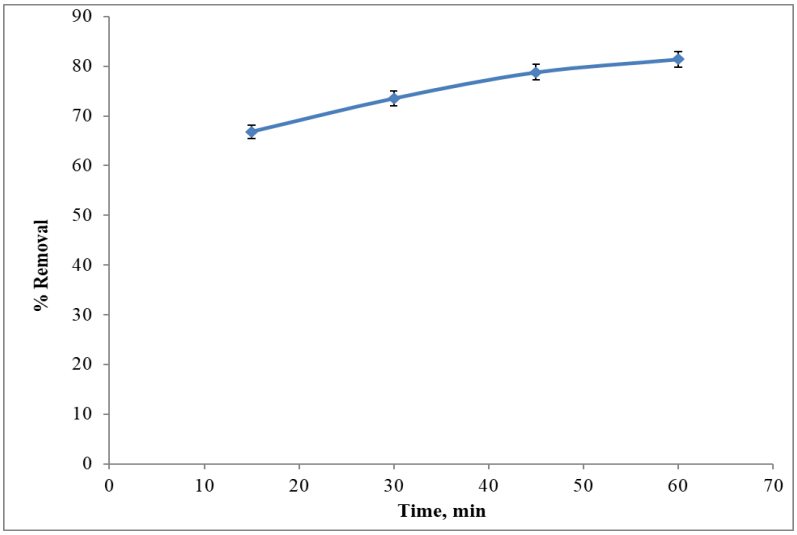

Fig 5.7 : Removal % of phenol from simulated wastewater at different time exposure by synergistic effect of gamma radiation and GOaN

5.3.2 OPTIMIZATION USING RESPONSE SURFACE METHODOLOGY

It was observed that as the pH decreased, removal of phenol from the solution increased. From ANOVA analysis, it was observed that the model developed by RSM was statistically significant and the model was quadratic model. P – value was 0.0002 (<0.05) and F value was 22.75. The goodness of fit of the model was also verified using multiple regression analysis and CV value. It was observed that R^2 value was 0.9669 suggesting that the regression analysis was statistically significant. The adjusted multiple regression value of 0.925 also suggested the model to be significant in this case. CV (2.75) was low suggesting that the model developed by RSM in this study was valid statistically.

$$\begin{aligned} R2 \;=\; 91.05 - 9.35 \text{ x pH} + 0.41 \text{ x dose} - 1.98 \text{ x time} - 8 \text{ x } 10^{-3} \text{ x pH x Dose} \\ + 0.064 \text{ x pH x time} - 1.70 \text{ x } 10^{-4} \text{ x dose x time} \\ + 0.636 \text{ x pH}^2 - 7.16 \text{ x } 10^{-4} \text{ x dose}^2 + 0.048 \text{ x time}^2 \end{aligned}$$

3

represents the predicted and experimental analysis of the study. It was observed that the predicted result was almost same as the experimental analysis and the error between the two was less than 5%.

Table 5.1 : The variable parameters with their range and coded levels for RSM

Table 1: The levels and ranges of the independent variables:					
Serial No	Variable	Notation	Range and levels (coded)		
			-1	0	+1
1	pH	A	3	6	9
2	Dose (g/L)	B	1	1	2
3	Time (min)	C	10	20	30

5.3.2.1 INTERACTION BETWEEN THE PROCESS PARAMETERS

The combined effect of solution pH and graphene oxide dosage on phenol removal is shown in the plot of Fig. 2b. It was observed that phenol removal increased as dose of graphene oxide was increased, the reason may be that as GO dose increased, surface area available for phenol adsorption increased and as a result removal of phenol from solution increased simultaneously. The same observation was observed in other reference papers. But in case of pH, it was observed that as pH decreased, removal increased. As phenol is weak acid and so at higher pH, due to ionization of phenol molecules, removal decreases. At higher pH, due to electrostatic repulsions between the negative charge present in GO and protonated phenol molecules, adsorption on the GO surface decreased and as a result removal decreased. The optimized condition was observed at pH 3.13 with dosage amount of 1.54 g/L of adsorbent (graphene oxide).

The combined effect of solution pH and time on exposure of phenol removal is shown in the plot of Fig. 2c. It was observed that phenol removal increased as time of exposure increases, the reason may be that due to more exposure of gamma irradiation and adsorption on phenol solution, removal of phenol from its aqueous solution culminates to near exhaustion. But in case of pH, it was observed that as pH decreased, removal increased. The optimized condition was thus observed at pH at 3.13 and dosage of 1.54 g/L of adsorbent dosage. Similar effect was also observed in case of time and dose.

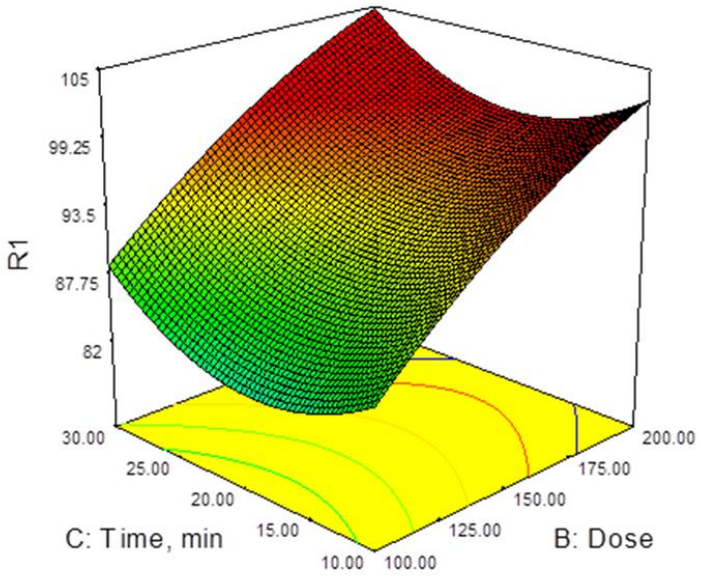

Fig 5.8 : Interaction between time and dose on the removal of phenol by GOaN + Gamma synergistic effect

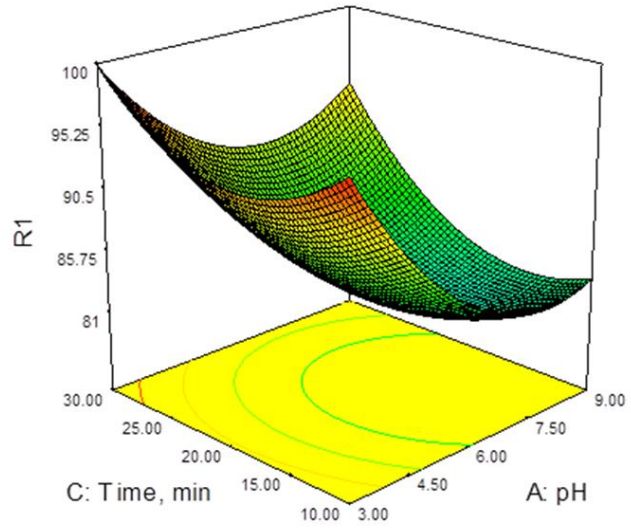

Fig 5.9 : Interaction between pH and time on the removal of phenol by GOaN + Gamma synergistic effect

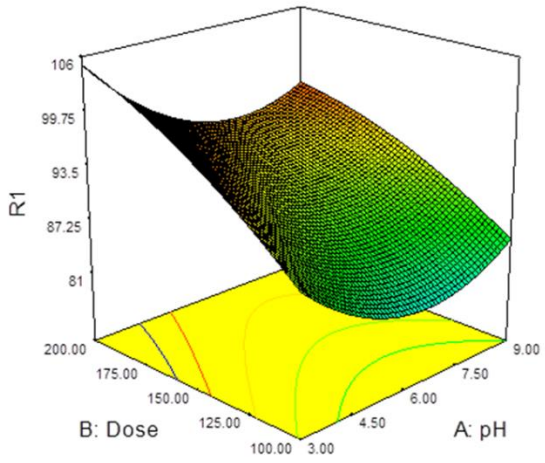

Fig 5.10 : Interaction between Dose and pH of the solution on removal of phenol by GOaN + Gamma synergistic effect

5.3.2.2 VALIDATION OF RESPONSE SURFACE METHODOLOGY

Optimized condition was found as to be around pH: 3.13, Dose of the adsorbent: 1.54 g/L, Time: 29.61 min and at this condition removal was found to be 98.81 from model value and 96.71% from actual experimental analysis. The error between the experimental and theoretical results was observed to be around 2.125%.

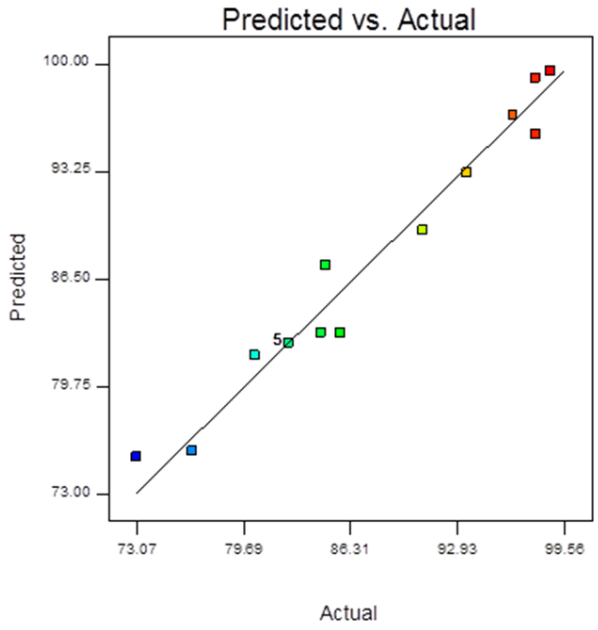

Fig 5.11 : Predicted and experimental removal using Response surface methodology

5.3.3: MODELING USING ARTIFICIAL NEURAL NETWORK

In this study, a three-layer feed forward backpropagation neural network with a linear transfer function was developed for modeling of phenol removal from its aqueous solution by using the effects of both gamma irradiation and adsorption by graphene oxide nano-materials in combination.

The trained network developed gave us a correlation coefficient of 0.9997. This high correlation coefficient of the experimental and theoretical plot signified the reliability of the neural model developed in this study.

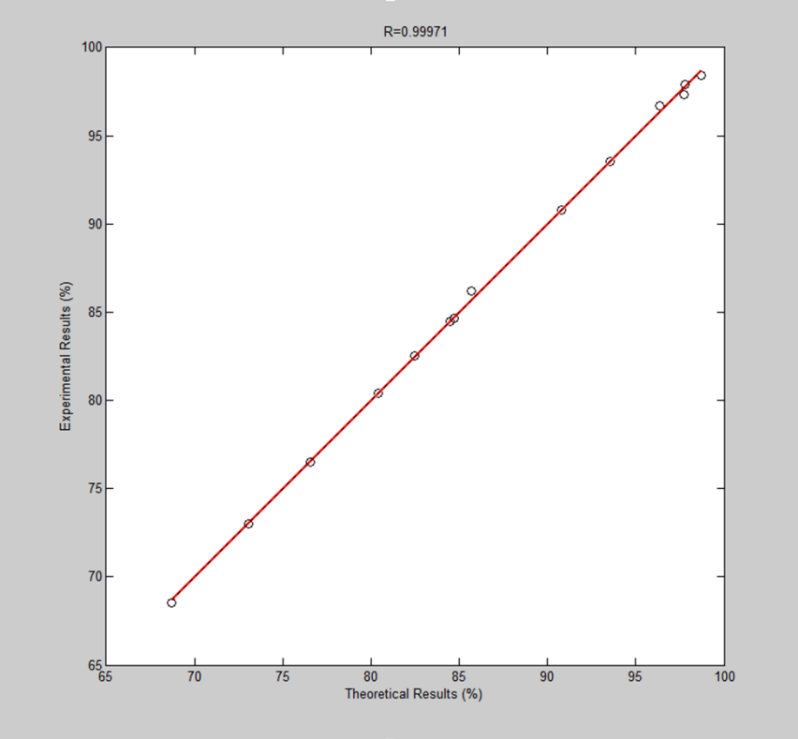

Fig 5.12 : Experimental and theoretical analysis using Artificial Neural Network

5.3.4: CHARACTERIZATION OF THE NANO-MATERIALS USING SEM, FTIR AND XRD

SEM (scanning Electron Microscope) analysis of the nano-materials were performed before and after exposure to gamma irradiation. From SEM analysis GO was observed as disordered solid of thin, overlapping, indiscriminately aggregated sheets closely associated with each other and also observed with many exposed surfaces or regions which might be used for adsorption purposes. A drastic change was observed in the surface texture of the treated adsorbent after exposure to gamma irradiation and adsorption of phenol on the surface. From FTIR figure it was observed no drastic change in the FTIR analysis pattern of GO nano-materials (before and after exposure) except the transmittance. Thus, it proves that no such change in the chemical composition of the sample has occurred due to the ionizing rays. The group present in the GO was observed as the spectrum exhibited the characteristic peaks at 1020, 1384, 1626, 2924 and 3423 cm^{-1} indicating C–O, C=C, C=O, O-H (acid) and O–H (hydroxyl) bonds respectively. Similar observation was observed for XRD analysis also. No significant effect was observed on the XRD profile before and after exposure of gamma on the GO nano-materials. The diffractogram is

characteristic of graphene oxide with diffraction peak at 2θ = 10.5. The peak at 26.5 and 42.5 denotes unreacted graphite bands as similar observation were reported in literature review. Thus, this shows that even at ionizing radiation dose of 6 kGy there was no change in the crystallinity of the sample and no reduction of graphene oxide. The shortening of the peak at 2θ = 26.5 maybe due to irregular stacking of unreacted graphene.

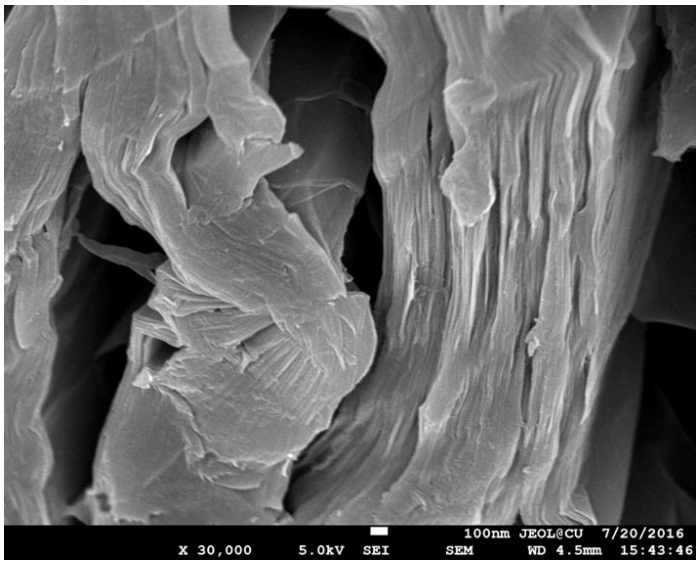

Fig 5.13 : SEM image of fabricated GOaN

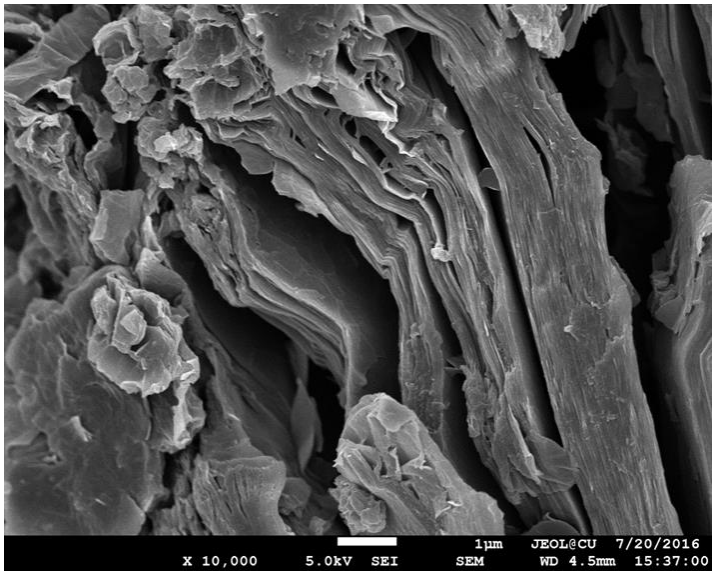

Fig 5.14 : SEM image of fabricated GOaN after gamma irradiation at 8kGy (KiloGray)

5.4 CONCLUDING REMARKS

In this present experimental study that we conducted, the combined effect of gamma irradiation along with the effect of nano-materials on removal of phenol from its aqueous solution was studied. For this, gamma irradiation along with graphene oxide as the wonder nanomaterial was used to remove phenol present in synthetic solution. It was observed that using the combined effect of gamma irradiation and nano-materials, removal of phenol was increased by 30% compared to individual effect of adsorption or gamma irradiation only. To scale up the process and to investigate the combined effects of various process parameters on the removal of phenol the response surface methodology was utilized. Optimization conditions for the maximum removal efficiency of phenol were obtained by applying a desirability function in RSM. Based on the statistical analysis the optimum conditions obtained were at pH 3.13, contact period of 29.61 minutes, with the dosage amount of graphene oxide of 1.54 g/L resulting in the removal condition culminating up to 98.8% and the final concentration of phenol in the solution was rendered to be around 0.24 mg/L which is well below the permissible limit. It was also observed that using the proposed simulated ANN model to predict the removal of phenol present in solution using the combined effect of both adsorption and gamma irradiation.

CHAPTER 6

6. REMOVAL OF PAHS AND PHENOL IN SYNTHESIZED AQUEOUS MATRIX BY GRAM POSITIVE AND GRAM-NEGATIVE BACTERIA

6.1 CONTEXTUAL INFORMATION

Biological treatment methods are attractive because they are easier, energy efficient, ecofriendly, viable, safer than chemical approaches. To achieve sustainable development goals along with economically viable options, bioremediation still remains the preferred choice (Imam et al., 2021). Biotechnology or biological technologies can be used as efficient and low-cost technology in comparison to other physical or chemical methods. Bioremediation is the green approach to mitigate waste products and other hazardous materials as they have no deteriorating effect on the environment and ecosystem. It uses the principle of treating waste products using biotic forms mainly microorganisms although phytoremediation and fungal remediation are of equivalent importance too. Biological treatment methods of aromatic hydrocarbons include

- Bioremediation using bacteria
- Fungal remediation
- Phytoremediation

By definition bioremediation is the inherent ability of microorganisms to mitigate organic and inorganic pollutants. Its success depends on few factors like the intrinsic biodegradable nature of the pollutant, the availability of microorganism to degrade the pollutant and the accessibility of the pollutant to its degraders. Biodegradation thus helps in recycling the nutrients and thereby an important parameter to maintain earth's nutrient balance (Remya et al., 2022) Biodegradation specifically using bacterial species has been researched over decades for proper degradation of complex compounds such as PAHs and phenolic compounds. Complete elimination of these toxic pollutants requires microorganisms to metabolize the products into utilizable produce. Degradation of environmentally persistent compounds is thus a never-ending process as with the increase of industrialization, newer complex byproducts are being disposed of into the environment. Thus, bioaugmentation or bio stimulation may be applied to degrade recalcitrant chemicals. Various bacterial species of *Acinetobacter* sp, *Achromobacter* sp, *Bacillus*

sp, *Pseudomonas* sp etc. have been isolated from contaminated regions and utilized for the degradation studies (Haritash & Kaushik, 2009; Lawal, 2017). Gram positive and Gram-negative microbial strains have been equally researched for elimination of complex PAHs and phenolic compounds (Baek et al., 2016). Taxonomic groups of prototypical gram-positive *Bacillus* and gram-negative *Pseudomonas* have been extensively studied for elimination of these recalcitrant products. *Bacillus* genus is one of the most ubiquitous and heterogenous with extensive phenotypic diversity. Generally, they are gram positive rods occurring in pairs or in chains. *Pseudomonas* is a widely known PAH degrader and occurs structurally as long rods singly or in pairs. Biotransformation of toxic pollutants into less complicated metabolites is achieved by biological degradation. The process depends on external parameters which influence the mineralization of pollutants to inorganic minerals, H_2O, CO_2 in case of aerobic degradation. The rate of biodegradation thus depends on pH, temperature, microbial inoculum volume, chemical structure and chemical partitioning in the pollutant media and accessibility of nutrients in the media. The metabolism of recalcitrant aromatic compounds initiates at the step of hydroxylation which breaks the resonance structure. The hydroxylase enzyme acts upon the degradation of the resonance bond structure. This is followed by dioxygenase (or monooxygenase) for fission of the benzoid ring structure thereby making the compound available for further degradation into simpler substance which eventually enters the TCA cycle as metabolites for assimilation of energy in the bacteria. Generally organic compound metabolism involves the catechol pathway by generating catechol as an intermediate product which is eventually degraded by ortho or meta trail giving rise to cis –cis intermediates.

6.2 EXPERIMENTAL SETUP

6.2.1 ISOLATION AND PROCUREMENT OF MICROORGANISMS FOR DEGRADATION STUDY

For the experimental study we selected pure cultures of *Pseudomona*s sp and *Bacillus* sp as the protypical Gram negative and gram-positive microbial strains. The pure cultures were purchased from IMTECH (Institute of Microbial Technology, Chandigarh, India and were MTCC (Microbial Type Culture Collection) coded. For the experimental study *Pseudomona*s *mendocina* (MTCC 11808) and *Bacillus pumilis* (MTCC 2466) were purchased. *Dietzia* sp. PD1 with GenBank accession number JQ414030 was also utilized for the degradation study. *Dietzia* sp was isolated from soil of a textile industry in Rajarhat, West Bengal. The detailed isolation procedure for the microorganism has been reported by the research study Saha et al., 2013.

Marine water was collected from Bakkhali region located in south western part of West Bengal, India. The location of the sampling site is denoted by geographical coordinates of latitude 21°43'3.13" N and longitude 88°16'9.60" E. Serial diluted samples were plated on Luria – agar plates containing phenol (50mg/L) and the isolates were collected. The dominant isolate was further grown in Luria Broth and Luria agar and send for identification.

All the selected microbial strains were maintained on nutrient agar slants (composition mentioned in the next section) with subculturing done every month to preserve the pure cultures. Glycerol stocks were also maintained at -80°C for longer storage of several months. For the experimental study, inoculum preparation was done by adding a loopful of the isolate to 50ml of broth (growth media) and kept in an incubator under controlled temperature of 30°C ±3°C and constant agitation of 120rpm. The inoculum is then added to estimate the pollutant degradation ability of each isolate. In case of degradation studies Minimal Media (composition mentioned in the next section) is used as it is devoid of carbon sources. Preweighed amount of organic pollutant (Naphthalene, Pyrene, Phenol) is added individually to the minimal media to substitute as carbon and energy source. The bio stimulated organisms are plated and stored at 4°C and used for further analysis.

6.2.2 HARVESTING OF MICROBIAL CELLS

Preculture of microbial cells were done in 50ml sterile Luria broth taken in a 100ml conical flask and kept at 30°C ±3°C under agitation speed of 120rpm for 30hrs. the microbial culture was then harvested at 5000rpm for 10mins and the pellet is washed and resuspended in 0.9% saline solution (isotonic saline solution) and cell density was adjusted according to O.D 1.0 (10^8 cells). The microbial inoculum is then used for further analysis. All the glassware were from Borosil® and the chemical used were of analytical grade and used without further purification.

The composition of Growth Media used in various microorganism related experimental study are as follows. All the broth were of similar composition in each case without the addition of agar:

Table 6.1 : Composition of growth media of microorganisms

MEDIA	AMOUNT (g/L)

Nutrient Agar Media	
Beef Extract	1.0
Yeast Extract	2.0
Peptone	5.0
Sodium chloride (NaCl)	5.0
Agar	15.0
Distilled water	1L
Luria Bertani Agar Media	
Tryptone	10.0
Yeast Extract	5.0
Sodium chloride (NaCl)	5.0
Distilled water	1L
Mineral Salt Agar Media	
Dipotassium hydrogen phosphate K2HPO4	7.0
Potassium dihydrogen phosphate KH2PO4	2.0
Ammonium sulfate (NH4)2SO4	1.0
Magnesium sulfate (MgSO4)	0.1
Sodium citrate	0.5
Distilled water	1L

6.2.3 IDENTIFICATION OF THE SELECTED STRAINS

The strains were identified by Gram staining, IMViC and other biochemical parameters. Gram staining Kit (LOBA Chemie) consisting staining solutions – Crystal violet solution, Gram's iodine solution, Safranine (0.5% w/v solution), acetone – alcohol (50% solution) as decolorizer. For gram staining bacterial smear was prepared on a clean grease free slide (Riviera). The slide was then stained by Crystal violet solution. The excess stain was washed off by water poured through a syringe. Gram's iodine solution was then added dropwise till the whole slide is flooded. It is kept for couple of minutes and then washed off by using decolourizer. Finally, safranine was added and kept for few minutes before removing the excess stain by distilled water. The prepared slide was then air dried at room temperature on a tissue paper to avoid contamination. The whole process is conducted within the laminar air flow chamber with air flowing from HEPA filter (G.B Instruments). Gram staining pics were obtained by Optika software of the microscope (OPTIKA). IMViC (Indole, Methyl Red, Voges – Proskauer and Citrate) kits were purchased from HiMedia. Biochemical Test Kit I (SRL) consisting of Peptone water (for carbohydrate utilization study), Triple sugar Iron agar, Phenylalanine agar, Urea Agar base and Biochemical Test Kit II (SRL) consisting of Nitrate agar, Malonate broth, Nutrient gelatin, Starch Agar were used to assess biochemical parameters of microorganisms.

The isolated microorganism was also sequenced by 16S rDNA and compared with Gene Bank database. The isolated microorganism was sent to Xceleris, Ahmedabad, Gujarat, India for 16S rDNA analysis. The phylogenetic tree helps to determine the percentage of similarity with other microbial strains. The gene sequences is analyzed by using BLAST (Basic Local Alignment Search Tool) at the online website of NCBI (National Centre of Biotechnology Information) [www.ncbi.nlm.nih.gov/BLAST]. The phylogenetic tree was constructed by comparing the sequences already present in the GenBank. Multiple alignments and cluster analysis was performed by neighbour – joining and maximum – likelihood approaches using MEGA 7.0 software.

6.2.4 ANALYTICAL TECHNIQUES

6.2.4.1 UV – ViS (UV – Visible) SPECTROSCOPY

In this study, Naphthalene is chosen as the model Poly Aromatic Hydrocarbon as it is the simplest PAH. It is a low molecular weight PAH and is toxic. Pyrene is chosen for the high molecular weight PAH as it has four aromatic rings in its structure and thus has increased complexity. Phenol is chosen as the model

organic pollutant and it is fairly soluble in water than the other two hydrophobic compounds. Biodegradation experiments are conducted using four microorganisms – *Pseudomonas mendocina* (Gram negative), *Bacillus pumilis* (Gram positive) *Dietzia* sp (Gram positive) and *Leclercia* sp (Gram negative) individually. Various physicochemical factors like pH, Temperature, Salinity, Rotation speed, Amount of Inoculum are taken into consideration to see the effects of these parameters on the degradation of the compounds. For biodegradation experiments minimal broth was used as the bacterial media to supplement the organic compounds as carbon sources. To minimize evaporation of the organic compounds the minimal media were pre sterilized by saturated steam autoclaving (G.B Equipments) at extreme pressure of 15 pounds/sq.inch at 121°C for 60 minutes with an additional 15mins standing time to cool down the highly heated constituents. The chemicals were dry sterilized before adding to the media. All the processes were conducted under the sterile air flow from HEPA filter in the Laminar Air Flow Chamber.

Concentration of the pollutants are estimated by UV – ViS diffuse reflectance spectrophotometer [Perkin Elmer] at their respective Lambda max values Naphthalene λmax 219nm; Pyrene λmax 293nm Phenol λmax 264nm. If the O.D reading is >1.5 appropriate dilutions were done to remove any possibility of false readings. The end result is multiplied by the dilution factor if and when necessary. The samples collected were subjected to centrifugation (10,000 *g for 10mins) [Remi]. The supernatants were utilized for estimation of residual pollutant concentration and the pellet was utilized to estimate specific growth rate of microorganisms used. Bacterial growth was also estimated with samples not subjected to centrifugation to give O.D (optical density) at 600 nm. pH of the experimental solutions was monitored by PCS multiparameter test kit with temperature function enabled.

$$Removal\% = \frac{Initial\ pollutant\ concentration - Final\ pollutant\ concentration}{Initial\ Concentration} * 100 \quad (1)$$

The samples were collected till the saturation is observed in the removal %. All the experiments were repeated several times to ensure reproducibility and statistically significant data.

6.2.4.2 FTIR SPECTROSCOPY

FTIR spectra as mentioned in Chapter 3 is a wonderful tool to ascertain about the state of the sample pre and post treatment by microorganisms. The spectra thus obtained and analyzed to conclude that the microorganisms selected were capable of degrading the organic pollutants used in this experimental study (Wulandari et al., 2019). The ATR (Attenuated Total reflectance) of the FTIR (Perkin Elemer) mode was utilized along with the KBr pelletization method. In the ATR mode the samples were directly observed without any further processing. In the KBr mode the sample was heated and then grinded with KBr to form pellets. Grinding helps in homogenizing the samples and thus get a homogenous spectra of the same (Kamnev et al., 2021).The scanning range remained between 450 – 5000 cm-1.

6.2.4.3 HPLC ANALYSIS

The obtained PAH resultant solution is preconcentrated by using rotatory evaporator (Buchi Rotavapour). The resultant solutions were also analyzed by HPLC using C18 general column (Waters). For HPLC 60:40 ratios were maintained for acetonitrile and water as the mobile phase, flow rate at 1.4ml/min and the detector was set at 254nm.

The supernatant of phenol solution was dissolved in distilled water to the desired concentration and then sterilized by filtration using 0.22-µm membrane filter, followed by HPLC analysis. HPLC was performed on a reverse phase C18 column (150 mm × 4.6 mm) with a methanol / water (60:40, v/v) mobile phase at a flow rate of 0.5 mL/min. Detection was performed with a UV detector (Perkin Elmer) at 270 nm. The concentration was measured using by comparing absorbance to a calibration curve.

6.2.4.4 GC – MS ANALYSIS

The preconcentrated resultant solutions is analyzed by Gas Chromatographic technique equipped with Mass Spectrophotometry (Thermo Scientific Trace 1300) using TG-5MS column (Thermo Scientific). In case of GCMS the operating conditions are as follows –MS source temperature 225℃, MS acquisition mode 45-450 amu, Transfer line temperature 300℃, Column flow rate 1.5ml/min, Injector temperature 275℃, Injection type split less, Oven temperature program 60℃ for 5mins then 300℃ for 10mins at the rate of 8℃/min

6.2.5 EFFECT OF OFAT ON DEGRADATION STUDY

Batch scale studies were conducted to estimate the effect of process parameters on the biodegradation. To estimate the process parameters on the degradation of aromatic pollutants, one variable at a time approach is included. Effect of various external process factors are studied including temperature, inoculum volume, initial pollutant concentration, rotational speed, pH, etc. Standard curves (R2 > 0.95) were made by using HPLC and GC-MS to quantify five gradients dilution of substrate stock solution and were used for translating peak area of sample into concentration (mg/L), which in order to further calculate the biodegradation rate. The biodegradation rates were calculated as the following formula:

$$Degradation\ rate\ = \frac{initial\ concentration\ of\ substrate\ (Ci\ ) - residual\ concentration\ of\ substrate\ (Cf)}{Ci}$$

(2)

6.2.6 BIODEGRADATION KINETICS

Biokinetics study can follow under two different conditions namely non inhibitory conditions and inhibitory conditions. When the pollutant load is smaller the microbial growth tends to follow Monod growth model which illustrates the kinetics of the bacterial growth. The equation for Monod model is as follows:

$$\mu = \frac{\mu m * S}{Ks + S}$$

(3)

μm = max specific growth rate (1/time) of the culture

μ = specific growth rate (1/time)

S = substrate concentration (mg/L)

Ks = Affinity constant or half – saturation constant (mg/L)

From the intercept the value of Ks and μm can be calculated. But many times, when the pollutant load is higher modified Monod model is used also named as Haldane model. It incorporates the inhibition factor due to substrate toxicity. The equation for modified Monod model is given as

$$\mu = \frac{\mu m * S}{Ks + S + \frac{S^2}{Ki}} \quad (4)$$

where Ki = inhibition constant (mg/L) for the substrate toxicity.

Experiments were performed at optimum environmental conditions using different initial pollutant concentrations (10 -50mg/L) to estimate the effect of pollutant on microbial growth. The value of μ was determined at the exponential phase of the growth curve. From the linear plot of X vs. ln (Sx/S), after a short lag phase, the value of μ for an initial phenol concentration (S) is obtained, where X is the cell concentration in absorbance unit at an OD of 600 nm. From the values of μ vs. S, the values of μmax, Ks, and Ki could be obtained using regression analysis. All the experiments were carried out under the optimum culture conditions for these strains.

6.3 DATA FINDINGS AND DISCUSSIONS

6.3.1 MORPHOLOGICAL IDENTIFICATION

The isolated organism from marine waters was identified as *Leclercia* sp according to 16S rDNA analysis and it is submitted at NCBI. The other pure microbial strains were purchased from Microbial gene bank of IMTECH (Institute of Microbial Technology), Chandigarh, India. The strains purchased were MTCC (Microbial Type Culture Collection) coded – *Pseudomonas mendocina* (MTCC 11808) and *Bacillus pumilis* (MTCC 2466). *Dietzia* sp was also used for the experimental set up which was isolated from textile industry. From Gram staining it was observed that both *Pseudomonas* sp and *Leclercia* sp are Gram negative whereas *Bacillus* sp and *Dietzia* sp are Gram positive. The gram negative ones have rod like structure , both having short rods but the gram positive ones vary between cocci and short rods. Sometimes chain formation was observed under the microscope.

Table 6.2 : Colony morphology of the selected microbial strains

morphology of a bacterial colony	*Pseudomonas* sp	*Bacillus* sp	*Dietzia* sp	*Leclercia* sp
Size.	Small	Medium	Small	Small
Shape.	Round	Round	Round	Round
Color	Yellowish white	White	Reddish yellow (pale coloured)	Creamish white
Texture.	Glossy	Opaque	Smooth	opaque
Height	Convex	Flat	Convex	Flat
Edge	Smooth	Rough	Smooth	Smooth

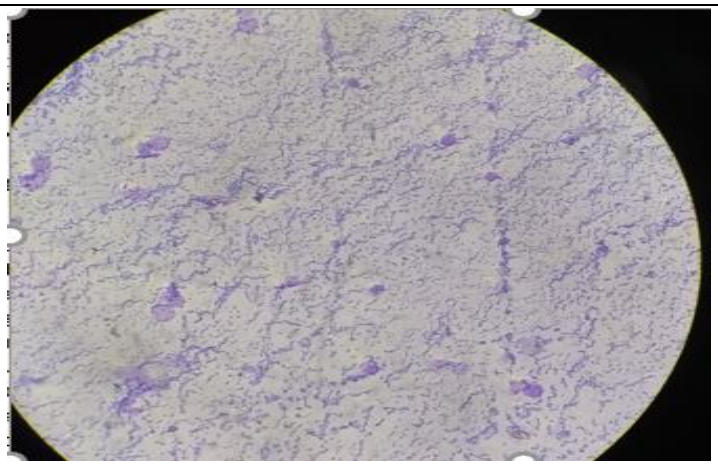

Fig 6.1 : Photographic illustration of Gram staining of *Bacillus* sp

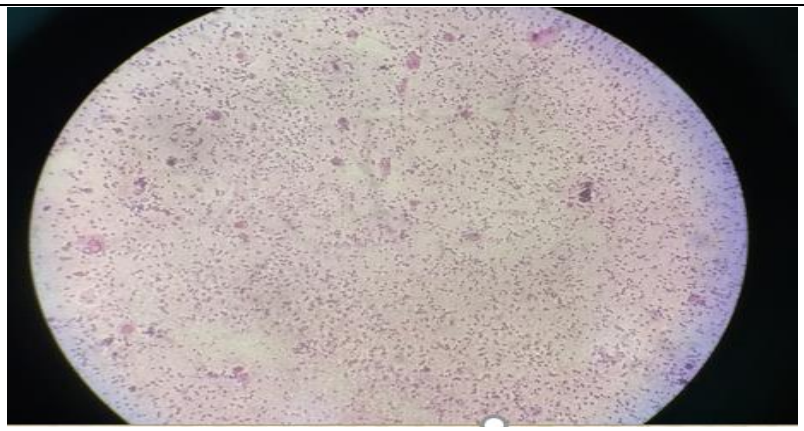

Fig 6.2 : Photographic illustration of Gram staining of *Pseudomonas* sp

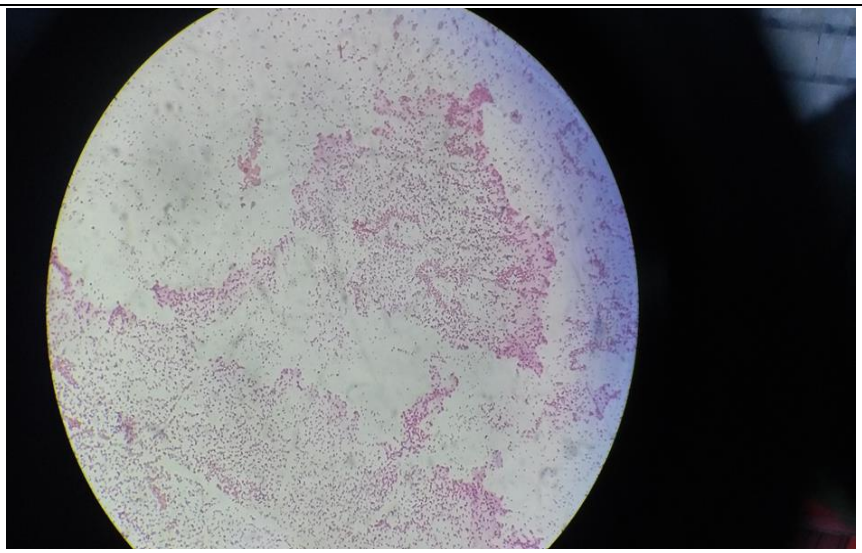

Fig 6.3 : Photographic illustration of Gram staining of *Leclercia* sp

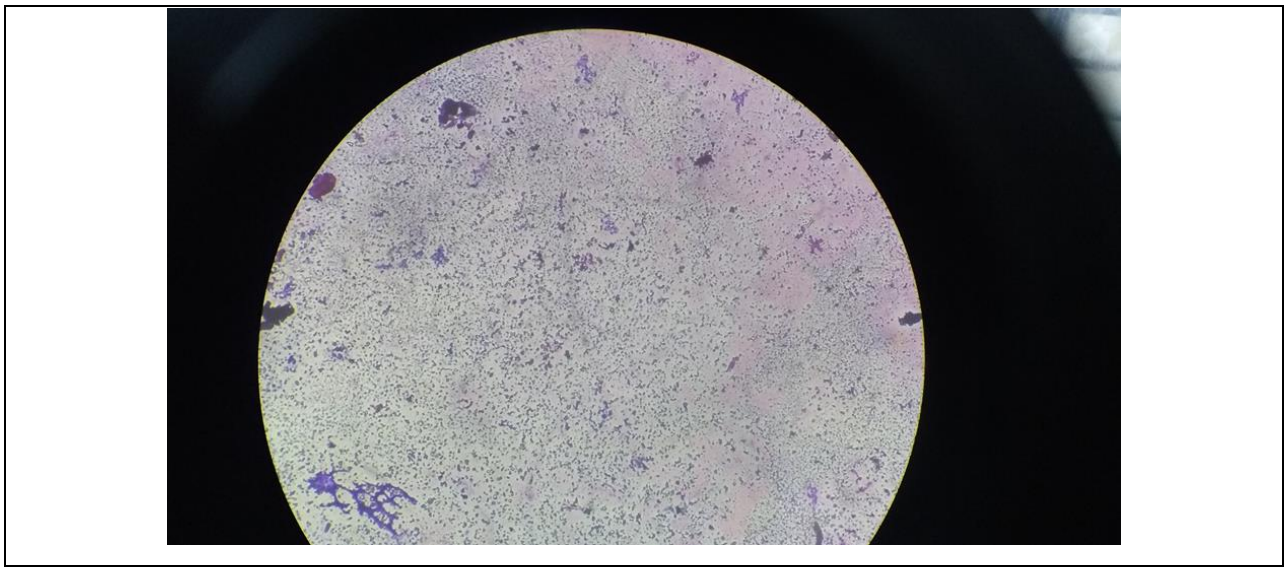

Fig 6.4 : Photographic illustration of Gram staining of *Dietzia* sp

6.3.2 BIOCHEMICAL IDENTIFICATION

The purchased biochemical test kits for IMViC assay was used under sterile conditions to inoculate the kit with microbial strains.

Fig 6.5 : Photographic illustration of IMViC test kits

Table 6.3 : IMViC tests of the selected microbial strains

Test	Original medium colour	Positive test	Negative test	*Pseudomonas*	*Bacillus*
Indole	Colourless	Reddish pink	Colourless	- ve	- ve
Methyl red	Colourless	Reddish	Yellowish orange	+ ve	- ve
Voges Proskauer's	Colourless	Red	Copper	+ ve	+ ve
Citrate utilization	Green	Blue	Green	+ve	+ ve
Glucose	Red	Yellow	Red	+ ve	+ ve
Adonitol	Red	Yellow	Red	- ve	- ve
Arabinose	Red	Yellow	Red	-ve	- ve
Lactose	Red	Yellow	Red	-ve	- ve
Sorbitol	Red	Yellow	Red	-ve	- ve
Mannitol	Red	Yellow	Red	-ve	- ve
Rhamnose	Red	Yellow	Red	-ve	- ve
Sucrose	Red	Yellow	Red	-ve	- ve

For *Dietzia* sp and *Leclercia* sp all the IMViC tests results obtained were all negative.

For *Leclercia* sp as it was mentioned the 16s rRNA gene analysis was done at NCBI and the test report is attached next page.

Nucleotide

The Nucleotide database will include EST and GSS sequences in early 2019. Read more.

GenBank

Leclercia sp. strain PD7 16S ribosomal RNA gene, partial sequence

GenBank: MK774724.1

FASTA Graphics

Go to:

```
LOCUS       MK774724               703 bp    DNA     linear   BCT 15-APR-2019
DEFINITION  Leclercia sp. strain PD7 16S ribosomal RNA gene, partial sequence.
ACCESSION   MK774724
VERSION     MK774724.1
KEYWORDS    .
SOURCE      Leclercia sp.
  ORGANISM  Leclercia sp.
            Bacteria; Proteobacteria; Gammaproteobacteria; Enterobacterales;
            Enterobacteriaceae; Leclercia.
REFERENCE   1  (bases 1 to 703)
  AUTHORS   Ganguli,A., Das,P. and S,D.
  TITLE     Degradation of phenol containing wastewater using isolated marine
            microorganism Leclercia sp PD7
  JOURNAL   Unpublished
REFERENCE   2  (bases 1 to 703)
  AUTHORS   Ganguli,A., Das,P. and S,D.
  TITLE     Direct Submission
  JOURNAL   Submitted (10-APR-2019) Chemical Engineering, Jadavpur University,
            Kolkata, Jadavpur University, Kolkata, West Bengal 700032, India
COMMENT     ##Assembly-Data-START##
            Sequencing Technology :: Sanger dideoxy sequencing
            ##Assembly-Data-END##
FEATURES             Location/Qualifiers
     source          1..703
                     /organism="Leclercia sp."
                     /mol_type="genomic DNA"
                     /strain="PD7"
                     /isolation_source="marine water"
                     /db_xref="taxon:1898428"
                     /country="India"
     rRNA            <1..>703
                     /product="16S ribosomal RNA"
ORIGIN
        1 tagagtctgt agaggggggt agaattccag gtgtagcggt gaaatgcgta gagatctgga
       61 gggaataccc ggtggcgaag gcggcccctg gacaaagact gacgctcagg tgcgaaagcg
      121 tggggagcaa acaggattag ataccctggt agtccacgcc gtaaacgatg tcgacttgga
      181 ggttgtgccc ttgaggcgtg gcttccggag ctaacgcgtt aagtcgaccg cctggggagt
      241 acggccgcaa ggttaaaact caaatgaatt gacgggggcc cgcacaagcg gtggagcatg
      301 tggtttaatt cgatgcaacg cgaagaacct tacctactct tgacatccag agaactttcc
      361 agagatggat tggtgccttc gggaactctg agacaggtgc tgcatggctg tcgtcagctc
      421 gtgttgtgaa atgttgggtt aagtcccgca acgagcgcaa ccctttatcct ttgttgccag
      481 cggttaggcc gggaactcaa aggagactgc cagtgataaa ctggaggaag gtggggatga
      541 cgtcaagtca tcatggccct tacgagtagg gctacacacg tgctacaatg gcgcatacaa
      601 agagaagcga cctcgcgaga gcaagcggac ctcataaagt gcgtcgtagt ccggattgga
      661 gtctgcaact cgactccatg aagtcggaat cgctagtaat cgt
//
```

6.3.3 BIODEGRADATION OF ORGANIC POLLUTANT BY DIFFERENT MICROORGANISMS

The various external and internal factors govern the biodegradation process - Temperature, pH of the solution, Initial concentration of the pollutant, Inoculum volume of the microbial biomass, Agitation speed, Contact time etc. The model organic pollutant utilized for the biodegradation assay is Phenol as it is fairly soluble in aqueous solution. Simulated synthetic solution of phenol were prepared from the stock solution (method mentioned in the previous chapter 4). All the experiments were conducted under sterile conditions in the laminar air flow chamber. Optimal conditions estimated to be pH 6, Temperature 30°C, RPM 120, Initial Concentration 10mg/L and microbial inoculum volume 1% of the total solution.

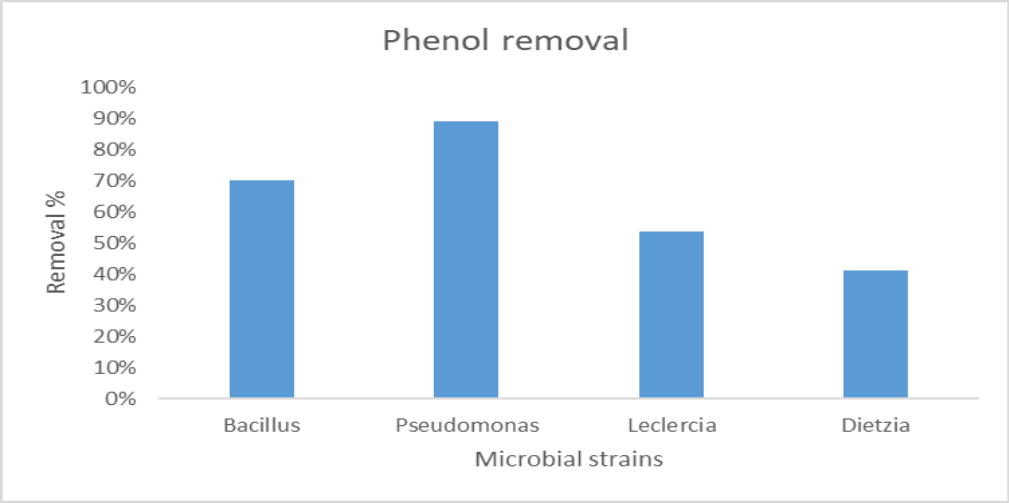

Fig 6.6 : Removal % of phenol by the selected microbial strains at optimal condition.

It was observed that both *Pseudomonas* sp and *Bacillus* sp had better removal % than the other two microorganisms. The contact time study showed the similar trend of *Pseudomonas* sp having higher removal % of phenol followed by *Bacillus* sp. Thus, the further studies were continued with the prototypical gram positive and gram-negative microorganisms - *Pseudomonas* sp and *Bacillus* sp showing higher degradation potential.

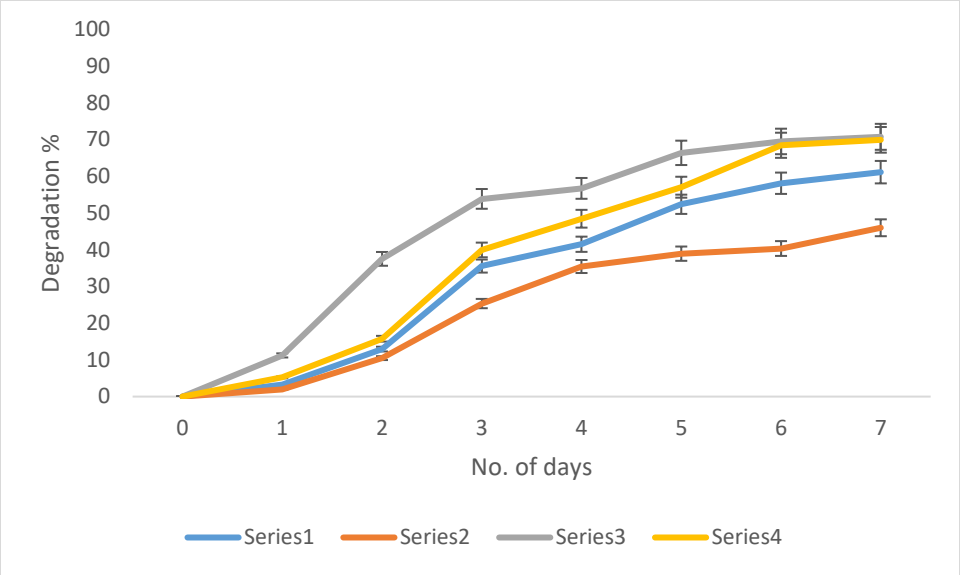

Fig 6.7: Effect of contact time on phenol removal % (Series 1 - *Leclercia* sp ; Series 2 – *Dietzia* sp ; Series 3 - *Pseudomonas* sp; Series 4 - *Bacillus* sp

6.3.3.1 EFFECT OF TEMPERATURE

Temperature is an important factor necessary for the viability of microorganisms and to keep the enzyme activity going without any interference. Both microorganisms and the enzymes secreted by them are temperature sensitive so temperature factor must be taken into consideration for biodegradation process. In the batch scale study temperature was monitored in the range of 25 °C to 40 and it was observed that maximum removal % was obtained at optimal temperature of 30°C. The other parameters were fixed – pH 6.5, initial contaminant concentration 10 mg/L, inoculum volume 1% of the 100ml simulated solution. Drastic reduction in the removal % was observed at higher temperature. This is in coherent with the sensitivity of microorganisms to higher temperature and inactivity of the microbial enzymes.(Roy et al., 2018). At higher temperature for a short duration also microorganisms may lose their culture ability (Munna et al., 2016).

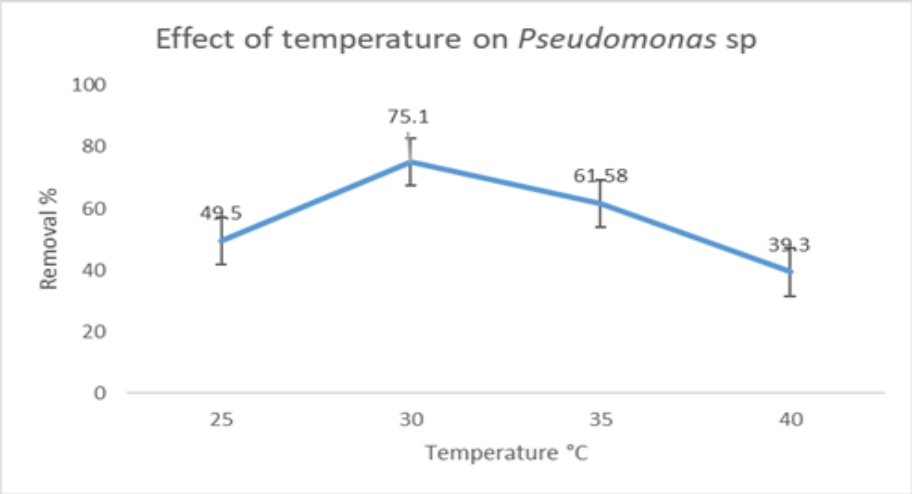

Fig 6.8 : Effect of temperature on phenol degradation by *Pseudomonas* sp

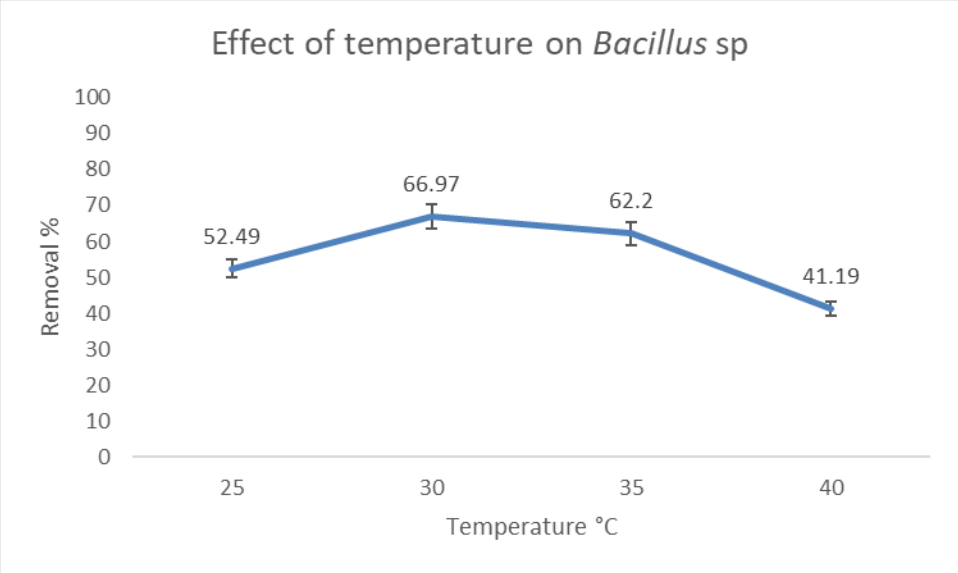

Fig 6.9 : Effect of temperature on phenol degradation by *Bacillus* sp

6.3.3.2 EFFECT OF pH

pH is a crucial factor to understand the stability of the system. To understand the effect of pH , the other variables were kept constant - initial contaminant concentration 10 mg/L, inoculum volume 1% of the 100ml simulated solution, temperature 30 °C. At extreme pH (acidic or basic), the viability of

microorganism may be questionable. Optimal pH is needed for proper growth of the microbial culture and thus degradation % may also increase. At extreme pH conditions the electrostatic effects may hinder the movement of the chemical molecules through the cell membrane. In this study it was observed that both the microorganisms showed highest degradation of phenol under optimal conditions of 6.2 . Although in slightly acidic conditions, the degradation potential of *Pseudomonas* sp is better than the *Bacillus* sp. But drastic reduction is seen in the alkaline range of pH. This may be explained by the chelation of phenol at higher pH making it difficult to degrade.

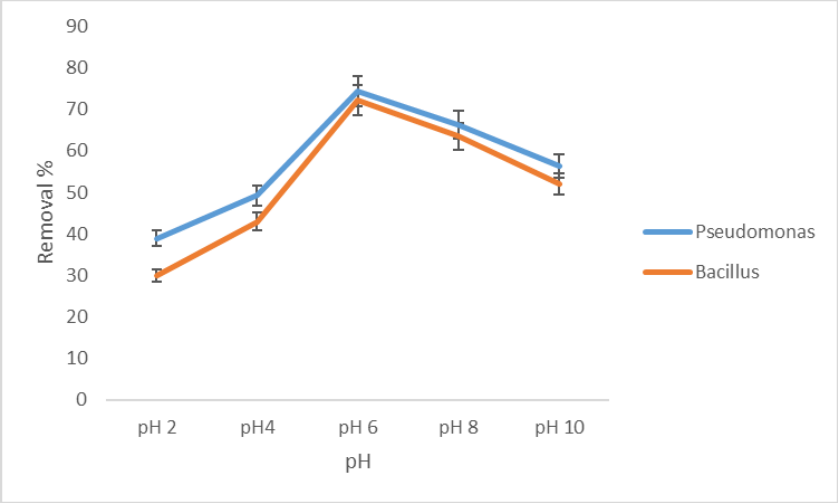

Fig 6.10 : Effect of pH on phenol degradation

6.3.3.3 EFFECT OF INITIAL CONCENTRATION

To understand the effect of initial concentration of phenol on the degradation % of the microorganisms, various concentration was studied – 5 mg/L, 10mg/L, 25mg/L, 50mg/L . the other factors were kept constant - inoculum volume 1% of the 100ml simulated solution, temperature 30 °C, pH 6.5. It was observed that the maximum degradation % was obtained at 10mg/L phenol concentration. This also infers that phenol also acts as a carbon source providing nutritional supplement and energy for the microorganisms to grow in the minimal media which is an incomplete growth medium devoid of any energy sources. It was observed that at higher concentration (50 mg/L), phenol acts an inhibitory agent and thus the degradation % reduces drastically. Another interesting fact was noted that at 5mg/L the degradation % was also less. This maybe explained by the fact that nutritional carbon source became a

limiting factor at such low concentration. Thus 10mg/L was chosen as the optimal dose for organic pollutants – Pyrene, Naphthalene, and Phenol.

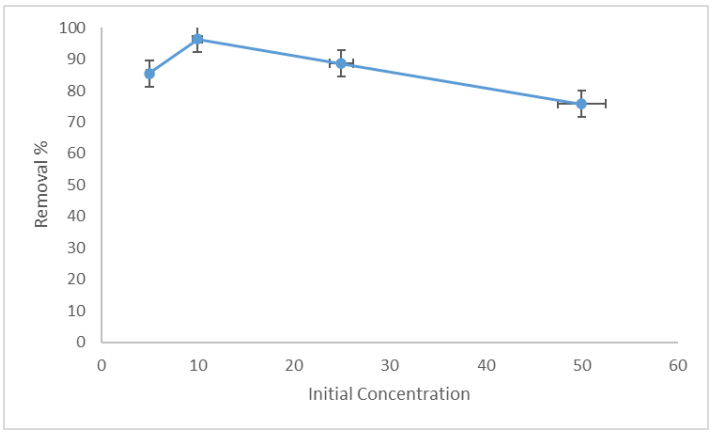

Fig 6.11 : Effect of initial adsorbate concentration (Phenol) on degradation by *Pseudomonas sp*

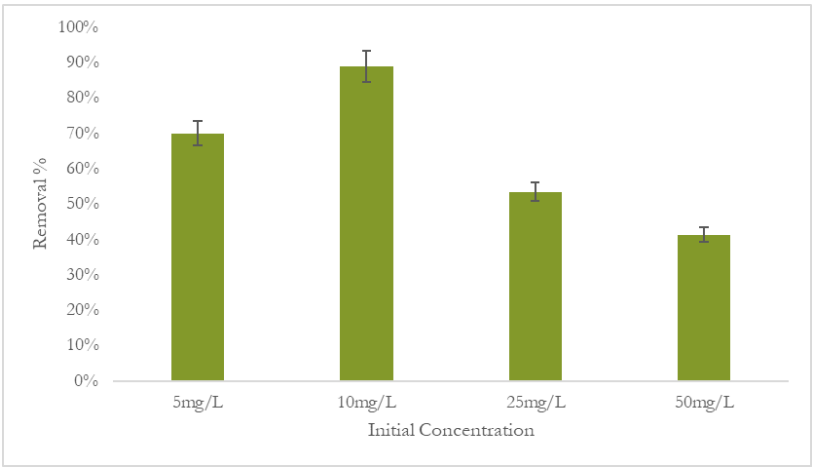

Fig 6.12 : Effect of initial adsorbate concentration (Phenol) on degradation by *Bacillus sp*

6.3.3.4 EFFECT OF INOCULUM VOLUME

Inoculum volume determines the amount bof inoculum given with respect to the fixed amount of adsorbate solution. For inoculum volume study we chose 0.5%, 1% and 2% volume of the original solution as the inoculum seed volume.The maximum degradation % was observed in the inoculum volume of 1ml/50ml of the adsorbate solution. Beyond that amount, decrease in the removal % is noticed which can be explained by the space constraint. Batch scale studies are done in conical flask with a fixed amount of solution in a finite space. The microbial population if grows more than the carrying capacity of the system then overcrowding and aggregation of the cells occur. This reflects in the decrease of the degradation %. Similar results were seen in Phenol

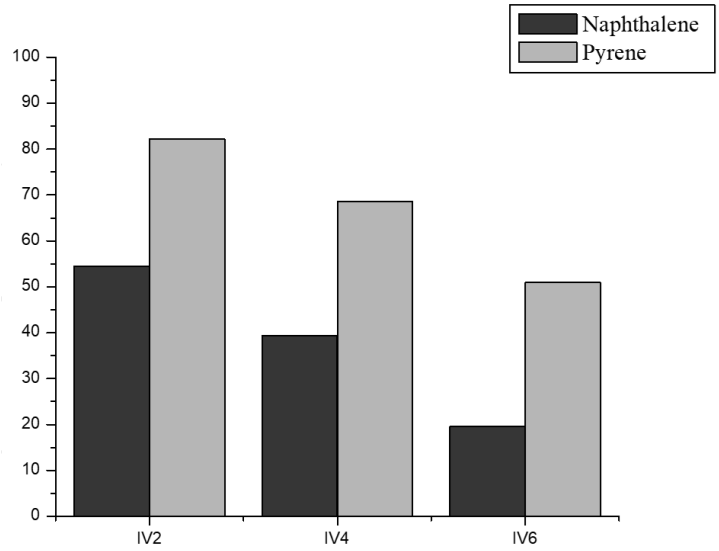

Fig 6.13 : Effect of inoculum volume on the degradation of organic pollutants (IV = Inoculum Volume).

6.3.4 BIOKINETICS OF BACTERIAL CELL GROWTH

The bacterial growth can be divided into many phases – lag phase, log / exponential phase, stationary phase and finally the death phase. In control group the microorganisms were grown in a complete media (Luria or Nutrient broth). The experimental group was grown in minimal media supplemented by phenol and naphthalene (20mg/L) as the carbon source providing them energy. Growth kinetics of *Pseudomonas* sp and *Bacillus* sp were assessed to understand the various growth phase of the individual microorganism and to obtain their doubling time. It was observed that from the start of the experiment the rate of growth is slow due to lag phase. After a considerable amount of time, log phase is started

early in case of complete nutrient media but it is slower in case of media supplemented with organic compounds. Generally, 24 hours – 48 hours is needed for bacterial culture to enter into log phase. In minimal media the duration might be longer sometimes depending on the complex aromatic rings present in the compound which are resistant to degradation. The bioavailability of the compound is important for degradation to occur.

The bacterial growth is observed by measuring the optical density at 600nm with the help of UV – ViS spectrophotometer (Perkin Elmer). The specific growth rate is calculated by subtracting successive OD readings and dividing the reading by the time interval between the readings. The doubling time is also measured from the exponential part of the growth curve. The doubling time of *Pseudomonas* sp is 29.12483 mins whereas the doubling time for *Bacillus* sp is 35.53740 mins. About 8.40 *10 ^10 cells grow per hour in case of *Pseudomonas* sp in normal broth at 360mins and about 8.12 *10^10 cells grow in case of *Bacillus* sp in normal condition. After addition of organic compounds, the growth rate for *Pseudomonas* sp is 7.7 *10^9 cells /hr whereas for *Bacillus* sp it is 7.5 *10^9 cells /hour.

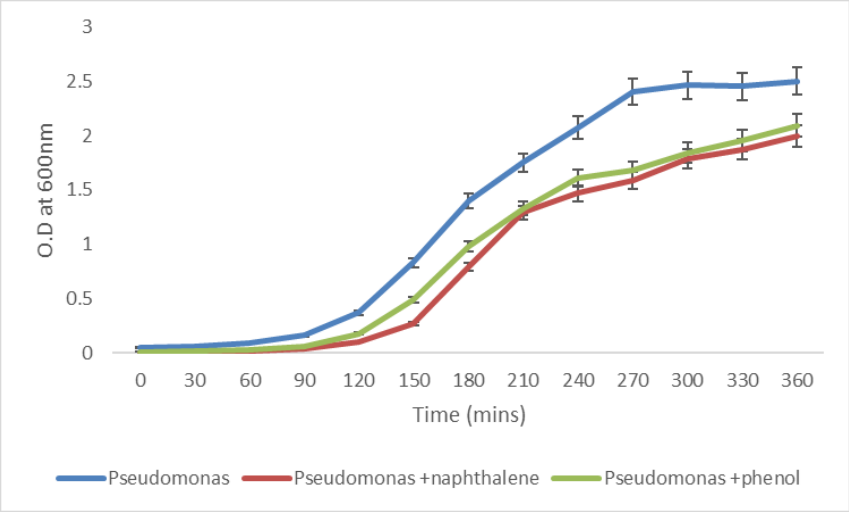

Fig 6.14 : Different phases of growth in *Pseudomonas sp* under normal condition and under supplemented conditions

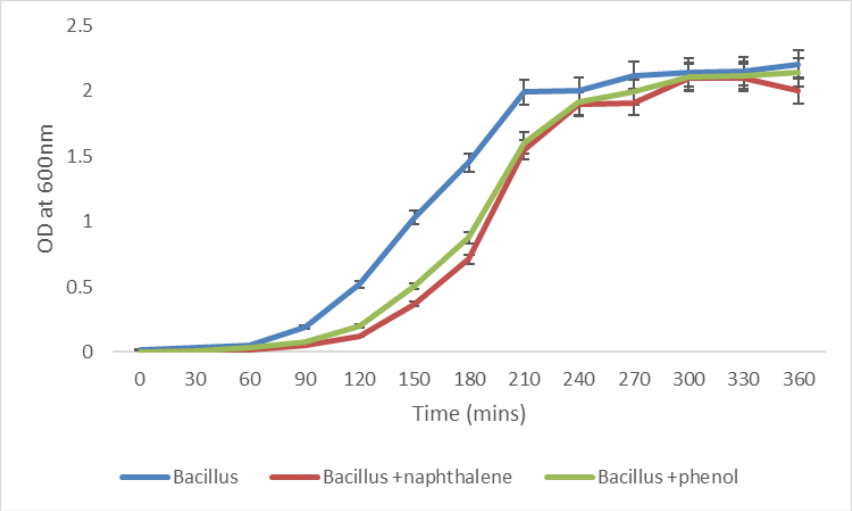

Fig 6.15 : Different phases of growth in *Bacillus sp* under normal condition and under supplemented conditions

6.3.5 FTIR SPECTRAL ANALYSIS

The FTIR spectral analysis of the adsorbate solution before and after degradation shows significant changes. The liquid part is analyzed by the ATR mode of the FTIR (Perkin Elmer) which requires minimal sample processing. Absorption bands below 1000 -1500 cm-1 indicates the compound to be aromatic in nature. After degradation by bacterial strains the benzene ring or aromaticity is reduced thereby indicated by loss of peaks below 1000 cm-1. Additional peaks were observed which are present in the spectra might have been generated due to degradation of organic pollutants. Absence of those peaks confirm the cleavage of the aromatic bonds. The intensity of the peaks has also reduced which confirms degradation of the organic compounds (Roy et al., 2018).

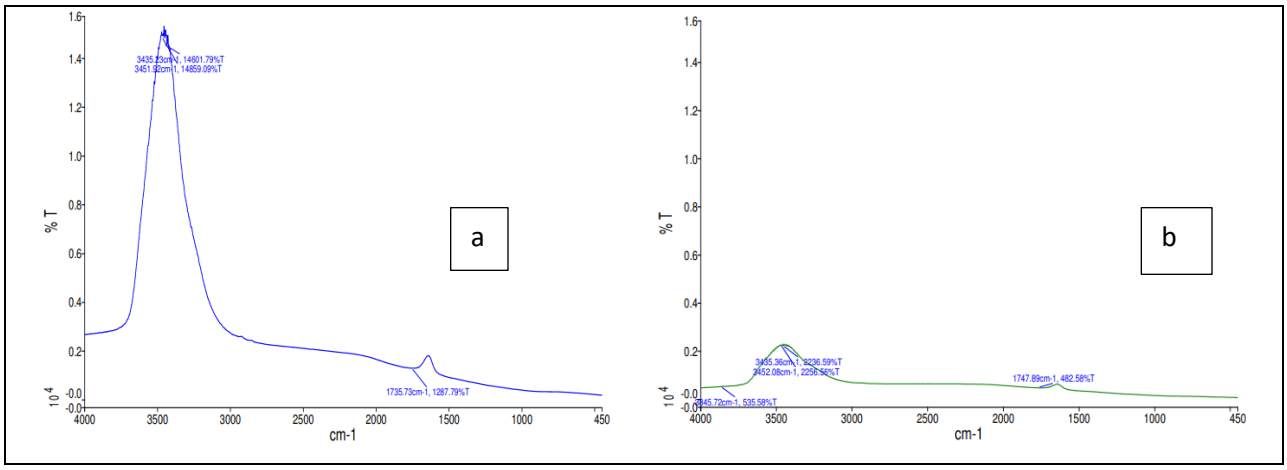

Fig 6.16 : FTIR spectra of phenol solution (a) Before degradation (b) After degradation by *Pseudomonas sp*

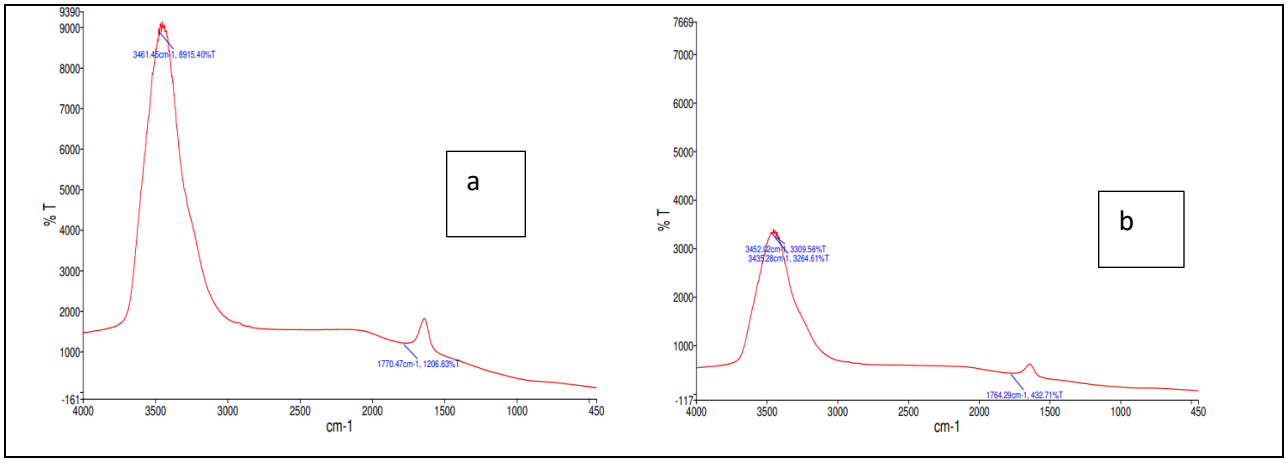

Fig 6.17 : FTIR spectra of phenol solution (a) Before degradation (b) After degradation by *Bacillus sp*

6.3.6 HPLC ANALYSIS AND GC-MS ANALYSIS

The following chromatograms were obtained when the resultant solution is analyzed by HPLC and GC -MS. Before analysis pre treatment of the sample was necessary and the operating conditions were mentioned in section 6.2.4.3 . The area analysis of the HPLC proves reduction in the concentration of the original phenol solution which confirms biodegradation of phenol. In the GC -MS chromatogram the shift in the peak area denotes metabolic products formation which have successive retention times as similar to phenol.

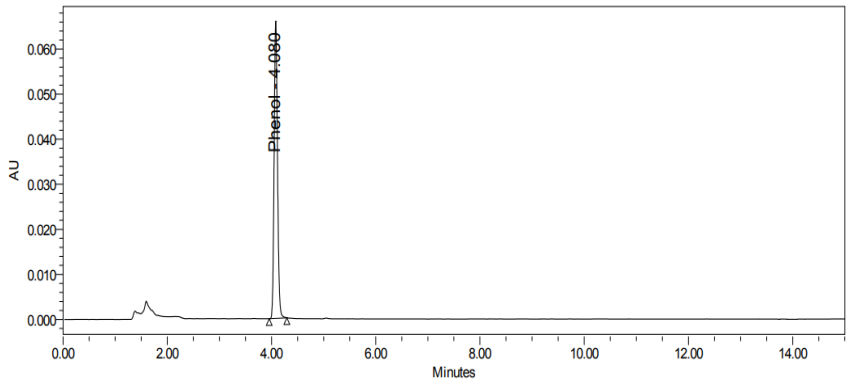

a

	Peak Name	RT (min)	Area (µV*sec)	% Area	Height (µV)	Amount	Units
1	Phenol	4.080	297378	100.00	65891	50.000	ppm

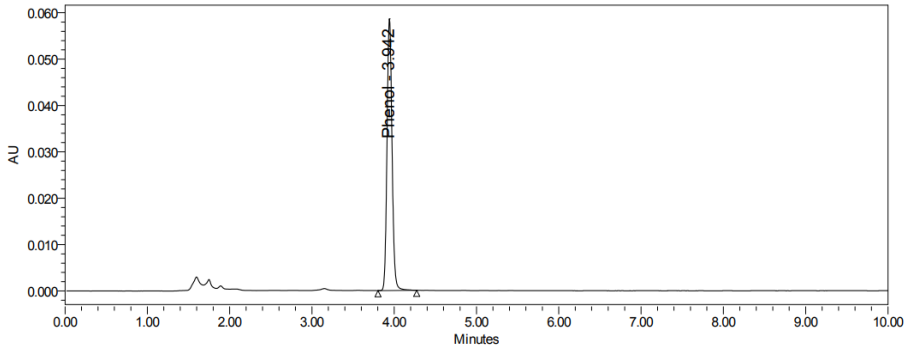

b

	Peak Name	RT (min)	Area (µV*sec)	% Area	Height (µV)	Amount	Units
1	Phenol	3.942	247729	100.00	58699	41.652	ppm

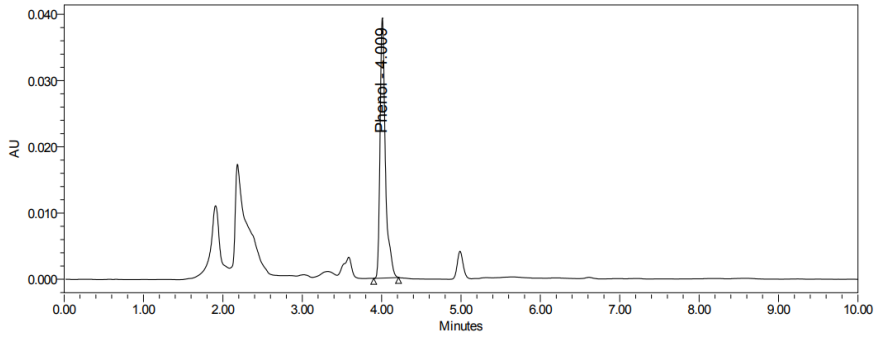

c

	Peak Name	RT (min)	Area (µV*sec)	% Area	Height (µV)	Amount	Units
1	Phenol	4.009	183221	100.00	39281	30.617	ppm

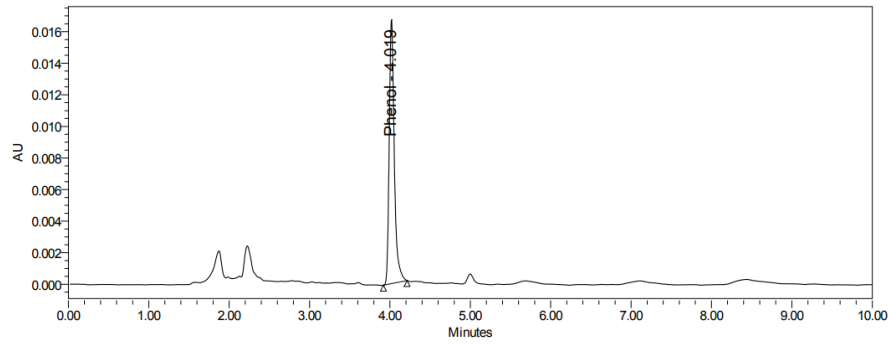

d

	Peak Name	RT (min)	Area (µV*sec)	% Area	Height (µV)	Amount	Units
1	Phenol	4.019	73161	100.00	16709	12.226	ppm

Fig 6.18 : HPLC Chromatograms of phenol – (a) Initial phenol solution (b) after degradation by isolated *Leclercia* sp (c) After degradation by *Bacillus sp* (d) After degradation by *Pseudomonas sp*

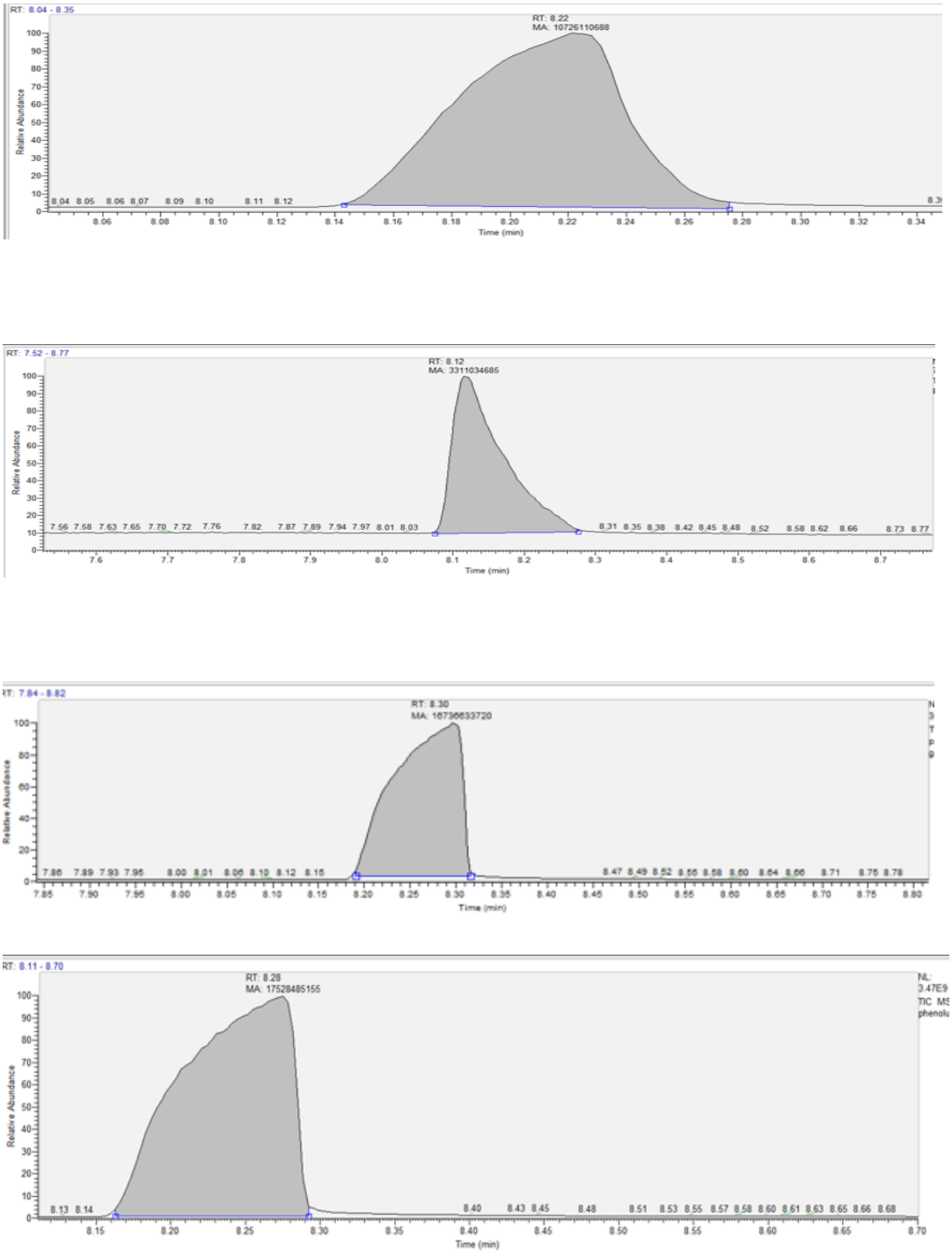

Fig 6.19 : Chromatograms of GC – (a) Original phenol Solution (b) After degradation by *Pseudomonas sp* (c) After degradation by *Bacillus sp* (d) After degradation by isolated *Leclercia* sp

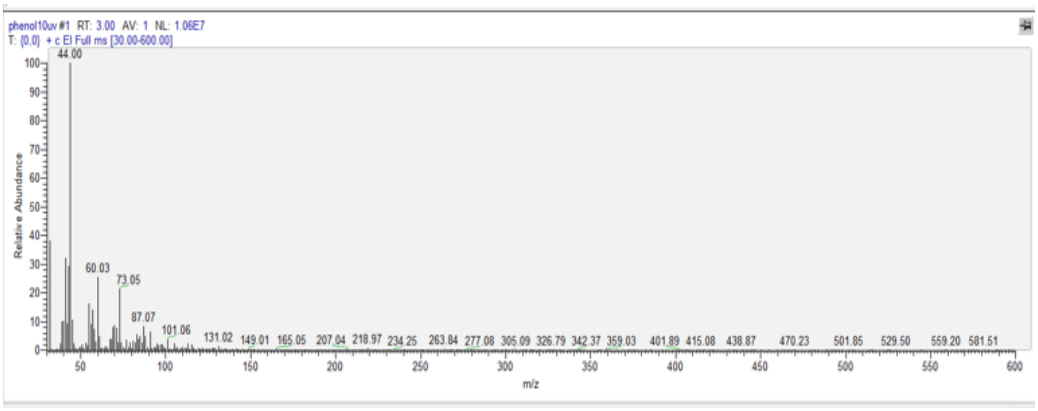

a

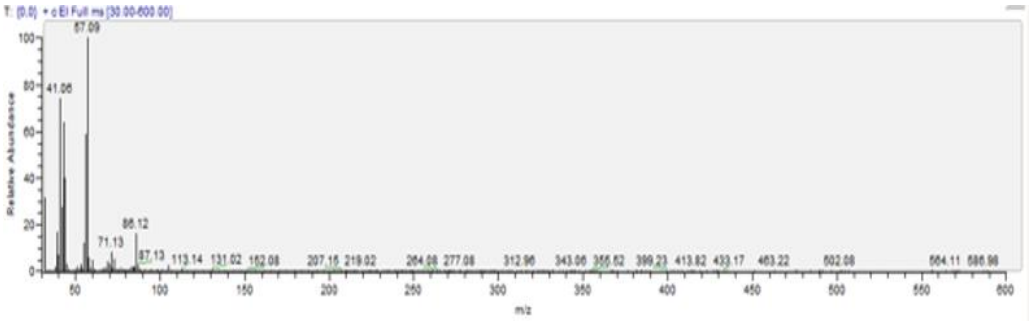

b

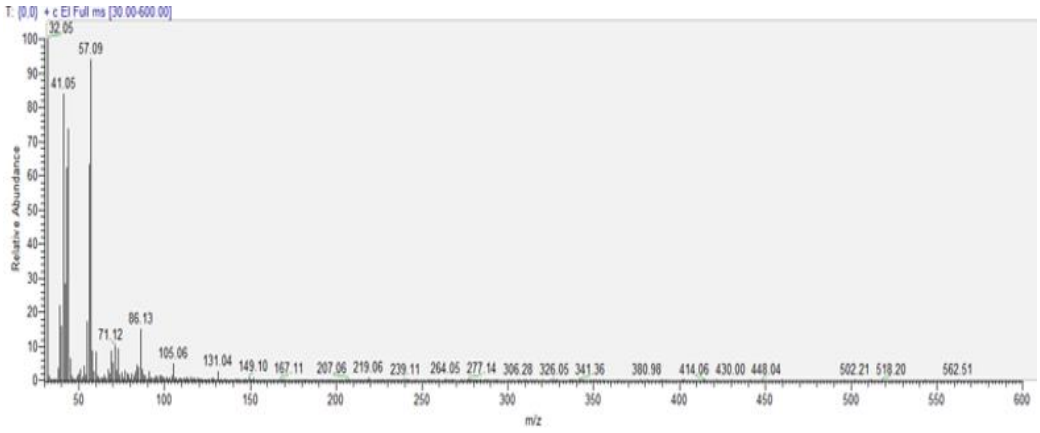

c

Fig 6.20 : Mass spectrum obtained from GCMS – (a) Original phenol Solution (b) After degradation by *Pseudomonas sp* (c) After degradation by *Bacillus sp*

Table 6.4 : Library search result of the mass spectrum (Thermo Xcalibur Qual browser)

Library Search Results

Hit	SI	RSI	Prob	Name	Library Name
1	950	953	71.53	Phenol	replib
2	930	938	71.53	Phenol	NISTDEMO
3	930	938	71.53	Phenol	mainlib
4	930	930	71.53	Phenol	replib
5	922	929	20.65	Phosph...	NISTDEMO
6	922	929	20.65	Phosph...	mainlib
7	869	870	4.08	2-Vinylfu...	mainlib
8	836	848	1.06	Formic a...	mainlib
9	827	829	0.77	Carbami...	NISTDEMO
10	827	829	0.77	Carbami...	mainlib
11	825	835	0.71	3-Methyl...	NISTDEMO

Hit	SI	RSI	Prob	Name	Library Name
1	796	869	55.05	Benzene, (2,4-cyclop...	mainlib
2	768	903	15.89	Acenaphthene	NISTDEMO
3	768	903	15.89	Acenaphthene	mainlib
4	759	934	11.54	Naphthalene, 2-ethe...	replib
5	759	844	11.54	Biphenyl	replib
6	746	839	15.89	Acenaphthene	replib
7	743	850	15.89	Acenaphthene	replib
8	740	848	15.89	Acenaphthene	replib
9	726	889	3.02	1,4-Ethenonaphthale...	mainlib
10	715	869	11.54	Biphenyl	replib
11	714	916	11.54	Naphthalene, 2-ethe...	replib
12	708	812	11.54	Biphenyl	replib

6.4 CONCLUDING REMARKS

Biodegradation is an important method for treatment of wide variety of pollutants. Biological treatment methods are attractive because they are easier, energy efficient, ecofriendly, viable, safer than chemical approaches. To achieve sustainable development goals along with economically viable options, bioremediation still remains the preferred choice (Imam et al., 2021). In this study, prototypical gram positive and gram-negative bacteria were selected for the experiment. It was observed that *Pseudomonas sp showed* better degradation results than *Bacillus sp .* Isolated microbial strain of *Leclercia sp* and *Dietzia* sp was also utilized for the degradation study. 16 S rRNA analysis of the isolated microorganisms were done. All other morphological and biochemical parameters were studied. To confirm degradation of organic contaminant by the bacterial species, the resultant solutions from batch scale studies were analyzed by HPLC and GC- MS analysis. The reduction in the peak intensity and the area confirmed degradation have been occurred and the introduction of new peaks is due to the metabolic products formed due to the biodegradation process.

CHAPTER 7

7 REMOVAL OF ORGANIC POLLUTANT BY INTEGRATED APPROACH OF SORPTION – BIODEGRADATION PROCESS

7.1 CONTEXTUAL INFORMATION

Intensification in the complexity of pollutants emitted via different methods into the environment have led researchers to adopt hybrid processes. With the advancement of science and technologies, hybrid techniques are gaining more preferences over conventional single approach for treatment of pollutants. Conventional treatment technologies and standard water treatment methods are being revamped by the introduction of nanomaterials to increase the process efficiency. Hybridization of processes leads to better removal of persistent pollutants in a coherent manner. As advancement of nanotechnology has occurred gradually, it has been incorporated and utilized in various fields with biological realm being the priority area. Combination of nanotechnology with biological remediation procedures have grab the attention of the researchers presently. Fabrication of various biofunctionalized materials in the nanoscale is thus the key agenda in combining both the fields of biotechnology and nanotechnology. Simultaneous adsorption – biodegradation combines the efficacy of adsorption process with the recyclability and cost effectiveness of biodegradation method. Pollutant degradation and remediation using these materials is thus the key hotspot of the researchers now a days as detailed understanding is needed to contemplate the interaction between the two. Graphene nanomaterials and its derivatives have acted as a scaffold for various bio compounds ranging from proteins to cells (S. Kumar & Parekh, 2020). Physical adsorption or chemical conjugation acts as a driving force of this interaction. Yet again, a huge voluminous literature is present which depicts graphene family nanomaterials having anti-bacterial property. The trend of this paradoxical situation is gradually being resolved with rise in research in the field of synergistic effect of graphene oxide nanomaterial and microorganism as shown in chapter 1. Advantage of addition of bio compounds with graphene family nanomaterial provides better compatible materials which are more soluble with specific selectivity of compounds. Embedding bacteria on adsorbent material provides certain advantages than free cells in terms of substrate attachment and colonization, nullifying the 'washing out' effect. Microbial cultures operate highly efficiently in immobilized form than its free cells. In free cell suspension the dilution effect sometimes cause hindrance with the process of degradation

making it more time consuming. The biodegradation step in the hybrid process helps in converting the pollutants to harmless compound (Y. Zheng et al., 2017).

The following chapter has been divided into **Section – A** Utilization of the prepared bio nano composite to remove organic pollutants from synthetic aqueous media and **Section – B** the mechanism of interaction at the interfacial level between the fabricated GOaN nanomaterial and the selected microbial strains.

SECTION – A

UTILIZATION OF THE PREPARED BIO NANO COMPOSITE TO REMOVE ORGANIC POLLUTANTS FROM SYNTHETIC AQUEOUS MEDIA

7.2 EXPERIMENTAL METHOD

7.2.1 FABRICATION OF GOaN NANOMATERIAL.

The fabrication of GOaN nanomaterial has been discussed in details in Chapter 3. Briefly, all the steps were similar to the previous method with the only major change in the protocol was about the method of drying of the adsorbent. The washed neutralized sample was freeze – dried by Lyophilizer (EYELA, Japan) to reduce the exposure time of the prepared adsorbent to the surrounding thus maintaining the aseptic conditions and thereby diminishing any chance of contamination. The flow chart of preparation process is as given below:

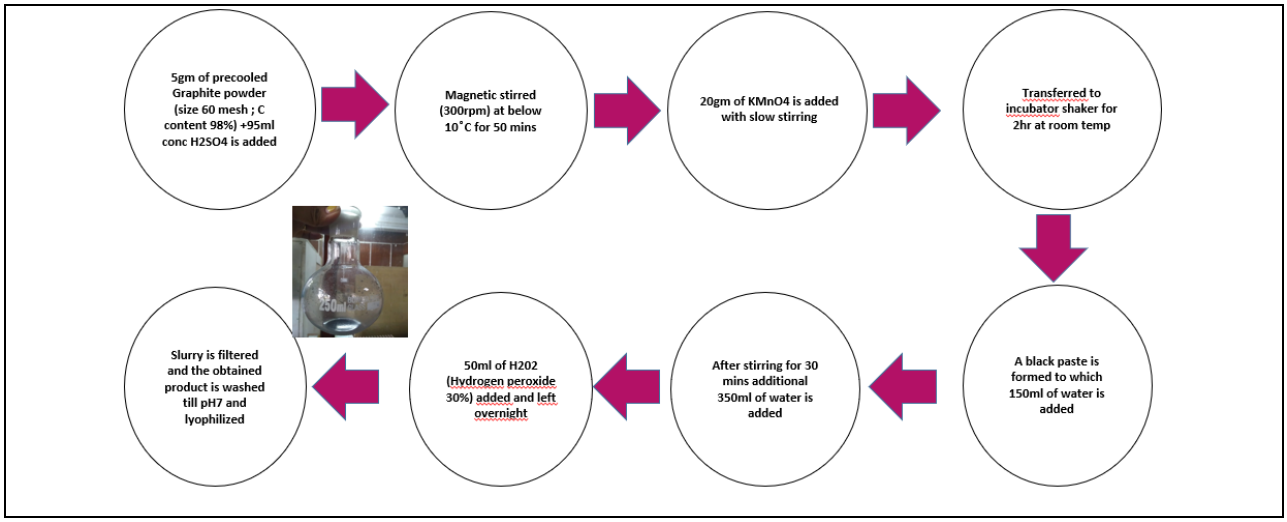

Fig 7.1 : Fabrication steps for GOaN nanomaterial conducive for bacterial attachment. [Inset – photographic visual of prepared material]

7.2.2 BACTERIAL STRAIN ACCLITAMIZATION AND HYBRID BIO - NANOCOMPOSITE FABRICATION

Prototypical Gram-positive and Gram-negative bacteria were chosen to study the effects due to interaction with Graphene oxide nanomaterial. Both *Pseudomonas* sp and *Bacillus* sp showed promising result in the earlier chapter for degradation of PAH(s) and Phenol. These two strains of bacteria are selected as prototypical microorganisms to study the interaction changes between them and fabricated graphene oxide analogous material. The preparation method of microbial culture inoculum has been discussed in earlier chapter 6. The composition of the growing media for bacterial culture – Luria Broth (Complete media – for acclimatization) and Minimal Broth (Specific media – for experimental study) has already been mentioned in chapter 6. The overnight grown cultures with exponential growing phase (10 ^8 cells) are subjected to various steps for formation of bio - nanocomposite (GOaN +P ; GOaN +B) by using fabricated graphene oxide material and Gram negative and Gram positive microorganism. Briefly, microbial cells from exponential phase were gathered by centrifugal force (REMI PR 24 Centrifuge) and washed in isotonic saline solution to minimize physiological changes of the culture condition. The cells (2ml) were resuspended in minimal media (98ml) containing prepared GOaN nanomaterial (2gm). The mixture is stirred in incubator shaker (REMI) at 30°C and left overnight. The final product is filtered via pre sterilized vacuum filtration unit (Tarson) using PTFE membrane (0.2um). The product is further dried using Lyophilizer (EYELA) and stored at 4°C for further studies. The steps of fabrication of the composite are shown in the figure(s) below:

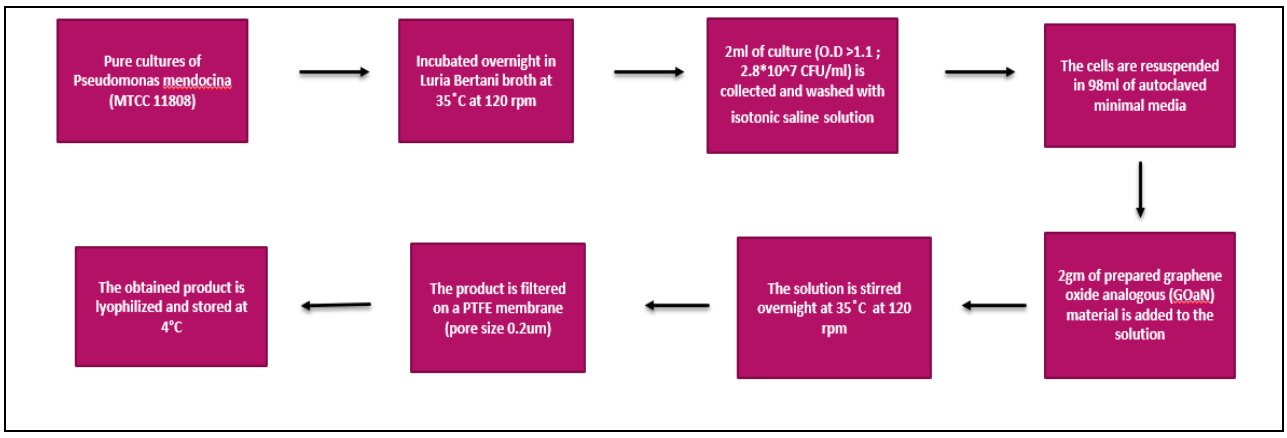

Fig 7.2 : Fabrication steps for GOaN + P bio nanocomposite

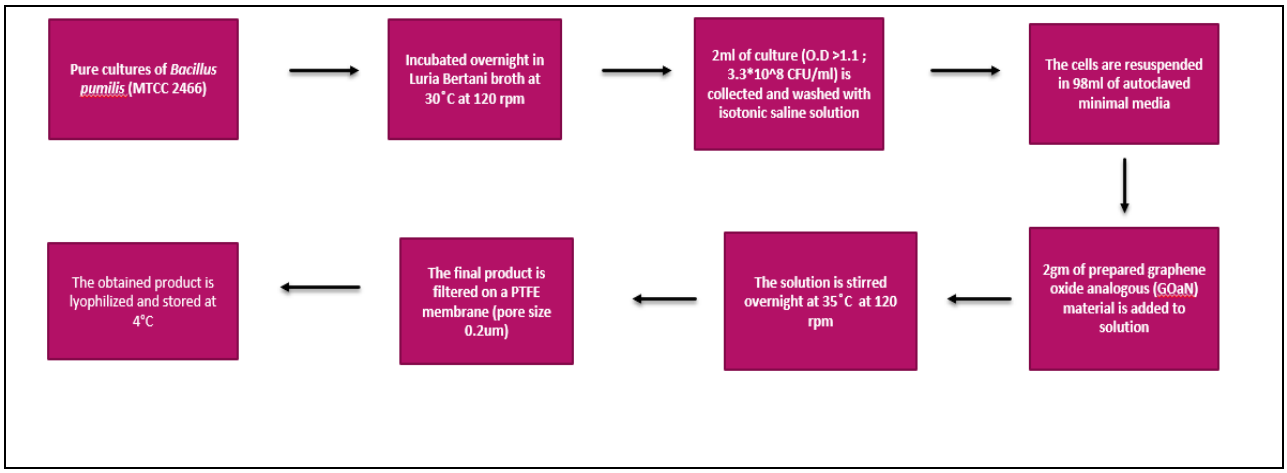

Fig 7.3 : Fabrication steps for GOaN + B bio nanocomposite

Fig 7.4: Photographic visual representation of bio nano composite formed.

7.2.3 CHARACTERIZATION OF THE FABRICATED BIO NANOCOMPOSITE

The characterization of the fabricated bio - nanocomposite was done by spectroscopic and microscopic analysis. Microscopic analysis by Scanning Electron Microscope (ZEISS, Germany) was utilized to prove the embedding of the organism to the material surface. Fluorescence microscopy (LEICA, USA) was applied to see the changes occurring in the aspect of viability of the organism after the interaction between the biological organism and fabricated GOaN nanomaterial interface. Laser based flow cytometer was applied

to estimate the changes in the microbial cells in the bio nanocomposite formation. FTIR (Perkin Elmer Spectrum, USA) spectroscopy method was used to observe the changes in the material due to interaction with bacterial cells.

7.2.3.1 SPECTROSCOPIC TECHNIQUE – FTIR

As mentioned earlier fast and reliable data about the structural fingerprint of the chemical composition of a material could be estimated by FTIR spectra (Legal et al., 1991). Broader chemicals like lipids, proteins, carbohydrates can be assessed which corroborates attachment of bacterial cells by physical means. The samples were observed by KBr Pellet method and also by ATR method. Pellet formation was done by previously discussed methods (Chapter 3) and the samples were scanned in the wavelength region of 450 - 4500 cm-1. The ATR method doesn't require pellet formation and thus samples can be directly assessed without any further preparation method. The scanning range for ATR is also in the wavelength region of 450 - 4500 cm-1.

7.2.3.2 MICROSCOPIC TECHNIQUE – SEM (SCANNING ELECTRON MICROSCOPE)

To study and analyze the surface morphology of biological samples SEM remains one of the preferred choices of the researchers. Excellent high-resolution images are produced by SEM which are not obtained from light optical microscope. As SEM operates under vacuum condition, the samples should be prepared carefully. Fixation and drying of biological samples during sample preparation should be done carefully to reduce errors. Among various methods of drying, Critical point drying (CPD) involves numerous time-consuming steps. Hexamethyldisilane (HMDS) is an alternative to CPD but it is not preferred due to toxic fumes evolution and high flammability (Ali et al., 2021). Air drying under sterile conditions may reduce artefact formation and gradual removal of water by ethanol is prescribed and used for biological sample preparation. To observe the surface morphology of the nanocomposite formed, scanning electron microscope is utilized. The preparation of the sample involved drop casting the sample diluted with PBS (Phosphate buffer solution) on to a glass surface. Fixation with 2% Glutaraldehyde (Sigma-Aldrich) for 20 minutes was done and again rinsed with phosphate buffer to remove excess glutaraldehyde. The sample was then immediately subjected to gradient dehydration by using 30 %, 50 %, 70 %, 90 %, and Absolute ethanol (Sigma-Aldrich) for 1.5 minutes at each concentration (Ali et al., 2021). The process was done in Laminar to reduce contamination and maintain sterilized conditions. Finally, the samples were coated by sample sputter coater (Quorum Q150R ES, UK) with a conducting material (Au – gold) and was observed under electron microscope under magnification of 1000X.

7.2.3.3 MICROSCOPIC TECHNIQUE – FLUORESCENCE MICROSCOPY

Fluorescence microcopy is an excellent tool to distinguish between living cells and dead apoptotic cells (Mansour et al., 1984). To ascertain the viability of the microorganism after interaction with nanomaterial fluorescent microscopy was utilized. Fluorescent dyes like ethidium bromide (EtBr) and acridine orange (AO) was used simultaneously to differentiate between normal living cells and dead apoptotic cells. In this dual AO - EtBr staining procedure it is observed that EtBr permeates non-living cells or damaged cell membranes imparting a reddish orange coloration whereas acridine orange is bound to DNA and retained by living cells showing green coloration under fluorescence microscope (Wu, 2015). In this process stock solutions of AO and EtBr are prepared in ethanol (3mg/ml of EtBr and 5mg/ml of AO). Equal volume of AO – EtBr (10ul:10ul) is added to 1 ml of PBS (Phosphate buffer saline) and it was added to 0.5ml cell solution to check the viability of cells. The microscope was operated using 495 nm and 515 nm filter to detect the stained cells.

7.2.3.4 LASER BASED TECHNIQUE – FLOW CYTOMETER

Flow cytometers present more sensitivity and it is utilized for more precise analysis (Tombolini & Jansson, 1998). They also give an idea about the apoptotic cells and normal living cells in the solution, although fluorescence microscopy with dual staining is more economical and easily available (Wu, 2015). Green fluorescent protein (GFP) has been used as a marker for different cell type as it formed at intra cellular level without any additional factors or co factors (M. Sharma et al., 2019). It is used to detect stress at cellular level of microorganisms. The emitted fluorescence intensity provides a direct data measured at the single- microbial cell level without any processing steps in in-situ and in real time. In this case the experiments were carried out on a BD Biosciences LSR II flow cytometer (USA) with a DPSS 488 nm detector. Briefly, the nanomaterial (GOaN) combined cells were harvested and pelleted by centrifugating at 5000×g for 15 mins at room temperature. Then the cells were washed and resuspended, in isotonic saline solution. 5 µl of PI (Propidium iodide) was added to the suspension of microbial cells and investigated by flow cytometry. The lower left quadrant of the cytograms shows the viable cells, which exclude PI (Propidium iodide). The upper right quadrant represents the non-viable, necrotic cells, with PI uptake. The lower right quadrant represents the early apoptotic cells, with cytoplasmic membrane integrity still left.

7.2.4 CELL VIABILITY ASSAY – BY AGAR PLATING

Agar plating method is the most convenient and easiest method to enumerate the viability of microbial cells. The microbial viability is estimated on the basis of colony forming units (CFU/ml) as each colony is estimated to be each bacterial cell capable of growth and division. The effect of prepared GOaN nano adsorbent on the viability of the microorganisms – Gram positive (*Bacillus* sp) and Gram negative (*Pseudomonas* sp) can be conferred from the visualization of agar plating of various concentration of prepared bio nanocomposite. Agar diffusion plates also helps to see the inhibitory effects of higher concentration (50mg/dl) of nanomaterial on the cell viability whereas growth can be observed in lower concentration (5mg/dl) of nanomaterial on the cell growth. The major obstacle while preparation of agar plates with fabricated GOaN nanomaterial is the change of the colour of agar plates. This causes hindrance while calculating the CFU units but it can be overcome by properly illumination of the agar pates with the help of a colony counter. The agar plates were estimated with the help of a colony counter and the number of CFU units are calculated accordingly to the following equation:

$$\frac{\text{CFU}}{\text{ml}} = \frac{\text{No. of colonies} \ * \ \text{Total dilution factor}}{(\text{Volume of culture plated in ml})} \quad (1)$$

7.2.5 ZETA POTENTIAL ANALYSIS – INDICATOR OF CELL VIABILITY AND MEMBRANE DAMAGE

Zeta potential is a useful tool for assessing the surface charge of any material. Its usage has also been extended to bacterial cells as recent studies correlate zeta potential as a tool for assessing membrane damage which in turn gives an idea about cell viability. In general, the surface charge of bacterial cells is negative which is balanced by the charge of the outer medium layer. The interfacial region between the bacterial cell surface and the stationary layer of media surrounding the cell plays a crucial role in maintaining the cell viability. Electrostatic interactions may affect the zeta potential which may alter cell membrane permeability and ultimately may cause membrane damage and cell death.

7.2.6 BATCH SCALE EXPERIMENTS

From the previous chapter it was observed that *Pseudomonas* sp (Gram negative) and *Bacillus* sp (Gram positive) showed higher removal of PAHs and Phenol from its aqueous phase. So, these two prototypical

microbial strains were chosen for henceforth experiments conducted. In this experimental study the above-mentioned bacterial species were immobilized on GOaN nanomaterial fabricated in the lab for utilizing the potency of co – adsorption – biodegradation. Degradation of PAH(s) – Naphthalene and Pyrene and degradation of Phenol is estimated to compare the simultaneous process with the individual processes when applied for pollutant removal. The supernatant was collected by centrifugating the experimental medium at 10000 g for 15 mins. The collected supernatant was analyzed by UV – ViS reflectance spectrophotometer (Perkin Elmer) using quartz cuvette (optical path length -1 cm).

The total percentage of pollutant removal was calculated by the following equation

$$\frac{a-b}{a} * 100 \quad (2)$$

a = Initial pollutant concentration (mg/L)

b = Final pollutant concentration (mg/L)

All the experimentations were recorded thrice to ensure accurateness, repeatability and reproducibility of the statistically significant data values and the error values were less than 5%. The data were analyzed by Origin Software, version 8.

7.2.7 OPTIMIZATION OF THE PROCESS PARAMETERS

Optimization of the design of experiments (DOE) can be done by applying RSM based D – optimal designs for screening of the experimental factors when the variables are less in number. To perceive the interaction effect between the two experimental factor D – optimal design is chosen. It also reduces the experimental run number thus providing cost effective, time saving, decision making solutions. The ANOVA was used for the creation of mathematical relation functions between the variables to establish a link between them (Rahman et al., 2022). R^2 measures the dispersion of data points around a fitted line of regression. Higher R-squared values indicates that there are fewer disparities between the observed and estimated values of the experimental similar set of data. ANOVA estimates whether the process factors and their interactions with each other has an impact on the response of removal % and is statistically significant (probability < 0.05).

7.3 DATA FINDINGS AND DISCUSSIONS

7.3.1 FTIR SPECTRUM ANALYSIS

The FTIR spectra of the prepared nano adsorbent (GOaN) were obtained before and after interaction with biological cell culture. The protuberant band at 3620 cm-1 is due to -OH absorption as with microbial cells the water content is increased in the material. The band at 1620 cm-1 refers to the amide groups and 1700 cm-1 is defined as carboxylate peak (– C=O) of fatty acids denoting presence of bacterial cell wall. A small peak around 1520 cm-1 refers to C-N bending of proteins and peptides. A prominent peak at 1260 cm-1 is due to C-O-C bending of esters. The region between 1200 cm-1 to 900cm-1 represents the saccharide region and thus presence of peaks in the region denotes successful impregnation of bacterial cells on the nanomaterial (GOaN) fabricated. The region between 900 cm-1 to 500 cm-1 is referred to as fingerprint region which is specific for the microorganism (Novais et al., 2019). This proves successful embedding of microorganism on fabricated graphene oxide analogous nanomaterial by physical attachment.

In case of GOaN + P (*Pseudomonas* sp) both amide I and amide II are observed as it may be due to the presence of cell wall in case of gram-negative bacteria. The cell wall is primarily composed of peptidoglycan where the glycan strands are interlinked with short peptides. Several smaller peaks are also observed in the saccharide region which may be accounted due to the presence of an extra layer of cell wall surrounding the cell membrane.

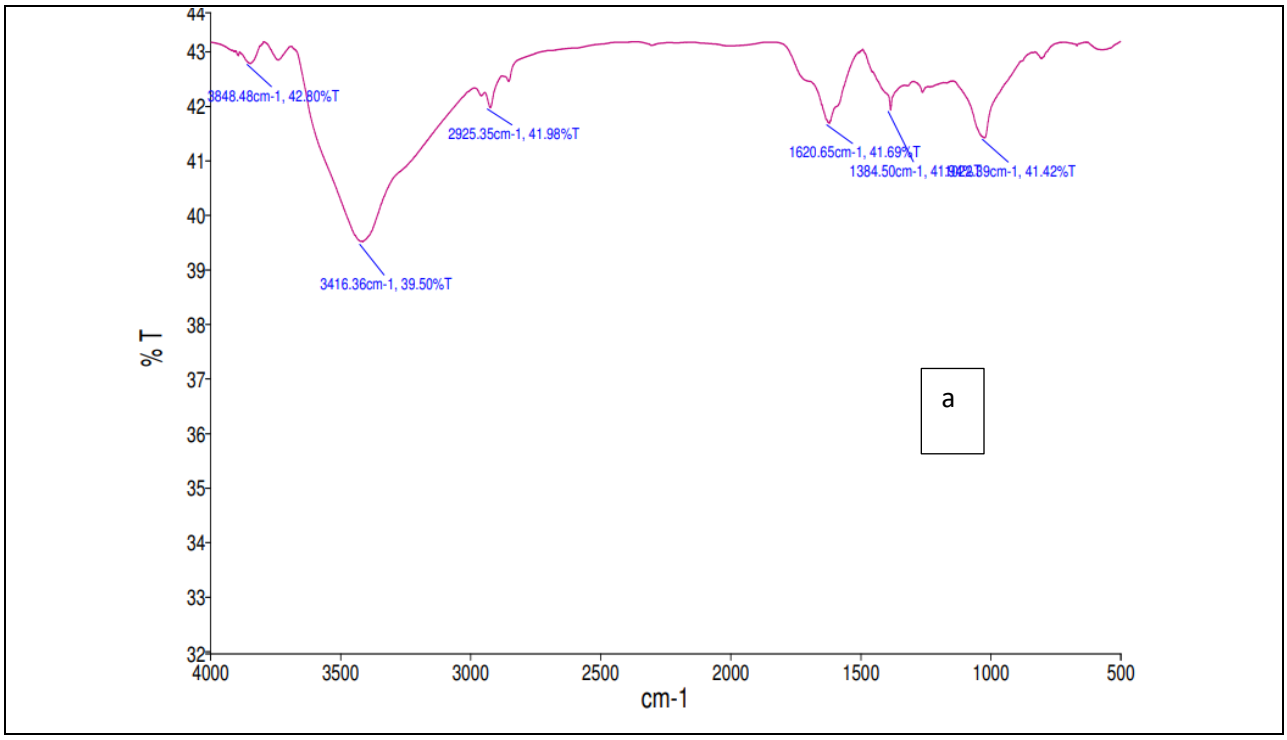
3848.48cm-1, 42.80%T
2925.35cm-1, 41.98%T
1620.65cm-1, 41.69%T
1384.50cm-1, 41.42%T
3416.36cm-1, 39.50%T
% T
cm-1
a

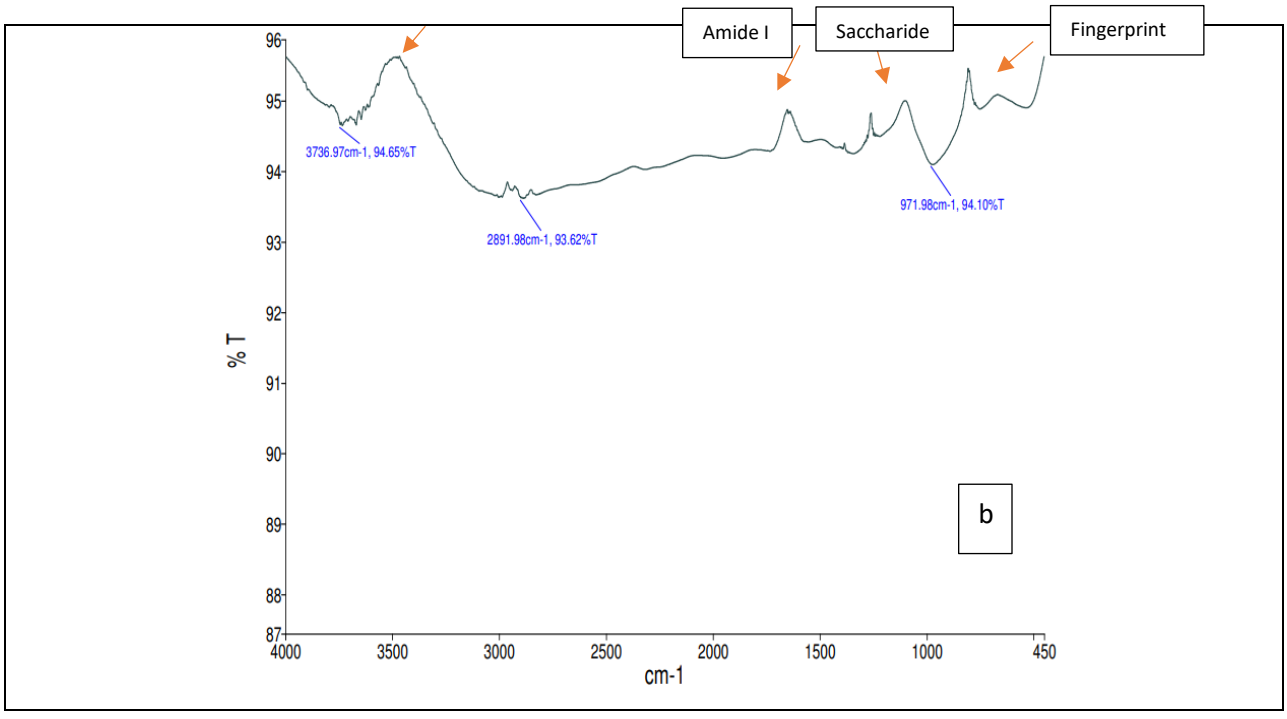
Amide I
Saccharide
Fingerprint
3736.97cm-1, 94.65%T
2891.98cm-1, 93.62%T
971.98cm-1, 94.10%T
% T
cm-1
b

Fig 7.5 : FTIR spectra of (a) GOaN nanomaterial before and (b) after interaction with microorganism (*Bacillus* sp) (c) after interaction with microorganism (*Pseudomonas* sp)

7.3.2 SEM IMAGE ANALYSIS

Cell morphology before interaction with fabricated GOaN nanomaterial and after interaction with fabricated GOaN nanomaterial can be illustrated by assessing surface morphology of bacterial cell with SEM (Scanning Electron Microscope) images**.** It can be observed that before interaction with nanomaterial the smooth surface of *Bacillus pumilis* short rods are present but after short term interaction (1hr) the surface is wrinkled although cell integrity is maintained without disintegration and leakage of internal cytoplasmic constituents. After long exposure (48hrs) it was observed that sporulation process has initiated as the surface was severely shrinked with shriveled cracks formed on the surface. Gram positive microorganisms has thicker peptidoglycan layer (more than 20nm thickness) but with increased time duration of interaction with GOaN nanomaterial spore formation has been initiated *as Bacillus pumilis* is known to form spores under stressed conditions.

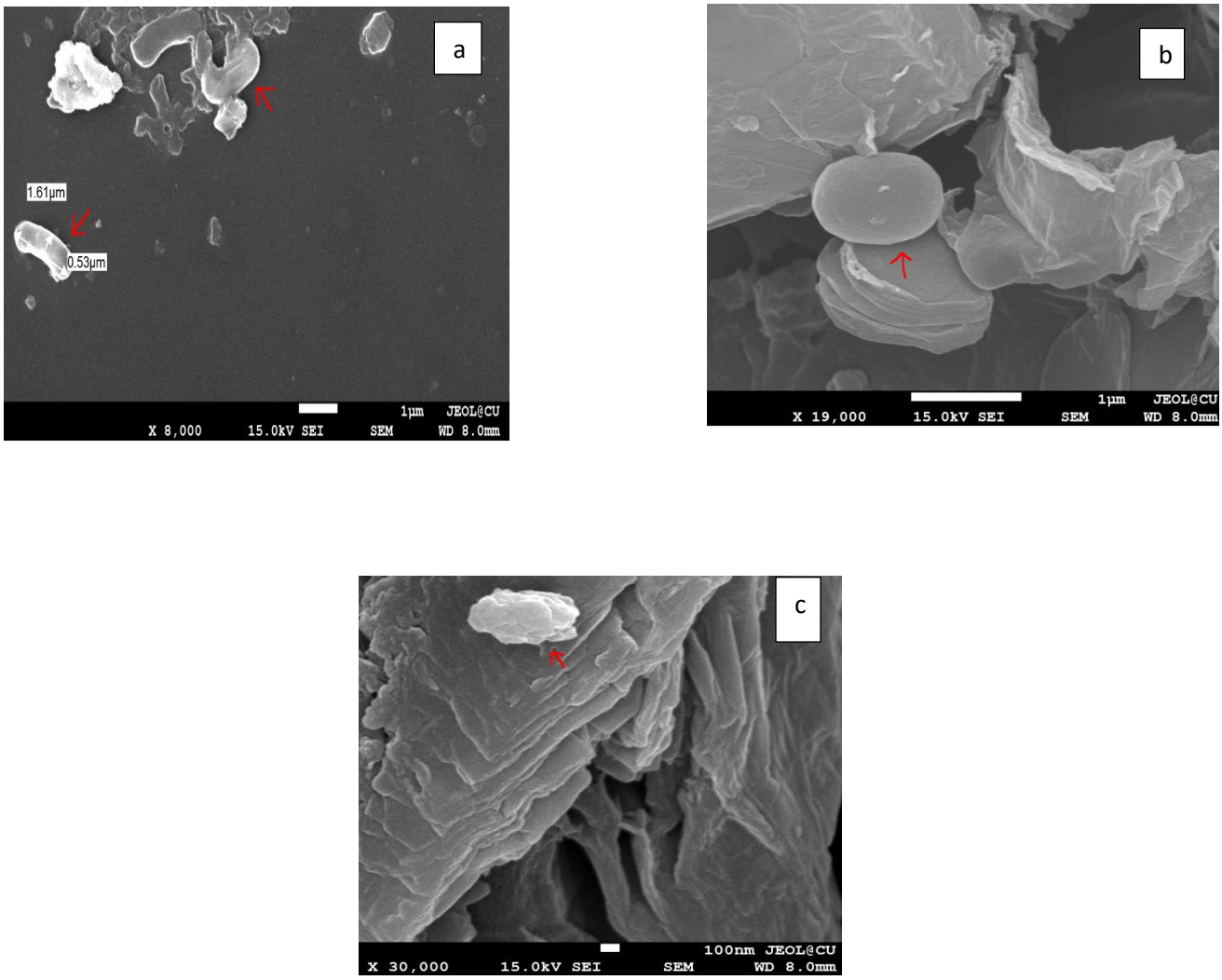

Fig 7.6 : **Surface scanning images of a) typical *Bacillus pumilis* cells b) after short term exposure to GOaN nanomaterial c) spore formation initiated after long term exposure with GOaN nanomaterial. Red arrow marks the *Bacillus* sp cells.**

In case of *Pseudomonas mendocina* it was observed that long rod cells are gradually clumped together and form a biofilm on exposure with fabricated GOaN nanomaterials on shorter exposure (1hr). On longer exposure (48hr) bacterial cell lawn formation is observed which further grouped the cells together.

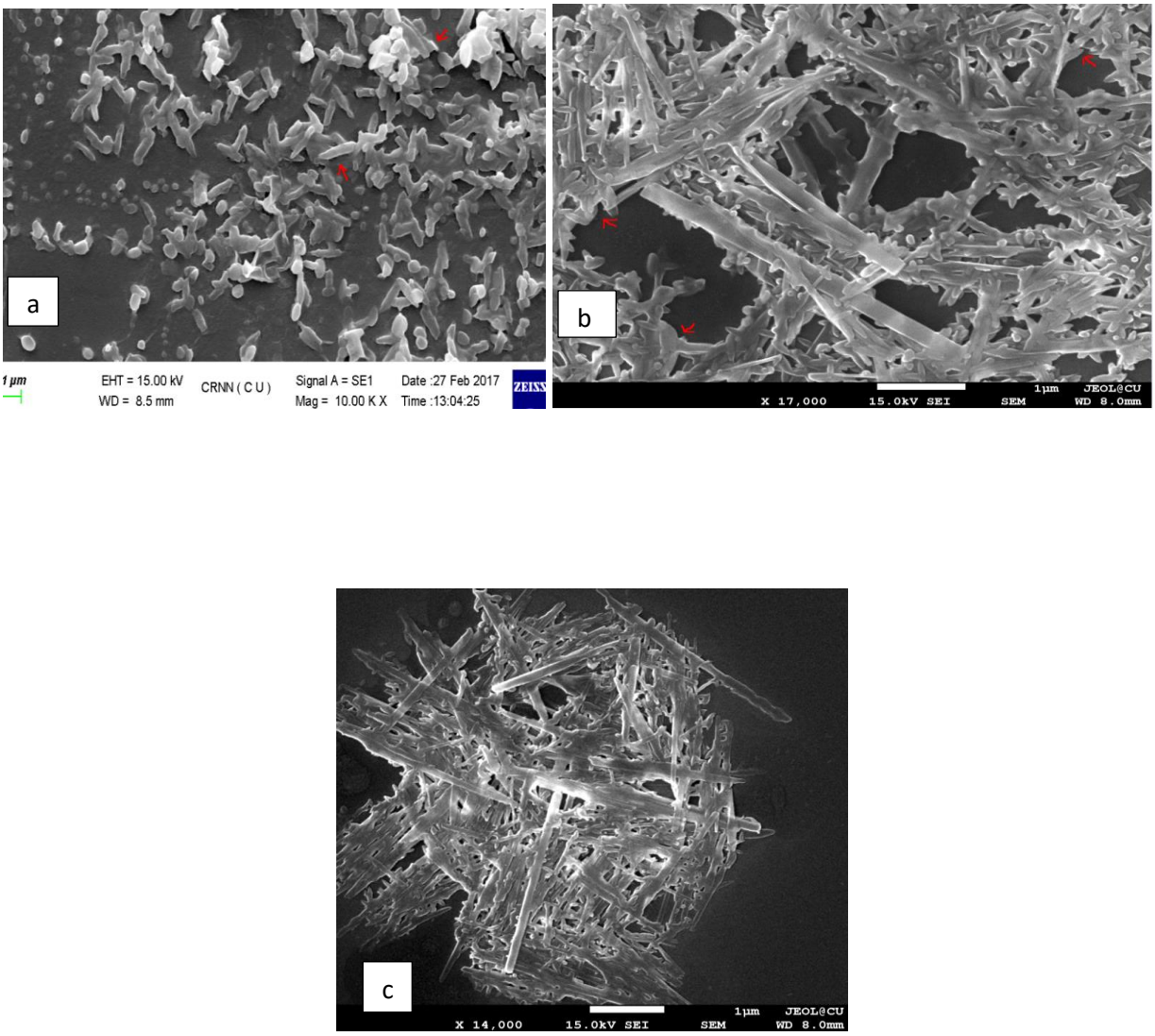

Fig 7.7 : **Surface scanning images of a) typical *Pseudomonas mendocina* cells b) after short term exposure to GOaN nanomaterial c) biofilm formation initiated after long term exposure with GOaN nanomaterial. Red arrow marks the *Pseudomonas* sp cells**.

During sample preparation for SEM imaging, extensive washing steps were performed but attached bacteria cells proved successful embedding of organism on prepared nanomaterial has occurred. The physical attachment is the reason behind adherence of bacteria to the nanomaterial. The nanomaterial

was combined with the growing medium and incubated overnight for successful bonding between the two.

7.3.3 FLUORESCENCE MICROSCOPE IMAGING - VIABILITY OF MICROBIAL CELLS ANALYSIS

Viability of the immobilized bacteria after contact with the fabricated GOaN nanomaterial could be ascertained by fluorescence microscopic imaging analysis using dual EtBr – AO simultaneously. The excitation maxima of EtBr and AO are 510 and 500nm respectively and the emission maxima of EtBr and AO are 595nm and 530nm respectively. The following series of pictorial representations shows the interaction phase between Gram positive (*Bacillus* sp) and fabricated GOaN on a short term (1hr) and long term (48hr). Similar observation was done in case of Gram negative (*Pseudomonas* sp) and fabricated GOaN on a short term (1hr) and long term (48hr). These microscopic images prove that Pseudomonas sp combined GOaN. The green stain indicates living cells whereas the reddish yellow stains indicate dead cells either in apototic or necrotic phases.

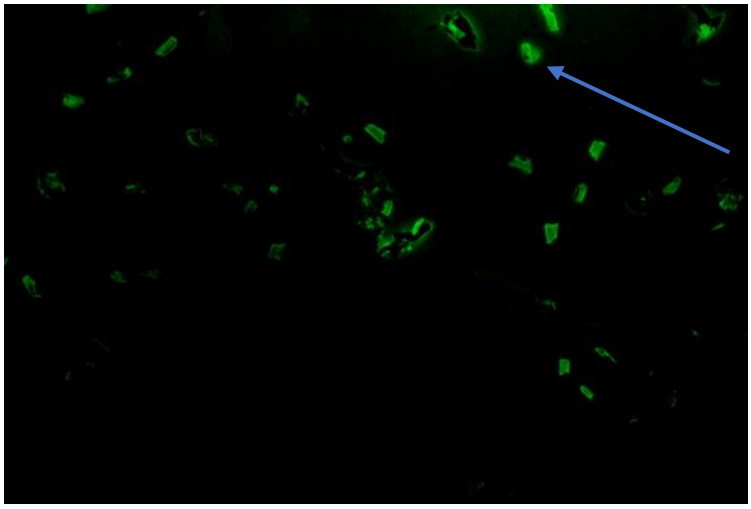

Fig 7.8 : Fluorescence imaging of *Bacillus sp* embedded GOaN nanomaterial (contact time 1hr)

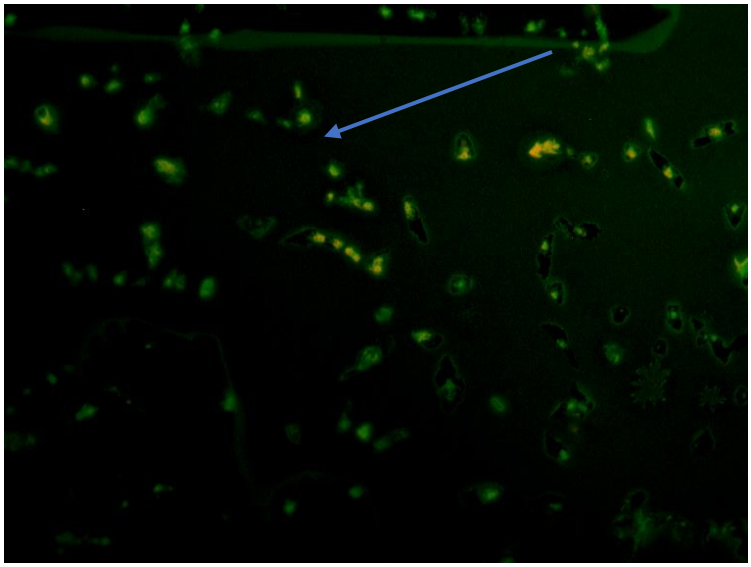

Fig 7.9 : Fluorescence imaging of *Bacillus sp* embedded GOaN nanomaterial (contact time 48hr)

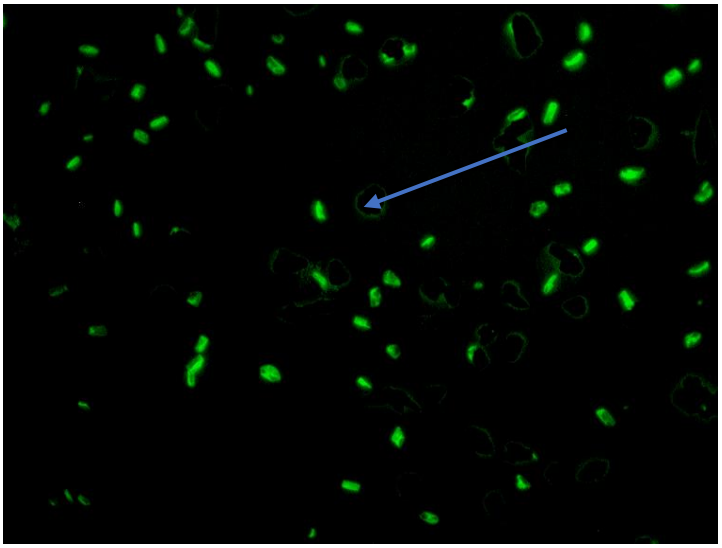

Fig 7.10 : **Fluorescence imaging of *Pseudomonas sp* embedded GOaN nanomaterial (contact time 1hr)**

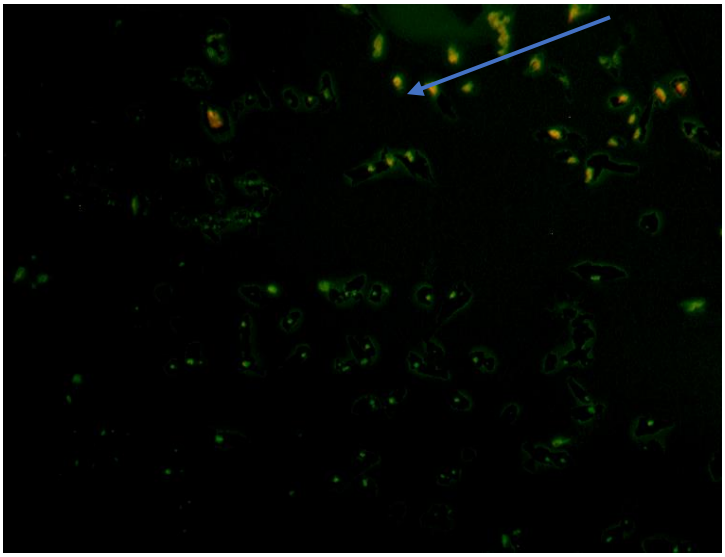

Fig 7.11 : **Fluorescence imaging of *Pseudomonas sp* embedded GOaN nanomaterial (contact time 48hr)**

7.3.4 FLOW CYTOMETER - VIABILITY OF MICROBIAL CELLS ANALYSIS

The result demonstrated that after contact period of 3 hours with laboratory fabricated GOaN nanomaterial, the number of living cells is higher in case of *Pseudomonas* sp than *Bacillus* sp. The lower left quadrant indicates the cell population living after the contact time of 3 days with the fabricated GOaN nanomaterial. Cell death is divided into two phases – Apoptosis and Necrosis. In apoptosis the cell membrane may still be intact which is not in the case of necrotic cells or late apoptotic cells where the membrane is disintegrated completely. PI stains the dead cells as it can enter via the disintegrated membrane. The upper right quadrant designates cells with necrotic phase and the lower right quadrant designates early apoptotic phases. The initial cell population in case of GOaN + P composite with respect to GOaN + B composite is greater indicating successful attachment and proliferation of cells.

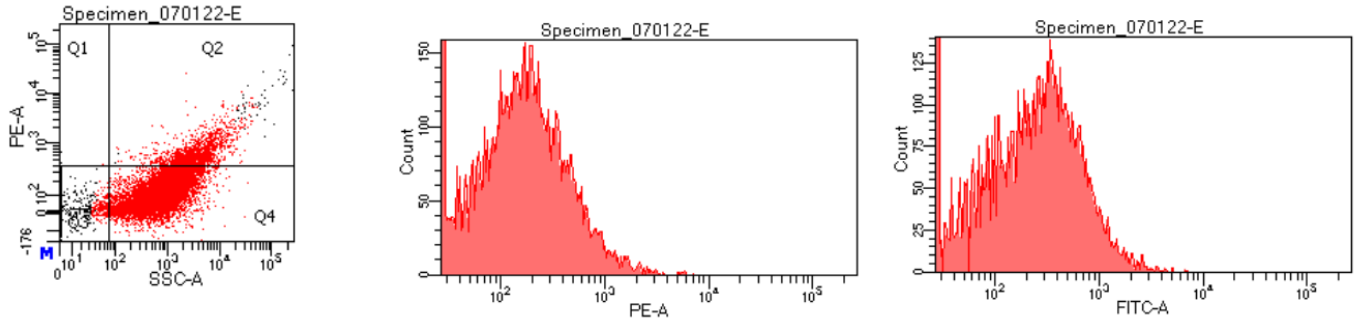

Fig 7.12 : Flow Cytometer analysis of *Pseudomonas* sp embedded GOaN nanomaterial (GOaN +P) after contact period of 3 days

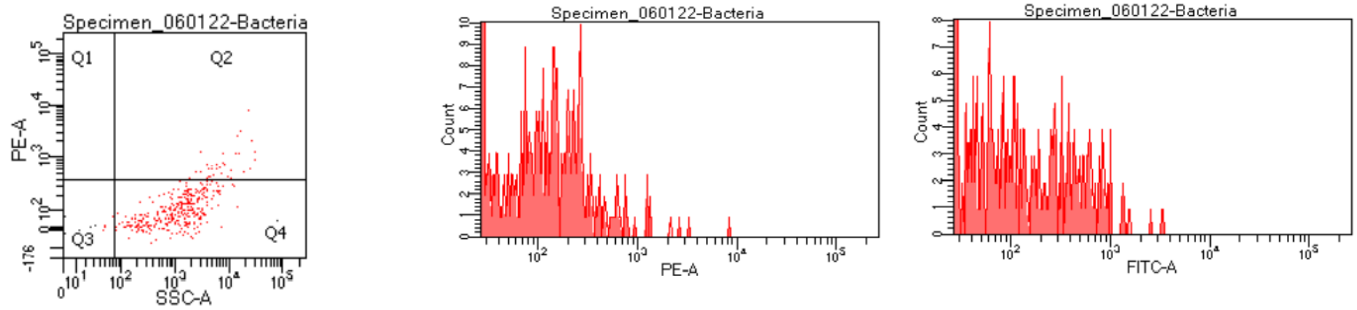

Fig 7.13 : Flow Cytometer analysis of *Bacillus* sp embedded GOaN nanomaterial (GOaN +B) after contact period of 3 days

7.3.5 INTEGRATED DIFFUSE AGAR PLATE METHOD

1ml of microorganism (10^8 cells/ml) were added to the ascending order of various concentrations of the adsorbent material (10 ug/ml, 25 ug/ml, 50 ug/ml,100 ug/ml) suspension under aseptic conditions in the laminar flow. The solution was then cotton plugged and kept in the incubator at 35C under 150 shaking speeds for 24hrs. 1ml of the samples were collected after every 6hrs for 24hrs and centrifuged at 5000g * 10mins. The pellets were resuspended in sterile saline solution and used for enumeration of viable cells by agar plating to check the cell viability by CFU (Colony Forming Unit) method. The Luria Bertani agar plates were kept in the incubator at 35°C for the colonies to grow overnight. The following table shows the effect of nanomaterial on cell viability of microorganism.

Table 7.1 : Bacterial CFU measure after exposure to GOaN and rGOaN nanomaterial

	Control	**After 6 hours**	**After 24 hours**
Adsorbent type	**CFU/ml (10^9)**	**CFU/ml (10^9)**	**CFU/ml (10^8)**
rGOaN + embedded *Bacillus sp*	8.0	6.1	3.7
GOaN +embedded *Bacillus* sp	7.8	7.5	6.3
rGOaN + embedded *Pseudomonas sp*	8.2	6.3	4.5
GOaN +embedded *Pseudomonas* sp	7.9	7.0	6.7

Thus, from the table it was observed that fabricated Graphene oxide (GOaN) nanomaterial shows less antibacterial effects than reduced GO (rGOaN) nanomaterial as reported by other researchers too (de Faria et al., 2014). Reduced GO (rGOaN) possess sharp edges due to exfoliation and reductive reactions as observed in the characterization (Chapter 3). This may be the reason behind decrease in the number of CFU along with absence of functional groups leads to less bacterial attachment and proliferation. The analysis from fluorescence microscopy also corroborates with the result of agar plating method. The agar diffusion study after 48hrs showed that at higher concentration of nanomaterial growth of microorganism is inhibited whereas at lower concentration the growth may be proliferated due to substratum effect.

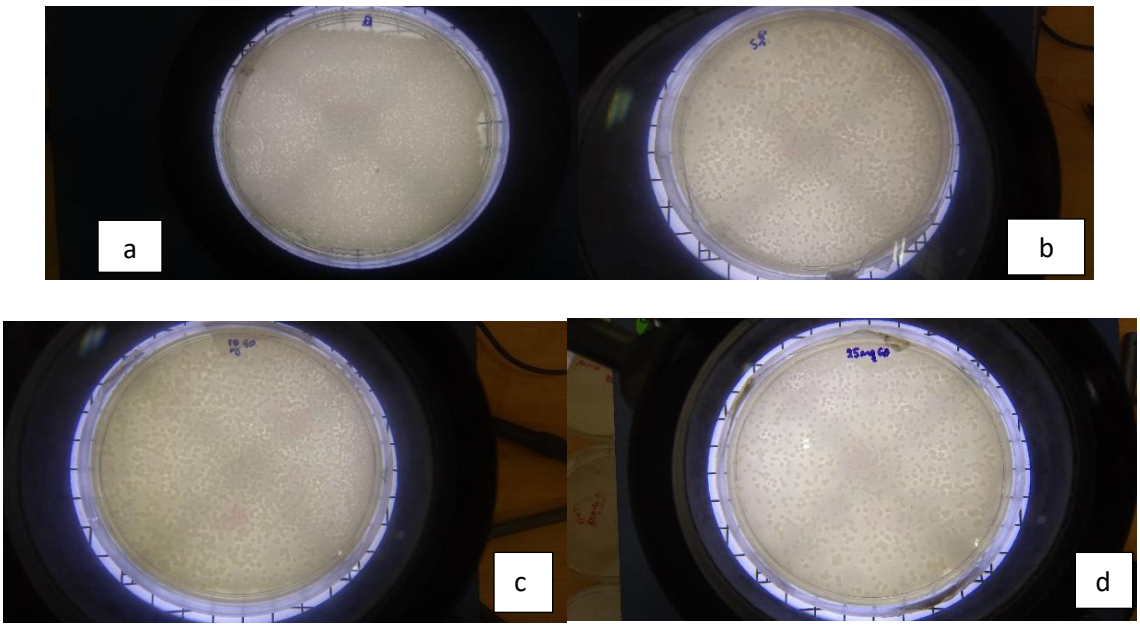

Fig 7.14 : Photographic visualization of Agar plate representation of CFU (*Bacillus* sp) at various concentration of GOaN nanomaterial – (a) Control

(b – d) Increasing concentration of GOAN nanomaterial

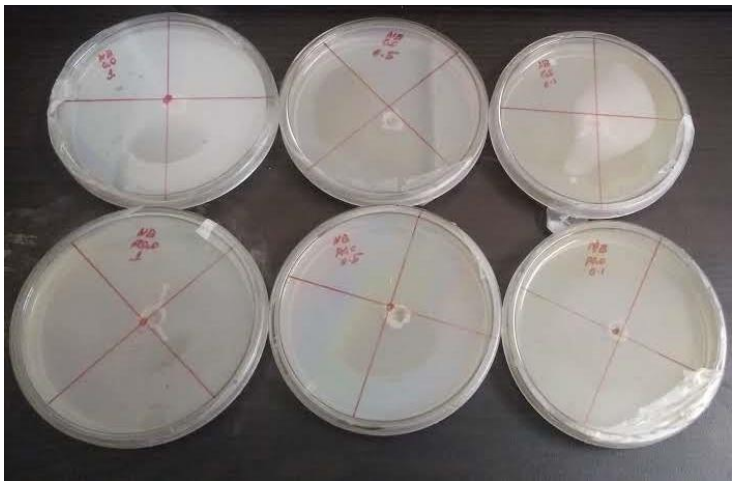

Fig 7.15 : Photographic visual representation of Agar diffusion plate upon amendment with GOaN nanomaterial (500mg/dl; high concentration)

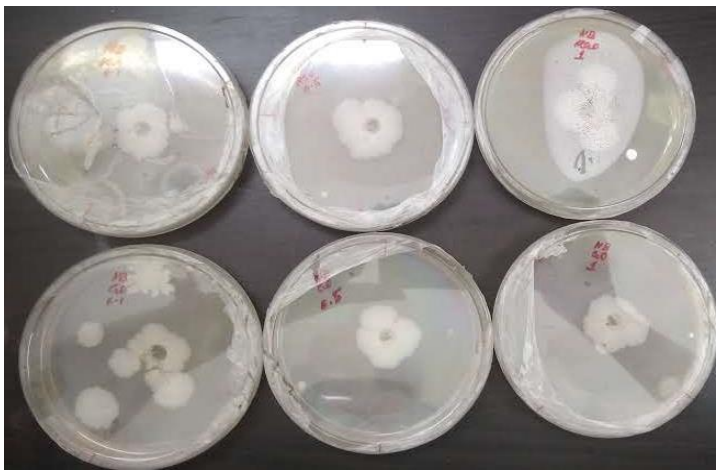

Fig 7.16 : Photographic visual representation of Agar plate (inoculum *Psueudomonas* sp) upon amendment with GOaN nanomaterial – (50mg/dl; low Concentration)

7.3.6 ZETA POTENTIAL ANALYSIS – INDICATOR OF CELL VIABILITY AND MEMBRANE DAMAGE

To validate the effect of electrostatic force on hybrid formation, the surface potential of GOaN was measured by the zeta potential analyzer (Zetasizer Nano), using distill water (H2O) as the dispersion phase of the nanomaterials**.** Zeta potential acts as a marker for cell health indicating damage at the cellular level which in turn corroborates with the cell viability. To ascertain the nature of electrostatic force of interaction between microorganism and nanomaterial at the interfacial region, zeta potential analysis is employed to do the same. In our study the zeta potential of *Pseudomonas* sp (Gram negative) is -20.7 mV and that of *Bacillus* sp (Gram positive) is -17.4 mV respectively under normal conditions. The higher negative potential in gram negative bacteria may be due to the presence of lipopolysaccharides and phospholipids in the additional layer of cell wall which is absent in gram positive bacteria. Gram positive bacteria includes peptidoglycan and teichoic acids as reported in other research studies (Halder et al., 2015). After addition of fabricated GOaN the zeta potential of the microorganisms changed with drastic reduction of zeta potential in terms of gram-positive bacteria. This may lead to alteration of membrane permeability and ultimately cell death which is explained by the fluorescence imaging and flow cytometer analysis. In case of gram-negative bacteria, the change in zeta potential is little which may be explained by the fact that the extra layer of cell wall protects the inner cell membrane and thereby resisting drastic

changes in surface potential of the membrane. The viability of gram-negative bacteria is better than the gram-positive bacteria in presence of fabricated GOaN is hereby corroborated.

Table 7.2 : Zeta potential measurements before and after addition of rGOaN and GOaN

Treatment	Zeta potential (mV)		Temp (°C)
	Pseudomonas sp	*Bacillus* sp	
Normal condition	-20.7	-17.4	25
GOaN added (0.1%)	-22.9	-11.24	25

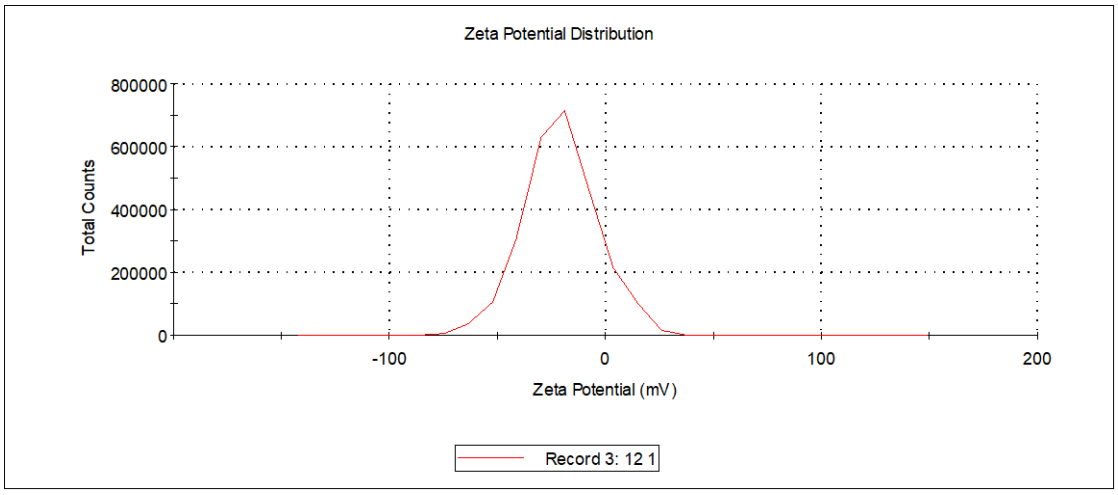

Fig 7.17 : Zeta potential distribution curve of *Pseudomonas* sp under normal conditions

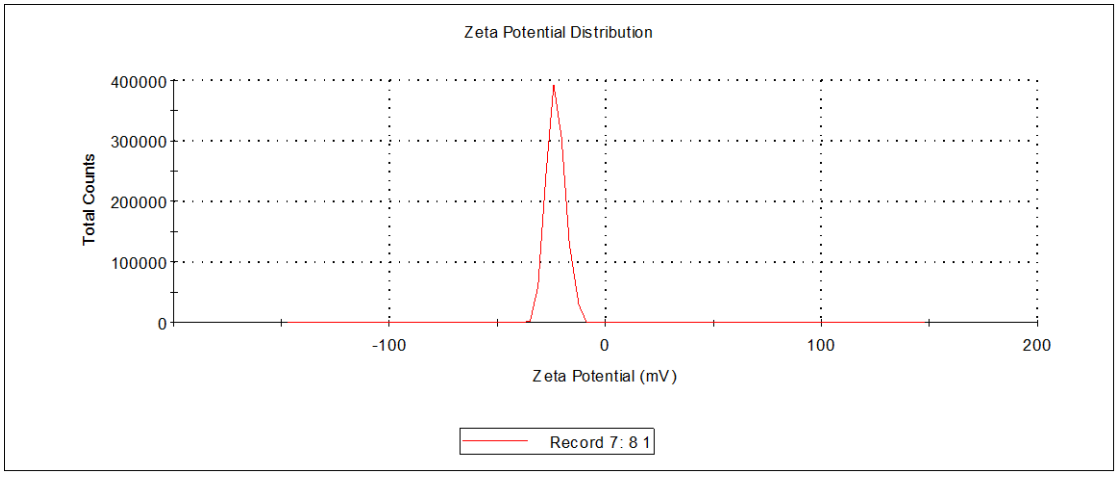

Fig 7.18 : Zeta potential distribution curve of *Pseudomonas* sp after GOaN addition

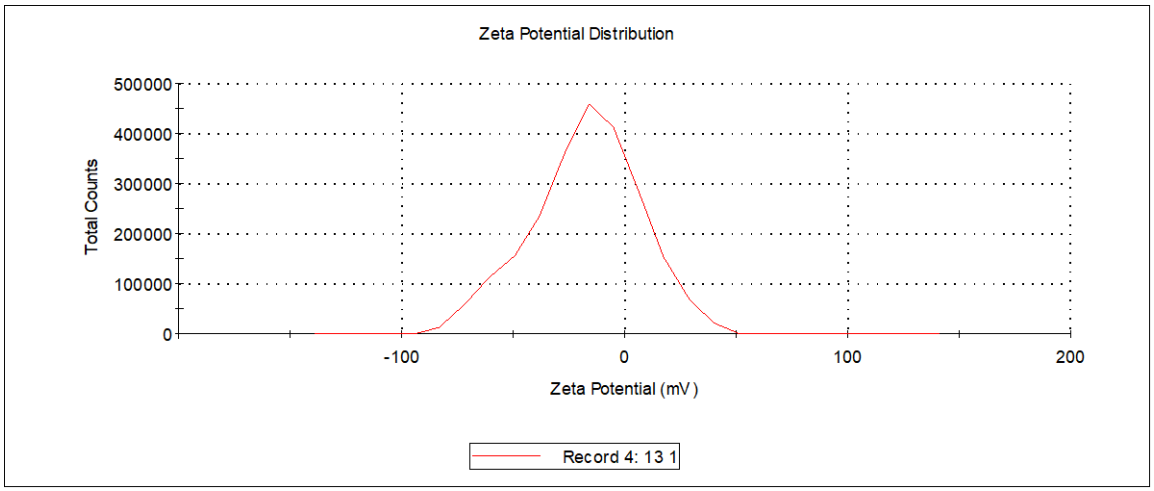

Fig 7.19 : Zeta potential distribution curve of *Bacillus* sp under normal conditions

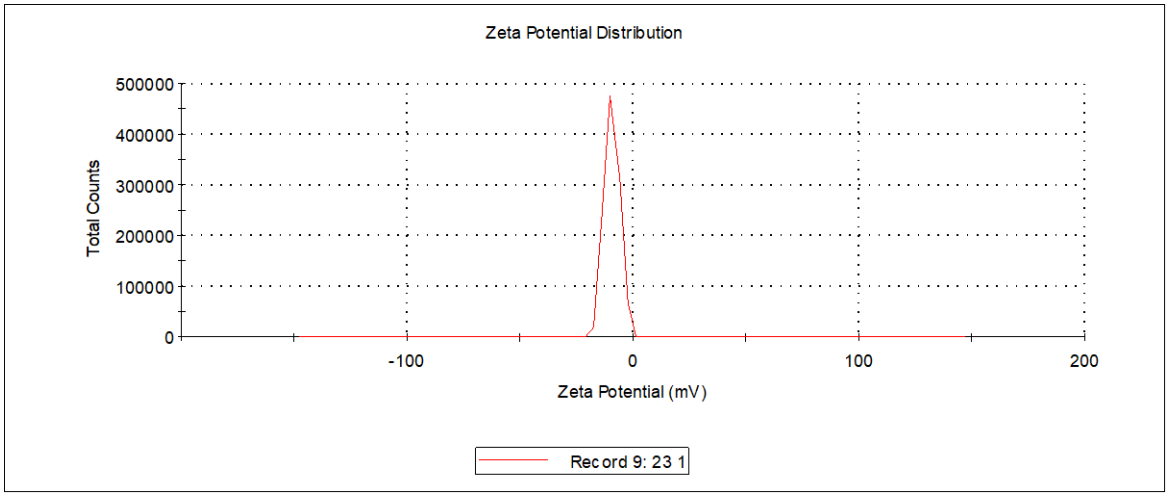

Fig 7.20 : Zeta potential distribution curve of *Bacillus* sp after GOaN addition

7.3.7 BATCH SCALE STUDY ANALYSIS

The mutual effect of adsorption and biodegradation on the removal of organic pollutants specifically PAHs and phenol are being investigated in this section. External factors influencing the process parameter is studied to get an idea about the optimal condition of maximal efficient removal of the pollutant from

synthetic media. The optimal conditions obtained from the previous chapters have been maintained to get the output result in the RSM software (Design Expert). As microbial attachment to the surface of the nanomaterial is a pH sensitive process and temperature dependent process so optimal conditions have been maintained for efficiency estimation. At higher temperature (> 37 °C) and at lower temperature (< 28 °C) diminishing of removal % occurs as biological organisms are temperature sensitive and specific range of temperature is needed for the microbial enzyme activity (Roy et al., 2018). Similarly, pH is an important factor which influences the surface charge of the microorganism and nanomaterial and thus impact the physical attachment and successful embedding of the microorganism and formation of the bio nanocomposite. Also acidic and basic pH interferes with movement of organic molecules across the cell membrane thereby affecting the metabolism of the pollutants to non-toxic by produce (Roy et al., 2018). Thus, the maximum potential for the nanocomposite is in the optimal range of 6 ±0.5 at 35 ± 2°C pH for the organic pollutants.

7.3.7.1 EFFECT OF INITIAL POLLUTANT CONCENTRATION

The maximum percentage of removal of organic pollutant was attained in the concentration range of 20 – 40 mg/L where the range of 10mg/L – 50mg/L was studied. The aromatic pollutants act as the sole energy source as it provides the necessary nutritional carbon source for the microorganisms to thrive and grow. Very low initial carbon concentration may affect the nutritional requirement of the microorganism and thus reduced result is obtained. On the other hand, higher pollutant concentration may pose toxic effect on the microbial cells. With the questionable viability of the cells, the removal percentage of pollutants is greatly diminished. For the integrated approach of adsorption coupled with biodegradation to be efficient the immobilized cells should be considered and it was observed that the integral system yields better result than the processes occurring individually. The nano adsorbents facilitate the attachment of organic pollutants on its surface and thereby eliminating dilution effect which occurs in case of planktonic bacteria. The nano adsorbent also occurs to provide a substratum for bacterial growth and proliferation.

7.3.7.2 EFFECT OF BIONANOCOMPOSITE DOSAGE

The effect of bio nanocomposite dosage on the removal of aromatic pollutants is also elucidated as an important criterion. The dosage of the bio nanocomposite was studied in the range 10mg/dL -100mg /dL

and the maximum removal was observed at 50mg/dL. After 50mg/dL the reduction percentage is not affected greatly with the amount of adsorbent added. This may be due to the reason of overcrowding of adsorbent in the finite space. Aggregation of the nanocomposite may reduce the efficiency as it may mask the active sites for attachment of the organic pollutants. Presence of high concentration of bacteria embedded nanocomposite may exaggerate the problem of less nutrients and competition between the microbial cells for oxygen and nutrients and thus viability and proliferation of microorganisms may be doubtful.

Below is the tabulated data which shows the removal % at optimal conditions in which GOaN + P showing better removal among the other nanocomposite forms. The amount of Phenol is 40 mg/L whereas 20mg/L was the chosen initial pollutant concentration for the PAHs for the experimental study.

Table 7.3 : Removal % of aromatic pollutants from aqueous phase by fabricated nanomaterial embedded with microorganism

Type of bio nano composite	Removal % of Phenol from synthesized aqueous media	Removal % of Pyrene (HMW PAH) from synthesized aqueous media	Removal % of Naphthalene (LMW PAH) from synthesized aqueous media
rGOaN + embedded *Bacillus sp*	87.12±1.2	70.10±0.7	86.60±1.1
GOaN +embedded *Bacillus* sp	96.56±0.5	85.04±0.3	94.28±0.1
rGOaN + embedded *Pseudomonas sp*	86.79±1.0	89.82±0.5	85.55±0.8
GOaN +embedded *Pseudomonas* sp	98.02±0.3	86.35±0.4	95.91±0.2

Results are indicated as Mean ±SD.

The data corroborated with our findings, that maximum removal can be observed for GOaN based nanocomposite as microorganism viability is better in case of GOaN nanomaterial. The viability of

microorganism in case of rGOaN is reduced which is also reported by other researchers that reduced Graphene oxide possess antimicrobial effects which is more pronounced with reduction of Graphene oxide (Kurantowicz et al., 2015). About 98.02% (Phenol) and 95.91% (Naphthalene, Simplest LMW PAH) could be removed by Pseudomonas sp embedded GOaN nanomaterial which is followed by Bacillus sp embedded GOaN nanomaterial which amounted to 96.56 % (Phenol) and 94.28% (Naphthalene, Simplest LMW PAH). An interesting feature is noted in case of pyrene as better results are obtained in case of reduced GO (rGOaN). This may be accounted due to the hydrophobic feature of complex PAH (more than two aromatic rings). Reduced GOaN also displays hydrophobicity by forming a layer on the surface of the aqueous media. Microorganism – rGOaN adsorbent thus settles at the bottom of the conical flask as aggregation of the nanoadsorbents occurred as shown in Fig 7.14. The results were less in case of rGOaN nanomaterial embedded with respective gram-positive (*Bacillus* sp) and gram-negative (*Pseudomonas* sp) microorganism.

7.3.8 OPTIMIZATION OF THE PARAMETERS

To decrease the cost, time and increase the efficiency, optimization of the process parameters by Design Expert Software 7.0 was done. The interaction between two factors with three level each – Initial concentration of organic pollutants (Naphthalene , Pyrene , Phenol) and the dosage of the adsorbent (GOaN + P) was studied and optimization was done based on them. The dosage for the bio nanocomposite was selected to be - 0.1 g/L, 0.5 g/L, 1 g/L and the initial concentration of the pollutants were selected to be – 10 mg/L, 25 mg/L and 50 mg/L. The D- optimal Design under the factorial study type of the software was selected to give the number of experiments to be run and to understand the interactive effect between the two factors. The experiments were conducted for 24hours and the results were obtained by above mentioned method. High "Model F-value" can occur when error due to noise is less. Model terms are important when the probability value is less than 0.0500. In this case, the model terms A, B, AB, A2 and B2 are crucial. If the p value is more than 0.1000, the model terms are insignificant. Total 9 runs were predicted by the software for two factor interaction by D – optimal design. The experimental runs are given in the table as below:

Table 7.4 : Model experimental analysis for organic pollutant removal by GOaN + P bio nanocomposite

Std	Run	Block	Factor 1 A:Adsorbent d g/L	Factor 2 B:Initial Concer mg/L	Response 1 Nap Removal %	Response 2 Pyr Removal %	Response 3 Phenol Removal %
1	1	Block 1	0.10	10.00	70.5	63.76	77.97
9	2	Block 1	1.00	50.00	52.77	50.91	65.83
6	3	Block 1	1.00	25.00	59.98	57.32	69.2
5	4	Block 1	0.50	25.00	88.43	70.07	92.07
7	5	Block 1	0.10	50.00	63.76	53.99	75.03
3	6	Block 1	1.00	10.00	74.83	72.97	77.48
2	7	Block 1	0.50	10.00	95.47	86.36	96.23
8	8	Block 1	0.50	50.00	82.11	57.93	92.93
4	9	Block 1	0.10	25.00	66.2	50.23	76.13

Table 7.5 : ANOVA table for Naphthalene removal % by GOaN +P bionanocomposite

Analysis of variance table [Partial sum of squares - Type III]

Source	Sum of Squares	df	Mean Square	F Value	p-value Prob > F	
Model	1535.45	5	307.09	96.50	0.0016	significant
A-Adsorbent dose	*35.63*	*1*	*35.63*	*11.20*	*0.0442*	
B-Initial Concentration	*307.08*	*1*	*307.08*	*96.50*	*0.0022*	
AB	*54.08*	*1*	*54.08*	*16.99*	*0.0259*	
A^2	*1124.27*	*1*	*1124.27*	*353.29*	*0.0003*	
B^2	*23.45*	*1*	*23.45*	*7.37*	*0.0729*	
Residual	9.55	3	3.18			
Cor Total	1545.00	8				

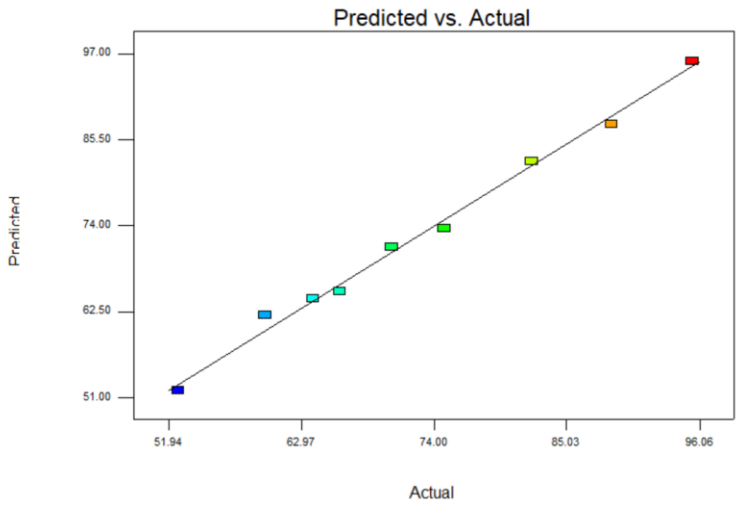

Fig 7.21 : Predicted vs Actual values of the experimental model for Naphthalene removal % by GOaN +P bio nanocomposite

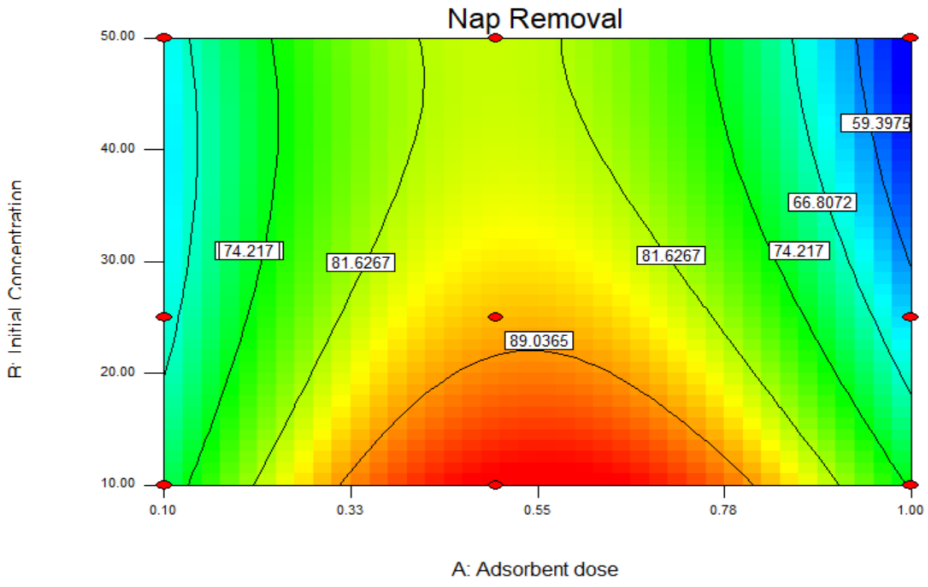

Fig 7.22 : Contour plot of Naphthalene removal by GOaN + P bio nanocomposite

Table 7.6 : ANOVA table for Pyrene removal % by GOaN +P bio nanocomposite

Analysis of variance table [Partial sum of squares - Type III]

Source	Sum of Squares	df	Mean Square	F Value	p-value Prob > F	
Model	1073.10	5	214.62	9.25	0.0483	significant
A-Adsorbent dose	*22.82*	*1*	*22.82*	*0.98*	*0.3945*	
B-Initial Concentration	*617.08*	*1*	*617.08*	*26.59*	*0.0141*	
AB	*34.99*	*1*	*34.99*	*1.51*	*0.3070*	
A^2	*363.09*	*1*	*363.09*	*15.65*	*0.0288*	
B^2	*113.88*	*1*	*113.88*	*4.91*	*0.1135*	
Residual	69.61	3	23.20			
Cor Total	1142.71	8				

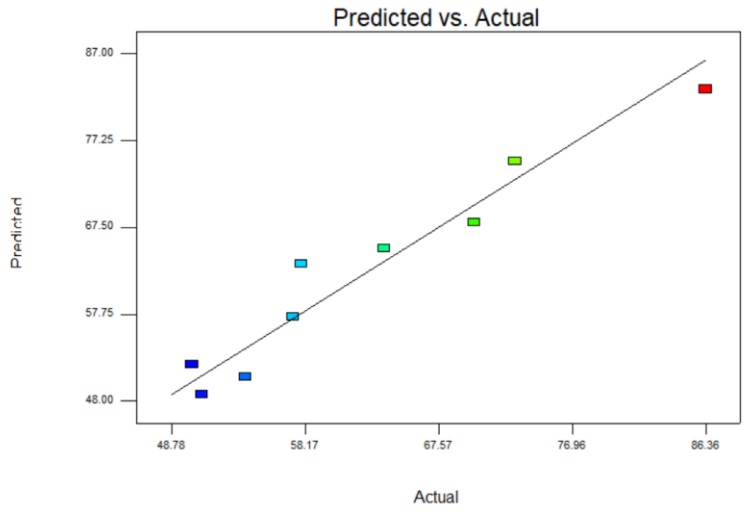

Fig 7.23 : Predicted vs Actual values of the experimental model for Pyrene removal % by GOaN +P bio nanocomposite

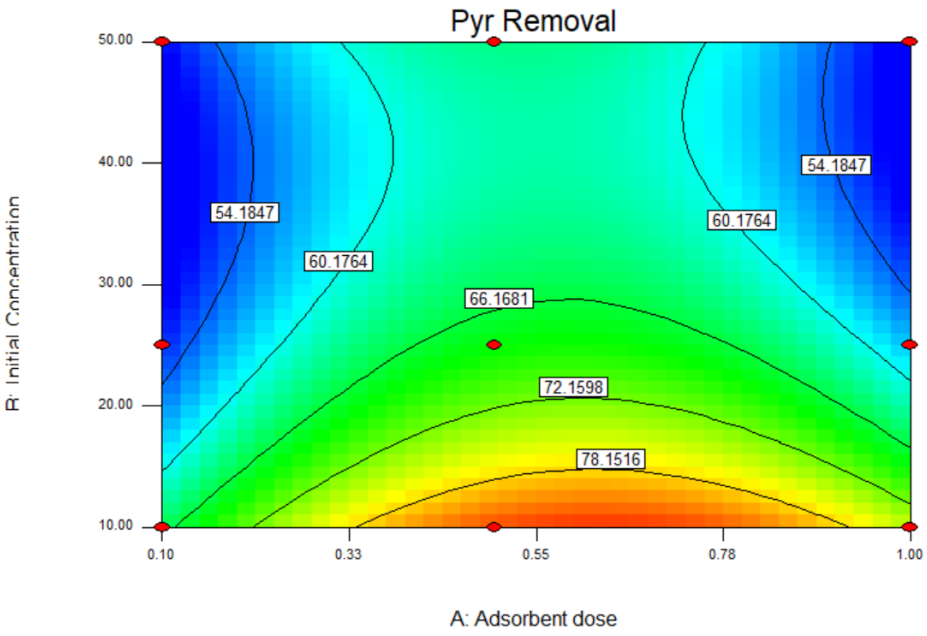

Fig 7.24 : Contour plot of Pyrene removal by GOaN + P bio nanocomposite

Table 7.7 : ANOVA table for Phenol removal % by GOaN +P bio nanocomposite

Analysis of variance table [Partial sum of squares - Type III]

Source	Sum of Squares	df	Mean Square	F Value	p-value Prob > F	
Model	935.02	5	187.00	70.76	0.0026	significant
A-Adsorbent dose	*51.56*	*1*	*51.56*	*19.51*	*0.0215*	
B-Initial Concentration	*56.07*	*1*	*56.07*	*21.21*	*0.0192*	
AB	*18.34*	*1*	*18.34*	*6.94*	*0.0780*	
A^2	*783.15*	*1*	*783.15*	*296.32*	*0.0004*	
B^2	*12.48*	*1*	*12.48*	*4.72*	*0.1181*	
Residual	7.93	3	2.64			
Cor Total	942.95	8				

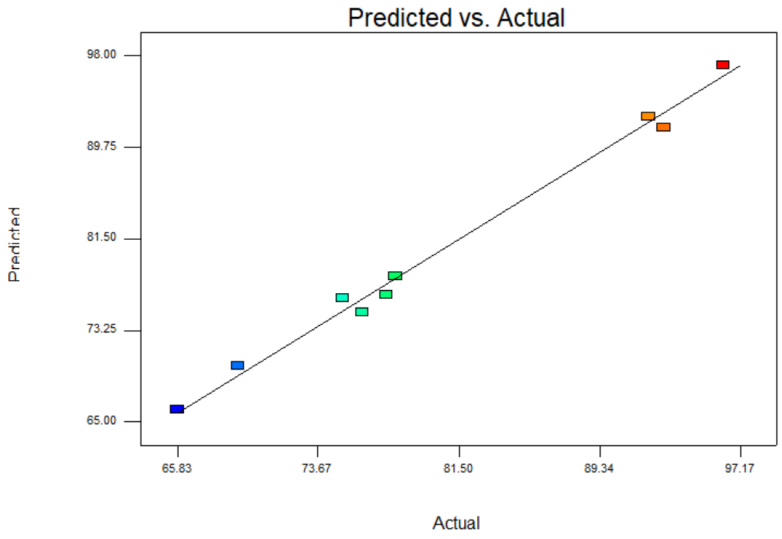

Fig 7.25 : Predicted vs Actual values of the experimental model for Phenol removal % by GOaN +P

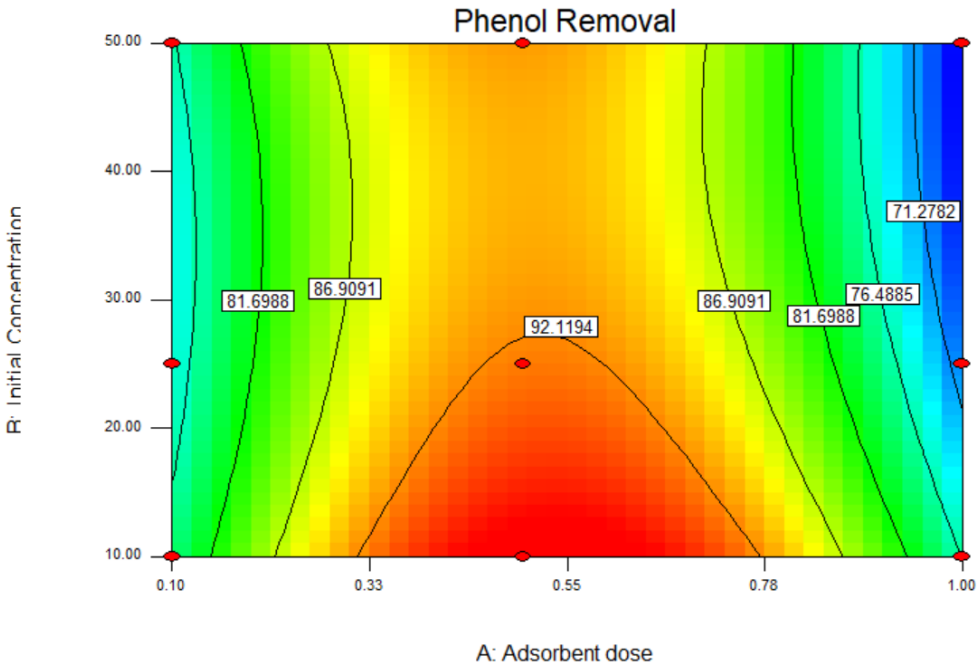

Fig 7.26 : Contour plot of Phenol removal by GOaN + P by GOaN + P bio nanocomposite

Table 7.8 : Summary of D- Optimal Design for optimization

Design Summary

Study Type	Factorial		**Runs**	9							
Initial Design	D-optimal	Coordinate Exchange		**Blocks**	No Blocks						
Design Model	2FI										
Factor	**Name**	**Units**	**Type**	**Low Actual**	**High Actual**	**Low Coded**	**High Coded**	**Mean**	**Std. Dev.**		
A	Adsorbent dose	g/L	Numeric	0.100	1.00	-1.000	1.000	0.533	0.368		
B	Initial Concentration	mg/L	Numeric	10.00	50.00	-1.000	1.000	28.333	16.499		
Response	**Name**	**Units**	**Obs**	**Analysis**	**Minimum**	**Maximum**	**Mean**	**Std. Dev.**	**Ratio**	**Trans**	**Model**
Y1	Nap Removal	%	9	Polynomial	52.770	95.470	72.672	13.102	1.809	None	Quadratic
Y2	Pyr Removal	%	9	Polynomial	50.230	86.360	62.616	11.268	1.719	None	Quadratic
Y3	Phenol Removal	%	9	Polynomial	65.830	96.230	80.319	10.236	1.462	None	Quadratic

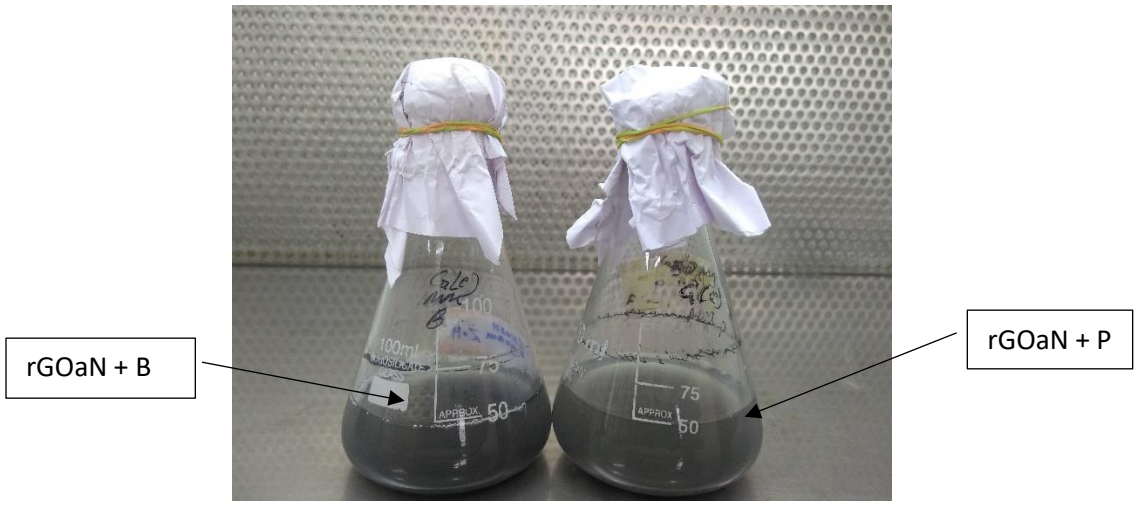

Fig 7.27 Photographic representation of rGOaN - microorganism experimental set

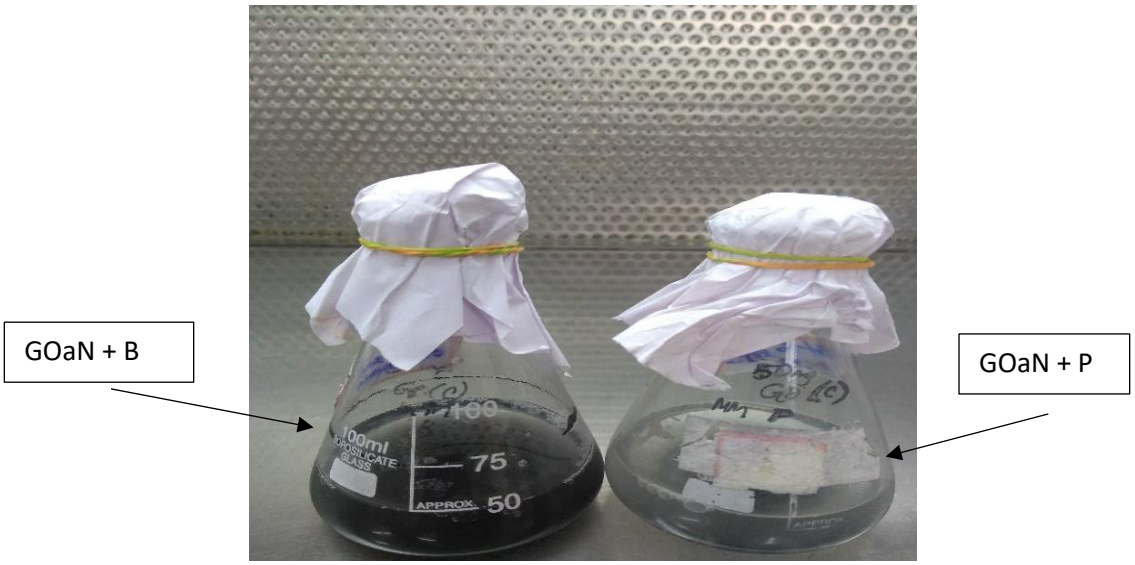

Fig 7.28 Photographic representation of GOaN - microorganism experimental set

7.4 CONCLUDING REMARKS

The attachment or physical entrapment of microorganism on the surface of the fabricated nanomaterials have been corroborated from the previous findings. FTIR, SEM, Fluorescence microscopy and Flow cytometer have been utilized to conclude successful attachment of microorganism and thus the fabricated GOaN particle is biocompatible by nature. Zeta potential studies confers the stability of gram-negative microorganism in presence of fabricated nanomaterial but gram-positive bacteria show less stability. Agar plating methods are utilized to estimate the effect of various dosage of fabricated nano adsorbent on the viability of the microorganism. Less or no toxicity is shown by the nanomaterial at minor dosage whereas inhibitory effect is evident at higher dosage. At low dosage the nanomaterial acts as substratum for bacterial growth and proliferation. The next section deals with the parameters influencing the synergistic effect of the microorganism in presence of GOaN nanomaterial.

SECTION B

INTERACTION MECHANISM BETWEEN NANOMATERIALS AND BACTERIA AT THE INTERFACIAL REGION

7.5 CONTEXTUAL INFORMATION : The uniqueness in the properties of graphene related nanomaterials such as graphene oxide (GO) and reduced form of graphene oxide (rGO) has created curiosity in the researchers to examine the interaction of such materials with microscopic organisms. Among the members of graphene related family of nanomaterials graphene oxide stands out to be an interesting choice for the study as it contains large amount of oxygen atoms in its various functional groups attached to the core basal planes as well as on the edges. This also helps in increasing the hydrophilicity of graphene oxide when compared to its hydrophobic counterparts. Graphene oxide also serves as substrate molecule for interaction with microorganism due to its dense oxygen rich sites. Various findings suggest that go possess antimicrobial effects with possible explanation ranging from wrapping bacteria to knifing effect of its sharp edges. The laceration leads do destruction of the phospholipid layer of the cell and may also result in oxidative stress. Also, literature suggests that GO may serve as a terminal electron acceptor thereby itself getting reduced due to bacterial respiration.

Bacteria are single celled prokaryotes which has been typified based on numerous parameters. Generally, morphologically it is distinguished into rod shaped bacilli or sphere-shaped cocci and sometimes it is spiral shaped too (spirilla). On the basis of composition of bacterial outer cell wall, it is divided into Gram-positive and Gram-negative types. Peptidoglycan forms the major structural component of bacterial exterior cell wall. Gram positive bacteria have several layers of peptidoglycan with an additional cell wall of lipoteichoic and teichoic acid thereby creating thicker cell wall than its counterpart gram negative bacteria which lacks in cell wall. Gram negative bacteria thus possess a thin layer of peptidoglycan and secretes lipopolysaccharides. The functionality of cell wall ranges from protection of the bacterial cell from external harm due to extrinsic factors and also maintains the structural integrity of the organism. Macromolecular adhesins presents on the bacterial cell surface are of utmost importance for interactions of bacteria on surface. the overall surface charge exhibited by bacteria in a physiological condition tends to be negative. For gram positive bacteria phosphoryl groups in the teichoic acids generates negative charges due to ionization. Although the electrochemical behavior is different in different bacterial strain and also on its surface characteristics. Thus, negative surface charge is a common physical property to both types of bacteria

Literature reviews showed mixed responses on the antibacterial effect of reduced Graphene oxide and Graphene oxide nanomaterial family. There has been an ambiguous in the response Accordingly, few papers mentioned that Gram positive bacteria characteristically has thicker peptidoglycan layer which gives innate protection against antibacterial effects of GO (Jaworski et al., 2018). But High concentration of graphene family materials as high as 250ug/ml or 250ppm(mg/L) inhibits growth of all microorganism as reported in several literature papers (Kurantowicz et al., 2015) but lower concentration around 25ug/ml /25ppm does not inhibit growth but may also act as nonspecific substrate for microbial growth. In case of graphene related nanomaterials oxygen rich functional groups acts as a site for bacterial attachment. But sometimes presence of more oxygenated functional groups creates ROS (Reactive Oxygen Species) which may affect the viability of the organism. So detailed analysis of material properties may be done to understand the successful attachment between the two. The size of the material also affects the attachment of bacteria as larger surface area is provided in case of larger sheet like structure for bacterial attachment. Successful attachment of the substrate helps in bacterial proliferation and creation of biofilm. Biofilm helps in enhanced pollutant removal as it contains other substances which cooperates with the pollutant removal. Thus, the attachment occurs at the edges for reduced graphene oxide or pristine graphene structure and in case of oxidized form of graphene the attachment occurs on the edges as well as on the surface due to the presence of oxygen rich groups in these places. Although few research paper have acknowledged and concluded nanoparticles as biodegradation enhancer agent which acts as a substratum for bacterial attachment and proliferation.

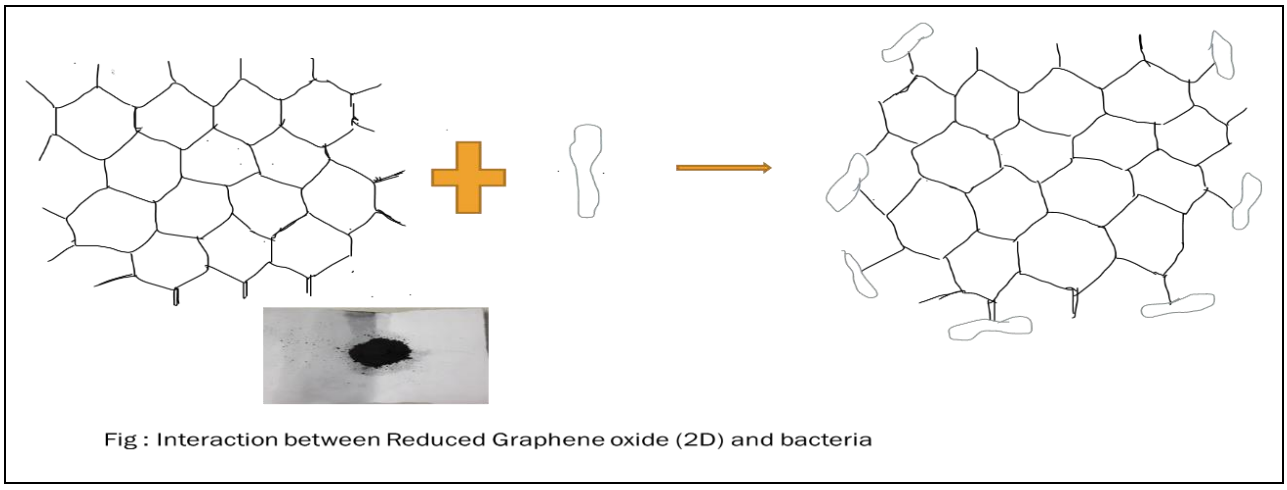

Fig 7.29 : rGOaN as substratum for bacterial attachment

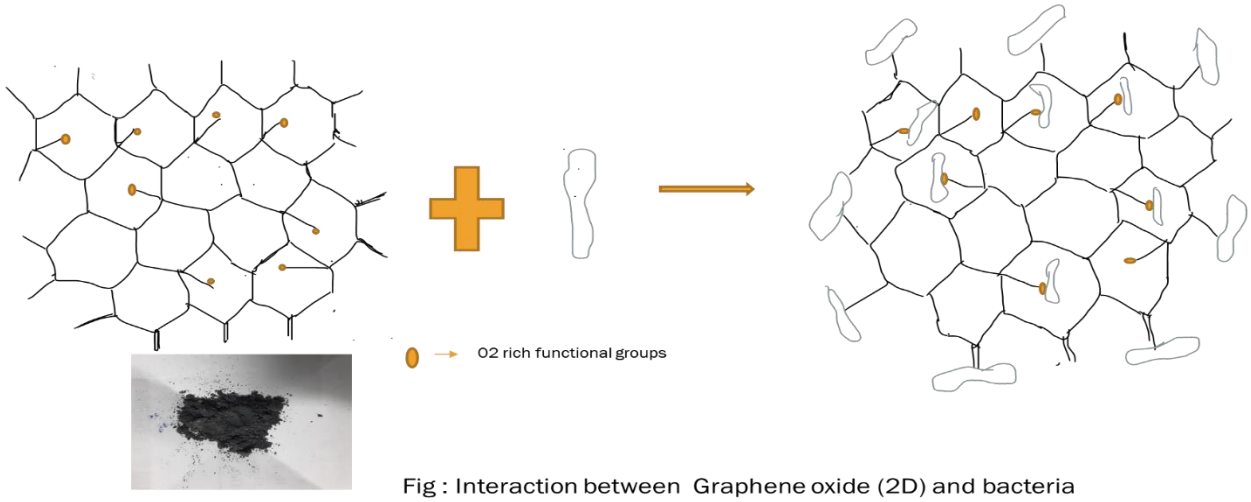

Fig 7.30 : GOaN as substratum for bacterial attachment

7.6 : STEPS OF BACTERIAL ATTACHMENT TO A NANOMATERIAL SURFACE

Bacterial attachment to a surface of a material in aqueous phase can be divided into several steps (Carniello et al., 2018; Y. Cheng et al., 2019; Zheng et al., 2021) -

a) Transport of the bacteria towards the material generally occurs by sedimentation (in stagnant conditions) or connective diffusivity (in flow displacement state)
b) Loose attachment of the bacteria on the surface of the material which maybe reversible or irreversible
c) After irreversible initial attachment takes place aggregation and colonization generally occurs.
d) Biofilm formation takes place after successful colonization leading to physio-chemical changes in the microbial surface and removal of interfacial water between the two systems.
e) Production of EPS **(extracellular polymeric matrix)** including polysaccharides, lipids, proteins strengthen the attachment.

The major binding force acting on the bacterial interaction to the surface of a material is the Lifshitz-van der Waals attractive binding forces between the surface of the material and the surface molecules present in the bacteria (Zheng et al., 2021). The surface parameters also play a pivotal role in attachment of bacteria and thus are briefly described below-

7.6.1 SURFACE TOPOGRAPHY AND SURFACE ROUGHNESS

The roughness of the material is also an important parameter for bacterial attachment. In the literature findings it was seen that roughness is positively related to growth or attachment of bacteria to the surface than polished surface which inhibits bacterial attachment(James et al., 2019; Yoda et al., 2014). Depending on the bacterial species used and surface protein secretions, the relationship may sometimes be ambiguous in nature(Zheng et al., 2021). In case of topography of the material it is reported that bacteria prefers structures with hollow spaces and pillar structures on to which greater attachment occurs.(Perera-Costa et al., 2014) .

As mentioned earlier (Section A) the fabricated GOaN nanomaterials showed no rough edges or sharp structure in SEM images but in case of extensive reduction process the edges were sharper in case of reduced GOaN. The SEM image below shows multi layered structure with crevices formed due to oxidation reactions. These gaps or crevices acts as attachment point for microorganisms as observed by other researchers (Ueshima et al., 2002). Thereby it proved to be compatible as a substratum for bacterial attachment and proliferation.

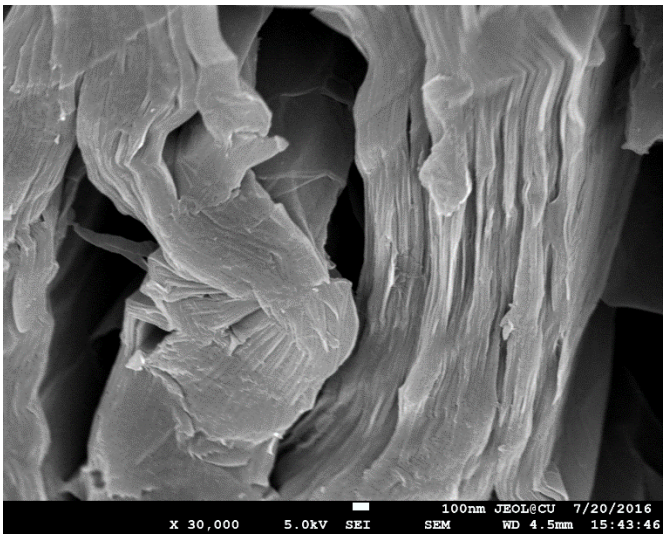

Fig 7.31 : SEM image of Multi layered GOaN nanomaterial

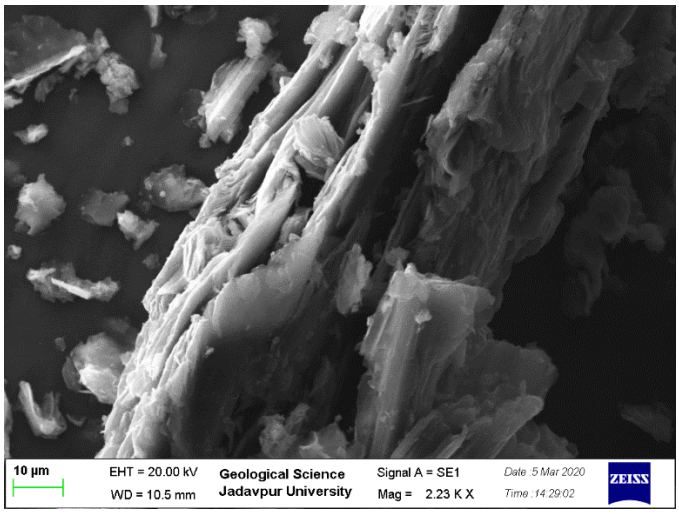

Fig 7.32 : SEM image of Multi layered rGOaN nanomaterial

7.6.2 PRESENCE OF OXYGEN RICH FUNCTIONAL GROUPS

According to Barrios et al (2019) important relationship parameters can be deduced from the interaction of surface chemistry of Graphene oxide and its antimicrobial function. From the FTIR spectrum the functional groups of the nanocomposite and the parent nanomaterial can be deciphered. Although the role of oxygen is doubtful as in some literature papers it is mentioned that the presence of oxygen may prove to be toxic to microorganisms and cause membrane damage. On the other hand, presence of oxygen rich functional groups renders the material hydrophilic thereby being easily available to the microorganisms for attachment.

In the previous section (section A) FTIR spectrum of the nanocomposite showed various stretching and bending due to the presence of oxygen rich moieties on the surface of the GOaN which made it conducible for bacterial attachment. The broader peak at 3416 cm-1 is due to intense OH stretching vibrations and smaller peak at 2925 cm-1 is due to CH3 CH2 (alkene and alkanes) and CH (aldehyde) stretching. Reduction in C=C symmetry gives rise to peaks at 1620cm-1. Due to incorporation of oxygen containing functional moieties C-O -H bending occurs and deformation in CH2 and CH3 gives rise to multiple peaks in the wavelength range of 1400 cm-1 – 1200cm-1 .

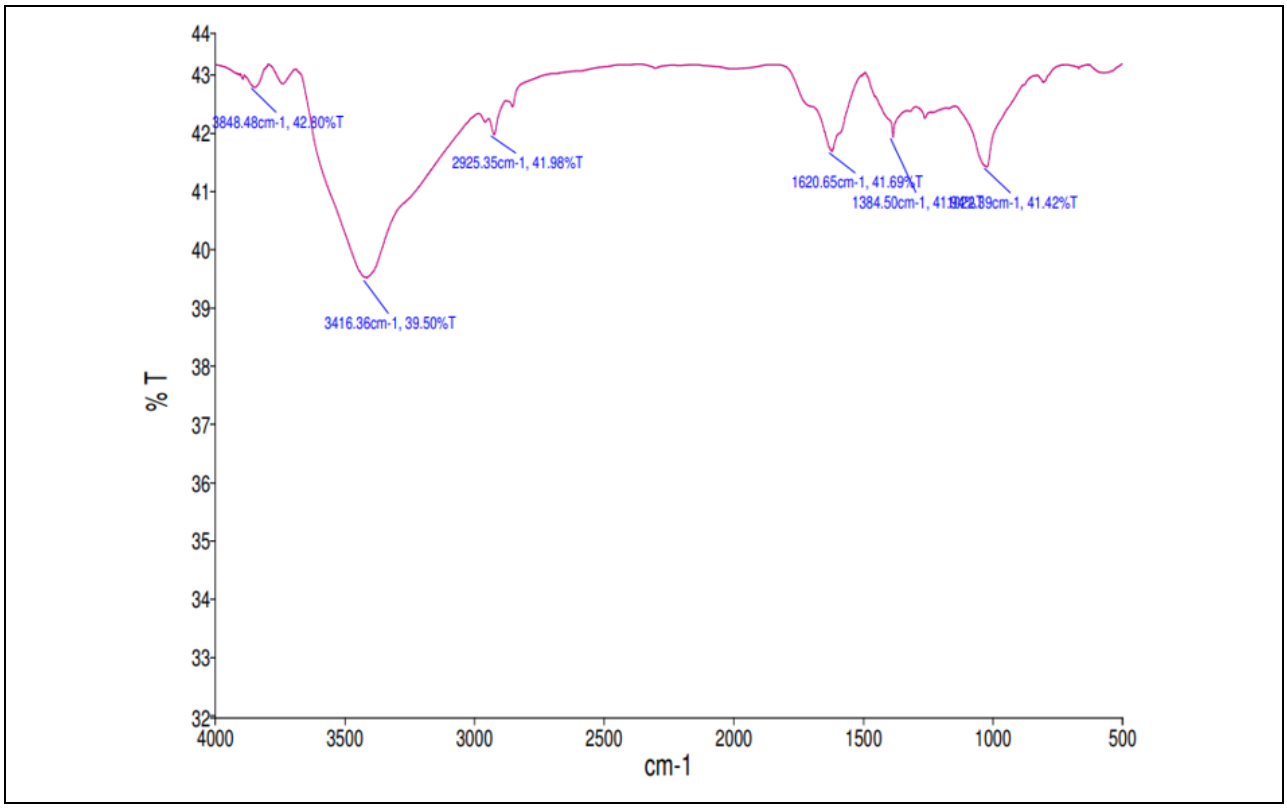

Fig 7.33 : FTIR spectrum of GOaN after lyophilization

7.6.3 INFLUENCE OF BASAL PLANE ON INTERACTION WITH MICROBES

According to Xue et al (2018) strong hydrophobic interactions play a key role in bacterial adhesion to GO functionalized surface. As per their literature bacteria of genus Pseudomonas has higher bio adhesion capability due to presence of adhesion proteins termed adhesins. Hydrophobic amino acids interact with the hydrophobic basal surface of graphene oxide and thus leads to attachment. They also reported horizontal flat surfaces to be better in terms of attachment thereby giving importance to spatial arrangement and conformation of graphene oxide surface for strong attachment. Electrostatic and steric forces reduce the adhesion between the bacteria and nanomaterial. Although this is contradicted by the fact that microbes can attach to rough surfaces rather than smooth polished surfaces.

According to Hui et al (2014) presence of basal planes in the structure of graphene oxide alleviates its antimicrobial activity. They demonstrated that if the basal planes are masked by non-covalent bonding, then it renders graphene oxide less lethal to microbes. Such masking can occur due to nutrients present

in Luria broth and Minimal broth used as growth medium and thus leading to reduce membrane permeabilization. Bare graphene oxide in saline solution shows more toxic effect on microorganisms.

In our case the remnants of media helped to mask the lethality of nanomaterial along with formation of exfoliated sheets due to oxidation gave rise to interconnected spaces and features which helped in bacterial attachment.

7.6.4 SIZE OF THE NANOMATERIAL

The size of nanomaterial proves to be an important factor for delineating its biocompatible or anti-microbial feature. As literature suggests the nanoparticle may harm microorganism by mechanism of "knife effect" which may puncture the cell wall and release the cytoplasmic contents leading to death of bacterial cells. Other ways of antimicrobial activity involve wrapping of microorganism and eventually leading to inactivation by devoid of its nutritional supply. This is known as the "wrapping effect". Generally smaller nanoparticles with size less than 500nm orthogonally pierce the cell with sharp edge culminating in "nano knives mechanism" (Xu et al., 2020). Larger particles in concentrated form may completely cover the microbial cell and induce inactivation by "wrapping mechanism". Interlayer spacing is an important virtue and influence bacterial attachment as thicker layer may induce more stronger attachment.

DLS is an important technique to estimate the size of the nanomaterial. It is a fast technique and easy to use and thus it is utilized by researchers for approximation of size of the nanomaterial. According to the size estimation by DLS the nanomaterials fabricated were greater than 500nm thus diminishing the knife effect and provided substratum for bacterial attachment as seen in the SEM images.

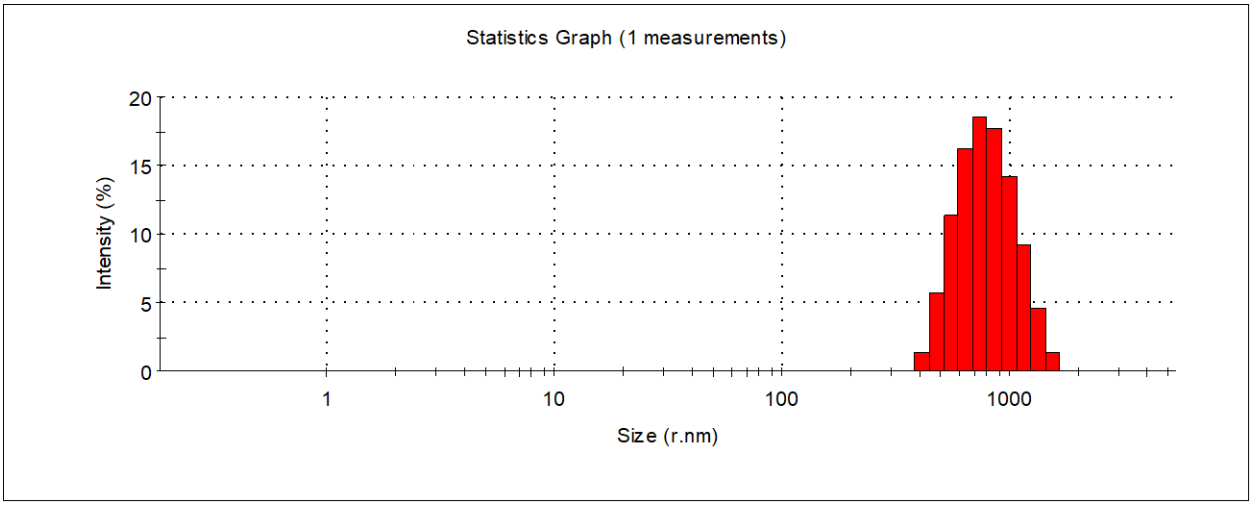

Fig 7.34 : Estimation of the size of fabricated GOaN by DLS

7.6.5 SURFACE CHARGE DENSITY

As bacteria possess net negative charge on the exterior surface due to presence of surface groups of carboxyl, phosphate, etc. it is more attracted towards positively charged substrate.(C. Chen et al., 2019; Guo et al., 2018; X. Zhu et al., 2015) But in literature findings mixed results is observed that sometimes the bacteria may overcome electrostatic repulsion forces and be overly attached to a negatively charged substratum specifically if they possess surface appendages like fimbriae or produce LPS (lipopolysaccharide).(Rzhepishevska et al., 2013; Ueshima et al., 2002).

Zeta potential study gives an idea about the net surface charge of the process and can determine the stability of the bond which has been discussed in Section A.

7.7 SEMI QUALITATIVE TEST FOR BIOSURFACTANTS PRODUCTION – CTAB BLUE AGAR TEST

CTAB (cetyltrimethylammonium bromide) blue agar plate assay is a type of semiqualitative method used for detection of presence of biosurfactants which are anionic in nature(Sabnis & Juvale, 2016).

In the Blue agar test cationic surfactant CTAB is added to the mineral salt agar plates in presence of basic dye methylene blue. If there is presence of anionic surfactant then a halo region is formed around the microorganism secreting the surfactant as an insoluble bond is formed between the reactants.

In this experiment, 20ul of previously grown mature microbial cultures is harvested and then centrifuged to collect the cell free suspension. The suspension is then aseptically transferred in the laminar air flow and inoculated in aseptically bored wells on the agar plate with the help of sterile gel puncher. The plates were then transferred to the incubator at 35C for 72hrs. It was observed halo region was formed in case of *Pseudomonas* sp in presence of GOaN (50ppm) nanomaterial whereas it was not observed in case of *Bacillus* sp.

Thus, the formation of biogel pattern (as shown in the picture) could be explained and the better removal efficacy of (Gram negative) *Pseudomonas* – GOaN than (Gram positive) *Bacillus* -GOaN could be possibly hypothesized. Segregation of dispersed negatively charged GO in water thus could be possible due to its intrinsic aggregation in presence of positively charged species like biosurfactants.

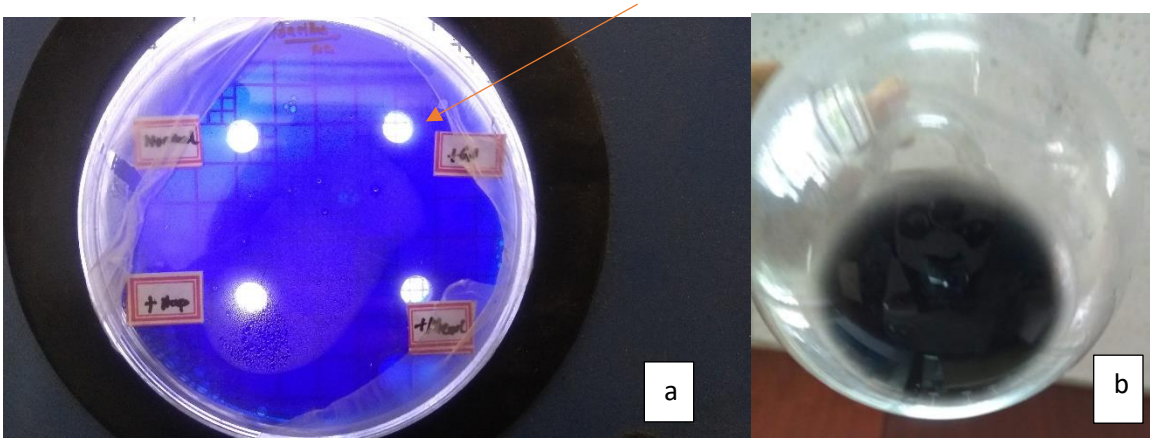

Fig 7.35 : Photographic visual of Blue Agar test for *Bacillus* sp – (a) CTAB agar plate visualization with no halo region (marked with arrow)

(b) No gel formation (self -assemble) observed in GOaN +B

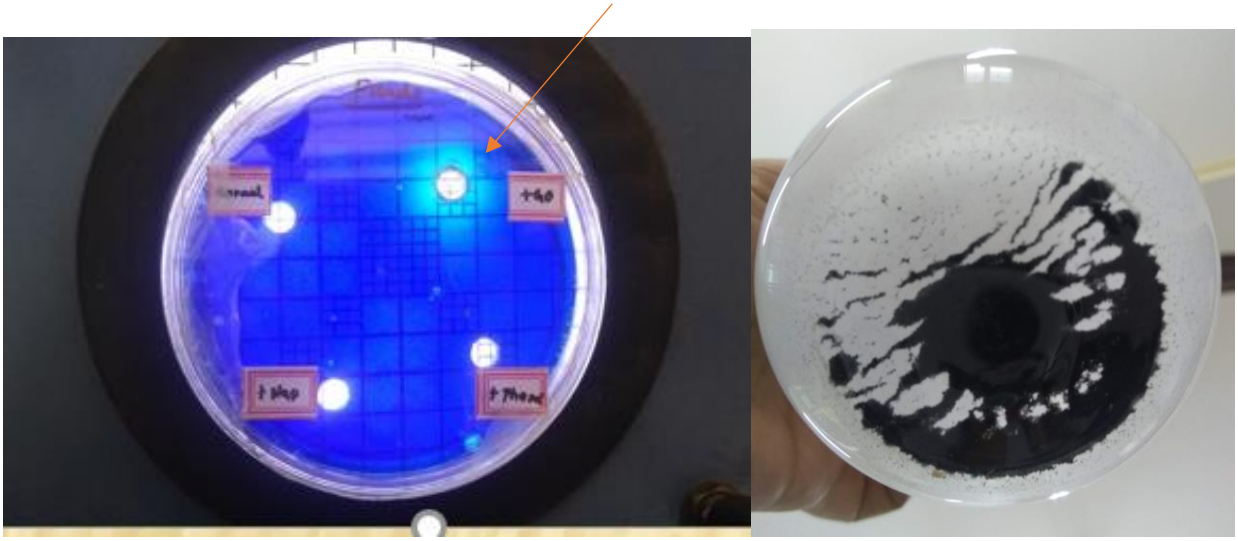

Fig 7.36 : Photographic visual of Blue Agar test for *Pseudomonas* sp – (a) CTAB agar plate visualization with a distinct halo region (marked with arrow)

(b) Gel formation (self -assemble) observed in GOaN +P

In current situation valorization of byproducts obtained during an experimental run is of great interest to many researchers. In our experiment, biosurfactant produced in presence of fabricated GOaN nanomaterial may be further used for better degradation of inorganic substances as comprehended in

other research papers (Shojaipour et al., 2020). This layer helps in retaining moisture which prevent drying of the microorganism, helps in better attachment to the substratum and thus biofilm matrix could be established. This corroborates the findings of better removal efficiency of GOaN +P than GOaN +B .

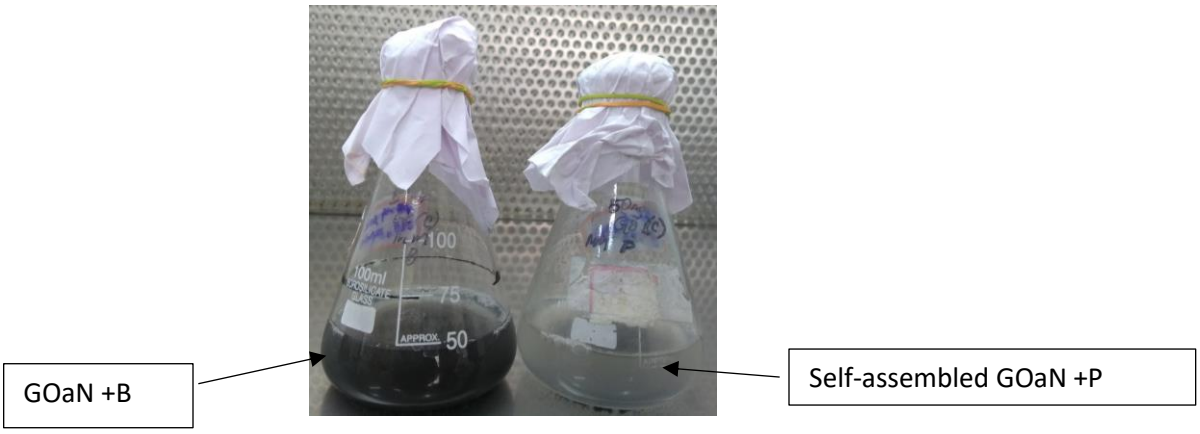

Fig 7.37 : Photographic representation of self-assembled GOaN + P nanocomposite

7.8 CONCLUDING DISCUSSIONS

Microbial degradation rate is increased in presence of nanomaterials (Kumari & Singh, 2016)**.** Whole cell nano bio preparations are thus mutualistic for both aspect as it helps to reduce dilution effect and concentrate the pollutant in the solution. Microorganism thus can act faster utilizing the pollutant as Carbon (energy source) and also the substratum helps in initiation of the biofilm formation thereby helping the bacteria to thrive in extreme conditions. Several other researchers have reported nanomaterial as enhancer of the process of biodegradation (Bhatia, 2013). Several studies with metallic nanomaterials have been observed but there is a dearth of literature regarding carbon-based nanomaterial and its effect to increase the efficiency of the degradation process by bacteria in hybrid mode (Remya et al., 2022). In this experiment it was observed that Gram negative microorganism – GOaN naomaterial hybrid composite formation

CHAPTER 8

8 TREATMENT OF REAL TIME EFFLUENT BY FABRICATED GRAPHENE OXIDE - MICROORGANISM NANOCOMPOSITE MATERIAL

8.1 CONTEXTUAL INFORMATION

In the last decade, materials with nano dimensional structures are enticing attention of researchers for real world problem solution (Panigrahy et al., 2022). Pollution of aquatic environment by industrial wastewater has increased profoundly with the ever increasing demography and technological advancement (Milon et al., 2022). Polluted aquatic environment is the leading cause of mortality and morbidity cases in the developing countries. To ameliorate the pollution scenario on the global scale and to manage the waste discharged in to the aquatic environment, various hybrid technologies are opted in the current decade. Although there are plethora of studies involving laboratory scale synthetic wastewater but real-world industrial wastewater researches are still few in number. Application of nanomaterials in combination with microorganisms is very limited due to the questionable antimicrobial effect of nanomaterials on the faunal world (Sanchez et al., 2012; L. Shen et al., 2018). The aim of the experiment lies in the fact to study the efficacy of the synergistic effect of the prepared microorganism embedded nanomaterials with comparison to adsorption or biodegradation applied individually in a real time effluent treatment which would ultimately lead to upscaling of its application. The laboratory bench scale fabricated composite of GOaN (Graphene oxide analogous nanomaterial) with embedded bacteria (*Pseudomonas mendocina*) was used for removal of Naphthalene (LMW PAH) Pyrene (HMW PAH) and Phenol (PH) with significant removal percentages of 95.03%, 87.68% and 98.32% respectively at optimal conditions as previously stated in previous chapters. In this present experimental setup industrial effluent treatment plant water was obtained from a local petrochemical industry, located in Haldia, Medinipur, West Bengal, India. The fabricated microorganism – nanomaterial composite was utilized as the adsorbent for the treatment of the ETP (Effluent Treatment Plant) water. The fabrication of the composite is mentioned in the earlier section of chapter 7. The conditions were kept similar to the optimal conditions at which the nanocomposites performed at maximal efficiency.

8.2 EXPERIMENTAL SET UP

8.2.1 COLLECTION, HANDLING AND STORAGE OF THE EFFLUENT

As mentioned previously the effluent was collected from a local petrochemical industry, located in Haldia, Medinipur, West Bengal, India. The location of the sampling site is denoted by geographical coordinates of latitude 22°03'58.90" N and longitude 88°07'04.80" E. The effluent water was transported in a 5lt plastic container made of non-reactive material with screw capped lid. The wastewater was transported immediately and was kept in the laboratory under normal conditions for 3 days without any disturbances. Larger particles and suspended solids were settled and the fluid from the upper surface was collected to minimize hindrances during experimental phase. The effluent water container was stowed in a cool dark and dry place to minimize loss due to volatilization and evaporation. The physical properties and chemical properties of the effluent was estimated after 3 days and before the initiation of the experiment. After experimental phase the properties were again estimated to measure the differences due to treatment by fabricated microorganism – nanomaterial composite.

8.2.2 PREPARATION OF GOaN – MICROORGANISM NANOCOMPOSITE

The process of preparation of microorganism embedded GOaN nanocomposite material has been discussed in details in the previous chapter 7. The characterization of the prepared nanocomposite and viability of the microbial cells in the conjugate formation has been thoroughly described in the previous chapter. As better results were opted in case of gram-negative microorganism – GOaN nanocomposite, hence it was further used for treatment of real-world effluent water. *Pseudomonas* sp is chosen as the prototypical gram-negative microorganism and thus the nanocomposite formed is termed as GOaN +P which is further utilized in this experimental study.

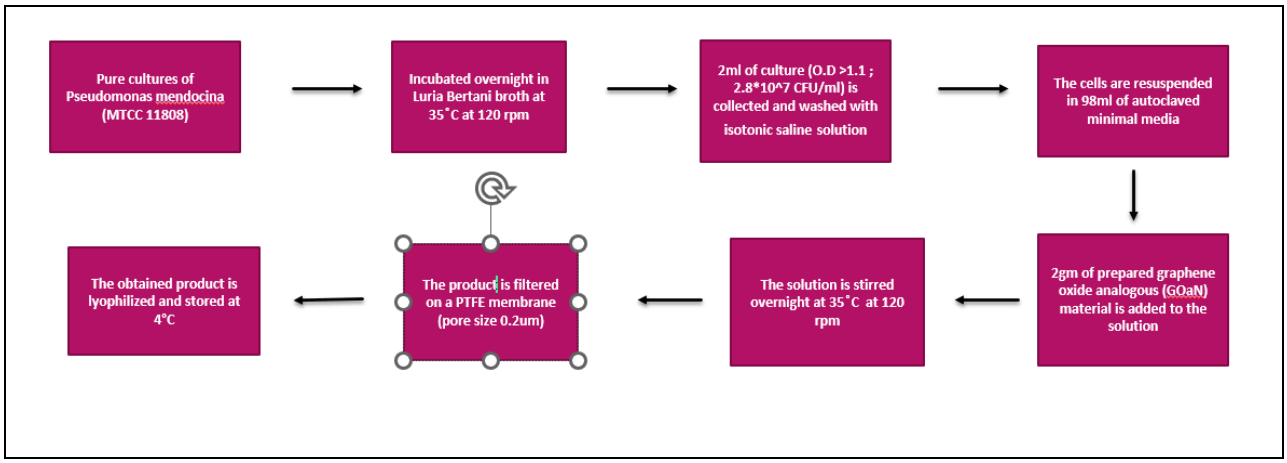

Fig 8.1 : Flow chart of the fabrication procedure of GOaN + P nanocomposite

8.2.3 CHARACTERIZATION OF WASTEWATER

The physical parameters of the wastewater were estimated by PCS multiparameter tester 35 including pH, Temperature,TDS (Total Dissolved Solids), TSS (Total Suspended Solids), Conductivity, etc. Oil and grease (O&G) test were estimated by the standard procedure of APHA. n-Hexane solution (30ml) was added to the acidified wastewater (pH =2) in a separating funnel and shaken vigorously for 10 minutes. The layers are separated with lighter water layer and heavier extracted oil and grease layer. The process is repeated few more times until the lighter part is reduced to minimum. Previously weighed flask is then filled with the heavier residues and heated. The flask is weighed (Sartorius) again to provide estimation of O&G test. FTIR spectra of raw wastewater and treated wastewater by GOaN +P was obtained by Perkin Elmer Spectrum Two. The wastewater organics also consist of estimating parameters like BOD (Biochemical oxygen demand) and COD (chemical oxygen demand) which is an important parameter for wastewater characterization and to estimate the toxicity of wastewater and is measured by APHA (American Public Health Association) techniques of water and wastewater analysis. COD is estimated by open reflux method with the aid of COD Digestor (Merck Spectroquant® TR 320). BOD is measured over a period of 5 days by measuring DO (Dissolved oxygen) with the help of DO probe (Hach) and unit is mg/L. Two BOD stoppered bottles (300ml) were used among which one was used for measuring initial DO and the other was used for measuring the final BOD after 5 days. The temperature was set at 20 – 25 °C for the BOD bottle and was kept under stirring conditions. The difference between the Initial DO and the Final DO after 5 days gives the BOD value of the sample and its unit is mg/L.

$$BOD\ (mg/L) = DOi - DOf$$

(1)

DOi = Initial DO (mg/L)

DOf = Final DO (mg/L)

8.2.4 COD REFLUX METHOD ESTIMATION

To estimate the amount of oxygen required for chemical oxidation of organic matter present in the wastewater, COD estimation is performed with distilled water as blank sample. In the digestion tube 3ml of sample is added with 1.5ml of potassium dichromate (strong oxidant). To this 4ml of silver sulphate acid reagent (1gm silver sulphate in 100ml of concentrated sulphuric acid) is added carefully and the solution is homogenized. Pinch of mercuric sulphate is added to the solution and the digestion tube is placed on the COD digestor unit (Merck). The heating program was selected to be 150 °C for 2 hours. After the stipulated time, digestion was over and the solution tubes was cooled at room temperature for 1 hour. 1.5 ml of distilled water is added to the solution and it is titrated against 0.1N FAS (Ferrous ammonium sulphate) solution with 2 drops of Ferroin reagent as indicator. To prepare 1 litre or 1000ml FAS reagent solution , 39.2g of Fe(NH4)2(SO4)2.6H2O is added to 20 ml of H2SO4 and the volume is diluted by double distill water. The titration end point is determined by color change from bluish green to reddish brown. The COD is measured by the following equation in mg/L.

$$\frac{[(A - B) * 8 * N * 1000]}{Vsample}$$

(2)

A = FAS volume used for blank titration (ml)

B = FAS volume used for sample titration (ml)

N = FAS normality

8 = milliequivalent (meq) weight of oxygen

8.2.5 BATCH SCALE STUDY UNDER OPTIMAL CONDITIONS

100ml of the effluent water was treated with pre-determined dosage of GOaN – microorganism (500 mg) i.e 5 gm/Lt of nanocomposite under optimum temperature conditions and the samples were collected. The 500 ml Erlenmeyer flasks were rotated on the shaker at 140rpm and the pH change to optimal 6.5 was done for the effluent water. The experimental set up was kept for 24hours for analysis. Samples were collected every 6 hours interval. Residual level of organic pollutants was estimated spectrophotometrically (Shimadzu UV - 1800) by scanning the supernatant at medium speed devoid of nanocomposite material from 200nm – 500nm. The slit width was set at 1.0nm and scanning interval was 0.2 secs. The physical properties and chemical parameters of the effluent wastewater were analyzed after the experimental period of 24hrs. The collected treated samples were centrifuged at 10,000 g for 15 mins and the resultant solutions were further analyzed for LMW PAH Naphthalene (NP) HMW PAH Pyrene (PR) and Phenol (PH) assay by spectrophotometric assay at their corresponding wavelength [Np λmax 219nm; Pr λmax 293nm Ph λmax 264nm]. The physical properties of the wastewater are assessed at the end of 24hr experimental time period. All the assays were done thrice and the statistically significant results are expressed as Mean +- SD. Zeta potential of the wastewater after treatment with GOaN + P was estimated by Zetasizer (Malvern). To estimate the stability of the colloidal dispersion due to electrostatic repulsive forces acting on zeta potential is an important parameter to be assessed (Rai et al., 2022).

8.3 DATA FINDINGS AND DISCUSSIONS

Wastewater characterization was done and the data obtained from before treatment and after treatment are tabulated as below:

Table 8.1 : **Wastewater parameters before and after treatment with GOaN + P nanocomposite**

PARAMETER	UNIT	BEFORE TREATMENT	AFTER TREATMENT
pH		8.9 ± 0.5	6.5 ± 0.2 (adjusted)
COD	mg/L	1983.2 ± 5.2	101.98 ± 0.5
BOD_5	mg/L	966.3 ± 0.3	59.6 ± 0.6

DO	mg/L	3.9 ± 0.2	7.8 ± 0.7
TDS	mg/L	1118.9 ± 1	23.8 ± 0.8
TSS	mg/L	180.9 ±0.5	5.2 ± 0.2
Conductivity	mS/cm	49 ± 0.5	2.5 ± 0.1
Turbidity	NTU	50.9 ± 0.3	8.98 ± 0.1

Results are indicated as Mean ± S.D

According to Central Pollution Control Board (CPCB) of India maximum permissible range for organics in the refinery wastewater is tabulated as follows (Narayan Thorat & Kumar Sonwani, 2022):

Table 8.2 : Maximum permissible limits for organics in refinery effluent water as set by CPCB, India and comparison with the experimental values generated by this experimental study.

PARAMETER	UNIT	MAXIMUM LIMIT (CPCB)	EXPERIMENTAL VALUES (THIS WORK)
pH		6 - 8	6.5 (adjusted)
COD	mg/L	125	101.98
TSS	mg/L	20	5.2
Oil and Grease	mg/L	5	1.5

The values in the above table shows that the experimental values are well within the range of permissible limits set by CPCB, India for effluent wastewater of petrochemical industry. For BOD the value depends on the number of days and is generally 20mg/L for BOD value of 3 days kept at 20°C. Thus, from the above tabulated data it is proven that the efficiency of fabricated GOaN + P nanocomposite which renders the dual function of sorption – biodegradation. Hybrid processes are thus advantageous over a single treatment process as it has more efficiency of treating the pollutants.

Main focal point of the study is on the organics part of the wastewater and so much importance is given on the BOD/COD ratio. Biodegradability index (BOD_5/COD) acts a conventional parameter for estimation of the quality of wastewater (Narayan Thorat & Kumar Sonwani, 2022). The BOD reading is taken after 5 days for the sample which is kept at 20-25°C with the help of DO probe. The value of the ratio of BOD_5/COD if more than 0.1 it is considered to be biodegradable although anything less than 0.4 is poorly biodegradable as the conditions are not suitable for microorganisms to survive. If the wastewater has ratio below 0.05 then it is completely nonbiodegradable by nature. The biodegradability index increased from 0.4 to 0.6 which is an indicator of improved biodegradation rate (Malik et al., 2020). Thus, pretreatment with the fabricated GOaN + P nanocomposite helps in improving the water quality of the effluent water and therefore making it more suitable for discharge into the natural environment. Thus, it can be concluded that the prepared nanomaterial is able to detoxify the ETP effluent and thus could be used for wider application.

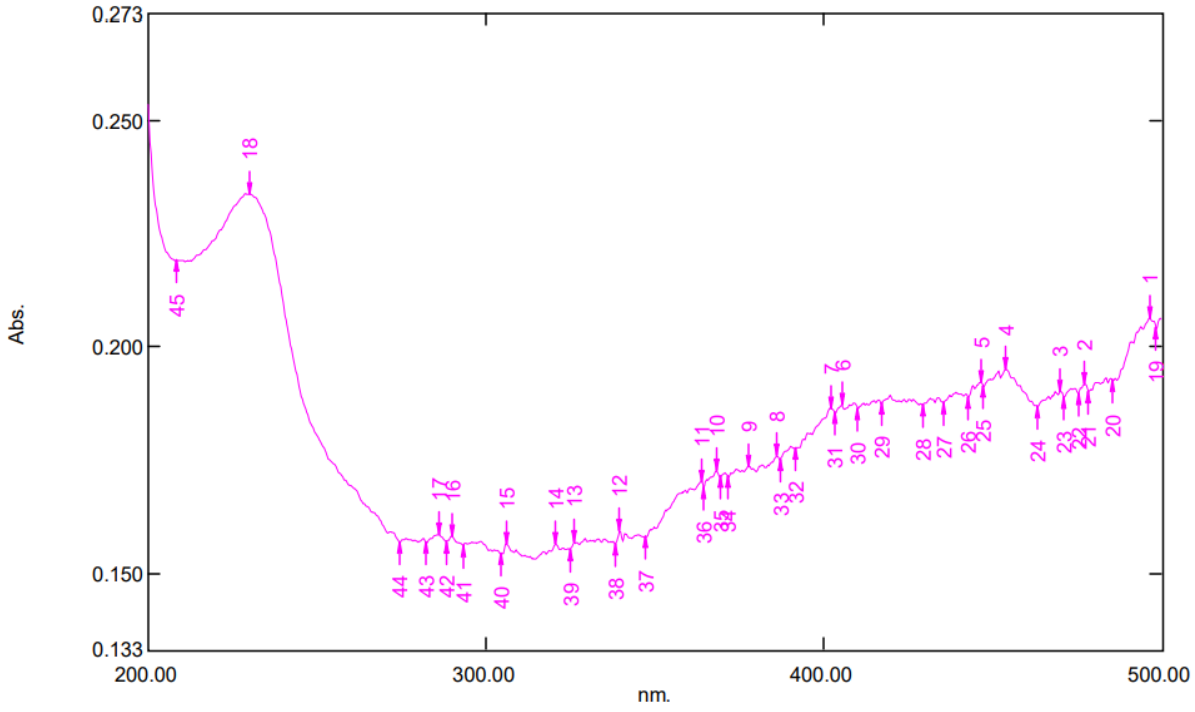

Fig 8.2 : Spectrophotometric spectrum of raw wastewater (diluted to 10^-1). The arrows indicate the peak pick points of the spectrum.

The UV spectrum of the raw and treated wastewater was obtained by Shimadzu spectrophotometer (UV -1800 series) using quartz cuvette. It is a fast nondestructive technique for routine analysis of the samples with ease and cost effectively. The samples were diluted by 10^-1 dilution for ease of spectrum analysis. After treatment of the wastewater by the GOaN + P nanocomposite, the spectrum was again obtained and the results were estimated by UVProbe software. The peak pick points were obtained by the software and it was observed that less amount of peak pick points was obtained in case of treated wastewater indicating removal of compounds. The peak pick points were estimated (±10nm) and it was observed that the absorbance value was reduced (hypochromic effect) in treated wastewater demonstrating reduction of the aromatic chemical species and thus less interference with transmitted light following Beer – Lambert law.

Table 8.3 : Peak pick points of the spectrum of the raw wastewater (10^-1 diluted) as generated by UVProbe software

No.	P/V	Wavelength	Abs.	Description
1	↑	496.40	0.206	
2	↑	477.40	0.192	
3	↑	470.20	0.190	
4	↑	454.00	0.195	
5	↑	446.40	0.192	
6	↑	405.40	0.187	
7	↑	402.00	0.186	
8	↑	386.20	0.176	
9	↑	377.80	0.174	
10	↑	368.20	0.173	
11	↑	363.80	0.170	
12	↑	339.60	0.159	
13	↑	326.20	0.157	
14	↑	320.80	0.156	
15	↑	306.20	0.156	
16	↑	289.80	0.158	
17	↑	286.20	0.159	
18	↑	230.00	0.234	
19	↓	498.60	0.204	
20	↓	485.80	0.193	
21	↓	478.60	0.190	
22	↓	475.40	0.190	
23	↓	471.20	0.189	
24	↓	463.60	0.187	
25	↓	447.40	0.191	
26	↓	443.00	0.189	
27	↓	435.40	0.188	
28	↓	429.20	0.187	
29	↓	417.20	0.187	
30	↓	410.20	0.186	
31	↓	403.40	0.185	
32	↓	391.40	0.178	
33	↓	387.00	0.175	
34	↓	371.80	0.171	
35	↓	369.40	0.171	
36	↓	364.60	0.169	
37	↓	347.00	0.158	
38	↓	338.40	0.157	
39	↓	324.80	0.155	
40	↓	304.60	0.154	
41	↓	293.20	0.156	
42	↓	288.20	0.157	
43	↓	282.40	0.157	
44	↓	274.60	0.157	
45	↓	208.20	0.219	

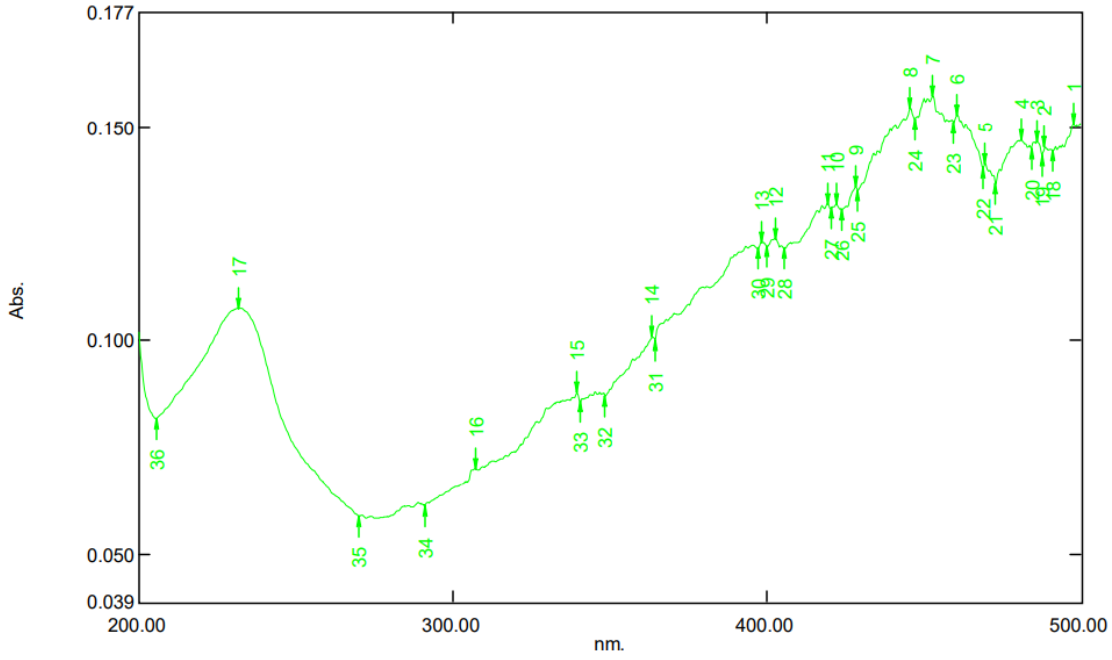

Fig 8.3 : Spectrophotometric spectrum of treated wastewater (diluted to 10^-1) by GOaN +P. The arrows indicate the peak pick points of the spectrum.

Table 8.4 : Peak pick points of the spectrum of the treated wastewater (10^-1 diluted) by GOaN +P as generated by UVProbe software

No.	P/V	Wavelength	Abs.	Description
1	↑	497.80	0.151	
2	↑	488.60	0.145	
3	↑	486.20	0.147	
4	↑	481.00	0.147	
5	↑	469.60	0.141	
6	↑	460.80	0.153	
7	↑	453.00	0.157	
8	↑	445.80	0.155	
9	↑	428.20	0.136	
10	↑	422.20	0.132	
11	↑	419.40	0.132	
12	↑	402.60	0.124	
13	↑	398.20	0.123	
14	↑	363.60	0.101	
15	↑	339.60	0.088	
16	↑	307.00	0.070	
17	↑	231.60	0.108	
18	↓	491.20	0.145	
19	↓	487.80	0.144	
20	↓	484.20	0.145	
21	↓	473.00	0.137	
22	↓	468.80	0.141	
23	↓	459.60	0.151	
24	↓	447.00	0.152	
25	↓	429.00	0.135	
26	↓	424.00	0.131	
27	↓	420.40	0.131	
28	↓	405.60	0.122	
29	↓	400.20	0.122	
30	↓	397.00	0.122	
31	↓	364.40	0.100	
32	↓	348.60	0.087	
33	↓	340.60	0.086	
34	↓	291.00	0.062	
35	↓	270.20	0.059	
36	↓	205.40	0.082	

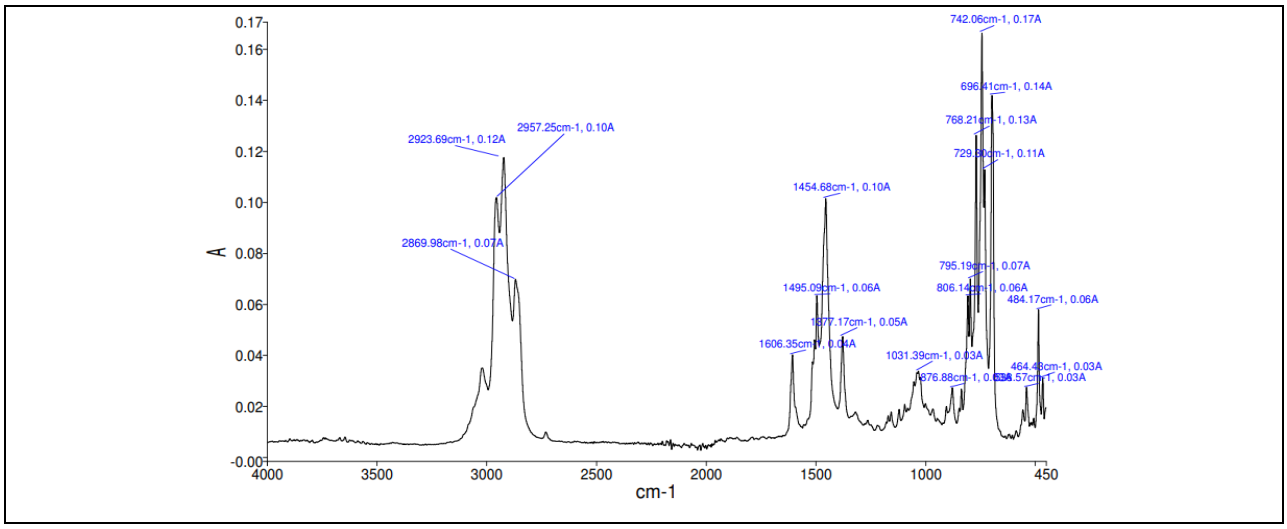

Fig 8.4 : FTIR spectra of raw wastewater

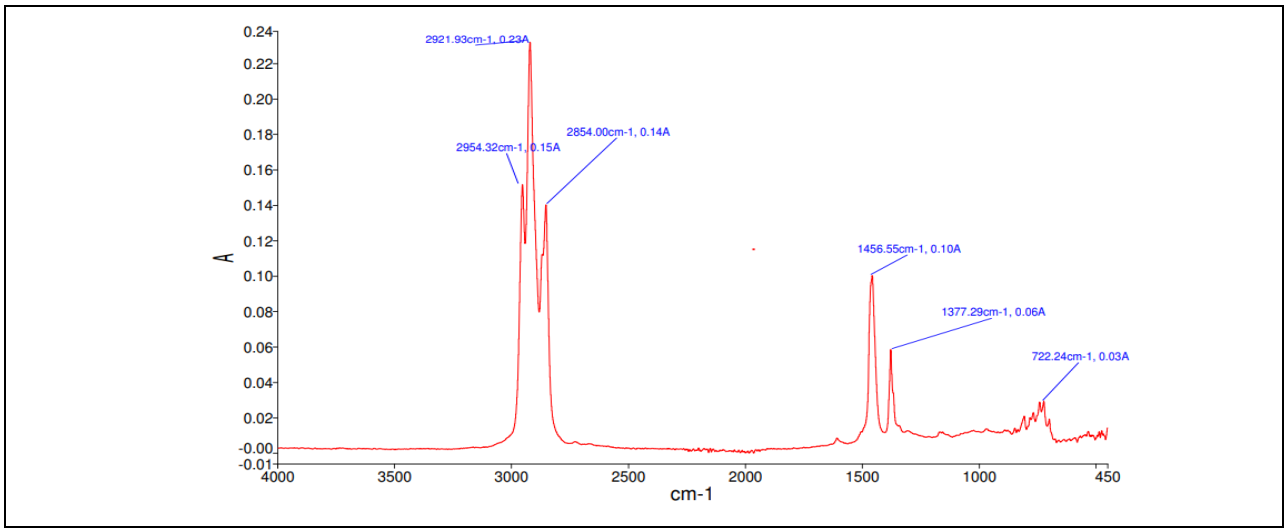

Fig 8.5 : FTIR spectra of treated wastewater by GOaN +P

.

The FTIR spectra was obtained in ATR mode where direct liquid sample can be analyzed without prior preparative measures. In the untreated sample peaks around 3000 cm-1 corresponds to O-H vibrations of hydroxyl groups and peaks at 2920 - 2950 cm-1 wavelength range is due to -CH2 and -CH3 bending of aromatic functional groups. Lesser peaks in treated type denotes adsorption and removal of aromatic functional groups from the sample by GOaN + P. About 72.56% of the Naphthalene and 65.60% of Pyrene is removed from the conjugated form present in ETP water within the stipulated time period of 24hrs. As Naphthalene is a LMW PAH so the reduction % is higher than the HMW PAH as it is easily available for degradation. The maximum removal is shown in phenol which is about 87.26% from its conjugated form

present in the wastewater. The conjugated form is proved by the shifting of the λmax values of the respective chemicals. As it was observed in the previous chapter that in interaction with the Graphene oxide (GOaN) nanomaterial embedded *Pseudomonas* sp initiates self-assembly of the nanomaterials into a bio gel formation which might help in better removal of the real time pollutants than GOaN + B nanocomposite. The data for GOaN + B nanocomposite remained inconclusive as erratic data for COD was obtained (not shown in the table). GOaN +B removal % of Np, Pr and Ph was only 49.35% Phenol, 42.01% Naphthalene and 23.22% of Pyrene in conjugated form were removed from real time effluent. The zeta potential was less than +30mV in case of GOaN + P whereas in case of GOaN + B the colloidal solution was not stable.

8.4 REUSABILITY STUDY OF PREPARED GOAN NANOCOMPOSITE

The adsorbents utilized in the bench top study of effluent treatment were filtered through vacuum filtration apparatus and were reused by suspending the particles into fresh batch of effluent water. The membrane filtration apparatus (Tarson) is used attached along with vacuum filtration pump (N.R Scientific, Kolkata). PTFE membrane (Merck) (pore size 0.22um) is used as the filter membrane so that the microbial cells are not washed out or the composite is not disintegrated by centrifugal forces. The ETP water obtained from local petrochemical industry along with the nanocomposite is passed through PTFE membrane (Merck) and thus the nanocomposite was drop casted on PTFE membrane (Merck) and air dried. All the materials used were pre sterilized to maintain decontamination phase for the experiment. The wastewater is then analyzed for estimating removal efficacy of the fabricated nano – micro composite material when re utilized the results were obtained thrice for statistical significance and the effect of PTFE membrane was also observed which was found to be negligible. Three successive cycles were estimated after which the efficiency is declined sharply. After the 3rd cycle, the bacterial cells were isolated by stirring at high speed with the help of a magnetic stirrer at room temperature. The composite disintegrated at such high speed and the solutions obtained is serially diluted and plated onto fresh Lura Bertani agar plates and the microbial CFU obtained are immobilized on new substrates.

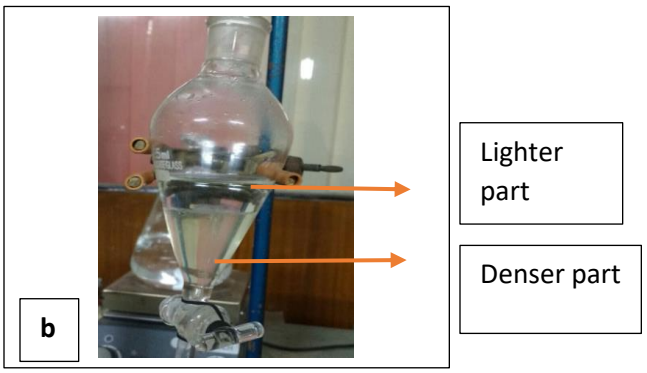

Fig 8.6: **a) Photographic visual representation of recollection of fabricated GOaN + P nanocomposite from treated wastewater for reusability study.**

b) Photographic visual representation of Oil and Grease (O&G) test of the collected effluent

8.5 CONCLUDING REMARKS

The above experimental setup concludes that the fabricated GOaN + P nanocomposite is suitable for application for treatment of real-world effluent produce treatment. As wastewater is characterized by Biodegradability index, it was observed that the biodegradability index increased from 0.4 to 0.6 which indicates in the improvement of the wastewater quality due to treatment with fabricated nanocomposite. The level of COD is decreased by 89% and oil & grease by 80% along with decrease in Suspended solids by 97%. The levels of organics are within the range as permissible by CPCB, India after treatment by the nanocomposite. Reusability study shows the potency of the composite formed to be applied for successive cycles of treatment. Zeta potential study shows the stability of the colloidal solutions formed.

CHAPTER 9

9. TOXICOLOGICAL ANALYSIS OF TREATED POLLUTANTS IN AQUEOUS PHASE BY FABRICATED GRAPHENE OXIDE NANOCOMPOSITE MATERIAL

9.1 CONTEXTUAL INFORMATION

As discussed in previous chapters water reuse and recycling of wastewater is an important strategy of water reclamation to overcome water scarcity and water shortage problems. Water reuse and recycle are major priorities for waste management under sustainable developmental goals proposed by United Nations (UN) (Hashemi et al., 2022). But before discharge in to the natural world, estimation about the quality of the treated water is priority. Phytotoxicity analysis is a way to quickly ascertain the fitness of the treated water to be able to discharge into the natural waters or used in secondary practices like washing, irrigation and all sorts of other activities etc. Phytotoxicity analysis includes estimation of germination rate and other morphological measurements including length of root, shoot, leaves etc. (Sonwani et al.,2021). To ascertain the quality and residual toxicity of the treated water by fabricated Graphene oxide analogous Nanomaterial (GOaN) and Microorganism (*Pseudomonas* sp) – Graphene Oxide Nanocomposite material (GOaN + P) [fabrication procedure in detailed form as mentioned in Chapter 3 and Chapter 7 respectively] and to investigate the detoxification efficiency of the abovementioned adsorbents prepared on the laboratory benchtop, the following experimental study is designed and conducted. To compare the efficacy of fabricated materials solely (GOaN) and in composite formation with embedded microorganisms (GOaN + P) to treat pollutants and to determine the residual toxic effects of aromatic pollutants present in synthetic aqueous phase after treatment, *Cicer arietinum* (Chickpea) germination and root analysis test is performed.

This macroscopic test provides a preliminary screening test of the residual toxicity and helps in estimation of the quality of the treated solutions to be rendered fit to discharge into the environment or to reuse the treated water in other secondary ways (Chowdhary et al., 2022; Evandri et al., 2000).

Cicer arietinum seeds (commonly known as Chickpea or Bengal gram) is a part of our staple diet as it is widely grown in the Indian subcontinent (Merga & Haji, 2019). Thus, these widely available seeds were used for the experiment as it is locally sourced, less costly, has shorter germination period and proper germination can occur under indoor conditions.

Germination and root length analysis provides us with a preliminary understanding of residual toxicity present in the water after treatment with ease and requiring less costly and widely available materials like Chickpea or Bengal gram.

To study the residual toxicity effect of the treated solution by nanomaterial fabricated in the laboratory bench top (GOaN) on the growth of the Chickpea seeds it was chosen. As it was observed in the previous study (Chapter 5) Gram negative microorganism – Graphene oxide analogous nanomaterial (GOaN +P) composite performed more efficiently with respect to removal of aromatic pollutants in comparison to Gram positive – Graphene oxide analogous nanomaterial composite (GOaN + B), thus GOaN + P nanocomposite (*Pseudomonas* sp embedded Graphene oxide analogous nanomaterial) had also been chosen for the following experimental study setup.

9.2 EXPERIMENTAL SETUP

The experimental setup consisted of 4 types of sets –

- Experimental synthetic untreated wastewater solutions [50mg/L concentration in case of phenol (Phe) and 20mg/L concentration in case of LMW PAH (Naphthalene) and HMW PAH (Pyrene)]
- Experimental synthetic wastewater solutions treated by fabricated GOaN nanomaterial.
- Experimental synthetic wastewater solutions treated by fabricated GOaN – *Pseudomonas* (GOaN +P) nanocomposite material.
- Experimental setup placed in only double distill water to be considered as standard [Blank]

9.2.1 PREPARATION OF ADSORBENT

All the above preparation methods of adsorbent and adsorbate have been discussed previously in other chapters in detailed form. Experimental simulated synthetic wastewater solutions were prepared in double distill water. The method for preparation of polyaromatic solutions (Np and Pr) and phenol (Ph) solutions have been previously described in chapter 4. The fabrication method of nano adsorbent and nanocomposite adsorbent used has been described in chapter 3 and chapter 7 respectively. The characterization of the prepared adsorbents has been discussed in details in earlier chapters. The flow chart of the fabrication processes is given below:

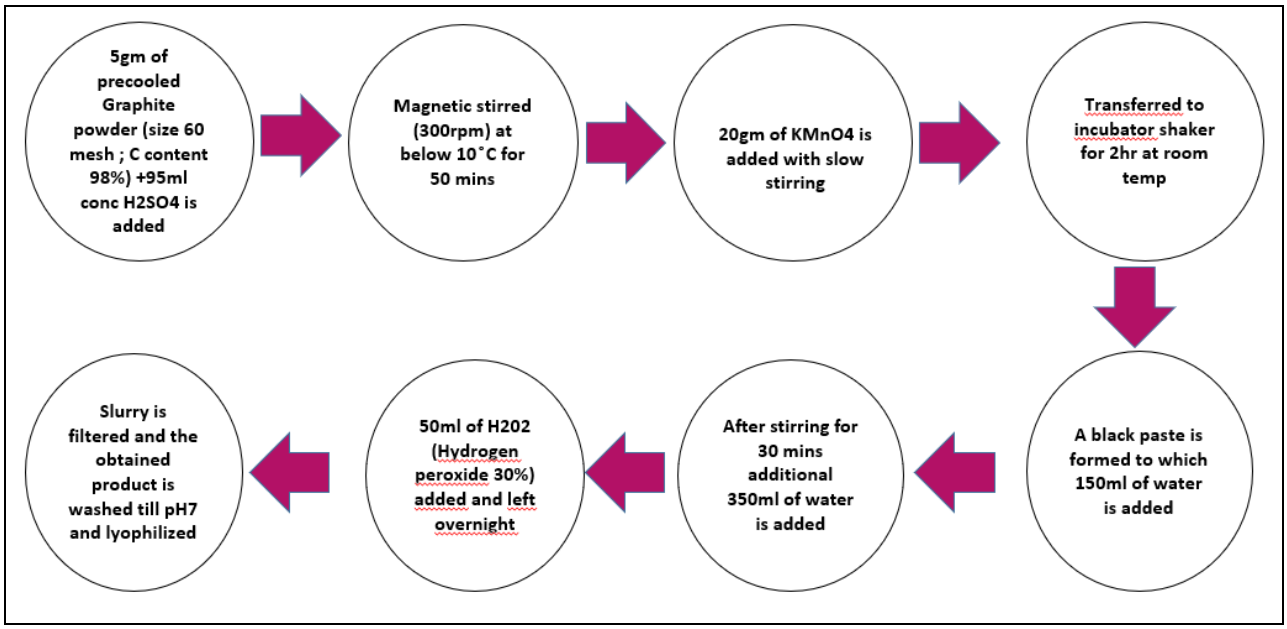

Fig 9.1 : Stepwise fabrication process of GOaN nanomaterial

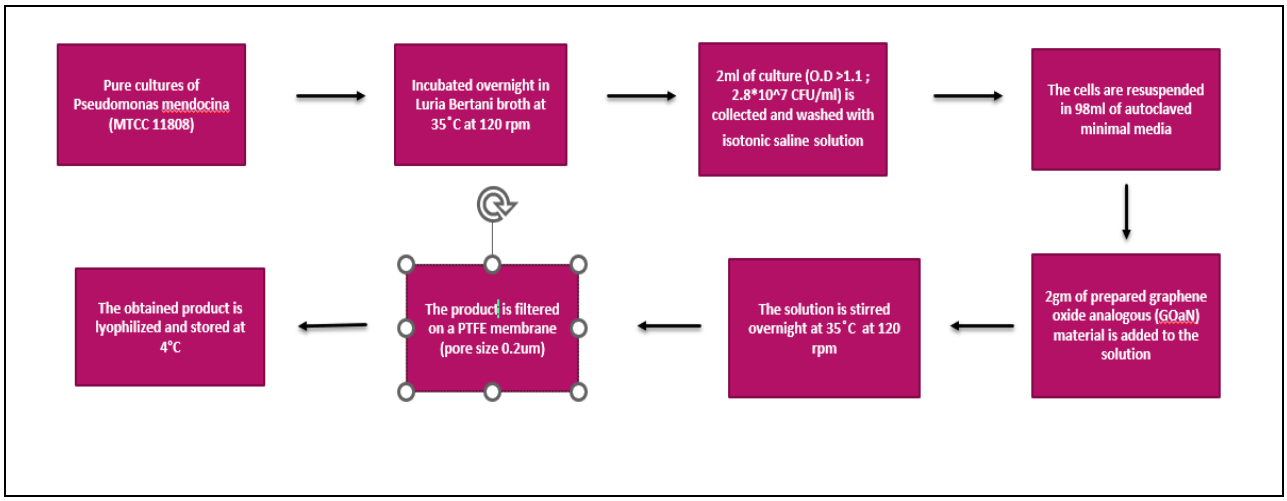

Fig 9.2 : Stepwise fabrication process of GOaN + P bionanocomposite material

9.2.2 PREPARATION OF EXPERIMENTAL SOLUTIONS

The method for preparation of synthetic waste water has been discussed in the previous chapters (chapter 4). Briefly, in case of PAH solutions acetone is added to increase the solubility of the chemicals into the

aqueous phase due to the low solubility of polyaromatics. The solution is then vortexed (REMI) to create a homogenous suspension and added to distilled water to form the required aliquots of experimental solution. In case of phenol the chemical is added directly to the aqueous phase due to its hydrophilic nature. The untreated and treated set(s) of experimental solutions are utilized for the phytotoxicity study to estimate the residual toxic level of the pollutants which indirectly ascertains the quality of the water after treatment. Solution pH is maintained according to the requirement of the experimental need. In case of pH change is needed, it is done by using 0.1N HCl or 0.1N NaOH. The pH is monitored by using handheld pH meter (Eutech Instruments)

9.2.3 PHYTOTOXICITY STUDY

The seeds of Chickpea were obtained from local market shop and washed thoroughly with distilled water before the onset of the experiment. Surface sterilization was done by soaking the seeds for 5mins in 0.1% (w/v) HgCl2 (Mercuric chloride) solution which is then washed off thoroughly. For each experimental setup 21 seeds were washed, sterilized and air dried. The seeds were placed on a filter paper (Whatman™®) in a Petri dish (Borosil 12.0 cm). 15.0 ml of the sample is added to the Petri dish and the experimental setup was kept under ambient conditions in a cool dry place. To reduce the effect of evaporative loss 5.0 ml of solution amount is added every day and the experiment was run till 5 days. The seeds were considered germinated if their root length is 1.0 mm and beyond and is thus measurable. With the help of a simple ruler, root (radicle) length of the seeds which are germinated are measured and percentage of seeds germinated were estimated. The samples obtained after treatment of phenol and other PAH(s) [Np (Naphthalene) and Pr (Pyrene)] in its aqueous phase by prepared graphene oxide analogous nanomaterial (GOaN) and by microorganism-GOaN composite [P (*Pseudomonas* sp)-GOaN set and B (*Bacillus* sp) – GOaN set] is analyzed for its detoxification efficiency. The experimental setup consists of replicative sets for statistical significance and equilibrium conditions were mentioned as described in chapter 4 and chapter 7 respectively for GOaN nanomaterial and GOaN + P nanocomposite. The mean root length as well as percentage of germinated seeds for each set were calculated which gave an idea about the germination index % (GI%) or relative seed germination % (RSG%) (Milon et al., 2022)

$$RSG\% = \frac{Number\ of\ seeds\ germinated}{Total\ seed\ number} * 100 \quad (1)$$

9.3 DATA FINDINGS AND DISCUSSION

The data from the experiments conducted are shown below in a tabulated manner. 50 mg/dL of Graphene oxide analogous nanomaterial (GOaN) and 50 mg/dL of Graphene oxide analogous material – *Pseudomonas* sp (GOaN +P) nanocomposite are used for the treatment of LMW PAH (Naphthalene) HMW PAH (Pyrene) and Phenol. The bar graphs and scatter plot graphs give a visual representation of the findings along with the pictorial representations:

Table 9.1 : Mean Root length of *Cicer arietinum* observed after 5 days of the experimental setup

ADSORBENT	SIMULATED SOLUTION	ROOT LENGTH (cm)		
		TREATED	UNTREATED	WATER
GOaN + P *(Pseudomonas* sp)	50.0 mg/L Phenol	3.4 ± 0.4	0.5 ± 0.2	4.0 ± 0.3
GOaN + P *(Pseudomonas* sp)	20.0 mg/L Naphthalene (LMW PAH)	3.1 ± 0.2	1.0 ± 0.1	4.0 ± 0.3
GOaN+ P *(Pseudomonas sp)*	20.0 mg/L Pyrene (HMW PAH)	2.7 ± 0.1	0.2 ± 0.1	4.0 ± 0.3
GOaN	50.0 mg/L Phenol	2.8 ± 0.3	0.5 ± 0.2	4.0 ± 0.3
GOaN	20.0 mg/L Naphthalene (LMW PAH)	2.5 ± 0.2	1.0 ± 0.2	4.0 ± 0.3
GOaN	20.0 mg/L Pyrene (HMW PAH)	2.2 ± 0.1	0.3 ± 0.2	4.0 ± 0.3

Results are indicated as Mean ± S.D

Table 9.2 : Relative Seed germination % (RSG %) after treatment by Graphene oxide - *Pseudomonas* (GOaN + P) nanocomposite

EXPERIMENTAL SOLUTIONS	NO. OF SEEDS GERMINATED		RSG%
	CONTROL	AFTER TREATMENT (by GOaN +P)	
Naphthalene (20mg/L)	21	17	80.952
Pyrene (20mg/L)	21	16	76.190
Phenol (50mg/L)	21	19	90.476

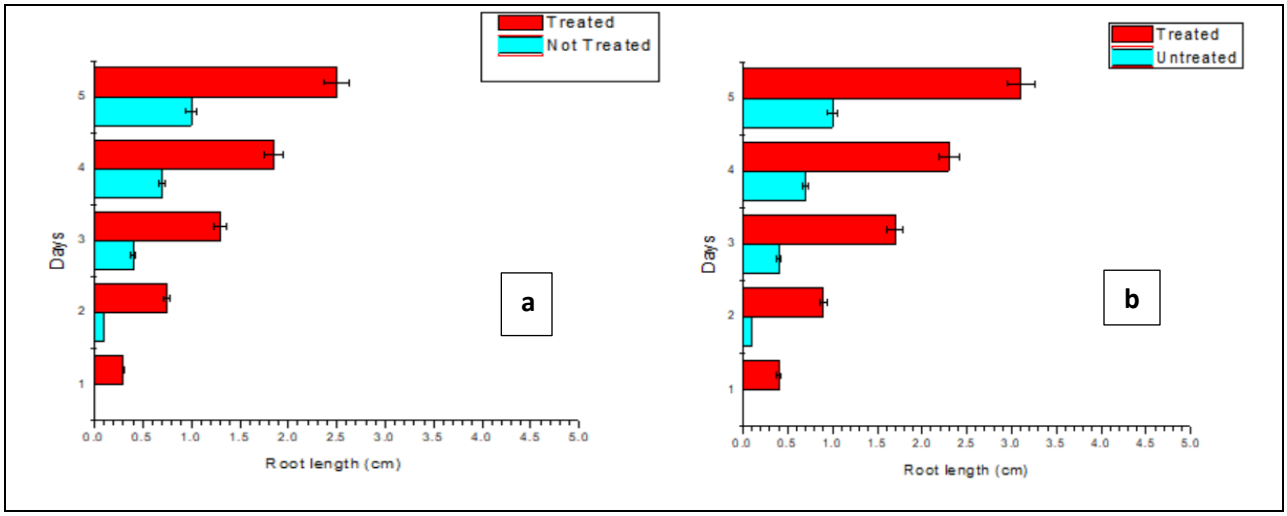

Figure a **Figure b**

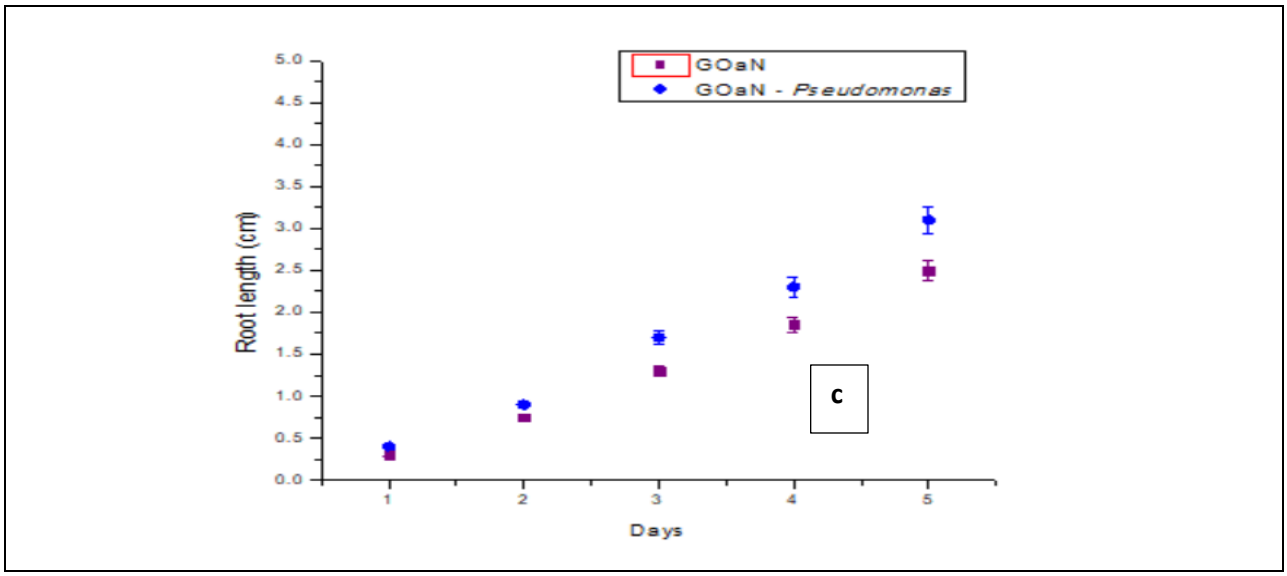

Figure c

Fig 9.3 : **Root length analysis of *Cicer arietinum* in LMW PAH (Naphthalene) solution a) Before treatment and after treatment by GOaN nanomaterial b) Before treatment and after treatment by microorganism *Pseudomonas* – GOaN (GOaN + P) nanocomposite and c) Comparison between root length in simulated wastewater treated by nanomaterial only (GOaN) and by nanomaterial – microorganism composite material (GOaN + P)**

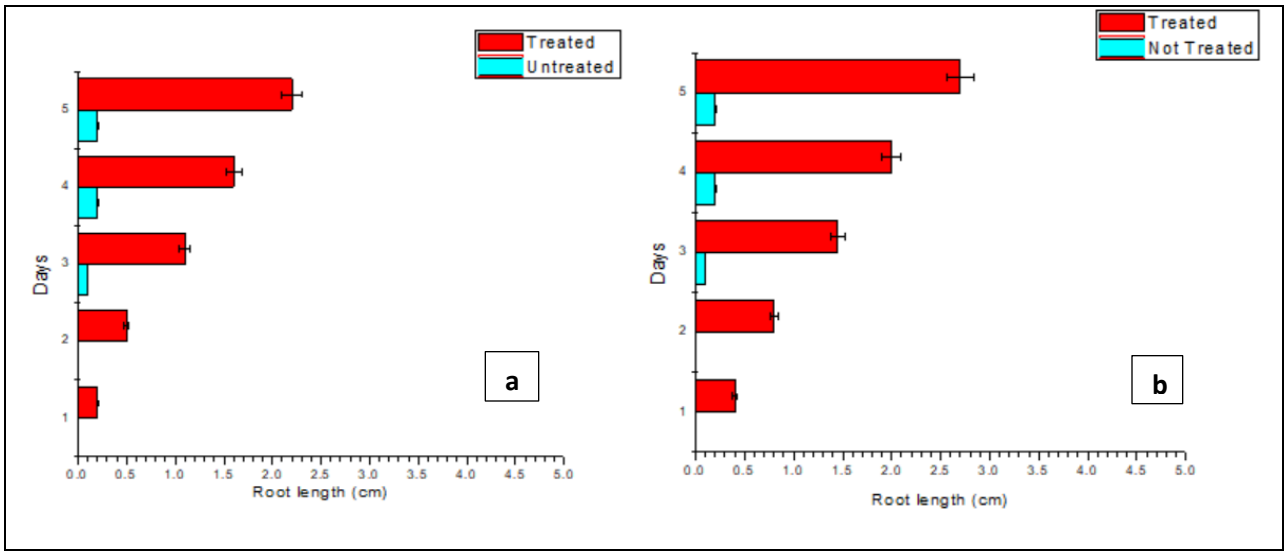

Figure a

Figure b

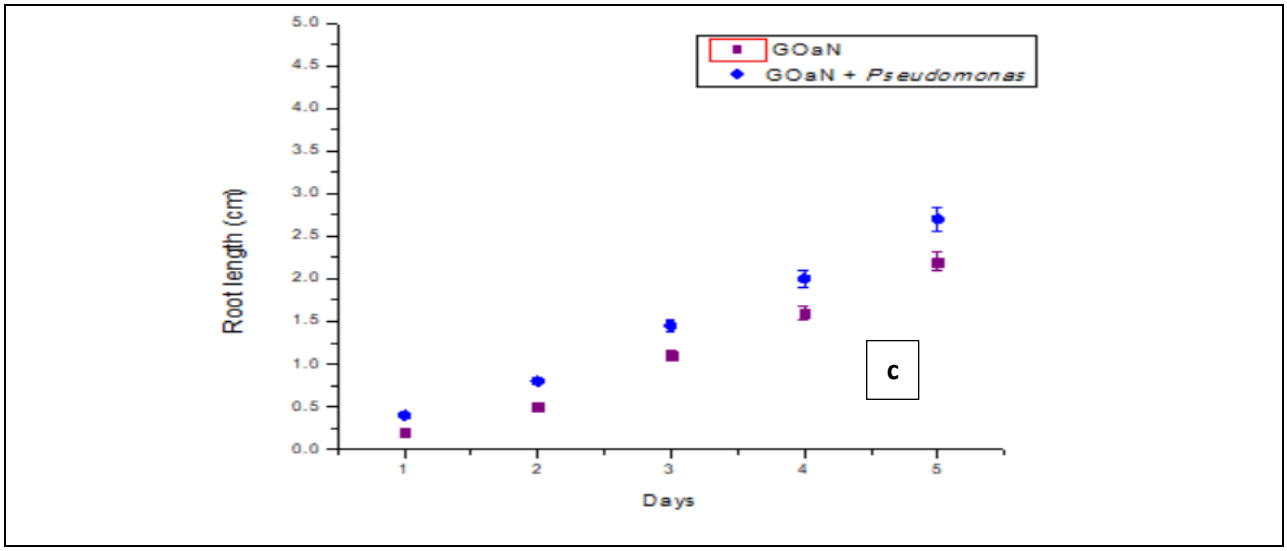

Figure c

Fig 9.4 : Root length analysis of *Cicer arietinum* in HMW PAH (Pyrene) solution a) Before treatment and after treatment by GOaN nanomaterial b) Before treatment and after treatment by microorganism *Pseudomonas*-GOaN (GOaN +P) nanocomposite and c) Comparison between root length in simulated wastewater treated by nanomaterial only (GOaN) and by nanomaterial – microorganism composite material (GOaN + P)

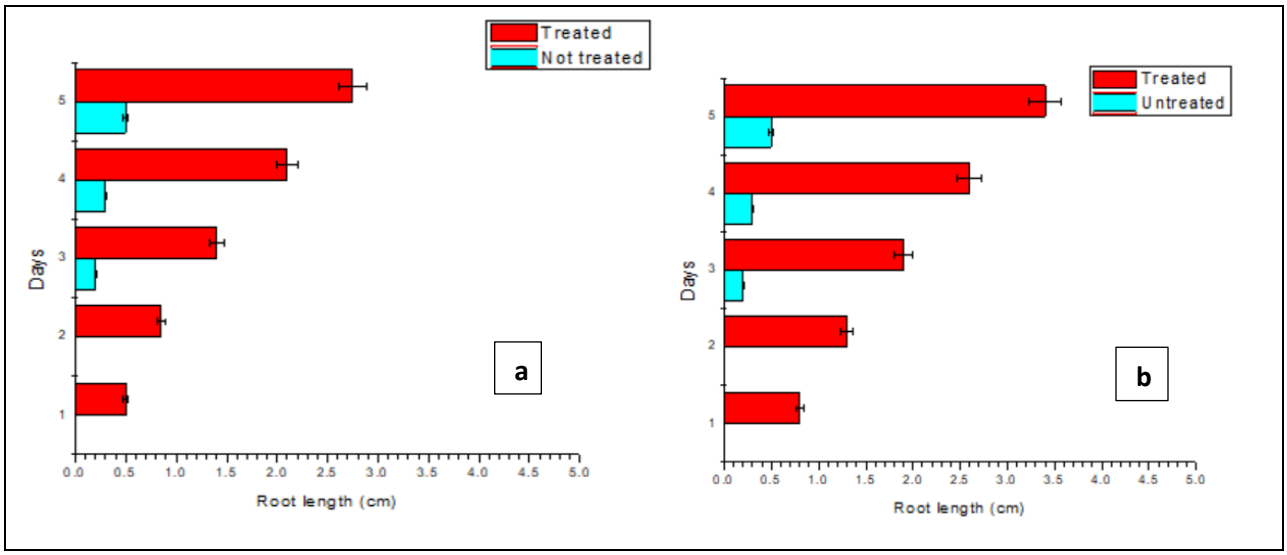

Figure a

Figure b

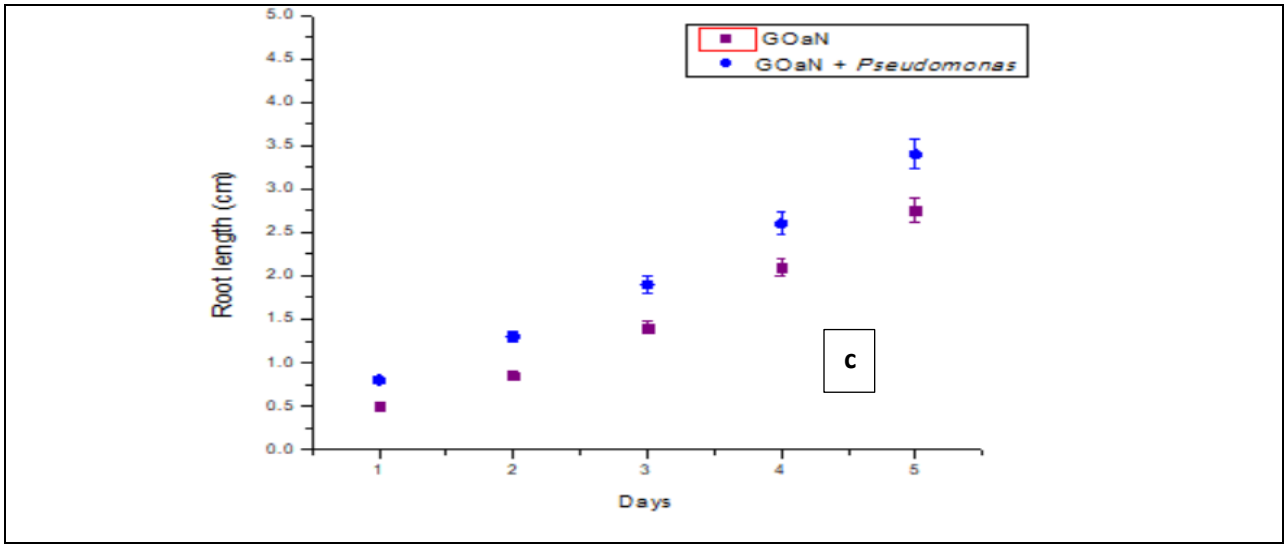

Figure c

Fig 9.5 : Root length analysis of *Cicer arietinum* in Phenol solution a) Before treatment and after treatment by GOaN nanomaterial b) Before treatment and after treatment by microorganism *Pseudomonas* – GOaN (GOaN + P) nanocomposite and c) Comparison between root length in simulated wastewater treated by nanomaterial only (GOaN) and by nanomaterial – microorganism composite material (GOaN + P)

Fig 9.6 : Photographic visual representation of experimental set up with *Cicer arietinum* seeds.

The growth was seen after 24 hours but delayed growth or shorter root lengths are observed in case of untreated samples whereas growth is observed in both kinds of treated samples. Thus, it proved that the materials fabricated during this doctoral study were all capable of removal of aromatic pollutants from aqueous phase and thereby reducing the toxic effects it may pose on aquatic ecosystem if left untreated. Another interesting fact was noticed that the growth of Bengal gram seeds was better in microorganism – nanomaterial composite (GOaN +P) treated water than only nanomaterial (GOaN) treated solution. This observation may be explained by the presence of microbial secretions of enzymes and amino acids which provides nutrients for better growth of the plant. It was observed in literature paper review that *Pseudomonas* sp possess plant growth enhancing factors and thus are used as biofertilizers (Chandra et al., 2020; Sah et al., 2021). Thus, we can conclude that reduced toxicity in the resultant solution has helped in the growth of *Cicer arietinum* seeds. As the data set is smaller non parametric Mann -Whitney U statistical test (Singh, 2019) is performed on the experimental data sets which showed $p<0.05$ thereby showing statistically significant data. Relative seed germination data and relative radicle length data estimated the germination index % which showed that the treated solutions showed little to no toxic effects on the growth of the Chickpea seedlings whereas the initial untreated simulated synthetic solutions of aromatic pollutants showed highly toxic effects on the germination and plant growth. Relative

seed germination data showed that about 80% of the Chickpea seeds were germinated in case of treated Naphthalene solution, 75% in case of treated Pyrene solution and 90% in case of treated Phenol solution presented in simulated wastewater. No plumule formation was noticed during the experimental timeframe.

HPLC and UV – Spectral analysis presented in earlier chapters has already shown the reduction of organic pollutant by GOaN – microorganism and thus the toxicity analysis result is in corroboration of the findings and exemplified the results obtained previously.

9.4 CONCLUDING REMARKS

Germination study and Root length analysis is an easier way to ascertain the residual toxicity effect present in treated synthetic wastewater. Relative seed germination % is an indicator of the toxicity imposed on the germination and growth of the seedlings. In this study it was observed that the detoxification efficiency of the laboratory fabricated composites is present and thus has promising application to treat poly aromatics as well as phenol from its aqueous phase. The synthetic wastewater treated by the fabricated composite materials is rendered fit for discharge into the environment and shows little to no residual toxicity. Negligible residual toxicity thus indicates that the pollutants were not only adsorbed by GOaN but the active biological component immobilized on it helps in remediation of the pollutants into metabolites. The water thus may also be utilized for agricultural practices, thereby ensuring reusing and recycling of the treated water. As Microbial – Nanomaterial (GOaN + P) composite materials also provide additional nutrients to the treated water thereby making it more conducive to possess plant growth promoting factors and utilization in agricultural practices.

CHAPTER 10

10 SUMMARY AND CONCLUSION

10.1 SUMMARY

Water is the utmost precious natural reserve available on our globe. The overdemanding effect on finite natural resources of the earth due to ever increasing population size has led to detrimental effects on the ecosystem. With the unprecedented growth the industrialization has increased rapidly thereby producing newer and persistent pollutants. Huge amount of literature suggests that the researchers are exploring various ways of minimizing pollution and maximizing reuse and recycling efforts. Literature review was done specifically considering pollutants or effluents released into the water bodies. Faster, safer and cost-effective ecofriendly strategies is the primary criteria to treat pollutants in aqueous phase. The treated water could be reused in other various activities and can also be safely discharged into the environment. This strategy of reusing treated polluted water for other activities is the solution to the problem of ever dwindling water resource of our planet. Treated water also helps in reduction of toxic effects on the ecosystem and thereby harmoniously balances the ecological cycle.

Every industrial process produces wastes which are considered as toxic pollutants. These pollutants are released into our water bodies, if unchecked they pose serious effects not only on aquatic sphere but also affects humans. The ecological balance intricately integrates every sphere of life and is well interconnected in all levels. Thereby we as humans is also a part of the ecological sphere and is interconnected with other levels. Aromatic compounds form the basic composition of many industrial sectors. Among the various aromatic compounds polyaromatic substances are regarded as persistent pollutants as they are not easily degraded. Due to its stability the toxic effect is prominent and has acute and chronic effects on all living beings. Many polyaromatic substances are classified as mutagenic, teratogenic and carcinogenic based on their effects. Thereby these substances are flagged as serious concern contaminants and are regulated and monitored by various Environmental Protection Agencies all over the globe. The standard limits are set for the maximum allowable limits for discharge into the environment by the guidelines given by WHO (World Health Organization).

Phenols acts as precursor material in various industries as well as it formed as a major byproduct in the wastewater of coke oven plant. Phenols also exert toxic effects on the aquatic organisms if present beyond

the tolerable limits. Thus, the wastewater containing phenol should be treated properly prior discharge into the environment. Various treatment methods have been described by the researchers all across the globe. Analyzing all the pros and cons of various treatment methods it was reckoned that adsorption is the easiest option of all. Adsorbent property greatly influences the process efficiency thus adsorbent with excellent adsorption capability is the primary requirement. Literature review recently has shown that nanomaterials is the promising material as adsorbent for various pollutants. The unique properties of material in its nano size are of research interest of various scientists all over the world. Carbonaceous nanomaterials with its excellent adsorption capability and mechanical stability along with other unique properties is one of the promising materials for adsorption. Recently scientists are exploring infinite possibilities of Graphene related family of nanomaterials to be used as adsorbents for treatment of pollutants. As nanomaterials acts as platform technology it can be merged with other techniques for better efficiency of treatment of persistent chemicals.

The overall study is thus emphasized on the feasibility on production of Graphene based nanomaterials at laboratory bench scale methods with lesser number of chemicals as well as application of fabricated graphene-based materials for the dealing of aromatic pollutants in a sustainable and practicable method. The adsorption process is governed by various external factors which were studied by batch scale methods using OFAT method. Isotherm, Kinetics and thermodynamic studies of the process were elucidated for better understanding of the process. Process optimization was done by RSM (Response Surface Methodology) using Box – Behnken and CCD (Central – Composite Design) feature available in the Design – Expert software to choose the best fitted optimal condition for maximum pollutant removal. It was seen that initially fabricated rGOaN (Graphene analogous nanomaterial) showed better removal but it was not stable as it forms a coating on the surface of the water. rGOaN thus formed showed hydrophobic tendency and therefore forms a film on the surface. GOaN (Graphene oxide analogous nanomaterial) fabricated showed stability as it forms fairly homogenous solution due to its hydrophilicity rendered by various oxygen containing functional groups integrated in its structure About 80 % of phenol and 67% of naphthalene can be removed by fabricated GOaN but the removal of pyrene was found to be around 55%. This may be explained due to the bigger structure of complex pyrene molecule which hindered attachment to adsorption sites.

Formation of nano sized materials having larger surface area and shorter diffusion path length makes the adsorbent active sites more accessible for the pollutant compounds. As nanomaterials can be merged with other treatment techniques so it was utilized with advanced gamma radiation for the treatment of

model organic pollutant. Pollutant removal by ionizing radiation is an advanced process for treatment of water. It was observed that the ionizing radiation did not have any alteration effect on the nanomaterial structure thereby proving the mechanical stability. Removal efficiency of aromatic pollutant is increased and treatment of the aqueous solution could be performed in shorter time. Utilization of graphene oxide and ionizing radiation for phenol removal is novel as few literature studies are present. About >90% of the phenol was removed from the simulated solution by gamma radiation in synergistic effect with GOaN nanomaterial. Although it has better efficiency than nanomaterial utilized separately but gamma radiation is an energy intensive process and has certain limitations due to its restrictive availability.

Biodegradation thus helps in recycling the nutrients and thereby an important parameter to maintain earth's nutrient balance (Remya et al., 2022) Biodegradation specifically using bacterial species has been researched over decades for proper degradation of complex compounds such as PAHs and phenolic compounds. Complete elimination of these toxic pollutants requires microorganisms to metabolize the products into utilizable produce. The major drawback of the adsorption process is the formation of pollutant laden sludge which maybe of concern. Thus, biodegradation is necessary to mitigate the drawback and to metabolize the toxic pollutants. Prototypical gram positive and gram-negative microorganisms were selected for the degradation of aromatic compound. It was observed that about 88% of the phenol was degraded by *Pseudomonas* sp followed by 79% by *Bacillus* sp. Water sample (marine) was collected and microorganism was isolated to be *Leclercia* sp. All the morphological and biochemical parameters were studied along with 16S rRNA phylogenetic analysis. About 67% of the phenol compound was degraded by *Leclercia* sp followed by Dietzia sp (isolated from soil of textile industry). But biodegradation takes place over a certain period of time involving several days. So to improve the efficiency of degradation formation of bio nanocomposite is necessary which involved important feature of adsorbents for fast removal of pollutants (within hours).

Interaction of biological material with the nanomaterials is studied thoroughly in this doctoral study. It was observed that in presence of the fabricated GOaN material *Pseudomonas* sp produces biosurfactant which helped in self-assembly of the nanomaterial into a composite formation. In current situation valorization of byproducts obtained during an experimental run is of great interest to many researchers. In our experiment, biosurfactant produced in presence of fabricated GOaN nanomaterial may be further used for better degradation of inorganic substances which might be a great future scope from this study. The fabricated graphene oxide material proved to be not having any antibacterial effects was confirmed by the integrated agar plate CFU counting and diffuse agar plate methods. The functionalization of the

graphene material with microorganism rendered the proposed material to be successful in executing treatment of pollutants in unary form as well as in real time effluent water. About >95% removal of organic pollutant is achieved by the bionanocomposite. In the real-world effluent treatment, it was observed that GOaN + *Pseudomonas* sp nanocomposite can increase the biodegradability index (ratio between COD: BOD) from 0.4 to 0.6 which indicates in the improvement of the wastewater quality due to treatment with fabricated nanocomposite. The level of COD is decreased by 89% and oil & grease by 80% along with decrease in Suspended solids by 97%. The levels of organics are within the range as permissible by CPCB, India after treatment by the nanocomposite. Reusability study shows the potency of the composite formed to be applied for successive cycles of treatment Although adsorption has many benefits but still the proper handling of the adsorbent material remains as a subject of concern after the process is over. Proper disposal of adsorbent is required and also integration of biodegradation makes the process more feasible and sustainable. Biodegradation takes place slowly if the cells are suspended in the solution. Co adsorption -biodegradation process could be integrated and removal of PAHs and phenols could be achieved. The efficiency of the process increased with integration of GOaN material as substratum for attachment of suspended cells of microorganism. The nanomaterial also helped in aggregating the pollutant molecule from the solution thereby making it easier for microorganism to degrade the toxicants. Toxicity study on the germination of Chickpea (*Cicer arietinum*) proves the potential of the prepared material to provide treated water safe for discharge in to the environment. It also shows that germination rate is increased which help us to give an option to utilize the treated water for agricultural practices. Relative seed germination data showed that about 80% of the Chickpea seeds were germinated in case of treated Naphthalene solution, 75% in case of treated Pyrene solution and 90% in case of treated Phenol solution presented in simulated wastewater. GOaN +P nanocomposite showed better result thereby proving the hypothesis of self-assembled nanocomposite formation by gram negative bacteria.

Thus, an overview of the present study constitutes fabrication of nanomaterial and its application for treatment of organic pollutants in unary form or in combination with other methods. Ionizing radiation in combination with nanomaterials fabricated were studied. Integration of microorganism with nanomaterial helps in immobilizing the suspended cell cultures and thereby reducing “wash out” effects. One-factor-at-a-time (OFAT) approach was utilized to evaluate the process parameters and to estimate the performance of the fabricated material. Standardization using RSM (Response Surface Methodology) was done for different pollutants. Co – adsorption – biodegradation process also aims to solve the problem of cross contamination of toxicants by the adsorbent after the treatment process is over. The treated aqueous phase can thus be directly discharged into the environment or used in various agriculture

or aquaculture processes. Limitations of conventional treatment methods (physical, chemical or biological) can be resolved by integration of two or more methods. Integration of treatment methods helps in resolving dead end products and also helps in removal of target chemicals with more efficiency and lesser amount of time.

10.2 LIMITATION OF THE PRESENT RESEARCH STUDY

Fabrication of biocompatible graphene analogous materials in bulk amount were not possible under the laboratory conditions.

Investigation of synergistic effect of prepared nanomaterial with other microorganisms could not be studied for time constraint.

10.3 FUTURE SCOPE

- Preparation of graphene family of nanomaterials with embedded magnetic properties for easier separation.
- Utilization of graphite from lithium-ion batteries to reduce battery waste dumped in our environment thereby implementing waste to wealth technique.
- Study the effect of model microorganism and magnetic nanomaterials in hybrid nanocomposite formation and to assess the effect of the particular interaction.
- Explanation of bacterial attachment to the nanomaterial surface by DLVO (Derjaguin-Landau-Verwey-Overbeek) theory and modelling of the process parameters.
- Investigation of the thermodynamic parameters of the above-mentioned interaction.

10.4 CONCLUDING POINTS

- **Fabrication of graphene-based nanomaterial is feasible at lab scale in a cost-effective manner.**
- **Oxidized form of graphene nanomaterial is utilized as nano adsorbents and is better suited to be applied with other treatment technologies for removal of organic pollutant.**

- **Gamma ionizing radiation is a type of de novo treatment of persistent organic pollutants. Concurrent methods utilizing the potency of ionizing radiation with nanotechnology helps in better removal of organic pollutants.**
- **The main drawback of adsorption process is the formation of pollutant laden sludge which is needed to be treated before elimination into the environment.**
- **Biodegradation is the only process where the pollutants are transformed to metabolites.**
- **Biodegradation process can be made more efficient when applied along with nanotechnology as it helps in reducing the "dilution effect" of microorganisms as nano sorbents acts as substratum for bacterial attachment.**
- **Optical imaging shows successful attachment of bacteria on nanomaterial and fluorescence imaging and agar plating proves its viability after attachment.**
- **Zeta potential and other bacterial growth studies shows that gram negative bacteria are better suited for interaction with nanomaterial than gram positive bacteria.**
- **The prepared hybrid nanomaterial is used as powder to attain negligible mass transfer resistances and shorter period of contact time is needed for attainment of steady state.**
- **The prepared nanomaterial induces formation of biosurfactant in case of *Pseudomonas* sp which might help in integration of the nanomaterial in a self-assembled bio gel formation and causes synergistic effect in treatment of organic pollutants.**
- **Toxicological study confirms the treated solution by the fabricated nano adsorbent and bio nanocomposite is devoid of harmful pollutants and is safe for utilization for other purposes or discharged into the environment.**
- **RSM study optimizes the process parameters applied during OFAT approach of pollutant treatment experiments**
- **The uniqueness of the study is in the preparation of graphene family nanomaterial conducive to be used with bacteria in a synergistic manner.**

REFERENCES

Abdel-Shafy, H. I., & Mansour, M. S. M. (2016). A review on polycyclic aromatic hydrocarbons: Source, environmental impact, effect on human health and remediation. *Egyptian Journal of Petroleum*, *25*(1), 107–123. https://doi.org/10.1016/j.ejpe.2015.03.011

Abu-Nada, A., Abdala, A., & McKay, G. (2021). Removal of phenols and dyes from aqueous solutions using graphene and graphene composite adsorption: A review. *Journal of Environmental Chemical Engineering*, *9*(5), 105858. https://doi.org/10.1016/j.jece.2021.105858

Adeniji, A. O., Okoh, O. O., & Okoh, A. I. (2018). Analytical Methods for Polycyclic Aromatic Hydrocarbons and their Global Trend of Distribution in Water and Sediment: A Review. In *Recent Insights in Petroleum Science and Engineering*. InTech. https://doi.org/10.5772/intechopen.71163

Ahmaruzzaman, M., & Sharma, D. K. (2005). Adsorption of phenols from wastewater. *Journal of Colloid and Interface Science*, *287*(1), 14–24. https://doi.org/10.1016/j.jcis.2005.01.075

Al-Asheh, S., Banat, F., & Abu-Aitah, L. (2003). Adsorption of phenol using different types of activated bentonites. *Separation and Purification Technology*, *33*(1), 1–10. https://doi.org/10.1016/S1383-5866(02)00180-6

Alam, S. N., Sharma, N., & Kumar, L. (2017). Synthesis of Graphene Oxide (GO) by Modified Hummers Method and Its Thermal Reduction to Obtain Reduced Graphene Oxide (rGO)*. *Graphene*, *06*(01), 1–18. https://doi.org/10.4236/graphene.2017.61001

Alcántara, M. T., Gómez, J., Pazos, M., & Sanromán, M. A. (2009). PAHs soil decontamination in two steps: Desorption and electrochemical treatment. *Journal of Hazardous Materials*, *166*(1), 462–468. https://doi.org/10.1016/j.jhazmat.2008.11.050

Ali, R., El-Boubbou, K., & Boudjelal, M. (2021). An easy, fast and inexpensive method of preparing a biological specimen for scanning electron microscopy (SEM). *MethodsX*, *8*, 101521. https://doi.org/10.1016/j.mex.2021.101521

Alkhuraiji, T. S., Boukari, S. O. B., & Alfadhl, F. S. (2017). Gamma irradiation-induced complete degradation and mineralization of phenol in aqueous solution: Effects of reagent. *Journal of Hazardous Materials*, *328*, 29–36. https://doi.org/10.1016/j.jhazmat.2017.01.004

Alvarez, P. J. J., Chan, C. K., Elimelech, M., Halas, N. J., & Villagrán, D. (2018). Emerging opportunities for nanotechnology to enhance water security. *Nature Nanotechnology*, *13*(8), 634–641. https://doi.org/10.1038/s41565-018-0203-2

Andersen, M. H. G., Saber, A. T., Clausen, P. A., Pedersen, J. E., Løhr, M., Kermanizadeh, A., Loft, S., Ebbehøj, N., Hansen, Å. M., Pedersen, P. B., Koponen, I. K., Nørskov, E.-C., Møller, P., & Vogel, U. (2018). Association between polycyclic aromatic hydrocarbon exposure and peripheral blood mononuclear cell DNA damage in human volunteers during fire extinction exercises. *Mutagenesis*, *33*(1), 105–115. https://doi.org/10.1093/mutage/gex021

Ba-Abbad, M. M., Kadhum, A. A. H., Mohamad, A. B., Takriff, M. S., & Sopian, K. (2013). Optimization of process parameters using D-optimal design for synthesis of ZnO nanoparticles via sol–gel technique. *Journal of Industrial and Engineering Chemistry*, *19*(1), 99–105. https://doi.org/10.1016/j.jiec.2012.07.010

Ba, S., Arsenault, A., Hassani, T., Jones, J. P., & Cabana, H. (2013). Laccase immobilization and insolubilization: from fundamentals to applications for the elimination of emerging contaminants in wastewater treatment. *Critical Reviews in Biotechnology*, *33*(4), 404–418. https://doi.org/10.3109/07388551.2012.725390

Baek, C., Chung, S. H., Kim, J., Yoon, S., & Min, J. (2016). Bacterial adsorption on nano graphene oxide-coated microbeads for molecular diagnosis. *Journal of Nanoscience and Nanotechnology*, *16*(11), 11887–11891. https://doi.org/10.1166/jnn.2016.13612

Bai, H., Wu, M., Zhang, H., & Tang, G. (2017). Chronic polycyclic aromatic hydrocarbon exposure causes DNA damage and genomic instability in lung epithelial cells. *Oncotarget*, *8*(45), 79034–79045. https://doi.org/10.18632/oncotarget.20891

Balati, A., Shahbazi, A., Amini, M. M., & Hashemi, S. H. (2015). Adsorption of polycyclic aromatic hydrocarbons from wastewater by using silica-based organic–inorganic nanohybrid material. *Journal of Water Reuse and Desalination*, *5*(1), 50–63. https://doi.org/10.2166/wrd.2014.013

Barik, M., Das, C. P., Kumar Verma, A., Sahoo, S., & Sahoo, N. K. (2021). Metabolic profiling of phenol biodegradation by an indigenous Rhodococcus pyridinivorans strain PDB9T N-1 isolated from paper pulp wastewater. *International Biodeterioration & Biodegradation*, *158*, 105168. https://doi.org/10.1016/j.ibiod.2020.105168

Basheer, A. A. (2018). New generation nano-adsorbents for the removal of emerging contaminants in water. *Journal of Molecular Liquids*, *261*, 583–593. https://doi.org/10.1016/j.molliq.2018.04.021

Bekkouche, S., Bouhelassa, M., Salah, N. H., & Meghlaoui, F. Z. (2004). Study of adsorption of phenol on titanium oxide (TiO2). *Desalination*, *166*, 355–362. https://doi.org/10.1016/j.desal.2004.06.090

Bhatia, M. (2013). Implicating Nanoparticles as Potential Biodegradation Enhancers: A Review. *Journal of Nanomedicine & Nanotechnology*, *04*(04). https://doi.org/10.4172/2157-7439.1000175

Bolden, A. L., Rochester, J. R., Schultz, K., & Kwiatkowski, C. F. (2017). Polycyclic aromatic hydrocarbons and female reproductive health: A scoping review. *Reproductive Toxicology*, *73*, 61–74. https://doi.org/10.1016/j.reprotox.2017.07.012

Boving, T. B., & Zhang, W. (2004). Removal of aqueous-phase polynuclear aromatic hydrocarbons using aspen wood fibers. *Chemosphere*, *54*(7), 831–839. https://doi.org/10.1016/j.chemosphere.2003.07.007

Brodie Benjamin Collins. (1859). XIII. On the atomic weight of graphite. *Philosophical Transactions of the Royal Society of London*, *149*, 249–259. https://doi.org/10.1098/rstl.1859.0013

Cabal, B., Ania, C. O., Parra, J. B., & Pis, J. J. (2009). Kinetics of naphthalene adsorption on an activated carbon: Comparison between aqueous and organic media. *Chemosphere*, *76*(4), 433–438. https://doi.org/10.1016/j.chemosphere.2009.04.002

Campbell, E., Hasan, M. T., Pho, C., Callaghan, K., Akkaraju, G. R., & Naumov, A. V. (2019). Graphene Oxide as a Multifunctional Platform for Intracellular Delivery, Imaging, and Cancer Sensing. *Scientific Reports*, *9*(1), 416. https://doi.org/10.1038/s41598-018-36617-4

Carniello, V., Peterson, B. W., van der Mei, H. C., & Busscher, H. J. (2018). Physico-chemistry from initial bacterial adhesion to surface-programmed biofilm growth. *Advances in Colloid and Interface Science*, *261*, 1–14. https://doi.org/10.1016/j.cis.2018.10.005

Chandra, H., Kumari, P., Bisht, R., Prasad, R., & Yadav, S. (2020). Plant growth promoting Pseudomonas aeruginosa from Valeriana wallichii displays antagonistic potential against three phytopathogenic fungi. *Molecular Biology Reports*, *47*(8), 6015–6026. https://doi.org/10.1007/s11033-020-05676-0

Chen, C., Petterson, T., Illergård, J., Ek, M., & Wågberg, L. (2019). Influence of Cellulose Charge on Bacteria Adhesion and Viability to PVAm/CNF/PVAm-Modified Cellulose Model Surfaces. *Biomacromolecules*, *20*(5), 2075–2083. https://doi.org/10.1021/acs.biomac.9b00297

Chen, H., Ma, S., Yu, Y., Liu, R., Li, G., Huang, H., & An, T. (2019). Seasonal profiles of atmospheric PAHs in an e-waste dismantling area and their associated health risk considering bioaccessible PAHs in the human lung. *Science of The Total Environment*, *683*, 371–379. https://doi.org/10.1016/j.scitotenv.2019.04.385

Cheng, X., Kan, A. T., & Tomson, M. B. (2004). Naphthalene Adsorption and Desorption from Aqueous C 60 Fullerene. *Journal of Chemical & Engineering Data*, *49*(3), 675–683. https://doi.org/10.1021/je030247m

Cheng, Y., Feng, G., & Moraru, C. I. (2019). Micro- and Nanotopography Sensitive Bacterial Attachment Mechanisms: A Review. *Frontiers in Microbiology*, *10*. https://doi.org/10.3389/fmicb.2019.00191

Chirman, D., & Pleshko, N. (2021). Characterization of bacterial biofilm infections with Fourier transform infrared spectroscopy: a review. *Applied Spectroscopy Reviews*, *56*(8–10), 673–701. https://doi.org/10.1080/05704928.2020.1864392

Chitose, N., Ueta, S., Seino, S., & Yamamoto, T. A. (2003). Radiolysis of aqueous phenol solutions with nanoparticles. 1. Phenol degradation and TOC removal in solutions containing TiO2 induced by UV, γ-ray and electron beams. *Chemosphere*, *50*(8), 1007–1013. https://doi.org/10.1016/S0045-6535(02)00642-2

Chowdhary, P., Singh, A., Chandra, R., Kumar, P. S., Raj, A., & Bharagava, R. N. (2022). Detection and identification of hazardous organic pollutants from distillery wastewater by GC-MS analysis and its phytotoxicity and genotoxicity evaluation by using Allium cepa and Cicer arietinum L. *Chemosphere*, *297*, 134123. https://doi.org/10.1016/j.chemosphere.2022.134123

Chu, L., Yu, S., & Wang, J. (2016). Gamma radiolytic degradation of naphthalene in aqueous solution. *Radiation Physics and Chemistry*, *123*, 97–102. https://doi.org/10.1016/j.radphyschem.2016.02.029

Das, P., Goswami, S., & Maiti, S. (2016). Removal of naphthalene present in synthetic waste water using novel Graphene /Graphene Oxide nano sheet synthesized from rice straw: comparative analysis, isotherm and kinetics. *Frontiers in Nanoscience and Nanotechnology*, *2*(1). https://doi.org/10.15761/FNN.1000107

Deemer, E. M., Paul, P. K., Manciu, F. S., Botez, C. E., Hodges, D. R., Landis, Z., Akter, T., Castro, E., & Chianelli, R. R. (2017). Consequence of oxidation method on graphene oxide produced with different size graphite precursors. *Materials Science and Engineering: B*, *224*, 150–157. https://doi.org/10.1016/j.mseb.2017.07.018

Diggs, D. L., Huderson, A. C., Harris, K. L., Myers, J. N., Banks, L. D., Rekhadevi, P. V., Niaz, M. S., & Ramesh, A. (2011). Polycyclic Aromatic Hydrocarbons and Digestive Tract Cancers: A Perspective. *Journal of Environmental Science and Health, Part C*, *29*(4), 324–357. https://doi.org/10.1080/10590501.2011.629974

Emiru, T. F., & Ayele, D. W. (2017). Controlled synthesis, characterization and reduction of graphene oxide: A convenient method for large scale production. *Egyptian Journal of Basic and Applied Sciences*, *4*(1), 74–79. https://doi.org/10.1016/j.ejbas.2016.11.002

Erawaty Silalahi, E. T. M., Anita, S., & Teruna, H. Y. (2021). Comparison of Extraction Techniques for the Determination of Polycyclic Aromatic Hydrocarbons (PAHs) in Soil. *Journal of Physics: Conference Series*, *1819*(1), 012061. https://doi.org/10.1088/1742-6596/1819/1/012061

Evandri, M. G., Tucci, P., & Bolle, P. (2000). Toxicological evaluation of commercial mineral water bottled in polyethylene terephthalate: a cytogenetic approach with *Allium cepa*. *Food Additives and Contaminants*, *17*(12), 1037–1045. https://doi.org/10.1080/02652030010014411

Gadi, R., Singh, D. P., Saud, T., Mandal, T. K., & Saxena, M. (2012). Emission Estimates of Particulate PAHs from Biomass Fuels Used in Delhi, India. *Human and Ecological Risk Assessment: An International Journal*, *18*(4), 871–887. https://doi.org/10.1080/10807039.2012.688714

Ganguli, A., Ganguly, P., Das, P., & Saha, A. (2020). Integral approach for the treatment of phenolic wastewater using gamma irradiation and graphene oxide. *Groundwater for Sustainable Development*, *10*, 100355. https://doi.org/10.1016/j.gsd.2020.100355

Geim, A. K., & Novoselov, K. S. (2007). The rise of graphene. *Nature Materials*, *6*(3), 183–191. https://doi.org/10.1038/nmat1849

Gholami, M. M., Mokhtari, M. A., Aameri, A., & Alizadeh Fard, M. R. (2006). Application of reverse osmosis technology for arsenic removal from drinking water. *Desalination*, *200*(1–3), 725–727. https://doi.org/10.1016/j.desal.2006.03.504

Gong, J., Zhu, T., Kipen, H., Rich, D. Q., Huang, W., Lin, W.-T., Hu, M., & Zhang, J. (Jim). (2015). Urinary polycyclic aromatic hydrocarbon metabolites as biomarkers of exposure to traffic-emitted pollutants. *Environment International*, *85*, 104–110. https://doi.org/10.1016/j.envint.2015.09.003

Gong, P., & Wang, X. (2021). Forest Fires Enhance the Emission and Transport of Persistent Organic Pollutants and Polycyclic Aromatic Hydrocarbons from the Central Himalaya to the Tibetan Plateau. *Environmental Science & Technology Letters*, *8*(7), 498–503. https://doi.org/10.1021/acs.estlett.1c00221

Guo, S., Kwek, M. Y., Toh, Z. Q., Pranantyo, D., Kang, E.-T., Loh, X. J., Zhu, X., Jańczewski, D., & Neoh, K. G. (2018). Tailoring Polyelectrolyte Architecture To Promote Cell Growth and Inhibit Bacterial Adhesion. *ACS Applied Materials & Interfaces*, *10*(9), 7882–7891. https://doi.org/10.1021/acsami.8b00666

Gupte, A., Tripathi, A., Patel, H., Rudakiya, D., & Gupte, S. (2016). Bioremediation of Polycyclic Aromatic Hydrocarbon (PAHs): A Perspective. *The Open Biotechnology Journal*, *10*(1), 363–378. https://doi.org/10.2174/1874070701610010363

Halder, S., Yadav, K. K., Sarkar, R., Mukherjee, S., Saha, P., Haldar, S., Karmakar, S., & Sen, T. (2015). Alteration of Zeta potential and membrane permeability in bacteria: a study with cationic agents. *SpringerPlus*, *4*(1), 672. https://doi.org/10.1186/s40064-015-1476-7

Haritash, A. K., & Kaushik, C. P. (2009). Biodegradation aspects of Polycyclic Aromatic Hydrocarbons (PAHs): A review. *Journal of Hazardous Materials*, *169*(1–3), 1–15. https://doi.org/10.1016/j.jhazmat.2009.03.137

Hashemi, F., Hashemi, H., Abbasi, A., & Schreiber, M. E. (2022). Life cycle and economic assessments of petroleum refineries wastewater recycling using membrane, resin and on site disinfection (UF-IXMB-MOX) processes. *Process Safety and Environmental Protection*, *162*, 419–425. https://doi.org/10.1016/j.psep.2022.04.027

Hernández, R., Vallés, C., Benito, A. M., Maser, W. K., Xavier Rius, F., & Riu, J. (2014). Graphene-based potentiometric biosensor for the immediate detection of living bacteria. *Biosensors and Bioelectronics*, *54*, 553–557. https://doi.org/10.1016/j.bios.2013.11.053

Holme, J. A., Brinchmann, B. C., Refsnes, M., Låg, M., & Øvrevik, J. (2019). Potential role of polycyclic aromatic hydrocarbons as mediators of cardiovascular effects from combustion particles. *Environmental Health*, *18*(1), 74. https://doi.org/10.1186/s12940-019-0514-2

Houari, M., Hamdi, B., Bouras, O., Bollinger, J.-C., & Baudu, M. (2014). Static sorption of phenol and 4-nitrophenol onto composite geomaterials based on montmorillonite, activated carbon and cement. *Chemical Engineering Journal*, *255*, 506–512. https://doi.org/10.1016/j.cej.2014.06.065

Hu, M., Yao, Z., & Wang, X. (2017). Characterization techniques for graphene-based materials in catalysis. *AIMS Materials Science*, *4*(3), 755–788. https://doi.org/10.3934/matersci.2017.3.755

Huang, R., Tian, W., Liu, Q., Yu, H., Jin, X., Zhao, Y., Zhou, Y., & Feng, G. (2016). Enhanced biodegradation of pyrene and indeno(1,2,3-cd)pyrene using bacteria immobilized in cinder beads in estuarine wetlands. *Marine Pollution Bulletin*, *102*(1), 128–133. https://doi.org/10.1016/j.marpolbul.2015.11.044

Huang, R., Yang, B., Liu, Q., & Liu, Y. (2014). Multifunctional activated carbon/chitosan composite preparation and its simultaneous adsorption of phenol and Cr(VI) from aqueous solutions. *Environmental Progress & Sustainable Energy*, *33*(3), 814–823. https://doi.org/10.1002/ep.11844

Huang, Y., Dong, X., Liu, Y., Li, L.-J., & Chen, P. (2011). Graphene-based biosensors for detection of bacteria and their metabolic activities. *Journal of Materials Chemistry*, *21*(33), 12358. https://doi.org/10.1039/c1jm11436k

Izquierdo-Colorado, A., Torres-Torres, G., Gamboa-Rodríguez, M. T., Silahua-Pavón, A. A., Arévalo-Pérez, J. C., Cervantes-Uribe, A., Cordero-García, A., & Beltramini, J. N. (2019). Catalytic Wet Air Oxidation (CWAO) of Phenol in a Fixed Bed Reactor Using Supported Ru and Ru-Au Catalysts: Effect of Gold and Ce Loading. *ChemistrySelect*, *4*(4), 1275–1284. https://doi.org/10.1002/slct.201802958

J., A. K., D., J. A., S., A. J., & S., S. (2016). Thermo-chemical sequestration of naphthalene using Borassus flabellifer Shell activated carbon: Effect of influencing parameters, isotherm and kinetic study. *African Journal of Biotechnology*, *15*(48), 2703–2713. https://doi.org/10.5897/AJB2016.15650

James, G. A., Boegli, L., Hancock, J., Bowersock, L., Parker, A., & Kinney, B. M. (2019). Bacterial Adhesion and Biofilm Formation on Textured Breast Implant Shell Materials. *Aesthetic Plastic Surgery*, *43*(2), 490–497. https://doi.org/10.1007/s00266-018-1234-7

Jia, X., Campos-Delgado, J., Terrones, M., Meunier, V., & Dresselhaus, M. S. (2011). Graphene edges: a review of their fabrication and characterization. *Nanoscale*, *3*(1), 86–95. https://doi.org/10.1039/C0NR00600A

Jin, X., Li, E., Lu, S., Qiu, Z., & Sui, Q. (2013). Coking wastewater treatment for industrial reuse purpose: Combining biological processes with ultrafiltration, nanofiltration and reverse osmosis. *Journal of Environmental Sciences*, *25*(8), 1565–1574. https://doi.org/10.1016/S1001-0742(12)60212-5

Johnsen, A. R., & Karlson, U. (2005). PAH Degradation Capacity of Soil Microbial Communities—Does It Depend on PAH Exposure? *Microbial Ecology*, *50*(4), 488–495. https://doi.org/10.1007/s00248-005-0022-5

Jung, K. H., Kim, J. K., Noh, J. H., Eun, J. W., Bae, H. J., Kim, M. G., Chang, Y. G., Shen, Q., Kim, S.-J., Kwon, S. H., Park, W. S., Lee, J. Y., & Nam, S. W. (2013). Characteristic molecular signature for the early detection and prediction of polycyclic aromatic hydrocarbons in rat liver. *Toxicology Letters*, *216*(1), 1–8. https://doi.org/10.1016/j.toxlet.2012.11.001

Kamnev, A. A., Dyatlova, Y. A., Kenzhegulov, O. A., Vladimirova, A. A., Mamchenkova, P. V., & Tugarova, A. V. (2021). Fourier Transform Infrared (FTIR) Spectroscopic Analyses of Microbiological Samples and Biogenic Selenium Nanoparticles of Microbial Origin: Sample Preparation Effects. *Molecules*, *26*(4), 1146. https://doi.org/10.3390/molecules26041146

Kongmany, S., Furuta, M., Matsuura, H., Okuda, S., Imamura, K., & Maeda, Y. (2014). Degradation of phorbol 12,13-diacetate in aqueous solution by gamma irradiation. *Radiation Physics and Chemistry*, *105*, 98–103. https://doi.org/10.1016/j.radphyschem.2014.05.022

Krishnamoorthy, K., Veerapandian, M., Yun, K., & Kim, S.-J. (2013). The chemical and structural analysis of graphene oxide with different degrees of oxidation. *Carbon*, *53*, 38–49. https://doi.org/10.1016/j.carbon.2012.10.013

Kumar, J. A., Amarnath, D. J., Kumar, P. S., Kaushik, C. S., Varghese, M. E., & Saravanan, A. (2018). Mass transfer and thermodynamic analysis on the removal of naphthalene from aqueous solution using oleic acid modified palm shell activated carbon. *DESALINATION AND WATER TREATMENT*, *106*, 238–250. https://doi.org/10.5004/dwt.2018.22066

Kumar, S., & Parekh, S. H. (2020). Linking graphene-based material physicochemical properties with molecular adsorption, structure and cell fate. *Communications Chemistry*, *3*(1), 8. https://doi.org/10.1038/s42004-019-0254-9

Kumari, B., & Singh, D. P. (2016). A review on multifaceted application of nanoparticles in the field of bioremediation of petroleum hydrocarbons. *Ecological Engineering*, *97*, 98–105. https://doi.org/10.1016/j.ecoleng.2016.08.006

Kurantowicz, N., Sawosz, E., Jaworski, S., Kutwin, M., Strojny, B., Wierzbicki, M., Szeliga, J., Hotowy, A., Lipińska, L., Koziński, R., Jagiełło, J., & Chwalibog, A. (2015). Interaction of graphene family materials with Listeria monocytogenes and Salmonella enterica. *Nanoscale Research Letters*, *10*(1), 23. https://doi.org/10.1186/s11671-015-0749-y

Kurnik, K., Treder, K., Skorupa-Kłaput, M., Tretyn, A., & Tyburski, J. (2015). Removal of Phenol from Synthetic and Industrial Wastewater by Potato Pulp Peroxidases. *Water, Air, & Soil Pollution*, *226*(8), 254. https://doi.org/10.1007/s11270-015-2517-0

Lacroix, C., Richard, G., Seguineau, C., Guyomarch, J., Moraga, D., & Auffret, M. (2015). Active and passive biomonitoring suggest metabolic adaptation in blue mussels (Mytilus spp.) chronically exposed to a moderate contamination in Brest harbor (France). *Aquatic Toxicology*, *162*, 126–137. https://doi.org/10.1016/j.aquatox.2015.03.008

Lamichhane, S., Bal Krishna, K. C., & Sarukkalige, R. (2016a). Polycyclic aromatic hydrocarbons (PAHs) removal by sorption: A review. *Chemosphere*, *148*, 336–353. https://doi.org/10.1016/j.chemosphere.2016.01.036

Lamichhane, S., Bal Krishna, K. C., & Sarukkalige, R. (2016b). Polycyclic aromatic hydrocarbons (PAHs) removal by sorption: A review. *Chemosphere*, *148*, 336–353. https://doi.org/10.1016/j.chemosphere.2016.01.036

Lawal, A. T. (2017). Polycyclic aromatic hydrocarbons. A review. *Cogent Environmental Science*, *3*(1), 1339841. https://doi.org/10.1080/23311843.2017.1339841

Legal, J. M., Manfait, M., & Theophanides, T. (1991). Applications of FTIR spectroscopy in structural studies of cells and bacteria. *Journal of Molecular Structure*, *242*, 397–407. https://doi.org/10.1016/0022-2860(91)87150-G

Leong, M. L., Lee, K. M., Lai, S. O., & Ooi, B. S. (2011). Sludge characteristics and performances of the sequencing batch reactor at different influent phenol concentrations. *Desalination*, *270*(1–3), 181–187. https://doi.org/10.1016/j.desal.2010.11.043

Li, N., Cheng, W.-Y., & Pan, Y.-Z. (2017). Adsorption of Naphthalene on Modified Zeolite from Aqueous Solution. *Journal of Environmental Protection*, *08*(04), 416–425. https://doi.org/10.4236/jep.2017.84030

Li, X., Cai, W., An, J., Kim, S., Nah, J., Yang, D., Piner, R., Velamakanni, A., Jung, I., Tutuc, E., Banerjee, S. K., Colombo, L., & Ruoff, R. S. (2009). Large-Area Synthesis of High-Quality and Uniform Graphene Films on Copper Foils. *Science*, *324*(5932), 1312–1314. https://doi.org/10.1126/science.1171245

Li, X., Xu, W., Tang, M., Zhou, L., Zhu, B., Zhu, S., & Zhu, J. (2016). Graphene oxide-based efficient and scalable solar desalination under one sun with a confined 2D water path. *Proceedings of the National Academy of Sciences*, *113*(49), 13953–13958. https://doi.org/10.1073/pnas.1613031113

Liang, L., Zhang, J., Feng, P., Li, C., Huang, Y., Dong, B., Li, L., & Guan, X. (2015). Occurrence of bisphenol A in surface and drinking waters and its physicochemical removal technologies. *Frontiers of Environmental Science & Engineering*, *9*(1), 16–38. https://doi.org/10.1007/s11783-014-0697-2

Liu, J., Xie, J., Ren, Z., & Zhang, W. (2013). Solvent extraction of phenol with cumene from wastewater. *Desalination and Water Treatment*, *51*(19–21), 3826–3831. https://doi.org/10.1080/19443994.2013.796993

Llosa Tanco, M., & Pacheco Tanaka, D. (2016). Recent Advances on Carbon Molecular Sieve Membranes (CMSMs) and Reactors. *Processes*, *4*(3), 29. https://doi.org/10.3390/pr4030029

Lohrke, J., Briel, A., & Mäder, K. (2008). Characterization of superparamagnetic iron oxide nanoparticles by asymmetrical flow-field-flow-fractionation. *Nanomedicine*, *3*(4), 437–452. https://doi.org/10.2217/17435889.3.4.437

Luo, P., Bao, L.-J., Li, S.-M., & Zeng, E. Y. (2015). Size-dependent distribution and inhalation cancer risk of particle-bound polycyclic aromatic hydrocarbons at a typical e-waste recycling and an urban site. *Environmental Pollution*, *200*, 10–15. https://doi.org/10.1016/j.envpol.2015.02.007

Mahgoub, H. A. (2019). Nanoparticles Used for Extraction of Polycyclic Aromatic Hydrocarbons. *Journal of Chemistry*, *2019*, 1–20. https://doi.org/10.1155/2019/4816849

Malik, S. N., Ghosh, P. C., Vaidya, A. N., & Mudliar, S. N. (2020). Hybrid ozonation process for industrial wastewater treatment: Principles and applications: A review. *Journal of Water Process Engineering*, *35*, 101193. https://doi.org/10.1016/j.jwpe.2020.101193

Manousi, N., & Zachariadis, G. A. (2020). Recent Advances in the Extraction of Polycyclic Aromatic Hydrocarbons from Environmental Samples. *Molecules*, *25*(9), 2182. https://doi.org/10.3390/molecules25092182

Mansour, J. D., Schram, J. L., & Schulte, T. H. (1984). Fluorescent staining of intracellular and extracellular bacteria in blood. *Journal of Clinical Microbiology*, *19*(4), 453–456. https://doi.org/10.1128/jcm.19.4.453-456.1984

Marcano, D. C., Kosynkin, D. V., Berlin, J. M., Sinitskii, A., Sun, Z., Slesarev, A., Alemany, L. B., Lu, W., & Tour, J. M. (2010). Improved Synthesis of Graphene Oxide. *ACS Nano*, *4*(8), 4806–4814. https://doi.org/10.1021/nn1006368

Martínez-Huitle, C. A., & Ferro, S. (2006). Electrochemical oxidation of organic pollutants for the wastewater treatment: direct and indirect processes. *Chem. Soc. Rev.*, *35*(12), 1324–1340. https://doi.org/10.1039/B517632H

Martínez-Morlanes, M. J., Castell, P., Martínez-Nogués, V., Martinez, M. T., Alonso, P. J., & Puértolas, J. A. (2011). Effects of gamma-irradiation on UHMWPE/MWNT nanocomposites. *Composites Science and Technology*, *71*(3), 282–288. https://doi.org/10.1016/j.compscitech.2010.11.013

Melnyk, A., Dettlaff, A., Kuklińska, K., Namieśnik, J., & Wolska, L. (2015). Concentration and sources of polycyclic aromatic hydrocarbons (PAHs) and polychlorinated biphenyls (PCBs) in surface soil near a municipal solid waste (MSW) landfill. *Science of The Total Environment*, *530–531*, 18–27. https://doi.org/10.1016/j.scitotenv.2015.05.092

Merga, B., & Haji, J. (2019). Economic importance of chickpea: Production, value, and world trade. *Cogent Food & Agriculture*, *5*(1), 1615718. https://doi.org/10.1080/23311932.2019.1615718

Milon, A. R., Chang, S. W., & Ravindran, B. (2022). Biochar amended compost maturity evaluation using commercial vegetable crops seedlings through phytotoxicity germination bioassay. *Journal of King Saud University - Science*, *34*(2), 101770. https://doi.org/10.1016/j.jksus.2021.101770

Mojiri, A., Zhou, J. L., Ohashi, A., Ozaki, N., & Kindaichi, T. (2019). Comprehensive review of polycyclic aromatic hydrocarbons in water sources, their effects and treatments. *Science of The Total Environment*, *696*, 133971. https://doi.org/10.1016/j.scitotenv.2019.133971

Munna, M. S., Zeba, Z., & Noor, R. (2016). Influence of temperature on the growth of Pseudomonas putida. *Stamford Journal of Microbiology*, *5*(1), 9–12. https://doi.org/10.3329/sjm.v5i1.26912

Narayan, P. S., Teradal, N. L., Jaldappagari, S., & Satpati, A. K. (2018). Eco-friendly reduced graphene oxide for the determination of mycophenolate mofetil in pharmaceutical formulations. *Journal of Pharmaceutical Analysis*, *8*(2), 131–137. https://doi.org/10.1016/j.jpha.2017.12.001

Narayan Thorat, B., & Kumar Sonwani, R. (2022). Current technologies and future perspectives for the treatment of complex petroleum refinery wastewater: A review. *Bioresource Technology*, *355*, 127263. https://doi.org/10.1016/j.biortech.2022.127263

Nesterenko-Malkovskaya, A., Kirzhner, F., Zimmels, Y., & Armon, R. (2012). Eichhornia crassipes capability to remove naphthalene from wastewater in the absence of bacteria. *Chemosphere*, *87*(10), 1186–1191. https://doi.org/10.1016/j.chemosphere.2012.01.060

Nguyen, D. H. K., Wang, J., Sbarski, I., Juodkazis, S., Crawford, R. J., & Ivanova, E. P. (2019). Influence of Amorphous, Carbon-Derived Wrinkled Surface Topologies on the Colonization of *Pseudomonas*

aeruginosa Bacteria. *Advanced Materials Interfaces*, *6*(7), 1801890. https://doi.org/10.1002/admi.201801890

Niu, J., Dai, Y., Guo, H., Xu, J., & Shen, Z. (2013). Adsorption and transformation of PAHs from water by a laccase-loading spider-type reactor. *Journal of Hazardous Materials*, *248–249*, 254–260. https://doi.org/10.1016/j.jhazmat.2013.01.017

Novais, Â., Freitas, A. R., Rodrigues, C., & Peixe, L. (2019). Fourier transform infrared spectroscopy: unlocking fundamentals and prospects for bacterial strain typing. *European Journal of Clinical Microbiology & Infectious Diseases*, *38*(3), 427–448. https://doi.org/10.1007/s10096-018-3431-3

Obayomi, K. S., Lau, S. Y., Danquah, M., Chiong, T., & Takeo, M. (2022). Advances in graphene oxide based nanobiocatalytic technology for wastewater treatment. *Environmental Nanotechnology, Monitoring & Management*, *17*, 100647. https://doi.org/10.1016/j.enmm.2022.100647

Otero, M., Rozada, F., Calvo, L. F., García, A. I., & Morán, A. (2003). Elimination of organic water pollutants using adsorbents obtained from sewage sludge. *Dyes and Pigments*, *57*(1), 55–65. https://doi.org/10.1016/S0143-7208(03)00005-6

Owabor, C. ., & Audu, J. . (2010). Studies on the adsorption of naphthalene and pyrene from aqueous medium using ripe orange peels as adsorbent. *Global Journal of Pure and Applied Sciences*, *16*(1). https://doi.org/10.4314/gjpas.v16i1.62822

Panigrahy, N., Priyadarshini, A., Sahoo, M. M., Verma, A. K., Daverey, A., & Sahoo, N. K. (2022). A comprehensive review on eco-toxicity and biodegradation of phenolics: Recent progress and future outlook. *Environmental Technology & Innovation*, *27*, 102423. https://doi.org/10.1016/j.eti.2022.102423

Patel, A. B., Mahala, K., Jain, K., & Madamwar, D. (2018). Development of mixed bacterial cultures DAK11 capable for degrading mixture of polycyclic aromatic hydrocarbons (PAHs). *Bioresource Technology*, *253*, 288–296. https://doi.org/10.1016/j.biortech.2018.01.049

Patel, A. B., Shaikh, S., Jain, K. R., Desai, C., & Madamwar, D. (2020). Polycyclic Aromatic Hydrocarbons: Sources, Toxicity, and Remediation Approaches. *Frontiers in Microbiology*, *11*. https://doi.org/10.3389/fmicb.2020.562813

Perera-Costa, D., Bruque, J. M., González-Martín, M. L., Gómez-García, A. C., & Vadillo-Rodríguez, V. (2014). Studying the Influence of Surface Topography on Bacterial Adhesion using Spatially Organized Microtopographic Surface Patterns. *Langmuir*, *30*(16), 4633–4641. https://doi.org/10.1021/la5001057

Priyadarsini, S., Mohanty, S., Mukherjee, S., Basu, S., & Mishra, M. (2018). Graphene and graphene oxide as nanomaterials for medicine and biology application. *Journal of Nanostructure in Chemistry*, *8*(2), 123–137. https://doi.org/10.1007/s40097-018-0265-6

Qiao, M., Fu, L., Li, Z., Liu, D., Bai, Y., & Zhao, X. (2020). Distribution and ecological risk of substituted and parent polycyclic aromatic hydrocarbons in surface waters of the Bai, Chao, and Chaobai rivers in northern China. *Environmental Pollution*, *257*, 113600. https://doi.org/10.1016/j.envpol.2019.113600

Qu, J., Wang, Y., Tian, X., Jiang, Z., Deng, F., Tao, Y., Jiang, Q., Wang, L., & Zhang, Y. (2021). KOH-activated porous biochar with high specific surface area for adsorptive removal of chromium (VI) and naphthalene from water: Affecting factors, mechanisms and reusability exploration. *Journal of*

Hazardous Materials, *401*, 123292. https://doi.org/10.1016/j.jhazmat.2020.123292

Rahman, S. M. A., Sharma, P., & Said, Z. (2022). Application of Response Surface Methodology based D-optimal Design for Modeling and Optimisation of Osmotic dehydration of Zucchini. *Digital Chemical Engineering*, *4*, 100039. https://doi.org/10.1016/j.dche.2022.100039

Rai, A., Amari, A., Yadav, V. K., Ismail, M. A., Elboughdiri, N., Fulekar, M. H., & Basnet, A. (2022). A Synergistic Effect of Moringa oleifera-Based Coagulant and Ultrafiltration for the Wastewater Treatment Collected from Final ETP. *Adsorption Science & Technology*, *2022*, 1–9. https://doi.org/10.1155/2022/1285011

Ramesha, G. K., Vijaya Kumara, A., Muralidhara, H. B., & Sampath, S. (2011). Graphene and graphene oxide as effective adsorbents toward anionic and cationic dyes. *Journal of Colloid and Interface Science*, *361*(1), 270–277. https://doi.org/10.1016/j.jcis.2011.05.050

Ranjan, P., Agrawal, S., Sinha, A., Rao, T. R., Balakrishnan, J., & Thakur, A. D. (2018). A Low-Cost Non-explosive Synthesis of Graphene Oxide for Scalable Applications. *Scientific Reports*, *8*(1), 12007. https://doi.org/10.1038/s41598-018-30613-4

Raza, W., Lee, J., Raza, N., Luo, Y., Kim, K.-H., & Yang, J. (2019). Removal of phenolic compounds from industrial waste water based on membrane-based technologies. *Journal of Industrial and Engineering Chemistry*, *71*, 1–18. https://doi.org/10.1016/j.jiec.2018.11.024

Remya, R. R., Julius, A., Suman, T. Y., Mohanavel, V., Karthick, A., Pazhanimuthu, C., Samrot, A. V., & Muhibbullah, M. (2022). Role of Nanoparticles in Biodegradation and Their Importance in Environmental and Biomedical Applications. *Journal of Nanomaterials*, *2022*, 1–15. https://doi.org/10.1155/2022/6090846

Rengaraj, S. (2002). Removal of phenol from aqueous solution and resin manufacturing industry wastewater using an agricultural waste: rubber seed coat. *Journal of Hazardous Materials*, *89*(2–3), 185–196. https://doi.org/10.1016/S0304-3894(01)00308-9

Roy, U., Sengupta, S., Banerjee, P., Das, P., Bhowal, A., & Datta, S. (2018). Assessment on the decolourization of textile dye (Reactive Yellow) using Pseudomonas sp. immobilized on fly ash: Response surface methodology optimization and toxicity evaluation. *Journal of Environmental Management*, *223*, 185–195. https://doi.org/10.1016/j.jenvman.2018.06.026

Rubio-Clemente, A., Torres-Palma, R. A., & Peñuela, G. A. (2014). Removal of polycyclic aromatic hydrocarbons in aqueous environment by chemical treatments: A review. *Science of The Total Environment*, *478*, 201–225. https://doi.org/10.1016/j.scitotenv.2013.12.126

Rzhepishevska, O., Hakobyan, S., Ruhal, R., Gautrot, J., Barbero, D., & Ramstedt, M. (2013). The surface charge of anti-bacterial coatings alters motility and biofilm architecture. *Biomaterials Science*, *1*(6), 589. https://doi.org/10.1039/c3bm00197k

Sabnis, S., & Juvale, V. (2016). Enrichment and Isolation of Biosurfactant Producers from Marine Environment. *International Journal of Current Microbiology and Applied Sciences*, *5*(4), 730–740. https://doi.org/10.20546/ijcmas.2016.504.084

Sah, S., Krishnani, S., & Singh, R. (2021). Pseudomonas mediated nutritional and growth promotional activities for sustainable food security. *Current Research in Microbial Sciences*, *2*, 100084. https://doi.org/10.1016/j.crmicr.2021.100084

Saha, P. Das, Bhattacharya, P., Sinha, K., & Chowdhury, S. (2013). Biosorption of Congo red and Indigo carmine by nonviable biomass of a new Dietzia strain isolated from the effluent of a textile industry. *Desalination and Water Treatment*, *51*(28–30), 5840–5847. https://doi.org/10.1080/19443994.2012.762589

Saha, P. Das, Srivastava, J., & Chowdhury, S. (2013). Removal of phenol from aqueous solution by adsorption onto seashells: equilibrium, kinetic and thermodynamic studies. *Journal of Water Reuse and Desalination*, *3*(2), 119–127. https://doi.org/10.2166/wrd.2013.070

Salvia, A. L., & Schneider, L. L. (2019). Overall Energy Efficiency and Sustainable Development. In *Encyclopedia of Sustainability in Higher Education* (pp. 1–8). Springer International Publishing. https://doi.org/10.1007/978-3-319-63951-2_463-1

Samburova, V., Connolly, J., Gyawali, M., Yatavelli, R. L. N., Watts, A. C., Chakrabarty, R. K., Zielinska, B., Moosmüller, H., & Khlystov, A. (2016). Polycyclic aromatic hydrocarbons in biomass-burning emissions and their contribution to light absorption and aerosol toxicity. *Science of The Total Environment*, *568*, 391–401. https://doi.org/10.1016/j.scitotenv.2016.06.026

Sanchez, V. C., Jachak, A., Hurt, R. H., & Kane, A. B. (2012). Biological Interactions of Graphene-Family Nanomaterials: An Interdisciplinary Review. *Chemical Research in Toxicology*, *25*(1), 15–34. https://doi.org/10.1021/tx200339h

Saputera, W. H., Putrie, A. S., Esmailpour, A. A., Sasongko, D., Suendo, V., & Mukti, R. R. (2021). Technology Advances in Phenol Removals: Current Progress and Future Perspectives. *Catalysts*, *11*(8), 998. https://doi.org/10.3390/catal11080998

Sarma, G. K., Sen Gupta, S., & Bhattacharyya, K. G. (2019). Nanomaterials as versatile adsorbents for heavy metal ions in water: a review. *Environmental Science and Pollution Research*, *26*(7), 6245–6278. https://doi.org/10.1007/s11356-018-04093-y

Sathish, S., Prasad, B. S. N., Kumar, J. A., Prabu, D., & Sivamani, S. (2021). Batch and column studies for adsorption of naphthalene from its aqueous solution using nanochitosan/sodium alginate composite. *Polymer Bulletin*. https://doi.org/10.1007/s00289-021-03926-0

Schwarzenbach, P., Egli, T., Hofstetter, T. B., Gunten, U. Von, & Wehrli, B. (2010). *Global Water Pollution and Human Health*. https://doi.org/10.1146/annurev-environ-100809-125342

Scott, T., Zhao, H., Deng, W., Feng, X., & Li, Y. (2019). Photocatalytic degradation of phenol in water under simulated sunlight by an ultrathin MgO coated Ag/TiO2 nanocomposite. *Chemosphere*, *216*, 1–8. https://doi.org/10.1016/j.chemosphere.2018.10.083

Shabeer, T. P. A., Saha, A., Gajbhiye, V. T., Gupta, S., Manjaiah, K. M., & Varghese, E. (2014). Removal of Poly Aromatic Hydrocarbons (PAHs) from Water: Effect of Nano and Modified Nano-clays as a Flocculation Aid and Adsorbent in Coagulation-flocculation Process. *Polycyclic Aromatic Compounds*, *34*(4), 452–467. https://doi.org/10.1080/10406638.2014.895949

Shah, M. P. (2014). Environmental Bioremediation: A Low Cost Nature’s Natural Biotechnology for Environmental Clean-up. *Journal of Petroleum & Environmental Biotechnology*, *05*(04). https://doi.org/10.4172/2157-7463.1000191

Shang, J., Ma, L., Li, J., Ai, W., Yu, T., & Gurzadyan, G. G. (2012). The Origin of Fluorescence from Graphene Oxide. *Scientific Reports*, *2*(1), 792. https://doi.org/10.1038/srep00792

Sharma, A., & Lee, B.-K. (2015). Adsorptive/photo-catalytic process for naphthalene removal from aqueous media using in-situ nickel doped titanium nanocomposite. *Journal of Environmental Management*, *155*, 114–122. https://doi.org/10.1016/j.jenvman.2015.03.008

Sharma, A., Singh, S. B., Sharma, R., Chaudhary, P., Pandey, A. K., Ansari, R., Vasudevan, V., Arora, A., Singh, S., Saha, S., & Nain, L. (2016). Enhanced biodegradation of PAHs by microbial consortium with different amendment and their fate in in-situ condition. *Journal of Environmental Management*, *181*, 728–736. https://doi.org/10.1016/j.jenvman.2016.08.024

Sharma, M., Tyagi, J. L., & Poluri, K. M. (2019). Quantifying bacterial cell lysis using GFP based fluorimetric assay. *International Journal of Biological Macromolecules*, *138*, 881–889. https://doi.org/10.1016/j.ijbiomac.2019.07.172

Shen, J., Liao, Y., Hopper, J. L., Goldberg, M., Santella, R. M., & Terry, M. B. (2017). Dependence of cancer risk from environmental exposures on underlying genetic susceptibility: an illustration with polycyclic aromatic hydrocarbons and breast cancer. *British Journal of Cancer*, *116*(9), 1229–1233. https://doi.org/10.1038/bjc.2017.81

Shen, L., Jin, Z., Wang, D., Wang, Y., & Lu, Y. (2018). Enhance wastewater biological treatment through the bacteria induced graphene oxide hydrogel. *Chemosphere*, *190*, 201–210. https://doi.org/10.1016/j.chemosphere.2017.09.105

Shin, K.-H., Kim, K.-W., & Ahn, Y. (2006). Use of biosurfactant to remediate phenanthrene-contaminated soil by the combined solubilization–biodegradation process. *Journal of Hazardous Materials*, *137*(3), 1831–1837. https://doi.org/10.1016/j.jhazmat.2006.05.025

Shojaipour, M., Ghaemy, M., & Amininasab, S. M. (2020). Removal of NO3− ions from water using bioadsorbent based on gum tragacanth carbohydrate biopolymer. *Carbohydrate Polymers*, *227*, 115367. https://doi.org/10.1016/j.carbpol.2019.115367

Singh, Z. (2019). Alteration in Morphological and Toxicological Properties of Copper Oxide Nano-particles: The pH Effect. *Journal of Applied Sciences*, *19*(2), 148–155. https://doi.org/10.3923/jas.2019.148.155

Sonwani, R. K., Swain, G., Giri, B. S., Singh, R. S., & Rai, B. N. (2019). A novel comparative study of modified carriers in moving bed biofilm reactor for the treatment of wastewater: Process optimization and kinetic study. *Bioresource Technology*, *281*, 335–342. https://doi.org/10.1016/j.biortech.2019.02.121

Strachowski, P., & Bystrzejewski, M. (2015). Comparative studies of sorption of phenolic compounds onto carbon-encapsulated iron nanoparticles, carbon nanotubes and activated carbon. *Colloids and Surfaces A: Physicochemical and Engineering Aspects*, *467*, 113–123. https://doi.org/10.1016/j.colsurfa.2014.11.044

Sun, X., Wang, C., Li, Y., Wang, W., & Wei, J. (2015). Treatment of phenolic wastewater by combined UF and NF/RO processes. *Desalination*, *355*, 68–74. https://doi.org/10.1016/j.desal.2014.10.018

Suzuki, H., Araki, S., & Yamamoto, H. (2015). Evaluation of advanced oxidation processes (AOP) using O3, UV, and TiO2 for the degradation of phenol in water. *Journal of Water Process Engineering*, *7*, 54–60. https://doi.org/10.1016/j.jwpe.2015.04.011

Tombolini, R., & Jansson, J. K. (1998). Monitoring of GFP-tagged bacterial cells. *Methods in Molecular Biology (Clifton, N.J.)*, *102*, 285–298. https://doi.org/10.1385/0-89603-520-4:285

Ueshima, M., Tanaka, S., Nakamura, S., & Yamashita, K. (2002). Manipulation of bacterial adhesion and proliferation by surface charges of electrically polarized hydroxyapatite. *Journal of Biomedical Materials Research*, *60*(4), 578–584. https://doi.org/10.1002/jbm.10113

Villegas, L. G. C., Mashhadi, N., Chen, M., Mukherjee, D., Taylor, K. E., & Biswas, N. (2016). A Short Review of Techniques for Phenol Removal from Wastewater. *Current Pollution Reports*, *2*(3), 157–167. https://doi.org/10.1007/s40726-016-0035-3

Vinodhkumar, G., Ramya, R., Vimalan, M., Potheher, I., & Peter, C. (2018). Reduced graphene oxide based on simultaneous detection of neurotransmitters. *Progress in Chemical and Biochemical Research*, 40–49. https://doi.org/10.29088/sami/pcbr.2018.1.4049

Volkov, Y., McIntyre, J., & Prina-Mello, A. (2017). Graphene toxicity as a double-edged sword of risks and exploitable opportunities: a critical analysis of the most recent trends and developments. *2D Materials*, *4*(2), 022001. https://doi.org/10.1088/2053-1583/aa5476

Wang, M., Niu, Y., Zhou, J., Wen, H., Zhang, Z., Luo, D., Gao, D., Yang, J., Liang, D., & Li, Y. (2016). The dispersion and aggregation of graphene oxide in aqueous media. *Nanoscale*, *8*(30), 14587–14592. https://doi.org/10.1039/C6NR03503E

Wentworth, G. R., Aklilu, Y., Landis, M. S., & Hsu, Y.-M. (2018). Impacts of a large boreal wildfire on ground level atmospheric concentrations of PAHs, VOCs and ozone. *Atmospheric Environment*, *178*, 19–30. https://doi.org/10.1016/j.atmosenv.2018.01.013

Wilcke, W., Bandowe, B. A. M., Lueso, M. G., Ruppenthal, M., del Valle, H., & Oelmann, Y. (2014). Polycyclic aromatic hydrocarbons (PAHs) and their polar derivatives (oxygenated PAHs, azaarenes) in soils along a climosequence in Argentina. *Science of The Total Environment*, *473–474*, 317–325. https://doi.org/10.1016/j.scitotenv.2013.12.037

Wu, X. (2015). Dual AO/EB Staining to Detect Apoptosis in Osteosarcoma Cells Compared with Flow Cytometry. *Medical Science Monitor Basic Research*, *21*, 15–20. https://doi.org/10.12659/MSMBR.893327

Wulandari, D. A., Zulys, A., & Kusrini, E. (2019). Samarium Complexes from 2,6-Naphtalenedicarboxylate: Synthesis, Photocatalytic Properties and Degradation of Methylene Blue. *IOP Conference Series: Materials Science and Engineering*, *546*(4), 042050. https://doi.org/10.1088/1757-899X/546/4/042050

Xu, W., Jin, Z., Pang, X., Zeng, Y., Jiang, X., Lu, Y., & Shen, L. (2020). Interaction between Biocompatible Graphene Oxide and Live Shewanella in the Self-Assembled Hydrogel: The Role of Physicochemical Properties. *ACS Applied Bio Materials*, *3*(7), 4263–4272. https://doi.org/10.1021/acsabm.0c00327

Yakout, S. M., Daifullah, A. A. M., & El-Reefy, S. A. (2013). Adsorption of Naphthalene, Phenanthrene and Pyrene from Aqueous Solution Using Low-Cost Activated Carbon Derived from Agricultural Wastes. *Adsorption Science & Technology*, *31*(4), 293–302. https://doi.org/10.1260/0263-6174.31.4.293

Yang, S., Chen, Q., Shi, M., Zhang, Q., Lan, S., Maimaiti, T., Li, Q., Ouyang, P., Tang, K., & Yang, S.-T. (2020). Fast Identification and Quantification of Graphene Oxide in Aqueous Environment by Raman Spectroscopy. *Nanomaterials*, *10*(4), 770. https://doi.org/10.3390/nano10040770

Yang, Z., Lin, Y., Wang, S., Liu, X., Cullinan, P., Chung, K. F., & Zhang, J. (2021). Urinary Amino-Polycyclic Aromatic Hydrocarbons in Urban Residents: Finding a Biomarker for Residential Exposure to Diesel Traffic. *Environmental Science & Technology*, *55*(15), 10569–10577.

https://doi.org/10.1021/acs.est.1c01549

Yang, Z., Yuan, Z., Shang, Z., & Ye, S. (2020). Multi-functional membrane based on montmorillonite/graphene oxide nanocomposites with high actuating performance and wastewater purification. *Applied Clay Science*, *197*(January), 105781. https://doi.org/10.1016/j.clay.2020.105781

Yates, B. J., Zboril, R., & Sharma, V. K. (2014). Engineering aspects of ferrate in water and wastewater treatment – a review. *Journal of Environmental Science and Health, Part A*, *49*(14), 1603–1614. https://doi.org/10.1080/10934529.2014.950924

Yoda, I., Koseki, H., Tomita, M., Shida, T., Horiuchi, H., Sakoda, H., & Osaki, M. (2014). Effect of surface roughness of biomaterials on Staphylococcus epidermidis adhesion. *BMC Microbiology*, *14*(1), 234. https://doi.org/10.1186/s12866-014-0234-2

Yuan, M., Tong, S., Zhao, S., & Jia, C. Q. (2010). Adsorption of polycyclic aromatic hydrocarbons from water using petroleum coke-derived porous carbon. *Journal of Hazardous Materials*, *181*(1–3), 1115–1120. https://doi.org/10.1016/j.jhazmat.2010.05.130

Zhang, H., Zhang, X., Wang, Y., Bai, P., Hayakawa, K., Zhang, L., & Tang, N. (2022). Characteristics and Influencing Factors of Polycyclic Aromatic Hydrocarbons Emitted from Open Burning and Stove Burning of Biomass: A Brief Review. *International Journal of Environmental Research and Public Health*, *19*(7), 3944. https://doi.org/10.3390/ijerph19073944

Zhao, W., Chen, I.-W., & Huang, F. (2019). Toward large-scale water treatment using nanomaterials. *Nano Today*, *27*, 11–27. https://doi.org/10.1016/j.nantod.2019.05.003

Zheng, S., Bawazir, M., Dhall, A., Kim, H.-E., He, L., Heo, J., & Hwang, G. (2021). Implication of Surface Properties, Bacterial Motility, and Hydrodynamic Conditions on Bacterial Surface Sensing and Their Initial Adhesion. *Frontiers in Bioengineering and Biotechnology*, *9*. https://doi.org/10.3389/fbioe.2021.643722

Zhu, M., Yao, J., Dong, L., & Sun, J. (2016). Adsorption of naphthalene from aqueous solution onto fatty acid modified walnut shells. *Chemosphere*, *144*, 1639–1645. https://doi.org/10.1016/j.chemosphere.2015.10.050

Zhu, X., Jańczewski, D., Guo, S., Lee, S. S. C., Parra Velandia, F. J., Teo, S. L.-M., He, T., Puniredd, S. R., & Vancso, G. J. (2015). Polyion Multilayers with Precise Surface Charge Control for Antifouling. *ACS Applied Materials & Interfaces*, *7*(1), 852–861. https://doi.org/10.1021/am507371a

Zhuan, R., & Wang, J. (2019). Degradation of sulfamethoxazole by ionizing radiation: Kinetics and implications of additives. *Science of the Total Environment*, *668*, 67–73. https://doi.org/10.1016/j.scitotenv.2019.03.027

1. INTRODUCTION AND LITERATURE REVIEW

1.1 CONTEXTUAL INFORMATION

The technological progression in addition to scientific advance
force leading to an exponential growth of human civilization. Th
and globalization which acts as a fillip for the exponential rise o
of novel scientific technologies and global increase in populati
the upsurge of industrialization to meet the current demand. Th
planet explicitly the atmosphere, biosphere, hydrosphere, litho
The Sustainable Development Goals (SDGs) were set up by Un
sustainable future for the progenies to come. The focal point
resources more judiciously and preserve the Earth's bounty for
on. As water remains an indispensable part of life, the increase i